EFFECTS OF OXIDATIVE STRESS AND NEUROPROTECTION IN APOPTOSIS IN NEURONAL CELL MODELS

VICKI SUZANNE BARBER

Doctor of Philosophy

THE UNIVERSITY OF ASTON IN BIRMINGHAM

June 2002

Aston University

Effects of oxidative stress and neuroprotection in apoptosis in neuronal cell models

Vicki Suzanne Barber Doctor of Philosophy, 2002

Summary

The PC12 and SH-SY5Y cell models have been proposed as potentially realistic models to investigate neuronal cell toxicity. The effects of oxidative stress (OS) caused by both H_2O_2 and Aβ on both cell models were assessed by several methods. Cell toxicity was quantitatied by measuring cell viability using the 3-(4,5-dimethylthiazol-2-yl)-2,5-diphenyltetrazolium (MTT) viability assay, an indicator of the integrity of the electron transfer chain (ETC), and cell morphology by fluorescence and video microscopy, both of which showed OS to cause decreased viability and changes in morphology. Levels of intracellular peroxide production, and changes in glutathione and carbonyl levels were also assessed, which showed OS to cause increases in intracellular peroxide production, glutathione and carbonyl levels. Differentiated SH-SY5Y cells were also employed and observed to exhibit the greatest sensitivity to toxicity.

The neurotrophic factor, nerve growth factor (NGF) was shown to cause protection against OS. Cells pre-treated with NGF showed higher viability after OS, generally less apoptotic morphology, recorded less apoptotic nucleiods, generally lower levels of intracellular peroxides and changes in gene expression.

The neurotrophic factor, brain derived growth factor (BDNF) and ascorbic acid (AA) were also investigated. BDNF showed no specific neuroprotection, however the preliminary data does warrant further investigation. AA showed a 'janus face' showing either anti-oxidant action and neuroprotection or pro-oxidant action depending on the situation.

Results show that the toxic effects of compounds such as Aβ and H_2O_2 are cell type dependent, and that OS alters glutathione metabolism in neuronal cells. Following toxic insult, glutathione levels are depleted to low levels. It is herein suggested that this lowering triggers an adaptive response causing alterations in glutathione metabolism as assessed by evaluation of glutathione mRNA biosynthetic enzyme expression and the subsequent increase in glutathione peroxidase (GPX) levels.

Keywords: PC12 cells SH-SY5Y cells, amyloid β peptide, oxidative stress, reactive oxygen species, apoptosis, glutathione, neurotrophic factors, nerve growth factor, brain derived neurotrophic factor.

I would like to dedicate this thesis to Helena McDougall – an inspirator, who taught me what could develop from a crystal garden.

ACKNOWLEDGEMENTS

I would like to thank my supervisor Dr Helen Griffiths for her support. Also thanks to Dr Peter Hanson for his help and collaboration with the crystal violet and caspase assays detailed in chapter seven.

I must also say thank you to Sarah and Mel for generally helping me through, and especially thanks to my 'Angel of the North – Sarah' for her directness, help and support with this thesis.

Finally I would like to thank Mum and Dad for their support throughout my studies especially the countless cups of tea! And Mark for all his help and support throughout the entire production of this ' tombe'.

ABBREVIATIONS

Aβ	Amyloid β protein/peptide
AA	Ascorbic acid
AD	Alzheimers disease
ALS	Amyotrophic lateral scerosis
AOX	Antioxidant
APOE	Apolipoprotein E
APP	Amyloid precursor protein
ATP	Adenosine 5-triphosphate
BCA	Bicinchoninic acid
BDNF	Brain derived neurotrophic factor
BFCN	Basal forebrain cholinergic neurons
BSO	L-Buthionine-[S,S]-sulfoxamime
CAT	Catalase
CNS	Central nervous system
COX	Cytochrome c oxidase
CSF	Cerebrospinal fluid
CTFs	C-Terminal fragments
DCF	2'.7'-dichlorofluorescin
DCFDA	2',7'-dichlorofluorescin diacetate
DHA	dehydroascorbic acid
DNA	Deoxyribonucleic acid
ELISA	Enzyme linked immuno sorbent assay
ETC	Electron transport chain
FBS	Foetal bovine serum

GAPDH	Glyceraldehyde-3-phosphate
GCS	γ–glutamylcystine synthetase
GDNF	Glial cell line-derived neurotophic factor
GFR	Growth factor receptor
GPX	Glutathione peroxidase
GRD	Glutathione reductase
GSH	Glutathione, reduced form
GSSG	Glutathione, oxidised form
GST	Glutathione transferase
H_2O_2	Hydrogen peroxide
HOCI	Hypochlorous acid
HS	Horse serum
KPI	Kunitz protein inhibitor
MtDNA	Mitochondrial DNA
MTT	3-(4,5-dimethylthiazol-2-yl)-2,5-diphenyltetrazolium
NAC	N-acetyl L-cysteine
NADPH	Nicotinamide adenine dinucleotide phosphate, reduced form
NFT	Neurofibrillary tangle
NGF	Nerve growth factor
NO	Nitric oxide
NOS	Nitricoxide synthetase
NTF	Neurotrophic factor
OS	Oxidative stress
PCR	Polymerase chain reaction
PD	Parkinson's disease

PI	Propidium iodide
RA	Retinoic acid
ROS	Reactive oxygen species
RT-PCR	Reverse transcription-polymerase chain reaction
SOD	Superoxide
SP	Senile plaque
TBARS	Thiobarbituric acid-reactive substance
TRX	Thioredoxin
US	United States of America

CONTENTS PAGE

FIGURES and TABLES

Chapter One – Introduction

CHAPTER ONE

INTRODUCTION

1.1 FREE RADICALS

1.1.1 What is a free radical?

In a stable molecule, pairs of electrons normally occupy orbitals surrounding the nucleus of atoms. If an orbital in the outer shell of a molecule loses an electron from a pair, the molecule becomes a radical, which is unstable and, therefore highly reactive. The radical, more commonly called a free radical, may then react with any other nearby molecule, converting that molecule to another free radical, which can then initiate another reaction, a chain reaction (Mason, 1995). A newly formed radical must either then react with another free radical, eliminating the unpaired electrons, or react with a free radical scavenger – a chain breaking or primary antioxidant, to become unreactive (Nordberg and Arnér, 2001). The respective half lives of some of the biologically relevant ROS are tabulated in Table 1.1.

Reactive oxygen species	**Half Life (T½)**
Hydrogen peroxide (H_2O_2)	Minutes
Organic hydroperoxides	
Hypohalous acids e.g. HOCl	
Nitric oxide (NO•)	Milliseconds
Peroxy nitrite (OONO-)	
Superoxide anion (O_2•-)	Microseconds
Singlet oxygen($^1O_2$•)	
Alkoxyl radical	
Hydroxyl radical (•OH)	Nanoseconds

Table 1.1 Half lives of radical species adapted from Kehrer, 2000.

Free radicals are capable of severely damaging cells either through reactivity with another radical or directly. Intracellular free radicals, i.e., free low molecular weight

molecules with an unpaired electron, are often oxygen derived. The term reactive oxygen species (ROS) is used to encompass oxygen derived species that are not only radicals, but also molecules, which have potent oxidising capacity.

Free oxygen radicals may be defined as any chemical species capable of independent existence that contains one or more unpaired electrons. Common free oxygen radicals include the hydroxyl radical (·OH), nitric oxide (NO·) and the superoxide anion (O_2·-). Non-radical ROS include molecules such as hydrogen peroxide (H_2O_2). Each of these ROS is capable of damaging most cellular constituents, either directly, or though reaction with other cellular constituents to produce new ROS. (Shackelford *et al.*, 2000).

Radical generation is a natural consequence of living in an oxidising environment. Cells generate small amounts of free radicals and other oxidants while performing their normal metabolic functions. Reactive products of oxygen are amongst the most potent and omnipresent threats faced by any living organism. O_2•- and H_2O_2 are released from mitochondria during adenosine-5-triphosphate (ATP) synthesis and haemoglobin during oxygen transport. Certain or specific enzymes also employ radicals for molecular synthesis; these include lipoxygenase, cyclooxygenase, tyrosine hydroxylase, nitric oxide synthase, and ribonucleoside reductase. However, these enzymes undergo a limited number of cycles before the protein matrix is damaged. The radical species generated after the destruction of these enzymes can initiate free radical oxidation in other parts of the cell (Thomas, 2000).

Radical species may perturb the cells natural antioxidant defence systems, resulting in damage to all of the major classes of biological macromolecules, including nucleic acids, proteins, carbohydrates and lipids (Chandra *et al.*, 2000).

1.1.2 Reactions of radicals

Reactions of radicals with non-radicals have a special feature and that is amplification of the consequences of the initiating event by a chain reaction. This happens because a reaction of a radical with a non-radical always forms another radical. An example is the oxidation of sulphite to sulphate, which can be initiated by $O_2^{\bullet -}$, thousands of sulphites can be oxidised per $O_2^{\bullet -}$ introduced, the chain of reactions are shown in reactions 1-4.

$SO_3^{2-} + O_2^{\bullet -} + 2H^+ \longleftrightarrow SO_3^{-\bullet} + H_2O_2$ (Reaction 1) **Initiation**

$SO_3^{-\bullet} + O_2 \longleftrightarrow SO_5^{-\bullet}$ (Reaction 2)

$SO_5^{-\bullet} + SO_3^{2-} \longleftrightarrow SO_5^{2-} + SO_3^{-\bullet}$ (Reaction 3)

Chain Propagation

$SO_5^{2-} + H_2O \longleftrightarrow SO_4^{2-} + H_2O_2$ (Reaction 4) **Chain termination**

(Formation of stable products)

The sulphur trioxy anion radical produced by reaction 1 and the sulphur pentoxy anion radical produced by reaction 2 are strong oxidants capable of oxidizing amines or alcohols, which act as antioxidants (AOX) because the radicals produced by their oxidation are not reactive enough to propagate the chain oxidation of sulphite. A chain mechanism similarly occurs during the oxidation of the polyunsaturated lipids, which are abundant in cell membranes, and this amplifies the damage caused by the initiating event (Fridovich, 1998).

1.1.3 Generation of ROS/ Biological oxidation states of oxygen

The reduction of O_2 to $2H_2O$ requires four electrons. Hence, intermediates are produced on this univalent pathway, these are O_2-•, H_2O_2 and ·OH. The step-wise reduction of molecular oxygen via single-electron transfers, connecting the ROS molecules is summarised in figure 1.1. It is these intermediates that are responsible for the toxicity of O_2, and defences against that toxicity must include minimising their production to the maximum extent possible and eliminating those whose production cannot be avoided (Thannickal & Fanburg, 2000; Markesberry & Carney, 1999). Most of the O_2 consumed by respiring cells is reduced by cytochrome c oxidase, which, by virtue of two ferrihaemes and two Cu(II) prosthetic groups, manages the four electron reduction of O_2 to $2H_2O$ without releasing intermediates. In addition, there are enzymes that reduce O_2 to H_2O_2, and there are both enzymic and spontaneous processes within cells that produce O_2-• (Fridovich, 1998).

Figure 1.1 Diagrammatic representation of the step wise reduction of molecular oxygen (Nordberg & Arnér, 2001).

1.1.4 Superoxide

The superoxide anion (O_2•-) is formed when molecular oxygen acquires an additional electron as shown in figure 1.1. It is the primary free radical in most oxygenated biological systems (Dean *et al.*, 1997).

$$O_2 + e^- \longrightarrow O_2^{\bullet-} \quad \text{(Reaction 5)}$$

$O_2^{\bullet-}$ is considerably less reactive than •OH, however, it is still quite capable of damaging DNA, and paradoxically is therefore potentially more damaging. Thus, OH• will react indiscriminately, perhaps acting on something expendable, within a very small radius of its site of generation, whereas $O_2^{\bullet-}$ can diffuse a considerable distance before it encounters a suitable, and possible critical target (Fridovich, 1998). $O_2^{\bullet-}$ is fairly abundant and approximately 2% of the oxygen consumed by cells is converted into $O_2^{\bullet-}$ (Shackelford *et al.*, 2000). It, however, lacks the ability to penetrate lipid membranes and is therefore enclosed in the compartment where it is produced. The formation of $O_2^{\bullet-}$ takes place spontaneously, especially in the electron rich aerobic environment in the vicinity of the inner mitochondrial membrane within the respiratory chain. It appears to do most of its damage through the production of •OH via the Haber-Weiss reactions as shown in reactions 9a and 9b. $O_2^{\bullet-}$ is also produced endogenously by flavoenzymes (Nordberg & Arnér, 2001).

1.1.5 Hydrogen peroxide

Hydrogen peroxide (H_2O_2) is produced by a variety of intracellular reactions, particularly oxidative electron transport in the mitochondria. One of the reactions occurs when the $O_2^{\bullet-}$ acquires an additional electron forming the hydroperoxyl radical, which then couples with another hydroperoxyl radical as shown in reaction 6. It appears to play a role in normal metabolism and is required for a number of cellular events such as thyroid hormone biosynthesis. By itself, H_2O_2 is relatively nonreactive toward biomolecules. Most of the H_2O_2 mediated molecular damage is due to the production of •OH via events such as the Haber Weiss reactions as shown in reactions 9a and 9b (Shackelford *et al.*, 2000).

Although H_2O_2 is not a free radical, it is nonetheless highly important because of its ability to penetrate biological membranes. H_2O_2 is widely regarded as a cytotoxic agent whose levels must be minimised by the action of AOX defence enzymes. In fact, H_2O_2 is poorly reactive in the absence of transition metal ions. Exposure of certain human tissues to H_2O_2 may be greater than is commonly supposed: substantial amounts of H_2O_2 can be present in common beverages (especially instant coffee), in freshly voided human urine, and in exhaled air. Levels of H_2O_2 in the human body may be controlled not only by catabolism but also by excretion, therefore under certain conditions it might be a valuable biomarker of oxidative stress (OS) (Halliwell *et al.*, 2000). H_2O_2 also plays a radical forming role as an intermediate in the production of more reactive ROS molecules including HOCl (hypochlorous acid) as shown in reaction 7, by the action of myeloperoxidase, an enzyme present in the phagosomes of neutrophils; and •OH, either by exposure to UV (Reaction 8) or the Haber-Weiss reactions (Reactions 9a and 9b).

(Halliwell *et al.*, 2000; Nordberg & Arnér, 2001).

1.1.6 Hydroxyl radical

The hydroxyl radical (•OH) is an extraordinary reactive oxidant, which attacks most organic compounds, it has been shown to react rapidly with DNA causing over 100 different types of DNA modifications (Blakely *et al.*, 1990). It can be produced by the reduction of H_2O_2 by metal cations such as Fe(II) or Cu(I). In the original paper published by Haber and Weiss in 1934 they discussed the need for a metal ion catalyst and illustrated that the net reaction created the hydroxyl radical. This can be broken

down into two chemical reactions as shown in reactions 9a and b. Although other transition metal ions are capable of catalysing this reaction, the iron-catalysed Haber-Weiss reaction, which makes use of Fenton chemistry as shown in reactions 10-13, is now considered by most groups to be the major mechanism by which the highly reactive •OH is generated in biological systems and can cause lipid peroxidation and cell injury (Kehrer, 2000).

O_2- + $Me^{(n)+}$ ⟷ O_2 + $Me^{(n-1)+}$ (Reaction 9a)

$Me^{(n-1)+}$ + H_2O_2 ⟶ $Me^{(n)+}$ + OH- + HO• (Reaction 9b)

} **Haber-Weiss Reaction**

$Fe(II) + HOOH \rightleftharpoons (Fe\text{-}OOH)^+ + H^+$ (Reaction 10)

$(Fe\text{-}OOH)^+ \rightleftharpoons (FeO)^{2+} + OH^-$ (Reaction 11)

$(FeO)^{2+} + H^+ \rightleftharpoons (Fe\text{-}OH)^{3+}$ (Reaction 12)

$(Fe\text{-}OH)^{3+} \rightleftharpoons Fe(III) + HO•$ (Reaction 13)

•OH is a very energetic, short-lived and toxic oxygen species. Some researchers suggest that the toxicity of H_2O_2 and O_2•-radicals may be due to their conversion to the •OH (Ackworth & Bailey, 1995). The •OH produced reacts rapidly with almost every cellular macromolecule including DNA, lipids, and proteins and produces functional as well as structural alterations in these biomolecules (Jang & Surh, 2001).

1.1.7 Singlet oxygen

Another form of active oxygen, singlet oxygen ($^1O_2$•), can be generated by sensitisation of molecules such as riboflavin and its derivatives flavin adenine dinucleotide and flavin mononucleotide, chlorophyll a and b, bilirubin, retinal, different porphyrins. $^1O_2$•

can also be generated during phagocytosis and by spontaneous dismutation of O_2•- (Matés & Sánchez-Jiménez, 2000).

1.1.8 Nitric oxide

Nitric oxide (NO•) is a reactive and unstable free radical gas that can cross cell membranes easily by diffusion without depending on any release or uptake mechanisms. NO• is generated from a guanido nitrogen of L-arginine by at least 3 distinct isoforms of NO•synthase (NOS) encoded by 3 distinct genes (Chandra *et al.*, 2000). NO• appears to damage biomolecules reacting with O_2•- to produce the peroxynitrite radical, which is similar in reactivity to •OH and readily damages biomolecules (Shackelford *et al.*, 2000). It is this damage to DNA, protein and lipids that makes the ROS so dangerous; especially if the body's natural defences are compromised (Ackworth & Bailey, 1995).

1.1.9 Biological sources of ROS

Oxidative insults emanating from within the cell can threaten homeostasis if they are not appropriately resolved. Mitochondria actively and continuously generate ROS during respiration, favouring a situation of mitochondrial OS. The electron transport chain (ETC) is an essential mechanism for generation of cellular energy and is localised to the mitochondrial inner membrane. Auto-oxidation of reduced respiratory chain components cause the production of free radical intermediates, O_2•- and H_2O_2, which is in the presence of iron can produce •OH. In the cytosol, the arachadonic acid cascade, yielding prostaglandins, and leukotrienes may generate ROS when the released lipid is metabolised, and some cytochrome P-450 isozymes are notorious O_2•- producers. Also, the auto oxidation reactions of ascorbic acid (AA), low molecular weight thiols,

adrenalin, and flavin coenzymes can cause ROS production. Other oxygen radicals with different sources of production and sites of action can also be deleterious to the cell such as NADPH oxidase and the endoplasmic reticulum (Chandra *et al.*, 2000).

The major ROS are tabulated in table 1.2 along with their metabolism. When there is an excessive production of ROS in the absence of adequate protection, OS can ensue.

ROS Molecule	Main cellular sources of production	Enzymatic defence systems	Product(s)
Superoxide ($O_2^{\bullet-}$)	'Leakage' of electrons from the ETC Activated phagocytes Xanthine oxidase Flavoenzymes	SOD Superoxide reductase (in some bacteria)	$H_2O_2 + O_2$ H_2O_2
Hydrogen peroxide (H_2O_2)	From $O_2^{\bullet-}$ via SOD NADPH-oxidase (neutrophils) Glucose oxidase Xanthine oxidase	GPX CAT PRX	$H_2O + GSSG$ $H_2O + O_2$ H_2O
Hydroxyl radical (•OH)	From $O_2^{\bullet-}$ and H_2O_2 via reduced transition metal ions (Fe or Cu)		
Nitric oxide (NO·)	Nitric oxide synthases	Glutathione-GRD/ Trx-TrxR	GSNO

Table 1.2 The Major ROS and their metabolism adapted from Nordberg & Arnér (2001). SOD – superoxide dismutase, GPX – glutathione peroxidase, CAT – catalase, PRX – peroxidase, GRD – glutathione reductase, Trx - thioredoxin and TrxR – thioredoxin reductase.

In addition to the production of endogenous free radicals, the body is exposed to many external sources of free radicals such as cigarette smoke and pollution e.g. nitrogen dioxide. Several drugs can also be metabolised to generate toxic products (e.g. nitrofurantoin, penicillamine and phenylbutazone) (Mason, 1995).

Figure 1.2 shows the generation of further ROS and the defence mechanisms against damage by active oxygen.

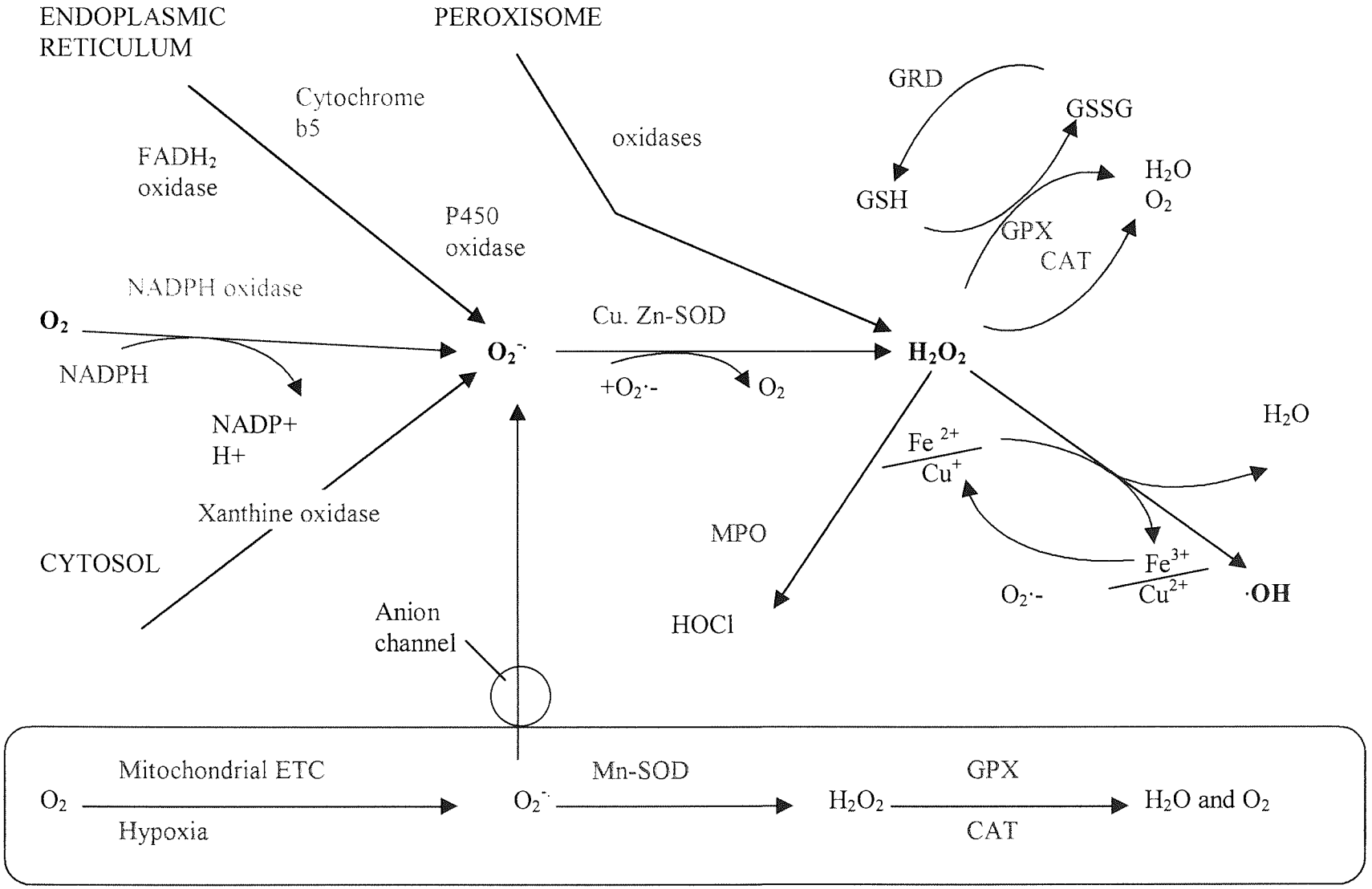

Figure 1.2 Generalised overview of the generation of reactive oxygen species and the defence mechanisms against damage by active oxygen. MPO=myeloperoxidase; GRD=glutathione reductase, CAT=catalase, GPX=glutathione peroxidase, SOD=superoxide dismutase

1.1.10 DNA damage

The presence of oxidised DNA bases is often used as a marker for ROS-mediated DNA damage (Helbock *et al.*, 1999). Oxidative damage to DNA is usually the result of DNA interaction with •OH. It is important to remember that while oxidised DNA bases always exist at some basal levels, if they occur at critical sites, or are not quickly repaired, oxidised purines (adenine and guanine) or pyrmidines (thymine and cytosine) can cause functional problems (Klaunig *et al.*, 1998). There are a multitude of modifications made by the •OH which can attack the deoxyribose moiety leading to the release of free bases from DNA and generates strand breaks. The other important target are the bases, with the resultant cross linking causing addition or elimination reactions. It has been estimated that endogenous ROS can result in about 200,000 base lesions per cell per day. DNA damage can lead to effects such as block of DNA modifications in hydrogen bonding, a decreased fidelity of DNA and/or RNA polymerase, conformational changes in the DNA template, and DNA replication. The guanine base is particularly sensitive to oxidation making this a reasonable biomarker for oxidative injury (Kehrer, 2000). Therefore 8-hydroxyguanine is a marker of OS in DNA, both in nuclear and in mitochondrial DNA (nDNA and mtDNA). An example of a DNA base lesion is shown in figure 1.3. Guanine normally pairs with cytosine during DNA replication, however the mutation to 8-hydroxyguanine causes the base to pair with adenine, resulting in a G ⟶ T mutation in the daughter strand of DNA.

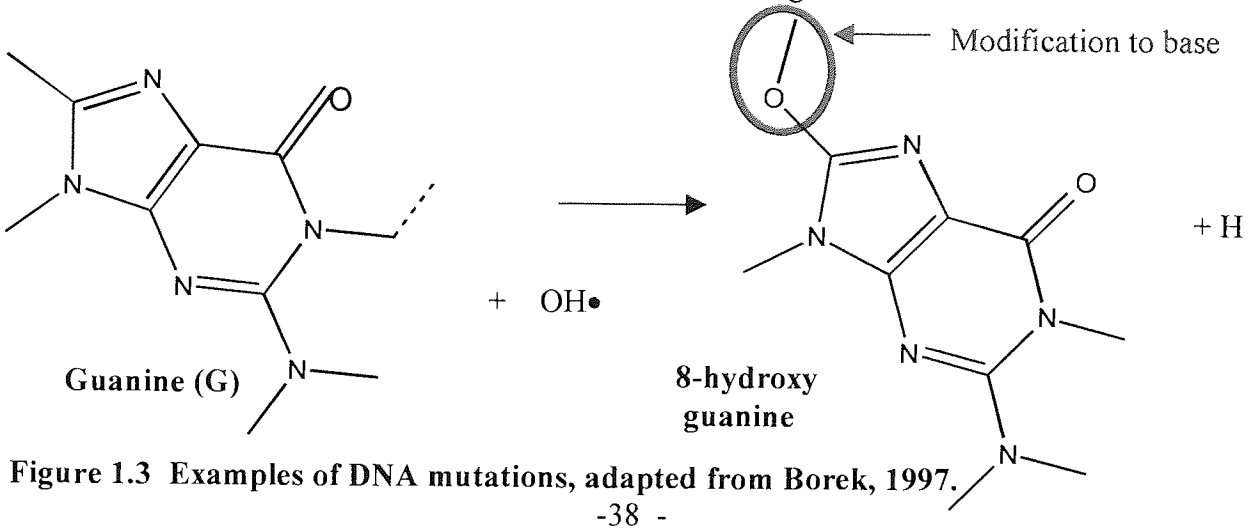

Figure 1.3 Examples of DNA mutations, adapted from Borek, 1997.

8-hydroxyguanine has been reported to be promutagenic, and oxidative base damage to DNA has been widely postulated to be a major contributory factor in the development of some degenerative diseases such as cancer and also natural aging. The oxidative damage is always most marked in mtDNA than in nDNA due to the large amount of ROS produced in mitochondria, the absence of bound histones and it has also been postulated that mitochondria may be deficient in certain repair mechanisms compared to the whole cell (Zastawny *et al.*, 1998).

1.1.11 Lipid damage

Lipids have a critical structural and functional role in membranes; any disruption of this role can lead to cell death. The double bonds in polyunsaturated fatty acids are ready targets for ROS attack. The abstraction of a hydrogen atom from one of these double bonds, which can be mediated by ROS, yields a new radical species that can readily interact with the diradical, O_2. The resultant lipid peroxyl radical can abstract a hydrogen atom from another fatty acid yielding another radical and a lipid hydroperoxide, thereby establishing a chain reaction. The lipid hydroperoxide formed is unstable and can decompose to various species including malondialdehyde, or it can be reduced to the more stable alcohol form. The lipid bilayer itself may also become more permeable thereby disrupting ion homeostasis. In addition, some of the oxidized fatty acid species that are formed such as the isoprostanes or the hydroperoxides have biologic activity in terms of an ability to affect signalling pathways including those that regulate the apoptotic form of cell death (Kehrer, 2000). A schematic figure shows the above events in Figure 1.4.

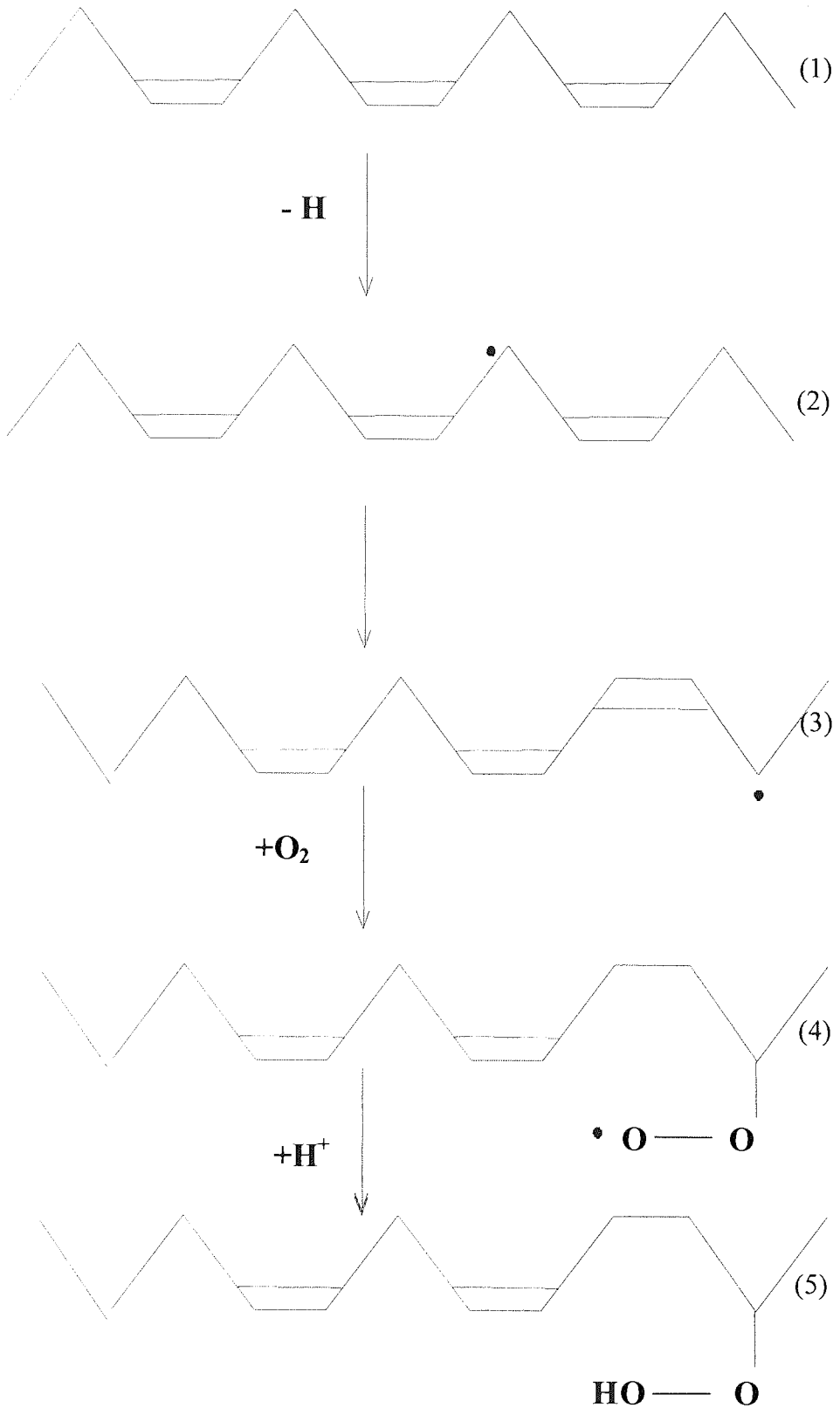

Figure 1.4 Schematic representation of ROS induced lipid damage in polyunsaturated fatty acid

1.1.12 Protein damage

Proteins constitute more than 50% of the dry weight of cells, and as such can be considered important targets for the effects of oxidising species (Griffiths, 2000). The oxidation of proteins by ROS can also generate a range of stable as well as reactive products, as these reactions progress, ion channels may be affected, membrane transport proteins or enzymes may be inactivated. Oxidised protein and amino acids components that have been found to be oxidised in biological systems are listed in Table 1.3.

Multiple reactions cause the introduction of carbonyl groups into proteins, and the measurement of protein carbonyl provides an integrated assessment of the burden borne by the cell as a consequence of OS. At least one out of every three proteins in the cell of older animals carries a carbonyl group and those modified proteins are likely dysfunctional either as enzymes or structural proteins. Normally oxidised proteins are degraded by proteosomal apparatus, but this declines in activity with age. Thus the level of dysfunctional proteins is sufficiently high that they are not simply markers of aging, but when observed may be the actual cause of the changes of aging (Levine & Stadtman, 2001).

Also products such as amino acid hydroperoxides can generate additional radicals when they interact with transition metals. The formation of oxidised moieties as listed in table 1.3 can alter protein functions, but this is often not quantitatively significant because of the sheer number of each type of protein. Although most oxidised proteins that are functionally inactive are rapidly removed, some can gradually accumulate with time and thereby contribute to the damage associated with aging as well as various diseases including diabetes, atherosclerosis and neurodegenerative diseases (Kehrer,

2000). The generalised mechanism of formation of protein carbonyls is shown in figure 1.5.

Oxidised protein and amino acids found in biological systems
2-Oxohistidine
3-Chlorotyrosine
3-Nitrotyrosine
5-Hydroxy-2-aminovaleric acid
Aminomalonic acid
Dimers of hydroxylated amino acids
DOPA
Hydro(pero)xyleucine
Hydro(pero)xyvalines
N-Formylkynurenine; kynurenine
o- and *m*-tyrosine
p-Hydroxyphenylacetaldehyde
Methionine sulphoxide
Nitrosothiols
Protein carbonyls

Table 1.3 Oxidised protein and amino acids found in biological systems, adapted from (Dean *et al.*, 1997)

1.2 ANTIOXIDANTS

Cellular antioxidants (AOXs) act in concert to detoxify ROS, being substances that either directly or indirectly protect cells against adverse effects of xenobiotics, drugs, carcinogens and toxic radical reactions (Halliwell *et al.*, 2000; Mates & Sanchez-Jimenez, 2000). Each ROS has a specific AOX, (Pitchumoni & Doraiswamy, 1998) with the toxicity of free radicals produced during normal cell metabolism being prevented by the naturally occurring protective AOX systems (Panet *et al.*, 2001).

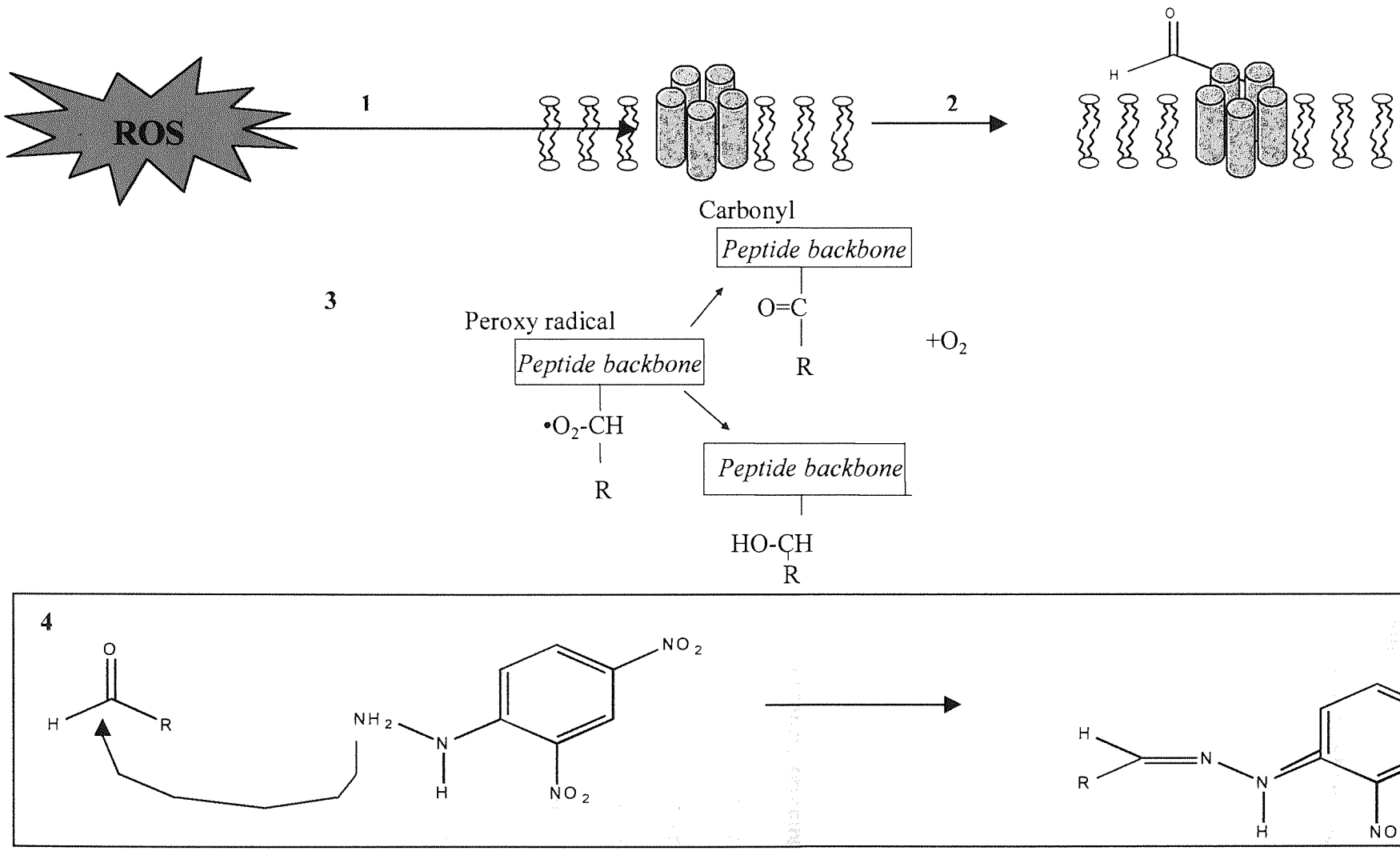

Figure 1.5 Formation and detection of protein carbonyls.
Reaction 1: ROS interact with membrane proteins and lipids
Reaction 3: Carbonyl formation

Taken from Butterfield *et al.*, 2001
Reaction 2: Introduction of protein carbonyls in an oxidised protein
Reaction 4: Reaction of protein carbonyls with 2,4-dinitrophenylhydrazine to form the protein bound hydrazone that is subsequently detected using spectroscopic or immunochemical means

Antioxidation includes all of the processes that slow down or stop free radical oxidation. Antioxidation processes include:

1) scavenging radicals to prevent their propagation
2) enzymatic hydrolysis of ester bonds to remove peroxidised fatty acids from lipids
3) sequestration of transitional metal ions
4) enzyme-catalysed reduction of peroxides.

Process 1 defines how an AOX can work, and the other three processes do not stop the reactions of radicals, instead, they prevent the accumulation of molecules that can promote free radical reactions (Thomas, 2000).

Various AOX systems have evolved to offer protection against ROS and to prevent damage to vital biological structures, including lipid membranes, proteins and DNA (Mason, 1995). The two important defence mechanisms that have been developed are (1) a thiol reducing buffer consisting of small proteins with redox-active sulphydryl moieties (e.g. glutathione (GSH) and thioredoxin (TRX)), and enzymatic systems (e.g. superoxide (SOD), catalase (CAT), glutathione peroxidase (GPX), glutathione reductase (GRD) and thioredoxin reductase (TRD)) (Davis *et al.*, 2001). Several biologically important compounds have also been reported to have AOX functions. These include vitamin C (AA), vitamin E (α-tocopherol), vitamin A derivatives, principally carotenoids such as β-carotene, and metallothionein, polyamines, melatonin, NADPH, adenosine, coenzyme Q-10, urate, ubiquinol, polyphenols, flavonoids, phytoestrogens, cysteine, homocysteine, taurine and methionine (Matés, 2000; Rice, 2000; Cassarino & Bennett, Jr, 1999; Halliwell, 1999; Ames, 1998; Benzi & Moretti, 1995; Frei, 1994).

The various AOX either scavenge O_2•- and ROS or stimulate the detoxification mechanisms within cells resulting in increased detoxification of free radical formation.

Specifically, SOD destroys O_2•- by converting it to peroxide that can in turn be destroyed by CAT or GPX reactions. A low level of O_2•- is constantly generated by aerobic respiration, O_2•- reduces Fe(III) to Fe(II), releasing iron from storage sites so that it can react with H_2O_2 and produce •OH (Matés, 2000). In humans, there are three forms of SOD: cytosolic Cu, Zn-SOD, mitochondrial Mn-SOD, and extracellular Cu-, Zn- SOD (Majima *et al.,* 1998). At a SOD concentration of approximately 10^{-5} mol/l and when O_2•- is at 10^{-10} mol/l, an O_2•- is 10^5 times more likely to encounter a molecule of SOD then it is to encounter another O_2•- (Fridovich, 1998). It is a strong catalyst and is ubiquitous, even though the uncatalysed dismutation of O_2•- is already a fast reaction (10^7/M/sec) under physiological conditions (Khan & Kasha., 1994). Interestingly, insertion of the cytosolic enzyme into mitochondria can protect cells lacking Mn-SOD from OS-induced apoptosis, suggesting that localisation supersedes differences between the SOD species (Wong, 1995).

CAT is one of the most efficient AOX enzymes, so much so that it cannot be saturated by H_2O_2 at any concentration (Lledias *et al.,* 1998). It reacts with H_2O_2 to form water and molecular oxygen as shown in reaction 15. It also reacts with hydrogen donors such as methanol and ethanol in a peroxidase manner (Matés, 2000). It also works with GPX to detoxify H_2O_2 as shown in figure 1.19. GPX, the principal peroxidase in mammals, specifically catalyses the reduction of alkyl hydroperoxides (ROOH) to the corresponding alcohols, and also acts on H_2O_2 using glutathione (GSH), thereby

protecting mammalian cells against oxidative damage, GPX is further discussed in section 1.11 and chapter five.

$$O_2^{\bullet-} + O_2^{\bullet-} + 2H^+ \xrightarrow{SOD} H_2O_2 + O_2 \qquad \text{(Reaction 14)}$$

$$2H_2O_2 \xrightarrow{CAT} 2H_2O + O_2 \qquad \text{(Reaction 15)}$$

$$ROOH + AH_2 \xrightarrow{CAT} H_2O + ROH + A \qquad \text{(Reaction 16)}$$

$$ROOH + 2GSH \xrightarrow{GPX} ROH + GSSG + H_2O \qquad \text{(Reaction 17)}$$

The specific functions of some of the other AOXs are tabulated in table 1.4.

An imbalance in the generation of ROS and AOX enzymes have been reported to play roles in some human diseases including atherosclerosis, cancer, neurodegenerative diseases (Price *et al.*, 1998) and bronchial asthma (Beasley *et al.*, 1991).

ANTIOXIDANT	FUNCTION
Carotenoids (β-Carotene)	Scavenges the lipoperoxy radical and thereby interferes with lipid peroxidation
Coenzyme Q10	Prevents $O_2^{\bullet-}$ formation in mitochondria by accepting electrons
Vitamin C (Ascorbic Acid)	Acts as a powerful reducing agent. Blocks the creation of nitrosamines by reducing nitrates
Vitamin E (α-tocopherol)	Protects against lipid peroxidation

Table 1.4 Specific functions of selected antioxidants, adapted from Pitchumoni & Doraiswamy, (1998).

1.3 OXIDATIVE STRESS

Oxidative stress (OS) is the result of excessive production of ROS, where there is a disturbance in the prooxidant-antioxidant balance in favour of the former (Sies, 1985).

It refers to the mismatched redox equilibrium between the production of ROS and the ability of the cell to defend against them. OS thus occurs when the production of ROS increases, scavenging of ROS or repair of oxidatively damaged macromolecules decreases, or both (Jang & Surh, 2001).

ROS readily react with cellular macromolecules, either damaging them directly or setting in motion a chain reaction wherein the free radical is passed from one macromolecule to another, resulting in extensive damage to cellular structures such as membranes. This paradoxical need for an ultimately toxic oxygen species must have been presented a major hurdle during the earliest stages of aerobic evolution. In order to exploit O_2 as a terminal electron acceptor for respiration energy production, early life forms had to simultaneously develop an effective defensive system to cope with an unwanted toxic ROS. This latter requirement took the form of an elaborate arsenal of antioxidants which function in concert to either: scavenge and detoxify ROS (such as SOD, CAT, GSH, GPX, GRD, TRX and TRD, block free radical chain reactions (examples include tocopherol, carotenoids and AA) or sequester transition metals which can serve as a ready source of free electrons (examples include lactoferrin, caeruloplasmin, and transferrin) (Buttke & Sandstrom, 1994).

Cells react rapidly to redox imbalance with a plethora of biological responses, including cell cycle-specific growth arrest, gene transcription, initiation of signal transduction pathways and repair of damaged DNA. These early events are likely to determine whether a cell will necrose, senesce, apoptose or survive and proliferate (Limoli *et al.*, 1998).

1.4 ASCORBIC ACID

The organic molecule L- *threo*-hexenon-1,4-lactone is commonly known as L-ascorbic acid (AA), or vitamin C, it is a well known reducing agent that is involved in several types of protective mechanism (Potters *et al.*, 2002). The interactions of AA with GSH are shown in figure 1.22. The brain contains much higher concentrations of AA (1-2mM), than in peripheral blood (0.02 – 0.08mM) suggesting that AA plays an important role in the CNS (Si *et al.*, 1998).

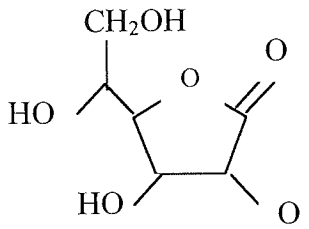

Figure 1.6a The chemical structure of ascorbic acid.

AA generally functions as an AOX by directly reacting with ROS and has a vital role in defences against OS, however, it also has pro-oxidant properties (Puskas *et al.*, 2000). AA has potent pro-oxidant activity in the presence of metal ions, where it acts as a reducing agent to provide catalysts for the Fenton reaction. Thus, low concentrations of AA enhance oxygen radical activity whilst high concentrations scavenge ·OH, $^1O_2$· and lipid peroxides (Griffiths & Lunec, 2001). It is also essential in the human diet for prevention of scurvy and other metabolic roles including collagen assembly and reduction of iron to aid intestinal absorption of iron.

AA can by oxidised by most ROS that are currently thought to contribute to tissue injury in several human diseases, included those implicated in AD. AA converts the ROS into poorly reactive AA derived products. The redox behaviour of AA ia associated with the enediol structure at C-2 and C-3. AA is utilised in the cell as an electron donor, and the first AA oxidation product is the semi quinone-like free radical

monodehydroascorbate (MDHA). Due to the highly delocalised free electron, MDHA radicals do not readily interact with other molecules, and are therefore generally considered to be less destructive. MDHA disproportionates spontaneously to AA or dehydroascorbate (DHA) (Potters *et al.*, 2002). The regeneration cycle of AA is shown in figure 1.6b.

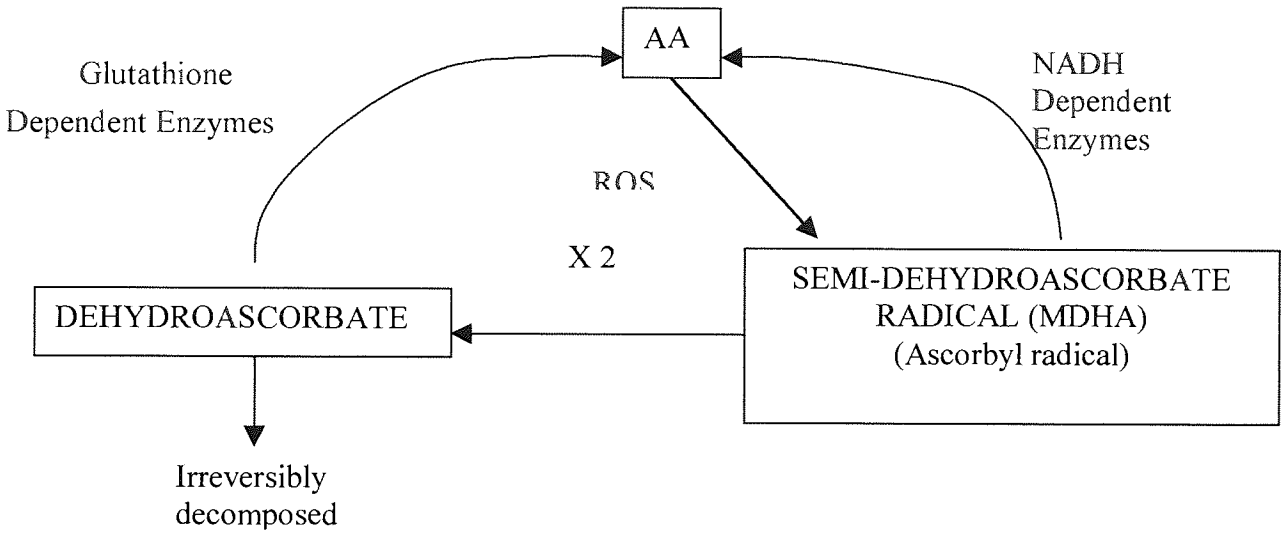

Figure 1.6b The regeneration cycle of ascorbic acid, adapted from Halliwell, 1999.

1.5 MITOCHONDRIA

Mitochondria -'the power houses' of the aerobic cell are composed of the two membranes that create two compartments, the matrix and the intermembrane space, each having unique activities. The matrix contains hundreds of types of enzymes including those involved in the fatty acid and pyrurate (both of which must be imported from the cytoplasm) oxidation cycles that yield acetyl CoA, the essential initial substrate of the citric acid cycle. The inner membrane is the site of the respiratory chain, the ATP – generating ATP synthase complex, and the function of a variety of proteins that regulate metabolite transport into the matrix (Gershon, 1999).

The ETC as a whole serves to oxidise NADH, with oxygen serving as the trial electron acceptor (respiration). The complexity of the ETC (complexes I, II, III, IV) is designed

to make use of the considerable free energy released from the oxidation of NADH. This energy is used to synthesize ATP, the 'energy currency' of the cell – a process referred to as oxidative phosphorylation (Scheffler, 2001). The ETC, present in the inner mitochandrial membrane, is comprised of more than 70 polypeptide components which are grouped into four (five) enzyme complexes (complexes I, II, III, IV), ATP synthase is sometimes known as complex V (Heales et al.,1999).

More than 90% of the oxygen consumed by aerobic living organisms, undergoes a concerted tetravalent reduction to produce water in a reaction catalysed by complex IV in the mitochondrial electron transport chain (ETC), as previously shown in figure 1.1 (Cadenas & Davies, 2000). The overall reaction is shown in reaction 18:

$$O_2 + 4e^- + 4H^+ \longrightarrow 2H_2O \qquad \text{(Reaction 18)}$$

A schematic diagram of the five major mitochondrial electron transport complexes are shown in figure 1.7. They are vulnerable to OS because of the high production of $O_2^{\cdot -}$ as a by-product of the ETC. In addition to these toxic ETC reactions of the inner mitochondrial membrane, the mitochondrial outer membrane enzyme monoamine oxidase catalyses the oxidative deamination of biogenic amines and is a quantitatively large source of H_2O_2 that contributes to an increase in the steady state concentrations of ROS within both the mitochondrial matrix and cytosol (Cadenas & Davies, 2000). Such damage is encountered in the DNA, lipid and protein components, the close proximity of mtDNA to this source of ROS probably accounts for the greater degree of oxidative damage (Gershon, 1999; Shackelford *et al.*, 2000). Recently however, mitochondria have been found to play an intimate role in a number of other cellular processes in addition to ATP production (Sherer *et al.*, 2001), including participating in a number of cellular signalling pathways (Biswas *et al.*, 1999).

It is becoming clear that subtle functional alterations in these essential cellular energy dynamos can lead to insidious pathological changes in cells. Impaired electron transport, in turn, in addition to the obvious impairment in cellular ATP production, also leads to diversion of electrons from their normal ETC recipients and further formation of damaging ROS. However, each of the complexes of the ETC exert varying degrees of control over respiration and substantial loss of activity of an individual respitatory chain complex may be returned before ATP synthesis is comprised (Darey and Clark 1996). As the AOX enzymes are generally relatively deficient in the brain (Marcus *et al.*, 1998; Reiter, 1995), a vicious cycle of increasing OS may slowly damage neurons over a period of years, leading to the eventual neuronal cell death characteristic of the sporadic, age-related neurodegenerative diseases – 'The mitochondrial theory of aging'. Damage to the mtDNA results in an enhanced rate of mutagenesis. The mutated genome expresses defective respiratory chain subunits, which are incorporated into the respiratory enzyme complexes leading to the generation of more ROS and more damage to mtDNA in an ever increasing cycle of destruction (Lightowlers *et al.*, 1999).

ROS are produced along the mitochondrial electron chain. At complex I, O_2 is converted to $O_2^{\bullet-}$ by the donation of an electron from NADH dehydrogenase. $O_2^{\bullet-}$ and/or H_2O_2 can also be formed following the autoxidation of reduced ubiquinone at Complex II (Succinate-coenzyme Q) and/ or Complex III (coenzyme QH_2-cytochrome c reductases) sites. Direct effects of oxidants have also been reported on mitochondrial respiratory chain enzymes. Glucocorticoids have been shown to inhibit cytochrome c oxidase activity by a direct action on the respiratory chain, by modulating cytochrome c oxidative activity (Complex IV) (Simon *et al.*, 1998).

MtDNA is especially susceptible to OS and mutation because it lacks protective histones, is close to the ROS producing systems, and is subject to a highly reducing environment in the mitochondrial matrix, supported by a high concentration of GSH (Cadenas & Davies, 2000). Mitochondria are often classed as the 'Achilles Heal' of the aerobic cell, and mitrochondrial breakdown could be the common aetiologic thread in most (if not all) GSH deficiency states. Healthy mitochondria avidly conserve their glutathione (GSH), but as cytoplasmic GSH levels decrease, mitochondrial GSH can fall below a critical threshold. The turning point in the face of sustained oxidative challenge, is that mitochondrial GSH becomes depleted. The membrane associated enzymes that transport GSH into the mitochondria then sustain damage, and GSH import is dealt a fatal blow. As a consequence, the mitrochondria become casualities of their own endogenously generated free radicals. Indeed, levels of OS in mtDNA are several times higher than those in nDNA and the former mutates several times more frequently than the latter (Camougrand & Rigoulet, 2001).

The inheritance of late onset neurodegenerative diseases, such as AD and Parkinson's disease (PD), appears to be sporadic. However, biochemical evidence has accumulated that the mitochondrial ETC is defective in these diseases. Specifically, NADH: ubiquinone oxidoreductase, or complex I, of the ETC is defective in PD; cytochrome c oxidase (COX), or complex IV, is defective in AD. These ETC defects may arise from mutated and oxidatively damaged mtDNA in sporadic PD and AD and may be the primary genetic basis of the sporadic forms of these diseases.

ETC defects can act as free radical generators by blocking the normal passage of electrons down the chain and their ultimate reduction of molecular oxygen to water.

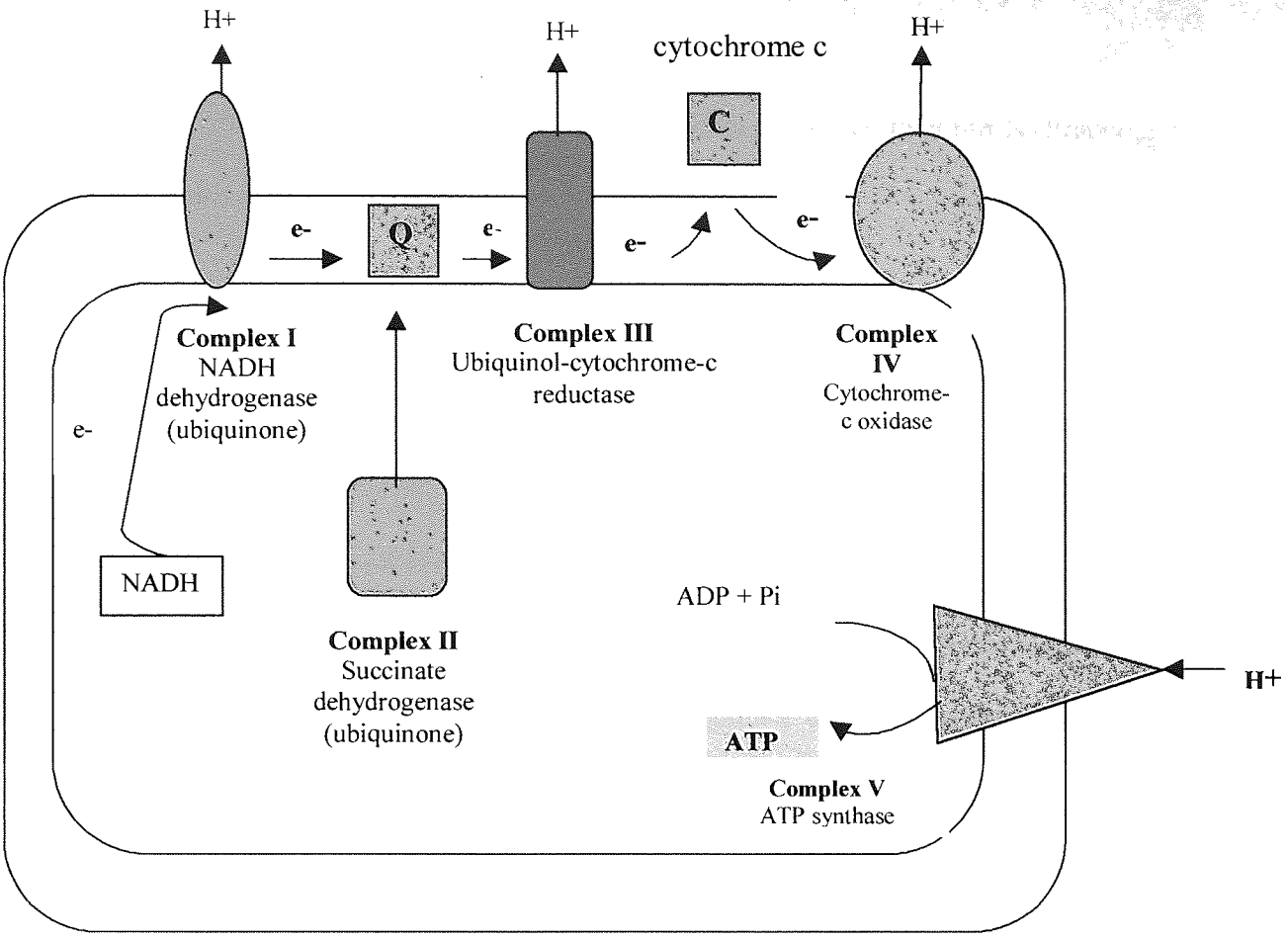

Figure 1.7 Schematic diagram of the five major mitochondrial electron transport complexes, each of which is composed of numerous subunits. A proton gradient generated by complexes I, III and IV is used by complex V to generate ATP from ADP. Adapted from Beal *et al.*, 1993.

Relevant to AD is the finding that the complex IV inhibitor, sodium azide, generates oxygen radicals both *in vitro* and *in vivo* and impairs the learning and memory in rats. There is a wealth of evidence for OS in the AD brain. Iron, which acts as a free-radical catalyst via the Fenton and Haber-Weiss reactions is elevated in the AD brain, especially in those regions that degenerate. In addition, Fe-binding proteins such as ferritin, transferrin, and melanotransferrin are elevated in AD brains, presumably as a compensatory response, hence those proteins may reduce Fe- catalysed free radical reactions (Cassarino and Bennett, Jr., 1999). Evidence has shown increased protein and lipid oxidation in AD brains compared to controls associated with increases in cell death. The oxidative damage to brain tissue manifests itself predominately as increases in lipid peroxidation, often measured are thiobarbituric acid reactive substances

(TBARS) and malondialdehyde (MDA) levels when compared to controls (Pratico, 2002; Smith *et al.*, 1998).

1.6 CELL DEATH

The cell death of neurons is induced by two mechanisms, necrosis or apoptosis, which are differentiated by morphological observation. Necrosis is induced by cellular injury, or the destruction of cell homeostasis. Cells swell, lyse and the intracellular contents spill into the extracellular space in an acute pathological process. Necrosis is followed by an inflammatory tissue reaction with the appearance of macrophages and activation of microglia in the brain. The major features of apoptosis and necrosis are stated in table 1.5.

	APOPTOSIS	NECROSIS
Stimuli	Physiologic and pathologic conditions	Physical changes, pH, hypoxia, ATP depletion
ATP requirement?	Yes	No
DNA	Intranucleosomal cleavage, (ladder formation)	Degeneration
Cell	Shrinkage	Swelling
Nucleus	Chromatin condensation, nuclear shrinkage (pyknosis), followed by nuclear fragmentation (karyorrhexis)	Chromatin clumping
Cytoplasm	Condensed apoptotic bodies	Hyperosinophilia
Plasma membrane	Intact, blebbed	Lysed
Cell integrity	Intact	Lost
Tissue reaction	No inflammation, Phagocytosis	Inflammation, Autolysis/Heterolysis

Table 1.5 Comparison of the major features of apoptosis and necrosis, adapted from Naoi *et al.*, (2000).

Figure 1.8 shows the sequence of ultra structural changes in apoptosis and necrosis. A normal cell is represented at 1. The process of necrosis is represented in 7 and 8, and the process of apoptosis is represented in 2, 3, 4, 5 and 6.

The occurrence of necrosis (7) is accompanied by clumping of chromatin without marked changes in its distribution, the appearance of dense bodies in the matrix of grossly swollen mitochondria, and focal disruption of membranes. At a later stage (8), organelles and membranes disintegrate, but the overall configuration of the cell is usually maintained. Early apoptosis is characterised in 2 by segmentation of the chromatin in sharply circumscribed masses that lie against the nuclear envelope, condensation of the cytoplasm, and convolution of the nuclear and cell outlines. In the next phase shown in 3, the nucleus fragments and the cell as a whole bud to produce membrane-bounded apoptotic bodies of varying size and structure, which are phagocytosed as shown in 4 by nearby cells and degraded within lysosomes as shown in 5. Finally the bodies are reduced to unrecognisable residues as shown in 6.

Figure 1.8 The sequence of ultra structural changes in apoptosis and necrosis. Taken from Harmon *et al.*, 1998.

1.7 APOPTOSIS

The term 'apoptosis' is derived from the Greek for falling away, this refers to cellular blebbing and subsequent apoptotic body formation, and was discovered by Carl Voigt in 1842 (Bowen *et al.*, 1998; Peter *et al.*, 1997). It is often seen as the opposite to

mitosis, however, it is only one of several modes of cell death (Bowen *et al.*, 1998). Apoptosis (or programmed cell death) is an active physiological cell death that controls cell populations during embryogenesis, immune response, hormone regulation, and normal tissue homeostasis (Esteve *et al.*, 1999). It is an orchestrated form of cell death, in which cells commit suicide for the greater good of the body (Joaquin & Gollapudi, 2001). Virtually all tissues harbour apoptotic cells at one time or another, examples include the lens of the eye which forms during embryonic development, it consists of apoptotic cells, that have replaced their innards with the clear protein crystallin; skin cells begin life in the deepest layers and then migrate to the surface, undergoing apoptosis along the way, the dead cells form the skin's protective outer layer (Duke *et al.*, 1996).

When apoptosis control fails there are two possible outcomes: diseases such as cancer and autoimmune diseases occur when there is too little apoptosis, and possible stroke damage or the neurodegeneration of AD when there is too much (Miller & Marx, 1998). Table 1.6 shows further disorders and diseases, which are related to changes in the levels of apoptosis.

Apoptosis, requires specialised machinery; the central component of this machinery is a proteolytic system involving a family of proteases called caspases. These enzymes participate in a cascade that is triggered in response to proapoptotic signals and culminates in cleavage of structural proteins and DNA resulting in disassembly of the cell (Thornberry & Lazebnik, 1998).

Disease associated with the inhibition of apoptosis	Disease associated with increased apoptosis
Malignancies	Multiple sclerosis
Autoimmune diseases including systemic lupus erythamtosis and rheumatoid arthritis	Neurodegenerative disorders
Many viral infections including herpes viruses and pox viruses	Bacterial infection
Chronic inflammation	Insulin-dependent diabetes mellitus
Lymphoma	AIDS and diGeorge syndrome
Leukaemia	Liver failure
Solid tumours	Tissue ischemic injury
	Cancers including melanoma & hepatoma
	Wilson's disease
	Aplastic anaemia

Table 1.6 Diseases and conditions associated with disregulation in apoptosis, adapted from Peter *et al.*, (1997) and Joaquin & Gollapudi, (2001).

Caspases are proteases, which contain a serine-rich region, composed of about 100 amino acids in the middle of protein and cleave peptides after an aspartic acid residue hence their name ***c***ysteinyl-***aspa***rtate-specific protea***ses***. Caspases are constitutively expressed and synthesized as inactive proenzymes, which are activated by cleavage at the specific aspartate cleavage site (Naoi *et al.*, 2000; Nicholson & Thornberry, 1997) to exert their roles. There are fourteen identified mammalian caspases that have been implicated in different aspects of cell death. Caspases are usually classed according to their function, either as upstream (initiator) caspases or downstream (effector) caspases. The proforms of upstream initiator caspases possess large N-terminal prodomains, which function as protein interaction molecules, allowing them to interact with various proteins that trigger caspase activation. In contrast, the proforms of downstream

(effector) caspases contain only short N-terminal prodomains, serving no apparent function. Downstream caspases are largely dependent on upstream caspases for their proteolytic processing and activation (Reed, 2000).

Caspases are activated by an extrinsic (death receptor signalling) or an intrinsic (death receptor independent/mitochondrial pathway involving cytochrome c as shown in figure 1.9). Whether cells die or survive depends largely on the interactions between the different modulators (Creagh & Martin, 2001; Joaquin & Gollapudi, 2001; Moriya *et al.*, 2000; Hengartner, 1998). Caspase-3 has a major role in apoptosis; when it is activated it in turn activates other executioner caspases and leads to the subsequent characteristic features of apoptosis, including the cleavage of fodrin and lamin, chromatin condensation, and nuclear fragmentation (Moriya *et al.*, 2000). The nuclear lamins part of the nuclear membrane component cause nuclear shrinking and blebbing. The expression of the cytoskeletal proteins fodrin and also gelsolin cause the loss of the overall cell shape. Caspase activated DNase cuts genomic DNA between the nucleosomes causing nuclear DNA fragmentation. However, caspase-3 inhibition has been shown to prevent H_2O_2-induced DNA fragmentation but was insufficient to prevent H_2O_2-mediated cell death in cell models (Jiang *et al.*, 2001). Caspase-3 and caspase-9 deficient mice have also been shown to exhibit increased brain size associated with decreased apoptosis (Kim *et al.*, 1999b). Therefore caspase-3 is a downstream caspase which has a role in apoptosis but the apoptotic cascade can proceed via an alternative pathway still culminating in cell death. Also the fact that a general caspase inhibitor (DEVD) was able to prevent cell death, as shown in figure 1.10 suggests that there may be other executioner caspases beside caspase-3 that act to execute cytotoxicity in H_2O_2 treated cells (Jiang *et al.*, 2001).

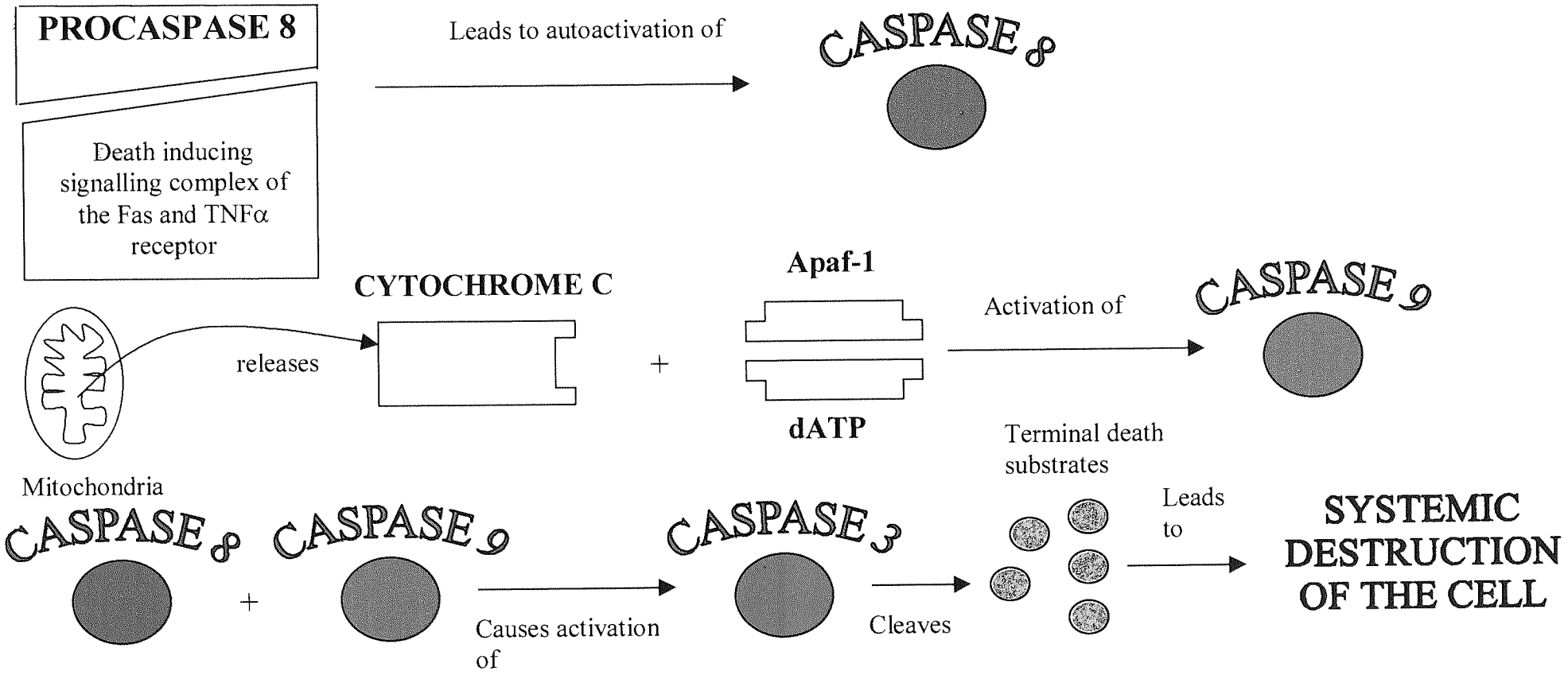

Figure 1.9 The relationship of caspases to cell death, adapted from Kim *et al.*, (1999b)

There are also several classes of proteins that act either as inhibitors or promoters of apoptosis: **Anti-Apoptosis modulators**

- Bcl-2, Bcl-xl – act by stabilising mitochondrial membrane

Pro-Apoptosis modulators

- Bax, Bad, Bim, Bid – act by destabilising mitochondrial membrane

(Joaquin & Gollapudi, 2001).

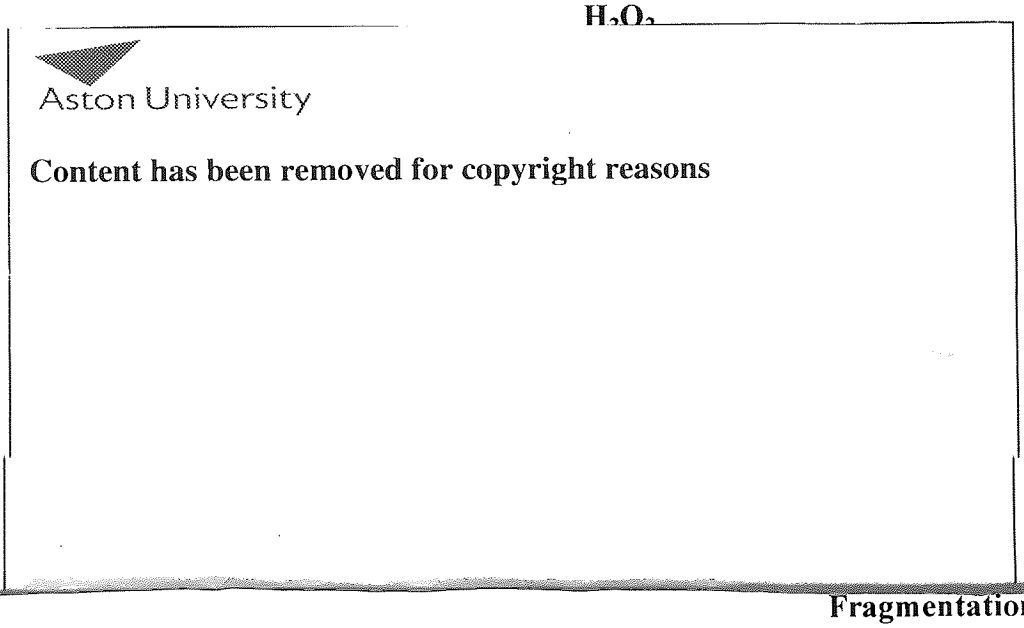

Figure 1.10 Possible caspase effects caused by H_2O_2 treatment of cells, from Jiang *et al.*, 2001.

The mitochondria-dependent pathway for apoptosis is governed by the Bcl-2 family of proteins. Bcl-2 family proteins are conserved throughout metazoan evolution, with homologues found in mammalian, avian, fish, and amphibian species, as well as in invertebrates such as *C. elegans*. Both pro-apoptotic and anti-apoptotic Bcl-2 family proteins exist and many of these proteins physically bond each other, forming a complex network of homo- and hetero-dimers. Bcl-2 protein is widely distributed in many parts of the CNS during embryonic development, but declines with age. In the PNS, neurons and supporting cells of sympathetic and sensory ganglia retain this protein throughout life (Sastry & Rao, 2000). The relative ratios of anti-and pro-

apoptotic Bcl-2 family proteins dictate the ultimate sensitivity or resistance of cells to various apoptotic stimuli, including growth factor deprivation, hypoxia and oxidants (Reed, 2000).

The gene product called bcl-2 first identified in human B-cell lymphomas, as a common translocation from its normal site on chromosome 18, to a region close to the immunoglobulin heavy chain promoter on chromosome 14. It is homologous to a negative regulator of cell death (ced-9) found in the nematode *Caenorhabditis elegans* (Slater *et al.,* 1995). In humans, 20 members of the Bcl-2 family gene family have been described to date. These genes encode the anti-apoptotic proteins, Bcl-2, Bcl-X_L, Mcl-1, Bfl-1, Bcl-W, and Boo (Diva) as well as the pro-apoptotic proteins Bax, Bak, Bok (Mtd), Bad, Bid, Bim, Bik and Bcl-X_S. Some of the Bcl-2 family genes produce two or more proteins through alternative mRNA splicing, sometimes exerting opposing effects on cell death regulation (e.g. Bcl-X_L versus Bcl-X_S) (Reed, 2000).

In spite of extensive research, the mechanism by which Bcl-2 blocks apoptosis remains elusive. However the fact that Bcl-2 is localised in the mitochondrial membrane has generated considerable scrutiny of the role of mitochondria play in facilitating aspects of apoptosis and Bcl-2's ability to block them at that site in the cell (Zamzami *et al.,* 1998). Hockenberry *et al.,* (1993) reported that Bcl-2 functioned in an AOX pathway to prevent apoptosis and so emerged the idea that ROS might be produced during apoptosis and mediate downstream events associated with the apoptotic process. The ROS could be suppressed by AOX present in the cell and, if Bcl-2 functioned in an AOX pathway, Bcl-2's inhibition of apoptosis could be explained on this basis. Furthermore, induction of apoptosis by ROS in neuronal cells can be suppressed by

Bcl-2 overexpression (Kane *et al.*, 1993).

Finally, transcription factors can be modulated by H_2O_2; nuclear translocation of p53 is caused by H_2O_2, (Uberti *et al.*, 1999) and the ubiquitous transcription factors, NF-κB and AP-1 are also activated by H_2O_2. Once activated, these transcription factors might drive transcription of pro-apoptotic genes or perhaps cause expression of inhibitors of survival-related proteins (Chandra *et al.*, 2000).

When considering whether OS and apoptosis are epiphenomenona or causal events in neuronal death, the following are important:

1. Oxygen radicals should be generated during the period of irreversible damage
2. Evidence of oxidative damage should be present
3. Free radicals should induce degeneration that appears to have identical characteristics
4. Free radical scavengers or inhibitors of processes generating oxygen radicals should prevent neuronal degeneration

(Bains & Shaw, 1997).

1.8 NEURODEGENERATION

Apoptosis may in fact serve a beneficial purpose in the mature brain by providing a controlled mechanism through which dysfunctional neuronal elements can be selectively removed without evoking inflammatory responses or the release of cellular products, which could endanger the surrounding network (Loo *et al.,* 1993).

The brain has a large oxidative capacity (in humans, the brain use approximately 20% of the oxygen used by the entire body and occupies 2% of the body weight), but its ability to combat OS is limited (Makar *et al.,* 1994). The brain is one of the most metabolically active organs of the body, and the amount of oxygen it uses varies with the degree of mental activity. Blood supplying the brain also contains glucose, the principal source of energy for brain cells. However, the CNS is also susceptible to oxidant damage due to low levels of AOX enzymes (Kitani *et al.,* 1999; Marcus *et al.,* 1998), high levels of free iron, which catalyse hydroxyl free radicals, and high concentrations of oxidisable substances such as catecholamines and peroxidizable fatty acids. Thus, oxidative damage to brain tissue manifests itself predominately as lipid peroxidation (Pratico, 2002). The further generation of ROS is highly toxic and results in neuronal degeneration (Pan & Perez-Polo, 1993).

A common pathological hallmark of various neurodegenerative disorders such as amyotrophic lateral sclerosis (ALS), AD and PD is the loss of particular subsets of neurons, further reviewed in section in 1.9. Neurodegeneration of those neural subsets maybe a consequence of various forms of neural cell death, e.g. necrosis and apoptosis. In turn, such forms of cell death maybe the result of a variety of cellular insults, including excitotoxicity and OS. Increasing age is the most reliable and robust risk

factor for susceptibility to neurodegenerative disease (Bains & Shaw, 1997). Lovell *et al.*, (1995) showed support for the concept that the brain in AD is under increased OS demonstrating lipid peroxidation changes in areas where degenerative changes occur. Further strong evidence suggesting that the pathogenesis of AD is as a result of oxidative damage includes:

1. Elevated levels of iron in AD brains
2. H_2O_2 mediated cytotoxic effect of amyloid β protein (Aβ)
3. Glutathione depletion
4. Damage to brain cellular macromolecules including lipids, proteins and DNA
5. Selective increases in lipid peroxidation

(Draczynska-Lusiak *et al.*, 1998; Good *et al.*, 1996).

1.9 ALZHEIMER'S DISEASE

Alzheimer's disease (AD) is the most common cause of age-related intellectual impairment occurring after the age of 60. It is a devastating degeneration, which accounts for half to two-thirds of all cases of late life intellectual failure in many developed countries where life expectancies are high and AD represents the fourth leading cause of death in the US, its' profound morbidity has a major socio-economic impact.

It is characterised by a progressive decline in cognitive function that correlates with a number of pathological changes in several different brain regions, one of the most prominent among the regions being the basal forebrain cholinergic neurons (BFCN) (Winkler *et al.*, 1998) Functionally, the disease causes synaptic and neuronal loss, which strongly correlates with the degree of cognitive impairment (Adamec *et*

al., 1999). Neuronal loss occurs in AD in the areas of the nucleus basalis of Meynert, locus coeruleus, hippocampus, amygdala and neocortical association areas. A loss of cholinergic neurones in the basal forebrain system is also a characteristic of AD (Connor *et al.*, 1996). An illustration of the human brain and the regions affected in the brains of AD patients is included as figure 1.11.

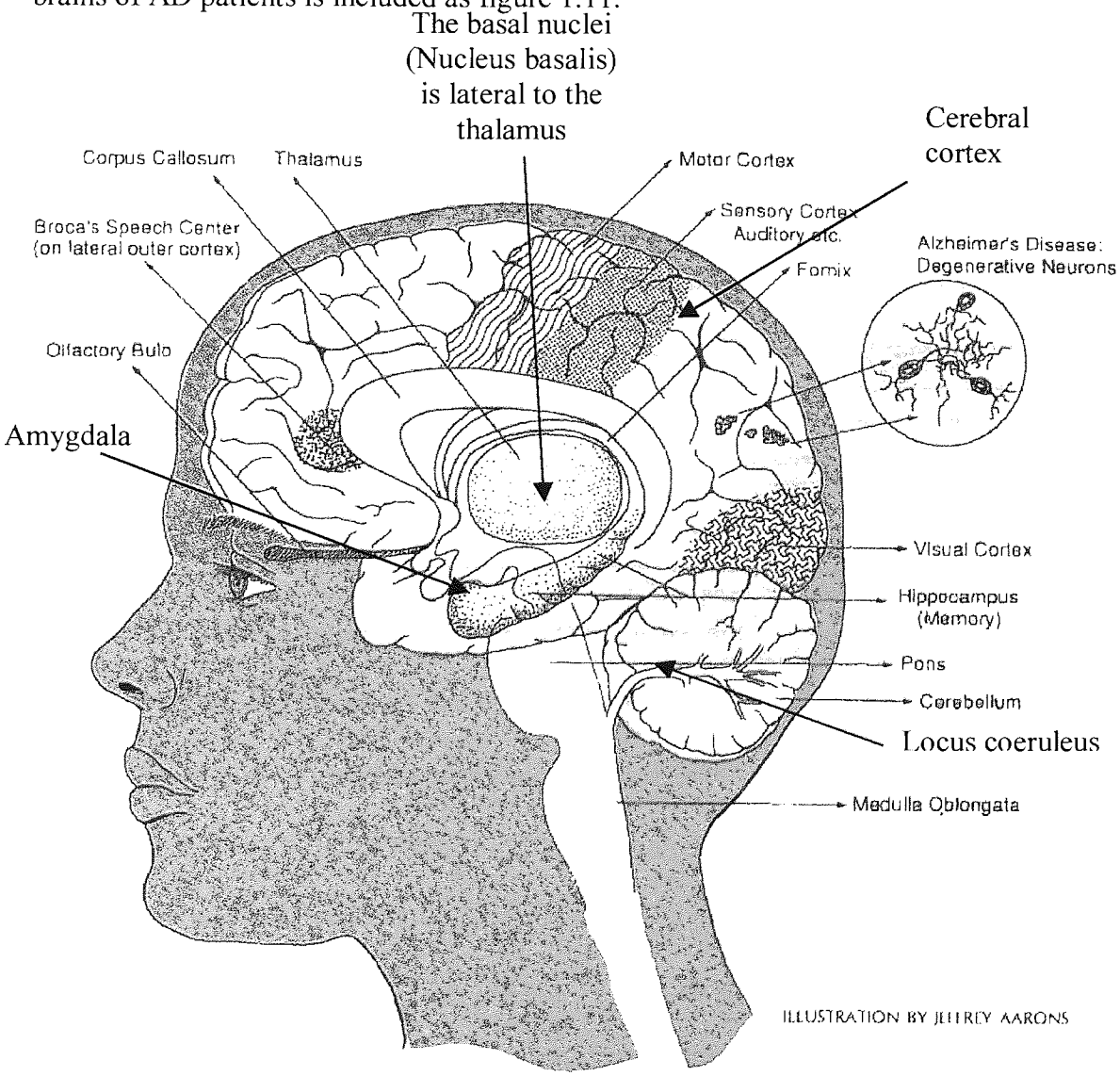

Figure 1.11 Diagram of the human brain and the occurrence of neuronal damage in the AD brain. Adapted from an illustration by Jeffrey Aarons

The disease is also characterised by neuropathological findings of neurofibrillary tangles (NFT) and senile plaques (SP). SPs are composed of a cluster of degenerative nerve terminals with a core that contains extracellular arrays of linear filaments characteristic of amyloid β protein (Adamec *et al.*, 1999).

The plaques consist of protein fibres, some 7-10nm thick, that are mixed with Aβ peptides. Mature plaques also contain degenerating nerve endings, and are surrounded by active astrocytes and microglia (de Strooper & König, 2001). NFTs inside neurons, are bundles of abnormal approximately 20nm cytoplasmic fibres derived from microtubule-associated tau proteins, which occur in both neuronal cell bodies (comprising NFTs) and in axons and dendrites referred to collectively as dystrophic neurites. The normal function of tau is probably to stabilise the microtubule network and the neuronal endoskeleton by site-specific phosphorylation and internal cellular transport mechanisms. In AD, brain tau is hyperphosphorylated microtubule-binding incompetent, and aggregates into paired helical filaments (PHFs) that form the NFTs (Mookherjee & Johnson, 2001).

Tau phosphorylation has been shown to be increased as a general outcome of apoptotic processes. It has been speculated that in AD brain apoptotic like processes contribute to the inappropriate expression of cell cycle kinases, and an outcome of this process is a pathological increase in tau phosphorylation (Nagy, 2000). In addition to AD, NFT are found in a number of other dementing neurodegenerative diseases, including Pick's disease and Parkinsonism linked to chromosome 17 (Spillantini & Goedert, 1998). No mutations have been detected in AD in the gene encoding tau on chromosome 17.

Presence of SPs together with numerous NFTs in the hippocampus, amygdala, cerebral cortex and certain other brain regions serves as the basis for a definitive pathological diagnosis of AD (Pascale & Etcheberrigaray, 1999; Selkoe, 1996; Wilcock & Harrold, 1996).

Fratiglioni (1996) has summarised the results of epidemiological research on the aetiology of AD, findings are tabulated in Table 1.7. Findings were divided into 3 categories:

1. Definite risk factors, in which the studies are numerous and findings are consistent
2. Possible risk factors, in which numerous studies have been performed, but results are inconsistent
3. Putative risk factors in which few studies have been conducted.

DEFINITE	POSSIBLE	PUTATIVE
- Age	- Head trauma	- Stressful life events
- Familial aggregation	- Thyroid disease	- Aluminium
- Apolipoprotein E gene, ε4 allele	- Advanced maternal age	- Alcohol
- Trisomy 21 (Down syndrome)	- Depression	- Manual work
	- Smoking (Protective)	- Anti-inflammatory drugs (Protective)
	- Illiteracy or low educational attainment	

Table 1.7 Epidemiological research on the aetiology of AD

The majority of AD cases are late in onset and show little or no genetic links; hence there are referred to as 'sporadic' (Cassarino & Bennett Jr, 1999). However, the aetiology is known in a minority of cases, where genetic abnormalities on 5 genes have been discovered, on chromosomes 1, 14, 19 and 21 (Hoyer, 1996) and recently chromosome 10q (Bertram *et al.*, 2000).

This is due to:

1. Polymorphism of the apolipoprotein (APOE) gene located on chromosome 19.
2. Mutations in the presenilin 1 and presenilin 2 genes located on chromosomes 14

This is due to:

1. Polymorphism of the apolipoprotein (APOE) gene located on chromosome 19.
2. Mutations in the presenilin 1 and presenilin 2 genes located on chromosomes 14 and 1 respectively, cause increased production of Aβ42 at age 40 and 50 (Ramassamy *et al.*, 1999)
3. Mutations in the APP gene located on chromosome 21
4. Dominant mutations on chromosome 10q have been recently located to have a positive linkage with late onset AD (Bertram *et al.*, 2000).

ApoE is a 37kDa protein, (Ramassamy *et al.*, 1999), its gene is located on chromosome 19, with the apoE4 polymorphism associated with an increased density of Aβ plaques and vascular deposits at age 60 and older (Selkoe, 1996). ApoE regulates plasma lipid transport and clearance by acting as a ligand for lipoprotein receptors. In the brain, apoE is predominately synthesized by astrocytes and its major physiological function seems to be the redistribution of lipids and the maintenance of cholesterol homeostasis (Hoy *et al.*, 2000). The apoE4 genotype is the major genetic risk factor for AD, with only two amino acid substitutions being responsible. In humans, apoE has 3 major isoforms apoE2, E3 and E4 which are the products of alleles differing from each other by a single mutation (Hoy *et al.*, 2000). People with two copies of the E4 allele are approximately ten times more likely to develop late-onset AD (Strittmatter *et al.*, 1993). People with E4 are also at greater risk for stroke and atherosclerosis, making E4 the most common risk factor yet described. There are, however, many people who have two copies of the E4 allele who are cognitively normal and at autopsy show no signs of AD pathology. Therefore E4 is a risk factor, not a causative factor, for late-onset AD (Fine, 1999; Selkoe, 1996). ApoE 3 is the most prevalent allele (Yankner, 1996). The

rare, but AD protective, apoE2 contains 2 cysteines at residues 112 and 158, the common apoE3 contains 1 cysteine at residue 112 and an arginine at residue 158,whereas apoE4, the risk factor for AD, contains no cysteine, both residues are arginines (Smith *et al.*,2000).

Some familial forms of AD arise from mutations in the amyloid precursor protein (APP); a large fraction of early-onset AD cases results from mutations in the presenilin genes that may be involved in APP processing and lead to deposition of excess amyloid β protein (Aβ). In the plasma and skin fibroblast culture media of humans bearing presenilin mutations linked to familial AD showed selective increases in $A\beta_{1-42}$ (Tomita *et* al., 1997; Scheuner *et al.,* 1996). Moreover persons with Down syndrome (trisomy 21) invariably develop the biochemical and neuropathological hallmarks of AD by their fourth decade of life, if they live sufficiently long, as APP is coded for chromosome 21 (Yamada & Nabeshima, 2000). These relatively rare genetic forms of AD together with the fact that all patients with Down syndrome show the neuropathology of AD in their 40s and 50s, provide strong evidence to support the amyloid hypothesis of AD, as there is an increase in the production of Aβ (Fine, 1999; Selkoe, 1996; Pollwein *et al.,* 1992). Finally, APP over expressing mice also exhibit at least some of the characteristics of AD, including OS (Yatin *et al.,* 1999a; Holscher, 1998). In another study, increased levels of $A\beta_{1-42}$ have been linked to a genetic contribution (chromosome 21) to Aβ generation in late onset-AD (Ertekin-Taher *et al., 2000).* A summary of current concepts of aetiological events underlying AD are listed in Table 1.8.

AETIOPATHOGENIC EVENTS IN ALZHEIMER'S DISEASE	
Primary events	Genetic factors
	Neuronal apoptosis
Secondary events	Protein aggregation
	β amyloid deposition
	Senile plaques
	Amyloid angiopathy
	Cytoskeletal changes
	NFT/paired helical filaments
	Tau protein hyperphosphorylation
	Synaptic loss
Tertiary events	Neurotransmitter deficits
	Neurotrophic alterations
	Neuroimmune dysfunction
	Neuroinflammatory reactions
Quaternary events	Excitotoxic reactions
	Changes in calcium metabolism
	Free radical formation
	Brain haemodynamics alterations
	Endothelial/cerebrovascular dysfunction

Table 1.8 Aetiopathogenic events in Alzheimer's disease, adapted from Cacabelos *et al.*, 1999.

There are several lines of evidence suggesting that Aβ plays a key role in the pathogenesis of AD. Current therapeutic approaches are based on enhancing neurotransmitter function, however, as table 1.8 indicates, an increase in understanding the mechanisms associated with AD can support the development of a breadth of novel pharmacological agents. These are summarised in table 1.9.

Pharmacological profile of novel compounds with potential anti-Alzheimer effects
Compounds acting on primary events
Regulators of AD-related genes
APP
APOE
Presenilins
Compounds acting on secondary events
Regulators of β-amyloid deposition
β-amyloid scavengers
Anti-proteolytic agents
Lysosomotropic agents
Regulators of cytoskeleton dysfunction
Cytoskeleton stabilisers
Anti-phosphorylating agents
MAP/tau regulators
Compounds acting on tertiary events
Neurotransmitter enhancers
Cholinergic
Monoaminergic
Neuropeptidergic
Aminoacidergic
Neurotrophic agents
Neuroimmunotrophins
Neuroimmunokinins
Anti-inflammatory agents
Chemokine regulators
Compounds acting on quaternary events
Inhibitors of exctitotoxic reactions
NMDA antagonists
Regulators of calcium homeostasis
Calcium channel blockers
Regulators of ROS
Free radical scavengers
Antioxidants
Antioxidant enzyme enhancers
Anti-peroxidating agents
Regulators of cerebrovascular function
Vasoactive agents
Vascular endotrophins

Table 1.9 Pharmacological profile of novel compounds with potential anti-Alzheimer effects, adapted from Cacabelos *et al.*, 1999.

1.10 AMYLOID β PEPTIDE

Amyloid β (Aβ) a 39-43 amino acid residue peptide is thought to be derived by proteolysis, from a much larger membrane spanning 110-130kDa β amyloid precursor protein (APP). Aβ was first isolated from the blood vessels of AD patients by Glenner & Wong, (1984), the amino acid sequence of Aβ peptide is shown in figure 1.12. Further breakdown of the amino acid sequence of Aβ peptide is shown in figure 1.13. Aβ is secreted constitutively by normal cells in culture and detected as a circulating peptide in the plasma and cerebrospinal fluid (CSF) of healthy humans and other mammals (Selkoe, 1998). It has been proposed to make a primary contribution to the pathogenesis of AD due to its toxicity, which has been observed both *in vitro* and *in vivo* (Xiao *et al.*, 1999).

The primary structure of APP closely resembles a cell surface receptor with a signal sequence, one large extramembranous N-terminal region, a single transmembrane domain and a small cytoplasmic C-terminal tail, as shown in Figure 1.14. Aβ represents only a small fragment of APP, therefore proteolytic processing of the precursor must be involved in Aβ generation. APPs have a number of important functions including the ability to bind metals and to inhibit a number of proteases (Fine, 1999). Mutations have been found in the APP gene. They include:

- **'Dutch'**

A missense mutation in the Aβ sequence with the glutamic acid base (E) changing to a glutamine (Q) base at residue 693. This mutation causes cerebral haemorrhages and death in victims.

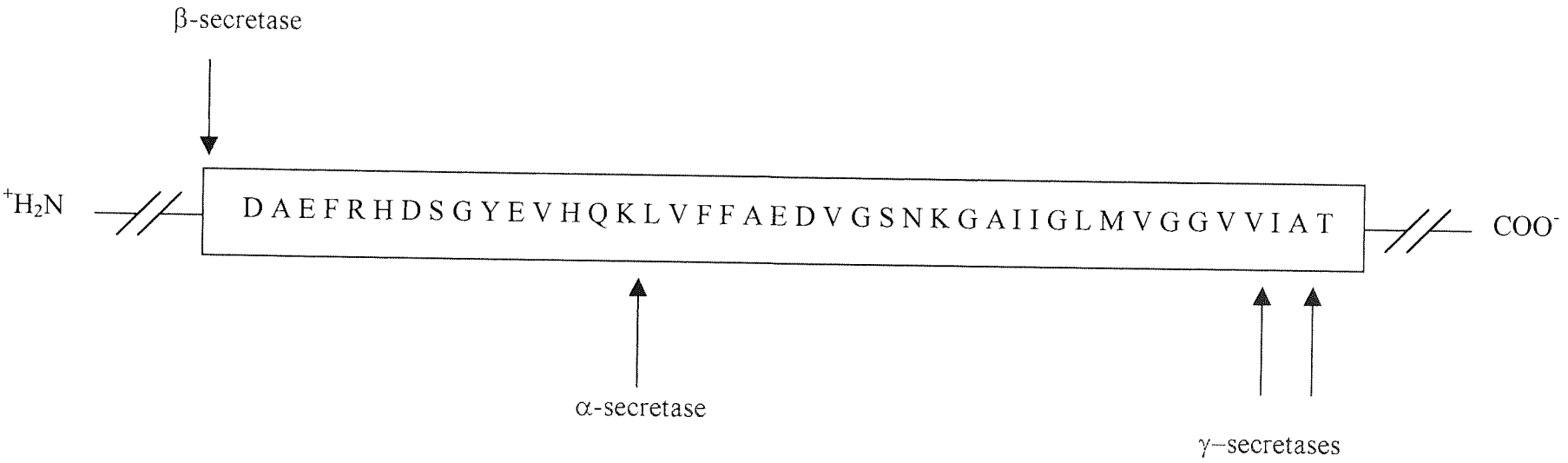

Figure 1.12 Amino acid sequence of amyloid β peptide (Aβ), showing α, β and γ secretase cleavage sites. Adapted from Allsop & Williams, (1994).

Aβ 1-42	**DAEFRHDSGYEVHHQKLVFFAEDVGSNKGAIIGLMVGGVVIA**	
Aβ 1-40	**DAEFRHDSGYEVHHQKLVFFAEDVGSNKGAIIGLMVGGVV**	
Aβ 25-35	(Neurotoxic domain)	**GSNKGAIIGLM**
Aβ 16-20	(Aggregation domain)	**KLVFF**
Aβ 18-20	(Amnesic domain)	**VFF**
Aβ 13-16	(Microglia activation domain)	**HHQK**
Aβ 31-34	(Cell surface-binding domain)	**IIGL**

Figure 1.13 Amino acid sequences of Aβ peptides. Adapted from Yamada & Nabeshima, 2000

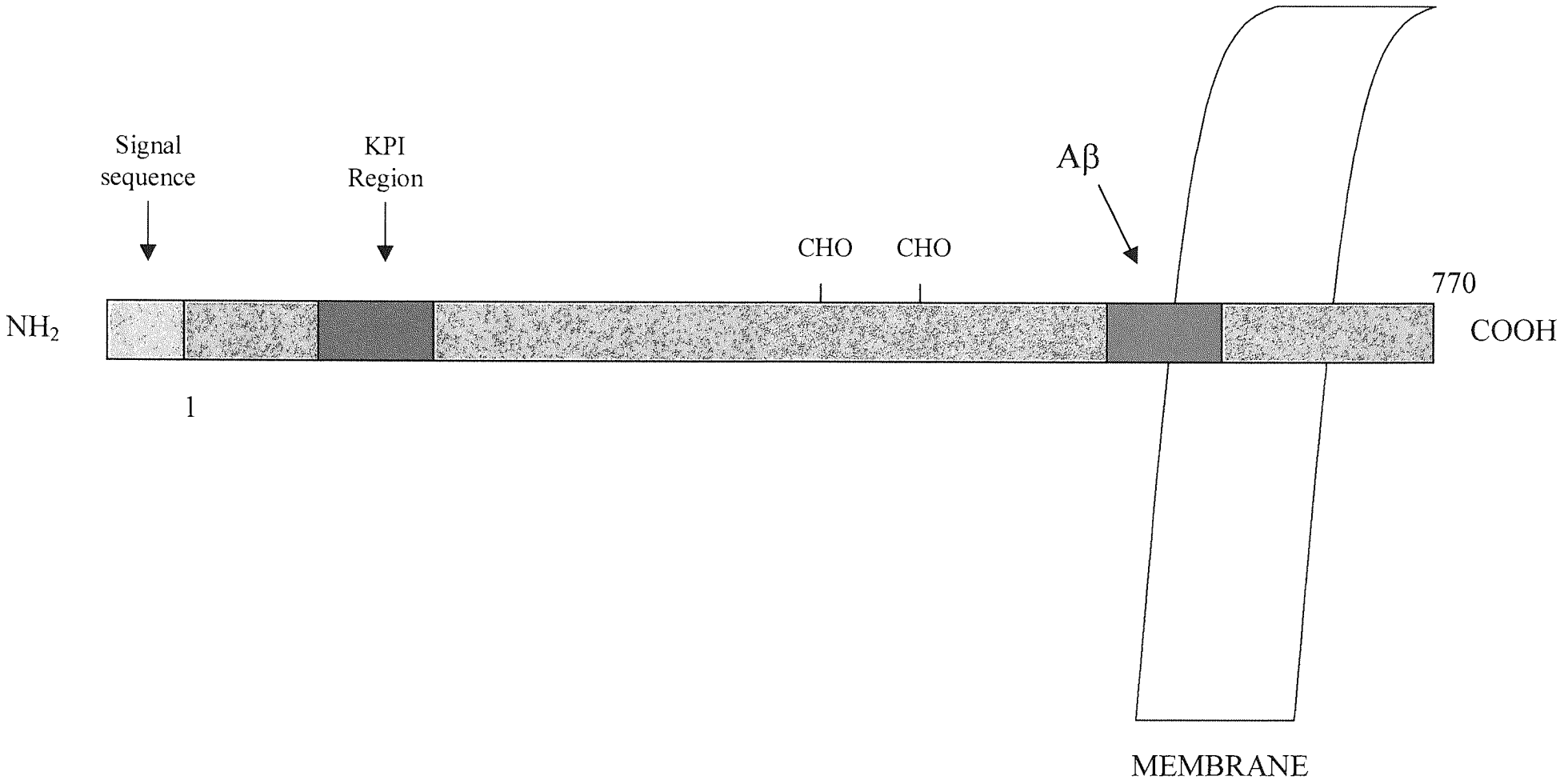

Figure 1.14 The structure of β-amyloid precursor protein (APP) adapted from Fine, (1999).

- **'Amino Acid 717'**

A missense mutation in APP with the valine (V) base at position 717 changing to either isoleucine, glycine or phenylalanine (I, G and F respectively). This mutation causes dominant early onset form of AD.

- **'Swedish – FAD 670/671'**

A double mutation in the amino acids adjacent to the beginning of the Aβ sequence with the lysine, methionine (KM) combination changing to asparagine leucine (NL). This mutation causes dominant early onset AD.

- **'CAA 692'**

A missense mutation in the Aβ sequence with the alanine base (A) changing to a glycine base.

Some of the mutations are shown in figure 1.15.

In normal APP processing there is constitutive proteolytic cleavage made by an unknown protease termed 'α-secretase' that enables secretion of the large soluble ectodomain of APP (APP_S-α) into the medium and retention of the 83 residue C-terminal fragment in the membrane. The C83 can undergo further cleavage by an unknown protesase(s) termed 'γ-secretase' at residue 711 or 713 to release the p3 peptide, as shown in figure 1.16. Alternatively proteolytic cleavage after residue 671 by an unknown enzyme(s) termed 'β-secretase' that results in the secretion of the slightly truncated APP_S-β molecule and the retention of a 99-residue C-terminal fragment. The C99 fragment can also undergo cleavage by 'γ-secretase' to release the Aβ peptides as shown in Figure 1.17. The site of cleavage by γ-secretase is either at 711 or 713, where $Aβ_{40}$ or $Aβ_{42}$ respectively, are produced . Whilst, precise quantitation is not available, it

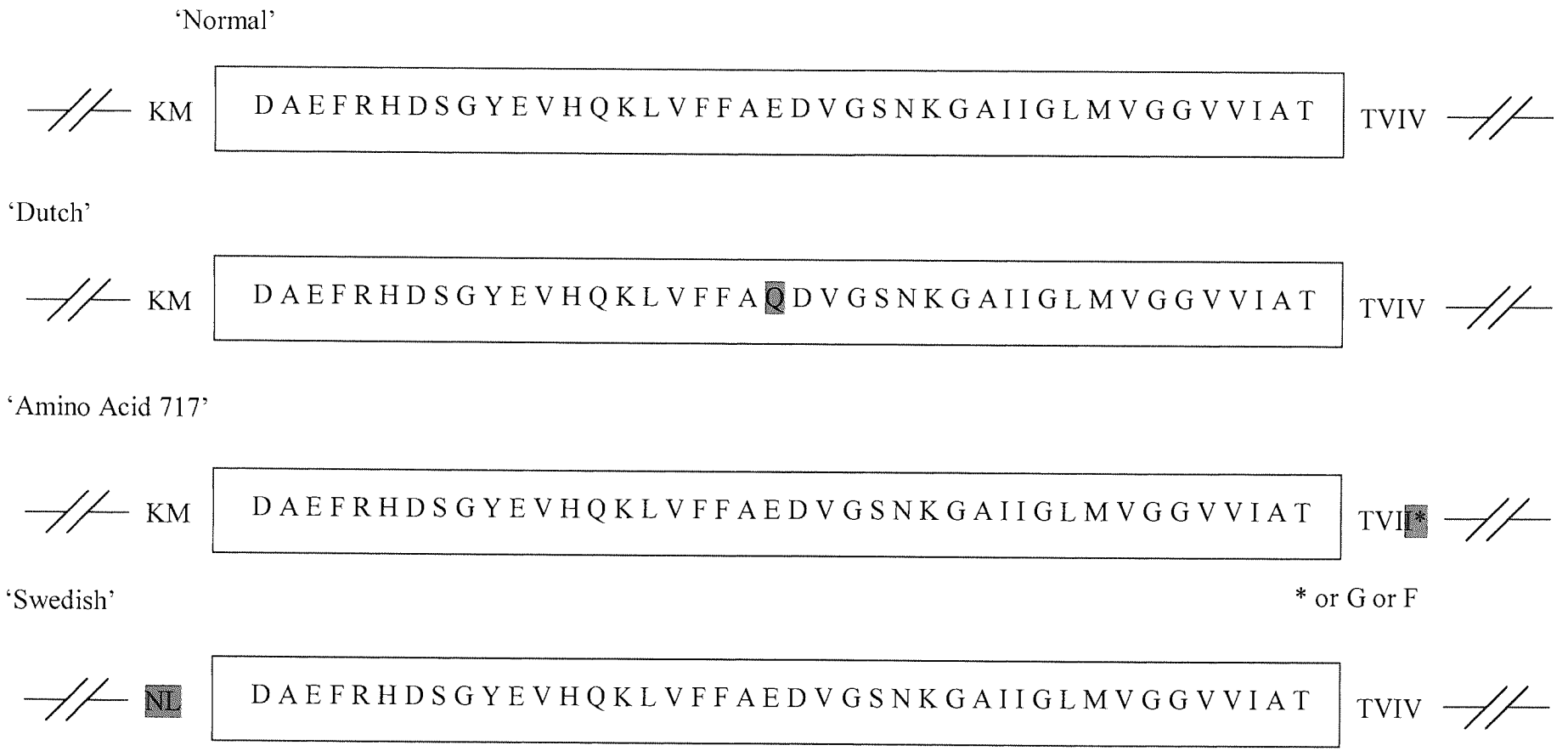

Figure 1.15 Mutations found in the APP gene. Amino acids changes are highlighted in red.

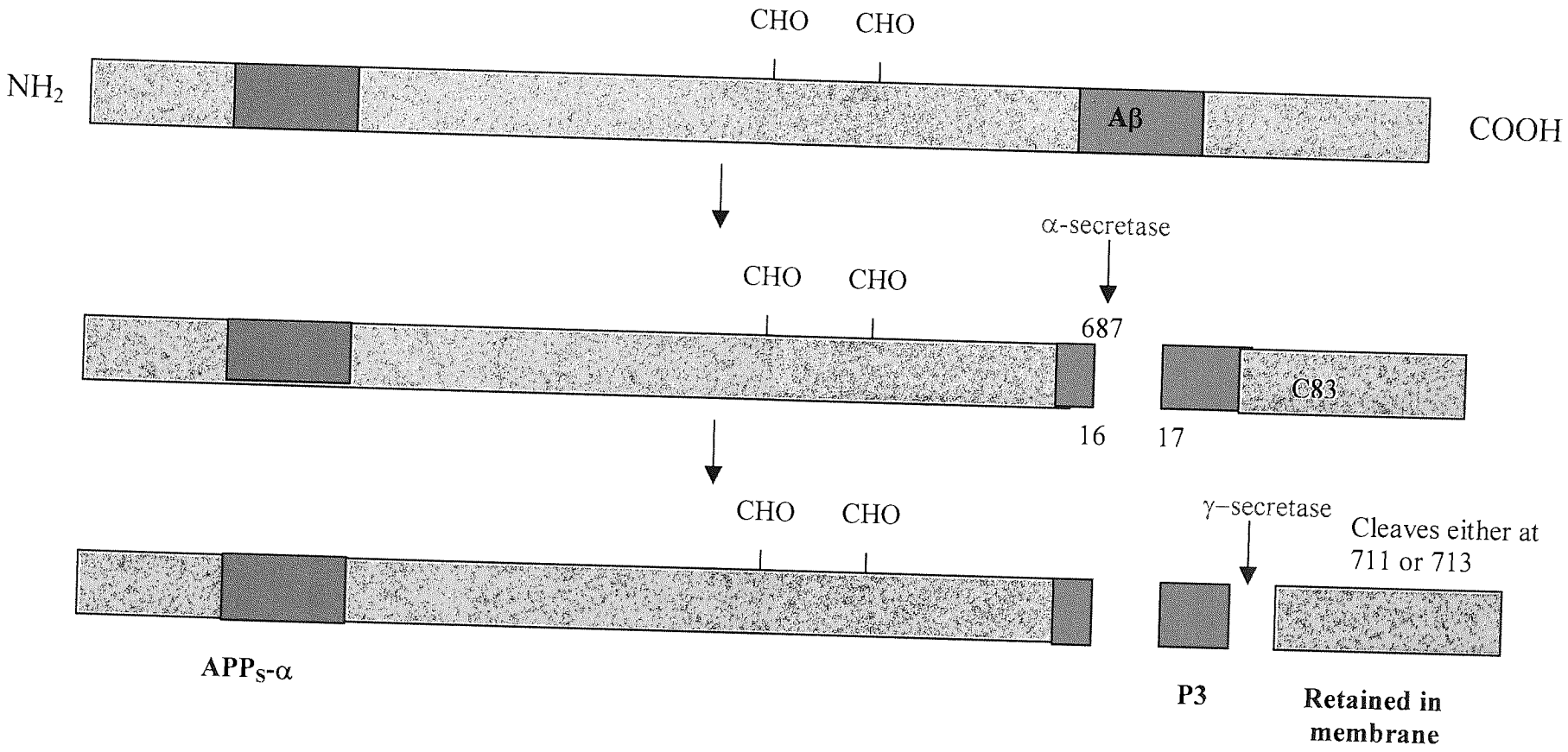

Figure 1.16 'Normal' APP processing

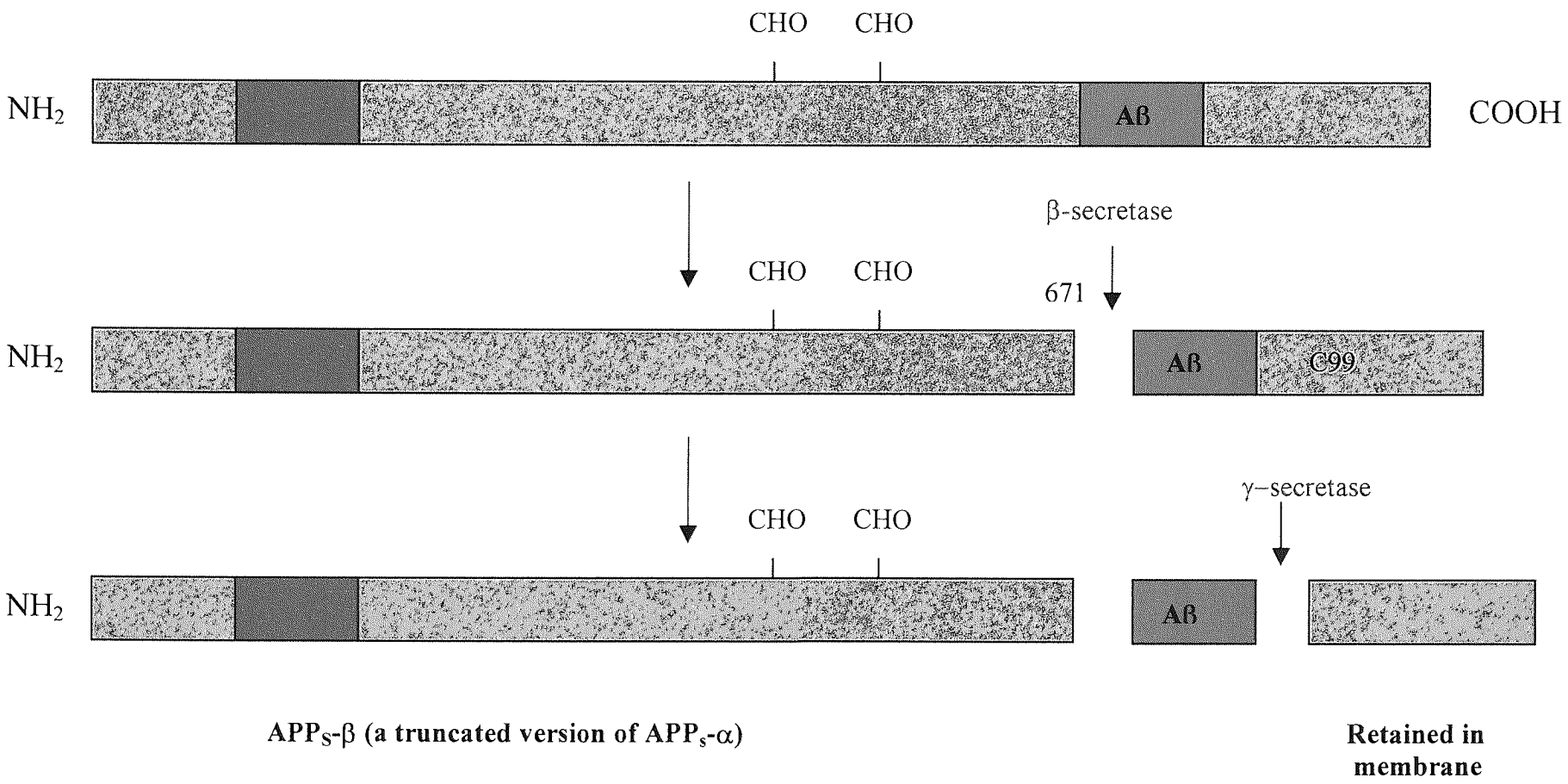

Figure 1.17 Alternative APP processing

appears that a substantially smaller portion of total cellular APP undergoes cleavage by 'β secretase'. Moreover, not all of the resultant C99 and C83 C terminal fragments (CTFs) are processed by 'γ-secretase' to Aβ and P3. Alternatively, proteolytic pathways can fully degrade these CTFs (Selkoe, 1998).

The Aβ peptide comprises 28 amino acids from the extracellular domain of APP and an additional 11-15 amino acids which are in the transmembrane region of APP (Fine, 1999). It has been shown that the cytotoxicity of Aβ residues in the sequence between amino acid residues 25 to 35 (Behl *et al.*, 1994b). Aβ is the major constituent of senile plaques (Monji *et al.*, 2001). It promotes neurite outgrowth, generates ROS, induces cytotoxic cellular OS and promotes microglial activation (DuYan *et al.*, 1996). It has also been shown that Aβ toxicity in culture is accompanied by multiple events culminating in apoptosis (Enkinci *et al.*, 2000).

Therefore in conclusion, AD is widely held to be associated with OS due, in part to the membrane action of Aβ aggregates (Periera *et al.*, 1999) including that Aβ and synthetic peptides homologous to different fragments of Aβ have been reported to be toxic to primary and clonal cell cultures (Forloni *et al.*, 1993). Su *et al.*, (1994) have provided evidence that apoptotic changes are present in AD based on the detection of DNA fragmentation and the morphological distribution of fragmented DNA. This study supports the hypothesis that apoptosis may be one mechanism leading to neuronal cell death in AD. OS has also been proposed as perhaps being contributory to an up regulation of APP expression. Figure 1.18 shows a possible cycling mechanism between Aβ and OS.

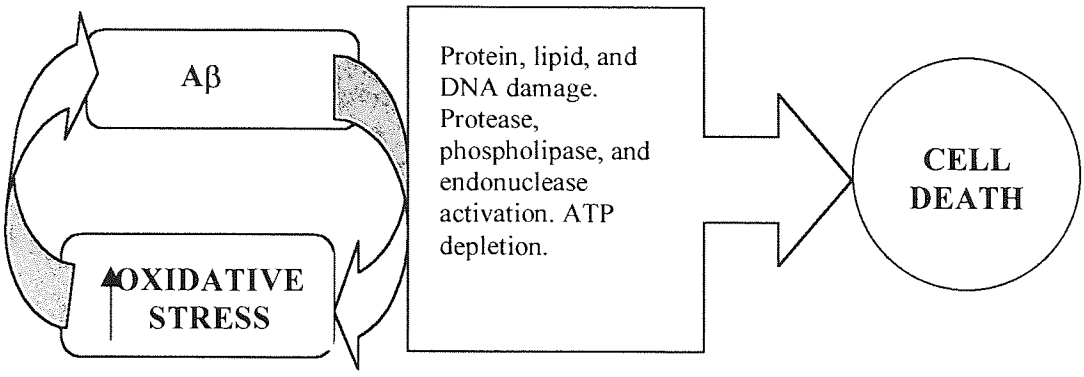

Figure 1.18 Proposed cycling mechanism between Aβ deposition and OS. Adapted from Bowling & Beal, (1995).

The more abundant form (approximately 90%) is 40 amino acids long ($A\beta_{40}$), whereas a very rare additional form is elongated at the C-terminus by two amino acids ($A\beta_{42}$). The longer peptide in particular $A\beta_{42}$ is thought to play a central role in Alzheimer's disease (AD) pathology (Steiner *et al.*, 1999). In particular, the $A\beta_{42}$ fragment is thought to be involved in AD for the following reasons: $A\beta_{42}$ is the predominant Aβ peptide in senile plaques. It aggregates faster than the other amyloid peptides, and the gene encoding some familial AD mutant APP results in overproduction of Aβ in cell models (Fagarasan & Efthimiopoulos, 1996).

It is believed is that APP leads to amyloid deposits resulting from abnormal processing, which over time, lead to plaque and tangle formation. The accumulation of amyloid itself may result in neurone death or synaptic loss. Once the plaques and tangles have formed, they induce glial activation and an inflammatory response that feeds back into the formation of more plaques and tangles and ultimately cell death (Hurley & Wells, 1999). The amyloid cascade theory, therefore, has proposed Aβ as the central trigger of these pathological changes (Sommer, 2002).

Since these plaques are associated with areas of nerve cell death, it has been suggested that Aβ may be either directly toxic to the neurons surrounding the plaques or participate in other neurodegenerative events (Behl *et al.,* 1994a). Aβ has been identified as a possible source of OS in the AD brain because it can acquire a free radical state contributing to its toxic effects. The demonstration of ROS production by Aβ (Huang *et al.,* 1999) and direct evidence of oxidative damage in neurons by Aβ has propelled research in this area.

It has been shown that Aβ possesses a strongly positive formal reduction potential, rapidly reduces Cu(II), and then traps molecular oxygen to generate H_2O_2. These effects are greatest for Aβ1-42 > Aβ1-40 >> rat Aβ1-40, a chemical relationship that correlates with the participation of these peptides in amyloid pathology, demonstrating the first direct evidence that accumulation of Aβ could be a direct source of OS in AD (Huang *et al.,* 1999). Martin *et al.,* (2001), have also shown apoptosis to be induced by Aβ 25-35, mediated at least in part by generation of ROS that probably includes H_2O_2 and superoxide anion. Further evidence for the activity of this peptide in ROS generation has been shown by Miranda *et al.,* (2000).

Therefore OS is likely to be involved in Aβ neurotoxicity. Some reports have indicated that Aβ 25-35 increases levels of H_2O_2 in neural cells and it has been suggested that H_2O_2 mediates Aβ neurotoxicity. However, it remains unknown whether Aβ and H_2O_2-mediated signal transduction and induction of apoptosis is identical (Saito *et al.,* 2001).

In summary, it appears that OS may play an important role in some forms of neuronal degeneration in various models. However, it must still be determined if OS is a final

common mechanism or a primary cause in the disease resulting from decreased cellular defence mechanisms or an over production of free radicals leading to neuronal death (Bains & Shaw, 1997). The AOX and free radical scavenger vitamin E has been shown to inhibit Aβ induced cell (PC12) death (Behl *et al.*, 1992). AA has also been shown to prevent Aβ induced cell (PC12) death (Yallampalli *et al.*, 1998). The AOX molecule, N-acetyl-L-cysteine (NAC) has also been shown to protect neuroblastoma cells from OS (Olivieri *et al.*, 2001). Lower plasma concentrations of vitamin E and retinol in AD patients compared to controls, have been suggested to result from consumption by excessive ROS (Bourdel-Marchasson *et al.*, 2001).

There has been some evidence published from post mortem studies that is consistent with the occurrence of OS in AD. In post mortem AD brains it has been reported that there is an altered AOX enzyme profile including changes in the levels of SOD and CAT, in several regions of histopathologically confirmed AD brains compared to control brains (Bruce *et al.*, 1997; Iwata *et al.*, 1997). The cumulative damage caused by ROS may explain the delayed onset and progressive characteristics of cell death in the various neurodegenerative disorders (Okuda *et al.*, 1998). Elevated OS has been recorded in models of normal brain aging and AD (Butterfield *et al.*, 1999; Matsuoka *et al.*, 2001; Pratico *et al.*, 2001; Yatin *et al.*, 1999c;).

All cells possess a network of AOXs and enzymes, which are involved in defence against ROS as discussed in section 1.2. However, the contribution in ROS detoxification of the various components of this network may differ in different brain cell types. Consequently, alterations in enzyme activities or in the concentration of small molecular weight AOXs as well as the availability of precursors for glutathione

synthesis and NADPH regeneration may contribute to the susceptibility or to the resistance against ROS of the different brain cell types under physiological and pathophysiological conditions (Dringen, 2000).

Increased consumption of fruit and vegetables, which contain AOX such as β-carotene and vitamins C and E, may act to diminish oxidative damage *in vivo* and because human endogenous AOX defences are not completely effective AOX obtained from the diet may be important in diminishing the cumulative effects of oxidative damage in the human body (Mason, 1995).

Since various AOX may serve their function in localised aqueous or lipid compartments, it is clear that an increase in any single AOX may not significantly alter overall oxidative balance. Further, AOX such as AA and vitamin E can, under some conditions, act as pro-oxidants by increasing the reduced forms of transition metal ions and thereby actually potentiate oxidative damage (Smith *et al.*, 1996).

Resveratrol, an AOX found in wine has been shown in neuronal cells to be a superior AOX in protecting cells from cell death through OS when compared with AA or vitamin E. This combination of resveratrol and AA and/or vitamin E has a greater protective effect that each individual AOX alone. The results indicated that resveratrol, not only possesses AOX and antimutagenic properties, but also can reduce cell death from OS, implying a beneficial value for preventing neurodegenerative diseases (Chanvitayapongs *et al.*, 1997). Free radical scavengers such as AOX have been suggested as being useful to prevent Aβ toxicity during ageing or AD (Yallampalli *et al.*, 1998).

A prospective study has been undertaken examining the relationship between the use of AA and vitamin E and incident AD of 633 persons aged 65 years and older. The study showed after a follow-up period of 4.3 years, that none of the vitamin E and AA supplement users had AD compared with the predicted number based on age, sex, years of education and length of follow-up interval and also based on the crude observed incidence among non-supplement users. The study suggested that the users of single doses of vitamin E and AA supplements may lower the risk of AD, therefore AOX may be associated with reduced occurrence of incident AD (Morris et al, 1998).

1.11 GLUTATHIONE

Glutathione (GSH) status may be involved in AD, however various levels have been reported. Some of these discrepancies may have arisen due to differing techniques: for GSH levels, the measurements of total rather than the crucial reduced GSH/GSSG ratio may hide real effects. Further, variations in post-mortem interval for tissue preparation may also contribute frequently to experimental discrepancies (Bains & Shaw, 1997). Decreases in GSH biochemistry and status and/or regulatory enzyme action have been reported in AD (Benzi & Moretti, 1997). However, GSH increases have also been reported in AD (Makar *et al.,* 1995). Increases in GSH have also been suggested to be compensatory responses as a consequence of OS.

GSH is a ubiquitous tripeptide thiol that serves essential functions in arobic species. It is composed of L-glutamate, L-cysteine and glycine. GSH is as a free radical scavenger particularly effective against the •OH radical. There are no known enzymatic defences against this species of radical. The ability of GSH to non-enzymatically scavenge both $^1O_2\cdot$ and •OH provides a first line of AOX defence. It is distributed in most cellular

organelles, and functions in anti-oxidation and detoxification (Hu *et al.*, 2000). GSH has been suggested to be a neuroprotectant, this is interesting as it is a storage form of cysteine in relation to the previous protective effects shown by ApoE alleles rich in cysteines.

Glutathione exists in both reduced form (usually abbreviated as GSH) and as an oxidised dimer (GSSG) form. They do not exist in equilibrium ratio under normal conditions because the majority of glutathione is in the reduced form, in a ratio of approximately (98:2). It is the most abundant bulk AOX in the cell, in neurons it is abundant at concentrations between 1-10mM. GSH and GSSG are interconvertible by the action of two enzymes, GPX and glutathione reductase (GRD). GSH strongly modulates the redox state (ratio of oxidizing to reducing equivalents) of the cell. GSSG is formed in AOX reactions that involve GSH, and accumulates with increased oxidative processing in the cell (Bains & Shaw, 1997; Ghibelli *et al.*, 1995). The ratio of GSH to GSSG is used as an indicator of OS status and DNA damage (Asensi *et al.*, 1999). Glutathione is synthsized *in vivo* by the consectutive action of two enzymes - γ-glutamylcysteine synthetase (γGCS) and glutathione synthetase (GS). GCS uses glutamate and cysteine as substrates forming the dipeptide L-γ-Glutatmyl-L-Cystine which is then combined with glycine in a reaction catalysed by GS to generate GSH. Adenosine triphosphate (ATP) is a cosubstrate for both enzymes (Dringen, 2000).

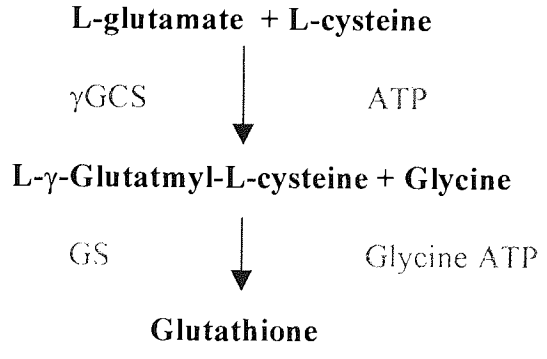

Figure 1.19a The synthesis of glutathione

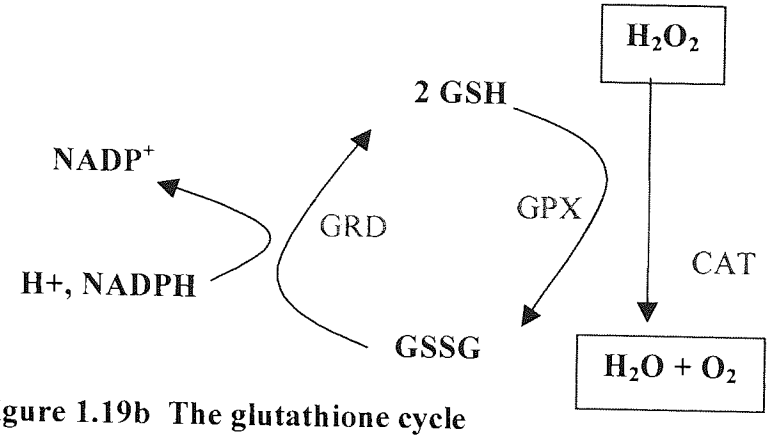

Figure 1.19b The glutathione cycle

γ-glutamylcysteine synthetase (GCS) is the rate-limiting enzyme in GSH synthesis, as the intracellular level of glutathione is regulated by a feedback inhibition of GCS by the endproduct GSH (Hu *et al.*, 2000). Other limiting factors for GSH synthesis include the availability of cysteine and selenium. Extracellularly, cysteine is rapidly oxidised to cystine. The GSH cycle, as shown in figure 1.19, is an important biochemical process that contributes critically to homeostasis of the intermediary metabolism of ROS through reduction of disulphide linkages of proteins in many cell types (Weber, 1999).

GSH protects the cell:

1. by reacting chemically with intracellular targets (mainly DNA)
2. by enzymatically reducing peroxides
3. by enzymatically detoxifying electrophiles
4. by maintaining the redox state of cellular thiols (Thomas *et al.*, 1995).

GSH is also present in the liver in millimolar concentrations, where it functions as an electrophile, radical scavenger, and a redox partner. It may also serve as a cofactor for (a) several drug metabolising enzymes (i.e. GSTs) where it is consumed, or (b) for AOX enzymes (i.e. GPX) where it functions as a redox partner (Twaroski *et al.*, 2001). It also plays a critical role in neuroprotection against H_2O_2 (Ibi *et al.*, 1999), and may play an important role in interactions under physiological levels of OS and consequently alter

the functional activity of cells (Denisova *et al.*, 2001). GSH is now recognised as a major modulator of OS, and cellular GSH content often dictates the relative susceptibility or resistance of a cell to the cytotoxic or apoptotic activities of a toxicant (Reinres Jr *et al.*, 2000).

Due to such multiple roles in normal tissue, there is a considerable potential for alterations in GSH to be causally associated with disease. OS arising from ROS formation can affect the ratio of reduced to total GSH and the GSH status of the cell as GSH is depleted to combat such radicals (Kleinman & Richie, Jr, 2000). Overall, while there is evidence for OS, perhaps arising from an altered GSH status in AD, consistent data has not been produced (Bains & Shaw, 1997). Figure 1.21 shows the proposed central role of glutathione in neuronal death. In addition to its critical role as an AOX/free radical scavenger, GSH may act as redox modulator of ionotropic receptors, serve as a neuroprotectant against the effects of glutamatergic excitotoxicity, and may also be a unique neurotranmitter (Bains & Shaw, 1997). Intracellular GSH levels can be artificially lowered in several ways for example by inhibiting its biosynthesis with buthionine sulfoxamine, binding free sulphydryl groups with diethyl maleate or simply withdrawing cysteine from the cell culture medium. When treated in this way, cells can usually tolerate GSH levels down to about 20% of normal, although they are usually very sensitive to any additional stress (Slater *et al.*, 1995). Depletion of GSH has also been shown to affect some of the GSH-dependent enzymes (GCS, GPX, glutathione transferase, leukotriene C4-synthetase, glutaredoxin system, glyoxylase I and II) making cells more susceptible to any further challenge (Benzi & Moretti, 1995). It is also clear that levels of endogenous AOX such as GSH decrease with age (Hu *et al.*, 2000). An impairment in GSH status occurring in particular neural populations sets in

motion a cascade of biochemical abnormalities culminating in various forms of neuronal cell death (Bains & Shaw, 1997).

There are multiple mechanisms by which ROS alter signalling pathways. Although not all are known, it appears that controlling the thiol status of a cell is critical (Sen, 1998). ROS can catalyse the formation of disulphide linkages between proteins, the formation of protein-glutathione mixed disulfides, or perhaps more directly alter protein-protein interactions. Cellular thiols appear to be an important regulatory target. ROS can oxidise a sulphydryl group resulting in the formation of disulphide linkages between proteins, or the formation of protein-glutathione mixed sulphides, or perhaps more directly alter protein-protein interactions as shown in figure 1.20 (Kehrer, 2000).

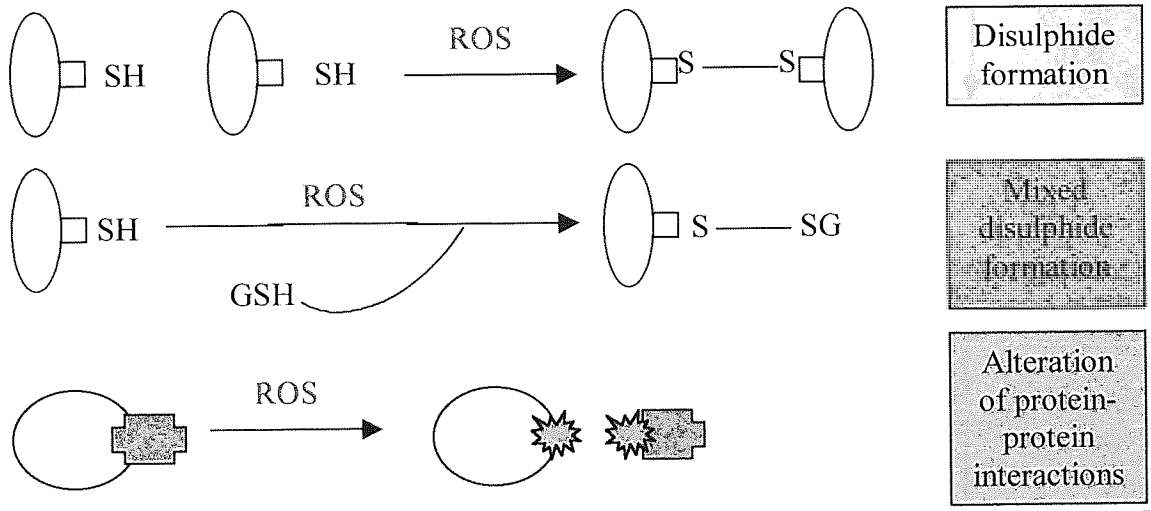

Figure 1.20 Mechanisms by which ROS may alter signalling pathways, adapted from Kehrer, 2000.

GSH can also interact with AA as shown in figure 1.22. A particularly important function of both AA and GSH has been proposed, as they both have the ability to neutralize reactive hydroxyl radicals (•OH). There are no enzymes analogous to SOD or GPX to scavenge •OH. In addition AA and GSH can interact as a redox couple. Depletion of either AA or GSH can be compensated for by the presence of the other. For example administration of GSH ester can prevent the onset of scurvy in AA-deficient guinea pigs, whereas AA administration of GSH ester can prevent tissue damage after inhibition of GSH synthesis. On a cellular level, the distinct AA-GSH interactions with greater reliance on AA in neurons and on GSH in glia (Oberdoerster & Rabin, 1999).

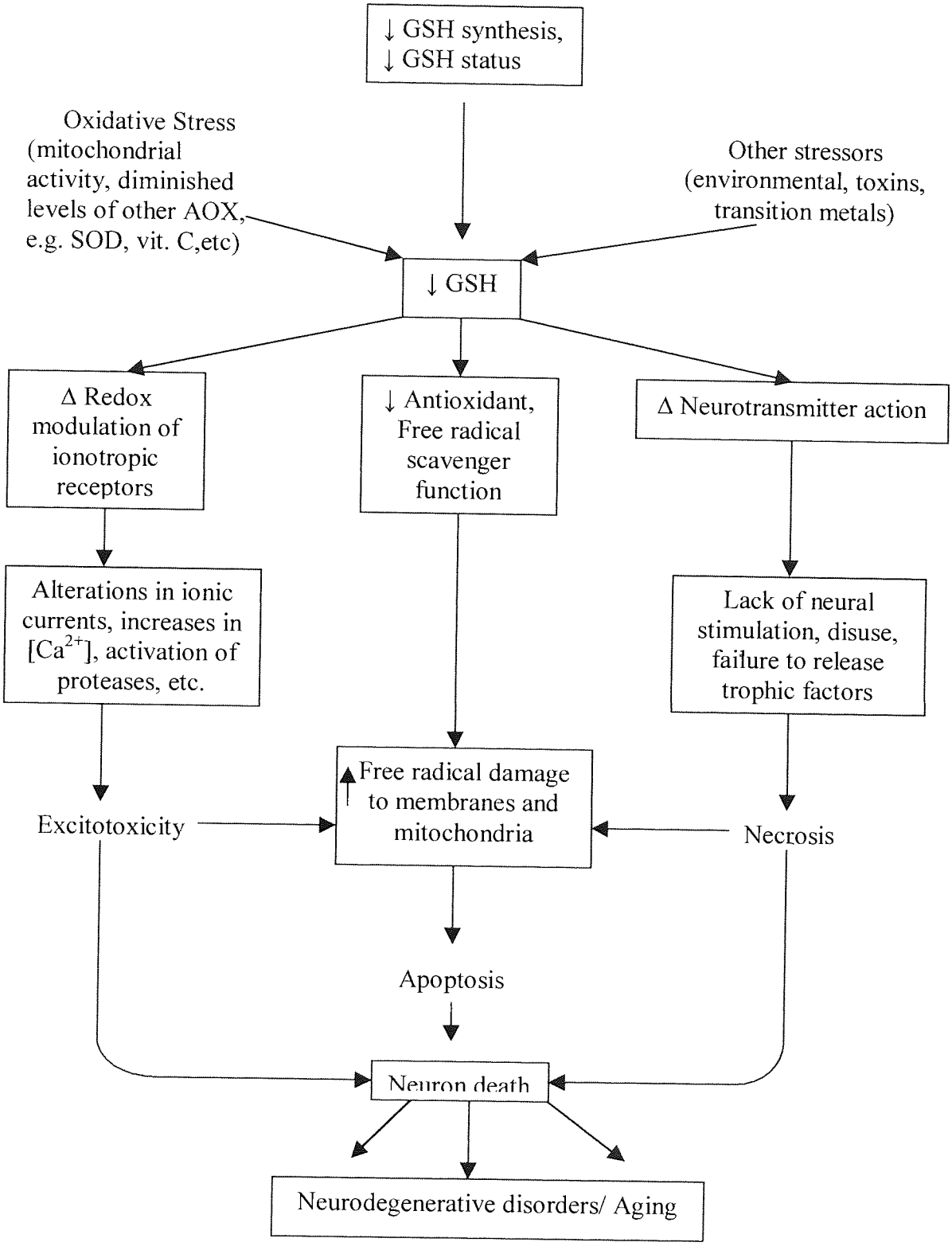

Figure 1.21 The central role of glutathione. Adapted from Bains & Shaw, 1997.

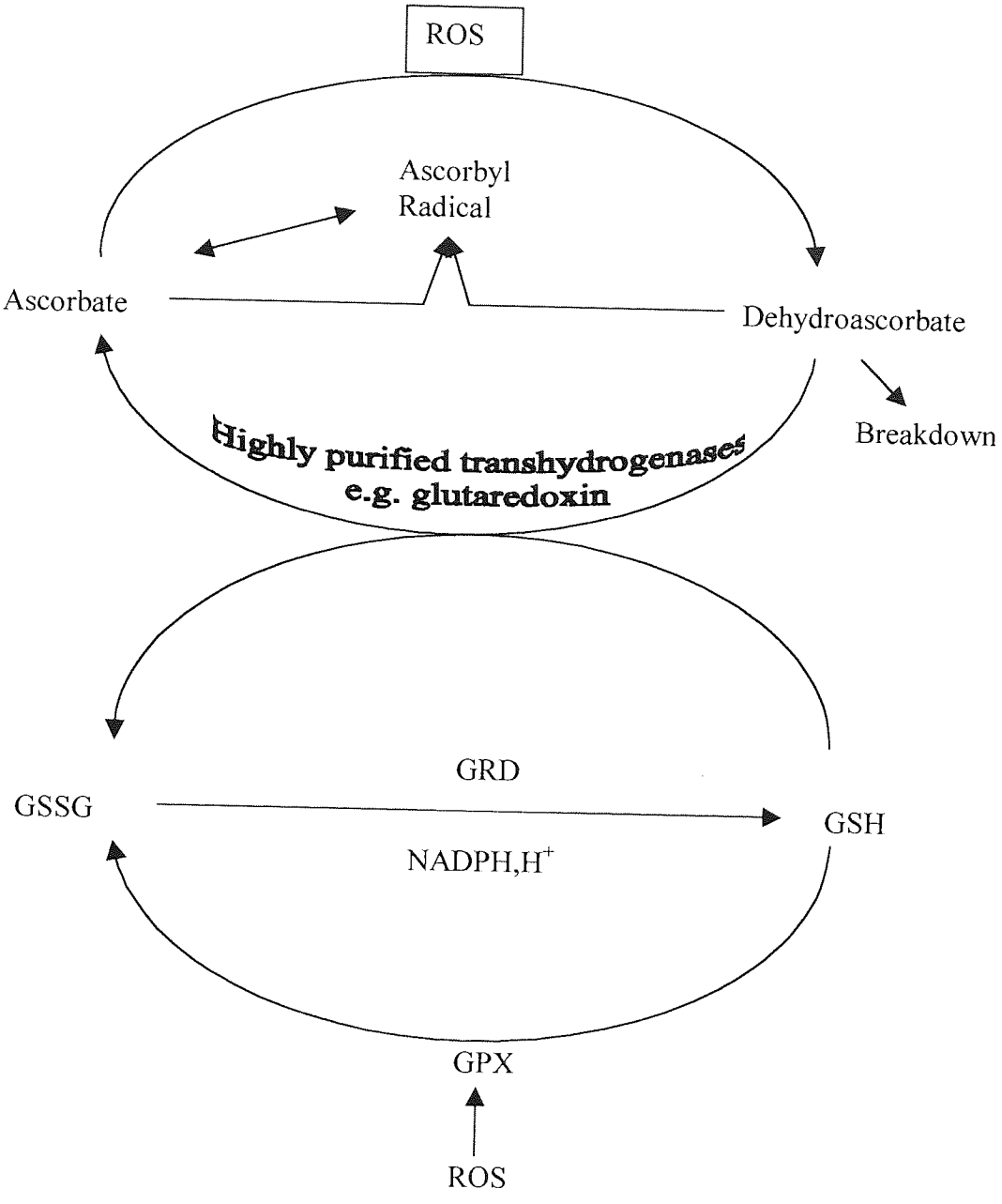

Figure 1.22 The interaction of AA and GSH. Adapted from Halliwell, 1999.

As depletion of GSH is associated with several disease states. The possibility of manipulating the availability of GSH has come to the forefront of treatment possibilities, to increase GSH levels by pharmaconutrition. Possible treatment

modalities include GSH itself, in the form of its sodium salt, GSH esters and GSH precursors (Valencia *et al.*, 2001).

1.12 NEUROTROPHINS

Neurotrophic factors (NTFs) promote the differentiation and growth of developing neurons and phenotypic maintenance. NTFs also promote the survival of adult mature neurons but also represent a potential means of modifying neuronal dysfunction, astrocytic activation and inflammatory reactions under pathological conditions. They are also essential in function in the adult brain (Siegel & Chauhan, 2000; Connor *et al.*, 1996).

Most NTFs belong to several families of structurally and functionally related molecules:

1. Neurotrophin super family
2. Glial cell line-derived neurotrophic factor (GDNF) family
3. Neurokine or neuropoietin super family
4. Non-neural growth factor super family.

The neurotrophins, now called the 'NGF super family' include nerve growth factor (NGF), brain derived neurotrophic factor (BDNF), Neurotrophin 3 (NT3), and Neurotrophin 4 (NT4), Neurotrophin 5 and 6 (NT-5 and NT-6) which are not expressed in humans. Neurotrophins bind to a specific family of receptors within the CNS known as tyrosine kinase (*Trk)* receptors. The low affinity neurotrophin receptor p75 promiscuously binds all of the neurotrophins. However *Trk A* binds specifically NGF whilst *Trk B* binds BDNF and NT 4/5. GDNF family receptors include a receptor complex of Ret and growth factor receptor (GFR) α1-4. The neurokine super family

ligands mediate via the receptors gp130 and leukaemia inhibitory factor receptor-β (LIFR-β) (Siegel & Chauhan, 2000).

The NGF super family are synthesised in many regions of the brain, a summary of the neuronal functions regulated by the neurotrophins are listed in table 1.10. Both NGF and BDNF support the function and survival of the basal forebrain cholinergic neurons, which has led to the suggestion that these factors are important in the prevention of AD (Holsinger *et al.*, 2000). It has been proposed that one mechanism whereby neurotrophic factors may exert their protection is by stimulating endogenous defences against OS and damage by ROS (Williams, 1995).

Table 1.10 Neuronal properties regulated by the neurotrophins. Taken from Cirulli, 2001.

It has been suggested that AD may be primarily due to a deficit in neurotrophin protein, or reciprocal receptor expression. Lower BDNF levels have been recorded in AD patients compared to controls as measured by specific ELISAs (Hock *et al.*, 2000).

1.13 NERVE GROWTH FACTOR

Nerve growth factor (NGF) was discovered in 1951 as a molecule that regulates the survival and maturation of developing neurons in the peripheral nervous system (Levi-

Montalcini & Hamburger, 1951), and is the best characterised of the neurotrophic factors.

The NGF gene is located on human chromosome 1. NGF exists in several different isoforms with various different molecular weights; its most biologically active form is β-NGF, which is similar in all tissues. It has a molecular weight of 26.5 kDa and consists of a covalently bound dimer of two 118 amino acid chains, each of which has 3 intrachain disulpide bridges (Sofroniew *et al.*, 2001; Smith, 1996). The NGF dimer has an elongated shape with a core, that is formed by twisted beta sheets: the molecule also features a cysteine-knot motif, a reverse turn at one end and three beta-hairpin loops at the other. It has twisted pairs of antiparallel beta strands linked by loops and anchored to a group of three disulphide bonds. The disulphide bonds form an unusual knot structure which has also been found in platelet-derived growth factor-BB and in transforming growth factor-beta 2.

Once mature, most neurons lose absolute dependence on target-derived growth factors for acute survival. In adults, the focus of NGF signalling shifts away from the regulation of neuronal survival to the regulation of neuronal phenotype and function. Substantial evidence suggests that amongst other functions, NGF acts to protect neurons from endogenous toxic events generated during the response to tissue injury and that NGF signalling facilitates regrowth and repair. The signalling mechanisms engaged in neuroprotection have not been defined. However, it appears that the protective effects of NGF extend both to neurons known to express *Trk A* receptors and to those that are not known to express such receptors (Sofroniew *et al.*, 2001).

There is incomplete information concerning NGF levels in body fluids. Normal values of NGF in serum from 157 normal subjects were determined. There were no statistically significant variations with age, but the NGF level were significantly lower in females (112±31 pg/ml) than in males (243±35 pg/ml). This NGF level appears to be a sexually dimorphic character in humans. It has been speculated that there may be a relationship between the lower NGF values in females and their higher prevalence of development of AD (Serrano *et al.*, 1996).

The neurotrophic factors (especially NGF) are of interest as neuroprotective agents. However, the therapeutical administration of these compounds seems to be quite complicated because of their chemical properties. Neurotrophic factors are large protein molecules that cannot easily pass the blood brain barrier (BBB) and do not distribute properly after systemic administration. Therefore the use of NGF proteins as neuroprotective therapeutics is limited by their hindered mobility through the BBB (Gozes, 2001). One approach to enhance the amounts of neurotrophic factors available to the CNS is to stimulate their synthesis in affected brain regions by systemically administered lipophilic compounds with a low molecular weight, such as beta-adrenoceptor agonists such as clenbuterol. Since degeneration of the basal forebrain cholinergic neurons occurs early in the course of AD and is correlated with cognitive deficits, cholinergic lesion paradigms have been used to study the role of the cholinergic system in cognitive function. Extensive studies have shown that the administration of NGF prevents or reduces this neuronal degeneration, in rodents and higher animals, including the primate brain. Thus, there is significant evidence to support the hypothesis that NGF may be neuroprotective as well as neurotrophic to cholinergic basal forebrain neurons (Hagg *et al.*, 1989; Hagg *et al.*, 1988; Tuszynski *et al.*, 1990).

Semkova and Krieglstein (1999) have suggested that data they have produced supports the hypothesis that active NGF inducers may have a potential as therapeutic agents for the treatment of neurodegenerative diseases. Potential NGF inducers include the neuroprotective agent 2,3-dimethoxy-5-methyl-6-(10-hydroxydecyl)-1,4-benzoquinone (CV-2619). CV-2619 has been shown to protect neurons (rat primary neurons) against Aβ induced neurotoxicity, have an anti-apoptotic effect in astrocyte injury models, by increasing NGF production and not affecting the levels of ROS. CV-2619 has also been shown to have its effect blocked by an anti-NGF antibody (Takuma *et al.,* 2000). Riaz *et al.,* (1999) have also shown that a vitamin D_3 derivative 1(S),3(R)-Dihydroxy-20(R)-(1-ethoxy-5-ethyl-hydroxy-2-heptyn-1-yl)-9,10-seco-pregna-5(Z), 7(E), 10(19)-triene (CB1093) induces increased NGF production, and depletions of NGF seen in diabetes were prevented by CB1093. Other agents have been found that are not necessarily NGF inducers but potentiate and mimic the effect of NGF including NG061 (a novel fungal metabolite) (Ito *et al.,* 1999).

Olson (1993) stated than an increased 'NGF tonus' might be beneficial in AD. It has been suggested that theoretically, this goal can be achieved in many different ways including:

- Intracerebral NGF infusion
- Slow release biodegradable implants
- Carrier-mediated transport across the blood-brain barrier
- Grafting NGF-producing cells
- Direct gene transfer to the brain
- Developing NGF receptor agonists
- Controlling endogenous NGF production

However, NGF has been shown to stimulate APP promoter activity in PC12 cells, thus increasing the expression of APP. If this also occurs in humans *in vivo*, the use of NGF, proposed as a palliative treatment in AD, could rather result in a risk factor for the disease. However, the neurotrophins can also increase the release of neurotrophic sAPP fragments, which very probably should be accompanied by a reduced generation and release of Aβ. It has been suggested that NGF could indeed be useful to define new strategies for the disease (Villa *et al.*, 2001). Gene therapy treatment for AD has begun, where autologous fibroblast cells obtained from skin biopsies are engineered to express human NGF and are then surgically implanted into the frontal lobe of the brain. In animal models, it has been shown that implanted fibroblasts expressing NGF prevent the death of cholinergic cells and reverse the effects of aging (Weitzman, 2001).

1.14 BRAIN DERIVED NEUROTROPHIC FACTOR

Brain derived neurotrophic factor (BDNF) is more highly expressed and widely distributed than NGF in the CNS and has survival promoting actions on a variety of CNS neurons. The mature form of human BDNF (hBDNF) is about 50% identical to human mature NGF (Murer *et al.*, 2001). All neurotrophins have six conserved cysteine residues and share a 55% sequence homology of amino acids. hBDNF is produced by the expression of a DNA sequence encoding a 247-amino acid precursor with a signal peptide and a proprotein that is cleaved to yield the 119 amino acid mature BDNF.

It has been suggested that BDNF may mediate neuronal protection as withdrawal of BDNF results in increased production of ROS and decreased survival of neurons. It has been suggested that the production of ROS can be ameliorated through supplementation

with BDNF (Gabaizadeh *et al.*, 1997). Spina *et al.*,(1992) have shown that BDNF enhances the activity of glutathione reductase, the enzyme responsible for the conversion of GSSG to GSH. They concluded that in SH-SY5Y cells, BDNF may protect against OS by maintaining GSH levels in the cell through increased glutathione reductase activity.

BDNF may play a role in AD: levels of BDNF mRNA levels have been shown to be 3.4 fold lower in parietal cortex of AD subjects compared to controls, and also lower BDNF mRNA and protein content has been reported in the hippocampal formation and temporal cortex. The loss of mRNA from these target areas of basal forebrain cholinergic neurons, suggests that BDNF may play an important role in cholinergic cell atrophy and dysfunction in AD (Hock *et al.*, 2000; Holsinger *et al.*, 2000; Connor *et al.*, 1997). Furthermore, it has recently been shown that BDNF inhibits free radical and apoptotic pathways in medium spiny neurons, but does so downstream from the point of commitment to cell death (Petersen *et al.*, 2001). This, therefore raised the fact that BDNF might be a potential therapeutic agent for PD and AD among other neurodegenerative disorders (Murer *et al.*, 2001).

1.15 CELL LINES

In slowly progressing diseases, which take 10-20 years to the final stage, the frequency of apoptotic death in neurons is so rare that the detection of apoptotic cells cannot be determined in post mortem brain samples. Considering that collapse of mitochondrial membrane potential takes place within 60 minutes, activation of caspase-3 within 24 hours and the whole apoptotic process within 72 hours, the possibility to detect apoptotic dying cells in clinical samples is unlikely. In addition, cells undergoing

apoptosis are phagocytosed, leaving fewer evidences to show occurrences of apoptosis. Therefore it has been proposed that the involvement of apoptosis in the neurodegeneration should be studied by the use of animal models or of cultured cell systems (Naoi *et al.*, 2000).

Two clonal cell lines, rat pheochromocytoma cells, PC12 and human neuroblastoma cells, SH-SY5Y, have widely been employed as neuronal models to investigate the effects of OS.

Clonal cell lines, such as the rat pheochromocytoma line PC12 cells provide a useful model system for the investigation of neuronal injury, and the study of numerous problems in neurobiology and neurobiology, at the single cell and molecular levels (Greene & Tischler, 1976). In contrast with CNS primary cultures which contain many types of nerve cells as well as glial populations, clonal nerve cell lines afford homogeneous populations and the ease of manipulation and degree of control that may be exerted over the extracellular milieu provide definite advantages over animal experiments facilitating the molecular dissection of complex mechanistic pathways (Xiao *et al.*, 1999; Iversen *et al.*, 1995). It has been shown that addition of Aβ to PC12 cells results in increased ROS production, mitochondrial dysfunction, apoptosis and cell death (Yao *et al.*, 1999).

SH-SY5Y cells represent a continuously dividing cell line, a neuroblastoma subclone of human origin. They have also been widely used in the study of neuronal functions such as transmembrane controls, and in AD-related research to study the effects of

aluminium or glycated tau protein, as well as Aβ induced apoptosis (Kohring & Zimmermann, 1998).

Neuroblastoma cell lines can be also differentiated into cells that are biochemically, ultrastructurally and electrophysiologically similar to neurons after being treated with different agents such as retinoic acid (RA) (Encinas *et al.,* 1999). RA, a product of vitamin A metabolism, causes different morphological and biochemical alterations including changes in receptors, ion changes and activation of DNA binding (Voigt *et al.,* 2000). It also mediates the biological responsiveness of the cells to the *Trk* B ligands BDNF and NT-3, by stimulating the expression of *Trk* B receptors (Kaplan *et al.,* 1993). RA also results in growth inhibited adherent cells, which have long neuritic cell processes (Påhlman *et al.,* 1995).

The cell models employed, have been shown to express the *trkA* and *p75* receptors in the PC12 cell line (Bournat & Allen, 2001; Wooten *et al.*, 1998), and the SY5Y cell line (Kaplan *et al.*, 1993).

Another reason for the use of the cell lines is for practical and ethical reasons, human neuronal and glial cultures cannot be used for routine neurotoxicity testing, but they may be very useful for validating results from murine cultures and to address specific toxicity questions. Besides primary cultures, human-derived clonal cell lines such as neuroblastoma SH-SY5Y can offer a first-step approach in neurotoxicity testing (Sanfeliu *et al.,* 1999). Differences are recorded between the cell lines in response to OS. This is due to each cell type being dependent upon their inherent capacity to derive energy from alternative substrate oxidative pathways, the functioning of normal

neuroprotective mechanisms, and the level of trophic support they require to maintain cell structure and function. These factors combine to limit the resultant damage due to excessive free radical generation and to restore calcium homeostasis and the balance of the phosphorylation/dephosphorylation cycles that control many types of enzymatic injury (O'Neill & Kaltschmit, 1997).

1.16 HYPOTHESIS, AIMS & OBJECTIVES

Neurotrophic factors provide survival signals for neuronal cells. It has been shown that specific neurons can amass Aβ both *in vitro* and *in vivo*. This appears to be associated with an increase in OS, and decreased glutathione levels (reduced form). These lowered pools of glutathione may lead to an incomplete detoxification of ROS, which in turn may cause an increase in cell death by means of apoptosis.

The hypothesis is that neurotrophic factors, specifically NGF and BDNF, can prevent OS induced apoptosis by modulating glutathione depletion or synthesis. This is summarised in figure 1.23.

Theory of Aβ mediated cell events

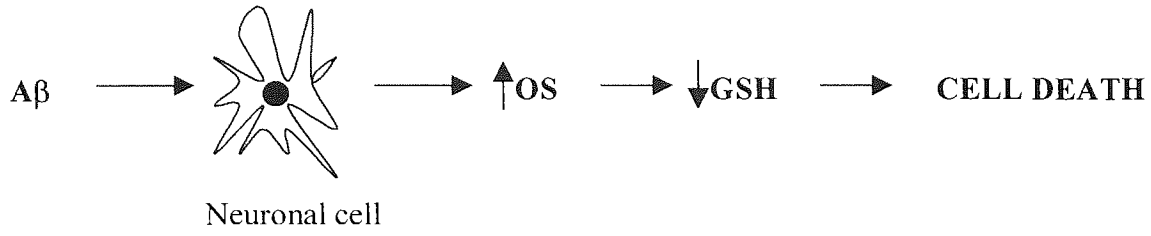

Expanded figure

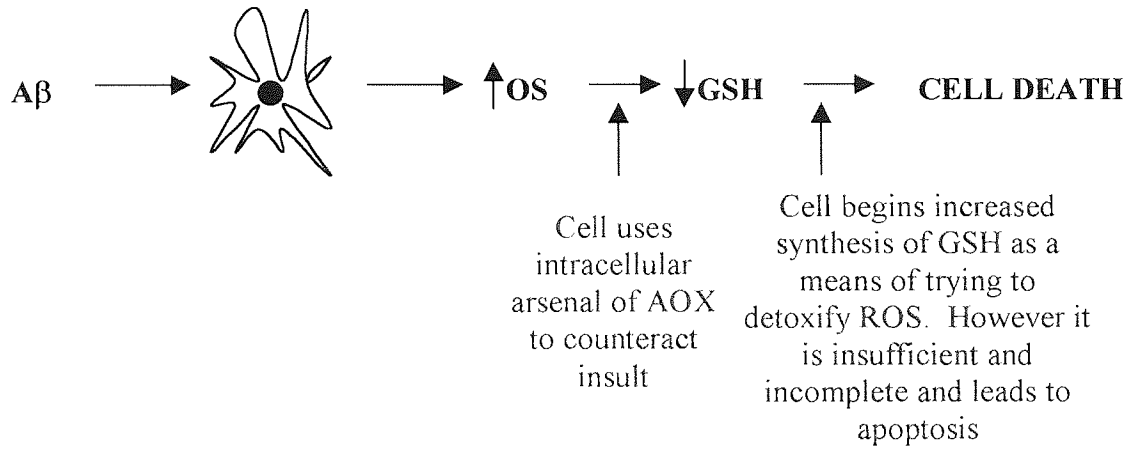

Hypothetical figure

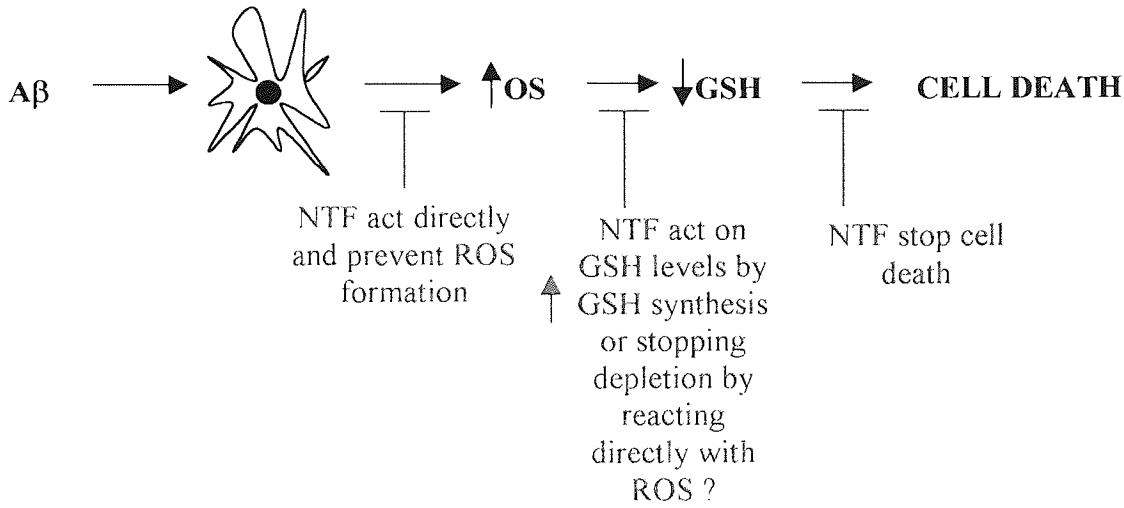

Figure 1.23 Proposed hypothesis of neurotrophic factor protection on cells

Specific aims and objectives are to :

- *Investigate the proposed hypothesis in three clonal cell models (PC12, SH-SY5Y undifferentiated and differentiated)*
- *Examine the effects of Aβ on ROS generation/ levels*
- *Examine the effects of ROS damage on proteins and viability*
- *Examine the effects of ROS on glutathione levels*
- *Examine the effects of neurotrophic factors specifically NGF and BDNF, on the intracellular glutathione AOX pool and induction of glutathione related genes induced by OS*
- *Investigate the effect of the classical 'antioxidant' ascorbic acid compared to the specified neurotrophic factors on ROS damage and glutathione levels*
- *Investigate the effects of novel NO-NSAIDS against Aβ induced damage.*

CHAPTER TWO

MATERIALS and METHODS

2.1 MATERIALS

2.1.1 Cell Culture

Roswell Park Memorial Institute 1640 media (RPMI 1640) with Glutamax I, Penicillin (10000 units/ml) streptomycin (10000μg/ml), horse serum, foetal bovine serum and trypsin-EDTA and Nunc Immunosorb 96 well plates were obtained from Gibco/BRL, Life Technologies Limited, Paisley, Scotland. PC12 rat pheochromocytoma cells, ECACC No. 8802241 were obtained from ECACC, Salisbury, Wiltshire, UK. SH-SY5Y human neuroblastoma cells were obtained from the department of anaesthesia, Leicester Royal, Leicester, UK. Minimal essential medium non-essential amino acids (100 x solution), trypan blue solution (0.04%), all trans-retinoic acid (RA), dimethyl sulfoxide (DMSO), polyoxyethylenesorbitan monolaurate (Tween 20), Sigma 104 tablets, magnesium chloride, sodium azide, bovine serum albumin, diethanolamine, alkaline phosphatase conjugated anti-rabbit IgG (whole molecule), sodium hydrogen carbonate, ethylenediaminetetraacetic acid (EDTA) and PBS (0.02M) tablets were obtained from Sigma-Aldrich Company Limited, Poole, Dorset, UK. Anti Trk B rabbit polyclonal IgG was obtained from Autogen Bioclear UK Limited, Calne, UK. All tissue culture plastics were obtained from Triple Red Limited, Thame, Oxfordshire, UK, or Helena Biosciences, Sunderland, UK. Olympus CK2 inverted microscope, haemocytometer, parafilm and 30ml sterile disposable universals were obtained from Appleton Woods Limited, Birmingham, UK. Sigma 2-15 centrifuge and Grant water bath were obtained from Phillip Harris, Shenstone, UK. Nalgene cryovials (1.8ml) and sodium carbonate were obtained from Fisher Scientific UK, Loughborough, Leicestershire, UK. A Shel Lab TC2323 CO_2 incubator was obtained from BoroLabs, Aldermaston, Berkshire, UK. Labsystems Wellwash 4 Mark 2 plate washer and a 20 - 50°C bench top incubator (hand warmer) were obtained from Thermo Life Sciences,

Hampshire, UK. Dynex MRX 96 well plate reader fitted with 340, 410, 490, 570 and 630nm filters was obtained from Prior Laboratories Services, Forest Row, East Sussex, UK.

2.1.2 3-(4,5-dimethylthiazol-2-yl)-2,5-diphenyltetrazolium (MTT) assay

PBS tablets (0.02M), 3-(4,5-dimethylthiazol-2-yl)-2,5-diphenyltetrazolium bromide (MTT), N, N-dimethylformamide (DMF), sodium lauryl sulphate (SDS, practical grade) were obtained from Sigma-Aldrich Company Limited, Poole, Dorset, UK. Acetic acid glacial (17.4M) was obtained from Fisher Scientific UK, Loughborough, Leicestershire, UK. Jenway 3310 pH meter was obtained from Appleton Woods Limited, Birmingham, UK. Microtitre plates (96well) were obtained from Triple Red Limited, Thame, Oxfordshire, UK. Dynex MRX 96 well plate reader fitted with 340, 410, 490, 570 and 630nm filters was obtained from Prior Laboratory Services, Forest Row, East Sussex, UK.

2.1.3 Microscopy

2.1.3.1 Video Microscopy

Digital camera was obtained from VideoLabs Incorporated, USA. Olympus CK2 inverted microscope was obtained from Appleton Woods Limited, Birmingham, UK. Stinger Pro PCI Capture Card which includes CineMarker software was obtained from Digital Vision, USA.

2.1.3.2 Fluorescence Microscopy

bisBenzimide Trichloride (Hoechst 33342), propidium iodide (PI), Kodak Ektachrome 64T (Tungsten) Colour Reversal film (EPY135-36) were obtained from Sigma-Aldrich

Company Limited, Poole, Dorset, UK. Centrifuge tubes (1.5ml), Pasteur pipettes (3ml), microscope glass slides sandblasted 76 x 26mm ground edge, thickness 1.0/1.2mm, cover slips square 22 x 22mm thickness 0 were obtained from Appleton Woods Limited, Birmingham, UK. Eppendorf Centrifuge 5415D was obtained from Helena Biosciences, Sunderland, UK. Zeiss Axioskop Fluorescent Microscope with filter set No.9 (405-490nm) and a 35mm camera x 2.5 projective Axio lens were obtained from Zeiss, Germany. A Nikomat 35mm EL camera was obtained from Nikon Industries, Japan. Films were developed by E6 processing at Greatrex Photographic Laboratories (Birmingham) Limited, Birmingham, UK and colour reversal prints produced.

2.1.4 Flow Cytometry

PBS tablets (0.02M), propidium iodide (made up at 50μg/ml in 0.1% sodium citrate (trisodium salt:dihydrate), 0.1% Triton-X100 (all molecular biology grade) and 2',7'-dichlorofluorescein diacetate (DCFDA) (made up at 75mM in DMSO) were obtained from Sigma-Aldrich Company Limited, Poole, Dorset, UK. Pasteur pipettes, centrifuge tubes (1.5ml) and aluminium foil were obtained from Appleton Woods Limited, Birmingham, UK. Flow cytometry tubes were obtained from Elkay Lab Products, Basingstoke, Hampshire, UK. Flow check fluorospheres, Cleanze solution, Isoton II and fluorescence activated cell sorter (FACS) – EPICS®XL-MCL were obtained from Beckman Coulter, High Wycombe, UK. Eppendorf centrifuge 5415D was obtained from Helena Biosciences, Sunderland, UK.

2.1.5 Glutathione Assays

5-Sulfosalicyclic acid (SSA), disodium ethylenediaminetetraacetic acid (disodium-EDTA), glutathione (reduced form) (GSH), glutathione (oxidised form) (GSSG), 5,5'-

dithio-bis(2-nitrobenzoic acid) (3-carboxy-4-nitrophenyl disulphide) (DTNB, Ellman's Reagent), β-Nicotinamide adenine dinucleotide phosphate, reduced form (β-NADPH), 2-vinylpyridine (2-VP), triethanolamine (TEA) and glutathione reductase (GRD) with an activity of 173 units/mg protein were obtained from Sigma-Aldrich Company Limited, Dorset, Poole, UK. Dynex MRX 96 well plate reader fitted with 340, 410, 490, 570 and 630nm filters was obtained from Prior Laboratories Services, Forest Row, East Sussex, UK.

2.1.6 Estimation of Protein Concentration

Bicinchoninic Acid Protein Assay Kit (BCA-1) containing (bicinchoninic acid solution, copper (II) sulphate pentahydrate (4% solution) and protein standard solution), sodium hydrogen carbonate and hydrochloric acid were all obtained from Sigma-Aldrich Company Limited, Poole, Dorset, UK. Sodium carbonate was obtained from Fisher Scientific UK, Loughborough, Leicestershire, UK. 96 well flat bottomed microtitre plates were obtained from Triple Red Limited, Thame, Oxfordshire, UK. Pasteur pipettes (3ml) and centrifuge tubes (1.5ml) were obtained from Appleton Woods Limited, Birmingham, UK. Eppendorf Centrifuge 5415D was obtained from Helena Biosciences, Sunderland, UK. Dynex MRX microtitre plate reader fitted with 340, 410, 490, 570 and 630nm filters was obtained from Prior Laboratory Services, Forest Row, East Sussex, UK. A 20 - 50°C bench top incubator (hand warmer) was obtained from Thermo Life Sciences, Hampshire, UK. GraphPad PRISM version 3.00 for Windows was obtained from GraphPad Software, San Diego, California, USA.

2.1.7 Protein Carbonyl Determination

Sodium hydrogen carbonate, 2,4-dinitrophenylhydrazine (DNPH), hydrochloric acid (HCl), polyoxyethylenesorbitan monolaurate (Tween-20) (molecular biology grade), hydrogen peroxide (H_2O_2) 30 % solution (8.8M), di-sodium hydrogen phosphate, o-phenylenediamine tablets (20mg substrate per tablet), sodium chloride, potassium chloride, PBS tablets (0.02M), 2,2'-Azobis(2-methylpropionamidine) dihydrochloride (AAPH), sodium borohydride, trichloroacetic acid (TCA), guanidine hydrochloride, anti-DNP antiserum mouse IgE were obtained from Sigma-Aldrich Company Limited, Poole, Dorset, UK. Peroxidase labelled rat anti-mouse IgE heavy chain was obtained from Serotec Ltd, Oxford, UK. PD-10 columns were obtained from Amersham Pharmacia Biotech UK Limited, Buckinghamshire, UK. Sodium carbonate, potassium di-hydrogen ortho phosphate, citric acid, sulphuric acid, ethyl acetate, ethanol and acetone were obtained from Fisher Scientific UK, Loughborough, Leicestershire, UK. Jenway Spectrophotometer, Stuart Scientific magnetic stirrer hotplate and Clifton cyclone vortex were obtained from Appleton Woods Limited, Birmingham, UK. Nunc Immunosorb 96 well plates were obtained from Gibco/BRL, Life Technologies Limited, Paisley, Scotland. Labsystems Wellwash 4 Mark 2 Plate Washer was obtained from Thermo Life Sciences, Hampshire, UK. A 20 - 50°C bench top incubator (hand warmer) was obtained from Thermo Life Sciences, Hampshire, UK. Dynex MRX 96 well plate reader fitted with 340, 410, 490, 570 and 630nm filters was obtained from Prior Laboratory Services, Forest Row, East Sussex, UK.

2.1.8 Gene Expression Studies

Polymerase chain reaction (PCR) buffer, expand reverse transcriptase (RT) buffer, expand RT, dithiothreitol (DTT) and Taq DNA Polymerase (Taq) were obtained from

Roche Molecular Biochemicals, East Sussex, UK. dNTPS were obtained from Advanced Biotechnologies Limited, Epsom, Surrey, UK. Agarose (electrophoresis grade) and ethidium bromide solution (10mg/ml) and primers were obtained from Gibco/BRL, Life Technologies, Paisley, Scotland. RQ1 ribonuclease (RNase)-free deoxyribonuclease (DNase), RNasin® ribonuclease inhibitor were obtained from Promega UK Limited, Southampton, UK. 123bp DNA ladder, gel loading solution, mineral oil, Polaroid 667 photographic film, diethyl dicarbonate (DEPC), boric acid, TRIZMA® Base (Tris[hydroxymethyl]aminomethane), and ethylenediaminetetraacetic acid, (EDTA) were obtained from Sigma-Aldrich Company Limited, Poole, Dorset, UK. PCR tubes (0.2ml), Techne Dri-Block DB•2A heating block, Techne Progene PCR machine and all RT grade filter tips were obtained from Appleton Woods Limited, Birmingham, UK. Eppendorf Centrifuge 5415D was obtained from Helena Biosciences, Sunderland, UK. mRNA direct kit, sample mixer and MPC®-E were obtained from Dynal (UK) Limited, Wirral, Merseyside. Needles (21 and 25 gauge), syringes (1ml) and RNase DNase free centrifuge tubes (1.5ml) were obtained from Fisher Scientific UK, Loughborough, Leicestershire, UK. Polaroid gel cam, electrophoresis hood, 312nm transilluminator table and horizontal gel tank were obtained from Flowgen, Shenstone, UK.

2.1.9 Preparation of stock solutions

all trans-Retinoic acid (RA), dimethyl sulfoxide (DMSO), amyloid β peptide (Aβ), fragments 25-35 and 1-42, L-ascorbic acid (AA),PBS (0.02M) tablets and nerve growth factor (NGF-7S) from Mouse Submaxillary Glands, deferoxamine mesylate (DFX) and PBS (0.02M) tablets were obtained from Sigma-Aldrich Company Limited, Poole, Dorset, UK. Foetal Bovine Serum was obtained from Gibco/BRL, Life Technologies

Limited, Paisley, Scotland. Human Brain Derived Neurotrophic Factor (hBDNF) produced in *E.coli* was obtained from TCS Cell Works Limited, Buckinghamshire. ^{14}C labelled ascorbic acid was obtained from Amersham, Uppsala, Sweden.

2.1.10 Investigations into the effects of nitroxybutyl ester of flurbiprofen (NO-FB) & novel compounds on PC12 cells

PC12 rat pheochromocytoma cells, ECACC No. 88022401 were obtained from ECACC, Salisbury, Wiltshire, UK. RPMI 1640 medium with Glutamax I, Penicillin Streptomycin (10000U/10000μg), horse serum, foetal bovine serum and trypsin-EDTA and Nunc Immunosorb 96 well plates were obtained from Gibco/BRL, Life Technologies Limited, Paisley, Scotland. Collagen type 1, crystal violet, propidium iodide, sodium citrate (trisodium salt:dihydrate), glycerol, phenylmethylsulphonyl fluoride (PMSF), aprotinin, pepstatin, leupeptin, dithiothreitol (DTT), ethylenediaminetetraacetic acid (EDTA), sodium dodecyl sulphate (SDS), PBS tablets (0.02M), Bicinchonic Acid protein assay kit (BCA-1), sodium hydrogen carbonate, 2,4-dinitrophenylhydrazine (DNPH), hydrochloric acid, polyoxyethylenesorbitan monolaurate (Tween-20) (molecular biology grade), hydrogen peroxide (H_2O_2) 30% solution (8.8M), di-sodium hydrogen phosphate, o-phenylenediamine tablets (20mg substrate per tablet), sodium chloride, potassium chloride, 2,2'-Azobis(2-methylpropionamidine) dihydrochloride (AAPH), anti-DNP antiserum mouse IgE were obtained from Sigma-Aldrich Company Limited, Poole, Dorset, UK. Peroxidase labelled rat anti-mouse IgE heavy chain was obtained from Serotec Limited, Oxford, UK. Sodium carbonate, potassium di-hydrogen ortho phosphate, glacial acetic acid, chloroform, citric acid, methanol and sulphuric acid were obtained from Fisher Scientific UK, Loughborough, Leicestershire, UK. All tissue culture plastics were obtained from Triple Red Limited, Thame, Oxfordshire, UK. Labsystems Wellwash 4

Mark 2 Plate Washer and a 20 – 50°C bench top incubator (Hand warmer) was obtained from thermo Life Sciences, Hampshire, UK. Pasteur pipettes, centrifuge tubes (1.5ml) and aluminium foil were obtained from Appleton Woods Limited, Birmingham, UK. Flow cytometry tubes were obtained from Elkay Lab Products, Basingstoke, Hampshire, UK. Caspase substrate Ac-Asp-Glu-Val-Asp-7-amido-4-methylcoumarin was obtained from Alexis Biochemicals, Nottingham, UK. Eppendorf centrifuge 5415D was obtained from Helena Biosciences, Sunderland, UK. A Victor and multilable counter and microtitre plate reader were employed. Flow check fluorospheres, Cleanze solution, Isoton II and a fluorescence activated cell sorter (FACS) -EPICS®XL-MCL were obtained from Beckman Coulter, High Wycombe, UK. Flurbiprofen (FB), nitroflurbiprofen (NO-FB) and the novel compounds NCX 2216 (trans 3-[4-2-fluoro-α–methyl-1-(1,1'-biphenyl)-4-acetyloxy]-3-methoxyphenyl]-2-propenoic acid 4-(nitrooxy)butyl ester were obtained from NicOx SA, Sophia Antipolis, France.

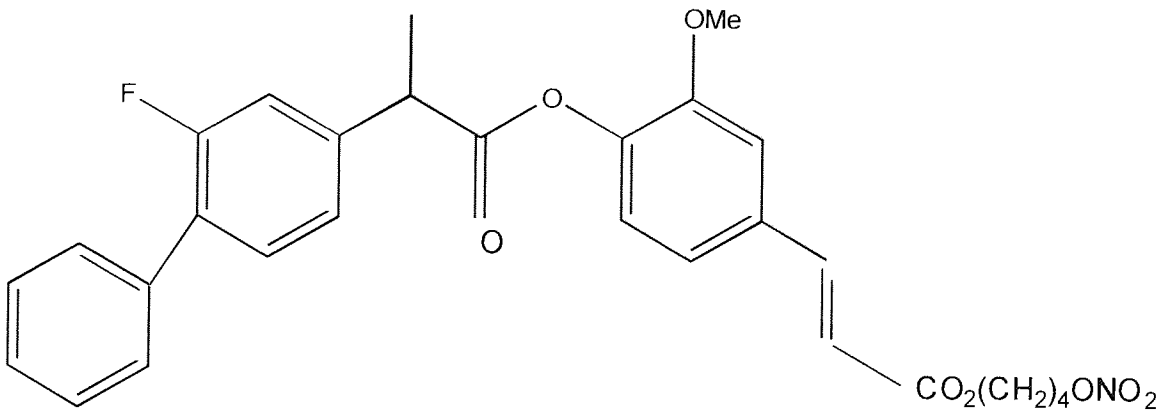

Figure 2.1 Structure of NCX 2216

2.1.11 Data analysis and statistics

All data analysis and statistical comparisons were performed using GraphPad Prism version 3.00 for Windows and GraphPad Instat version 3.00, GraphPad Software, San Diego, California, USA, www.graphpad.com.

Data sets were entered into Instat and the differences between experimental and control conditions were assessed by unpaired t-tests, one-way analysis of variance (ANOVA), repeated measures analysis of variance (ANOVA), Dunnett's multiple comparison tests and coefficients of variation.

2.2 METHODS

2.2.1 Cell culture

2.2.1.1 Cell lines

The cell lines used for the experiments described herein were rat adrenal pheochromocytoma PC12 (between passages 5 and 26) and human neuroblastoma SH-SY5Y (between passages 15 and 38).

2.2.1.2 Maintenance of Cell Lines

PC12

PC12 cells were routinely cultured in $75cm^3$ flasks in a water jacketed humidified 5% CO_2 incubator with maintenance media. (RPMI 1640 media with Glutamax I; 10% (v/v) HS, 5% (v/v) FBS, penicillin (0.5U/ml) and streptomycin (0.5mg/ml). Every 2-3 days, spent PC12 cell media was removed and replaced with fresh maintenance media, which had been pre-warmed to 37°C. Cells were passaged once a week, as described in section 2.2.1.3, when the cells were at a density of approximately 5×10^6 per ml.

SH-SY5Y cells

SH-SY5Y cells were routinely cultured in RPMI 1640 media with Glutamax I containing 5% (v/v) FBS, penicillin (50000 units per 500ml), streptomycin (50000µg per 500ml) and 1% non-essential amino acids (NEAA) solution. As described previously, the maintenance media was replaced every 2-3 days with media pre-warmed to 37°C, until the SH-SY5Y cells were 90% confluent. At this point, cells were passaged as described in section 2.2.1.4.

2.2.1.3 Passage of PC12 cells

Cells were harvested and centrifuged at 182 x g for 5 minutes at 22 - 25°C in a Sigma 2-15 centrifuge. The supernatants were removed and the cell pellet manually agitated and resuspended into maintenance media (10ml). An aliquot was taken for counting using a haemocytometer and cells were seeded into a 75cm^3 flask (25ml of 2 x 10^5 cells per ml).

2.2.1.4 Passage of SH-SY5Y cells

Maintenance media was removed from flasks and replaced with PBS (5ml). Rotation of the solution around the base of the flask ensured that all cells were soaked to remove remaining media. The PBS was replaced with trypsin-EDTA (2.5ml of 1x liquid, (0.5g/l trypsin (1:250) + 0.2g/l EDTA in HBSS without Ca^{2+} and Mg^{2+}). The flask was then incubated at 37°C for approximately 5 minutes. The flask was manually agitated to ensure that the cells had separated from the surface of the flask. To prevent further action of the trypsin on the cells, maintenance media (22.5ml) was added to the flask and thoroughly mixed with the trypsinised cells. The cells were centrifuged at 182 x g for 5 minutes at 22 - 25°C in a Sigma 2-15 centrifuge. The supernatants were removed and the cell pellet manually agitated and resuspended into 10ml of maintenance media. An aliquot was taken for counting using a haemocytometer and cells were seeded into a 75cm^3 flask (25ml of 2 x 10^5 cells per ml).

2.2.1.5 Cell Counts

Cells were split, centrifuged and resuspended in media (10ml). Trypan Blue (15µl) was added to cell suspension (15µl) and mixed by aspiration. 15µl of the mixture was transferred to both chambers of a haemocytometer. The chambers were allowed to fill using capillary action. Live cells actively exclude the dye, the number of blue cells

(dead) were counted as a percentage of the number of total cells. All the cells were counted in the 1mm centre square and four 1mm corner squares. This was repeated twice for each sample. Each square of the haemocytometer with cover slip in place represents a total volume of $0.1mm^3$. The cell concentration was the then determined by:

Cells per ml = average count per square x dilution factor x 10^4.

E.g If the average count per square is 20, the dilution factor is 2, the cells per ml of this solution would be:

$20 \times 2 \times 10^4 = 400000$cells per ml $= 4 \times 10^5$ cells per ml

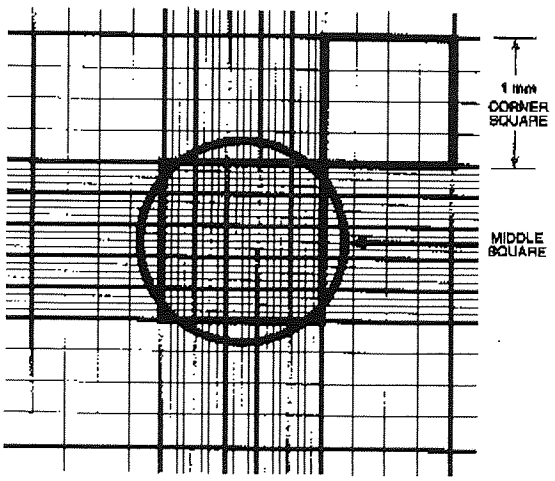

Figure 2.2
Standard Haemocytometer Chamber taken from Sigma Technical Information Resources

When counting only cells touching the top and left middle line were counted, cells touching the middle line on the bottom and the right were not counted.

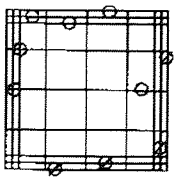

Figure 2.3 Corner Square (Enlargement) taken from Sigma Technical Information Resources

2.2.1.6 Cell Viability

Cells were only used for experiments with a viability of 90 – 95%. Total cell viability was calculated by:

Total viable cells (unstained) ÷ Total cells (unstained and stained) x 100

2.2.1.7 Differentiation of SH-SY5Y cells

Cells (40ml of $1x10^5$ cells per ml) were seeded into a $150cm^3$ flask in complete medium. Flasks were incubated for 24 hours at 37°C in a 5% CO_2 humidified atmosphere. The medium in the flasks was then changed to 1% FBS medium (80ml) and either DMSO (40µl) or retinoic acid (40µl of 3mg/ml in DMSO) was added. Medium was then subsequently changed every 48 hours with the addition each time of either DMSO or RA (40µl). After 9 days, cells were harvested by trypsinization and examined for differentiation.

2.2.1.7.1 Trk B ELISA of differentiated SH-SY5Y cells

A marker of differentiation in SH-SY5Y cells is expression of the Trk B receptor. An ELISA was developed against Trk B, in order to determine whether differentiation had occurred. Samples were diluted to 0.15mg/ml with coating buffer (15mM sodium carbonate, 35mM sodium hydrogen carbonate, pH9.2), plated out into separate microtitre plate wells in triplicate (50µl per well) and the plates covered. Plates were then incubated for 16 hours at 4°C. The antigen solution was removed by flicking and the plate was slapped dry. Blocking buffer (200µl of 0.2M PBS containing 1% BSA and 0.02% sodium azide) was added to block any non-specific protein binding for 1.5 hours at 22 - 25°C. Blocking buffer was removed by flicking and the plate slapped dry. The plate was then washed with washing buffer (250µl of 0.2M PBS with 0.02%

sodium azide) and slapped dry. Primary antibody, anti-Trk B rabbit polyclonal IgG diluted 1:100 and 1:250 in blocking buffer (50µl) was added to each well and incubated for 1 hour at 22 - 25°C. Plates were washed with a plate washer containing 0.02M PBS with 0.05% Tween-20. The plate was then slapped dry. Alkaline phosphatase conjugated secondary antibody, anti-rabbit IgG (whole molecule) diluted 1:100 in blocking buffer (50µl) was added to each well and incubated for 1 hour at 22 – 25 °C. Plates were washed as above, and agitated. The plate was then washed once with diethanolamine buffer (200µl per well of 10mM diethanolamine, 0.5mM magnesium chloride, pH 9.5) and agitated. Substrate was then added to each well (50µl of 1 SIGMA 104 tablet dissolved in diethanolamine buffer (5ml)) and plates were incubated in the dark for 25 minutes at 22 - 25°C. The colour reaction was stopped in each well by the addition of EDTA (50µl of 0.1M, pH 7.5). The absorbance of the plate was then read with a test filter of 410nm and a reference filter of 490nm.

2.2.1.8 Freezing cells

Cells ($5x10^6$ cells) were resuspended into 1.5ml freezing media (90% (v/v) FBS and 10% (v/v) DMSO). Cells were incubated at 0 - 4°C for 15 minutes before storage at -70°C for 24 hours, before indefinite storage of the cryo vials at -196°C in a cell bank liquid nitrogen facility.

2.2.1.9 Resuscitation of a cell line from frozen stocks

Frozen cell culture stocks were thawed rapidly at 37°C and the cells added to pre-warmed maintenance media (7.5ml) in a $25cm^3$ flask. Cells were incubated at 37°C and media changed every 48 hours for a week before use.

2.2.2 3-(4,5-dimethylthiazol-2-yl)-2,5-diphenyltetrazolium (MTT) assay

Cells ($2x10^5$ cells per ml, 100µl per well) were seeded into 96 well flat bottomed microtitre plates. Control wells consisted of complete medium (no cells) and exposed to the same conditions/additions as the cell containing wells, or untreated cells. Two hours prior to completion of the experiment, MTT solution (25µl of 5mg/ml in 0.01M PBS) was added to all wells including blanks. Plates were then incubated for a further 2 hours at 37°C, 5% CO_2. Lysis buffer (100µl of 20% w/v SDS, in DMF (50%), dH_2O(50%), pH 4.7 adjusted with 2.5% of 80% glacial acetic acid) was then added to each well and the plates incubated for a further 16 hours at 37°C, 5%CO_2. The absorbance of the each well was then read at 570nm in a 96 well plate reader.

2.2.3 Microscopy

2.2.3.1 Video Microscopy

A digital camera was attached to the inverted microscope by means of the appropriate attachments provided with the video camera, this allowed images to be taken of cell flasks and well plates. Images were captured using the software package CineMaker and saved as device independent bitmaps.

2.2.3.2 Fluorescence Microscopy

Cells ($2x10^5$ cells/ml) were used for all experiments. At the endpoint of each experiment minus 15 minutes, Hoechst 33342 solution (5.53µl of 1mg/ml in DMSO) was added. Plates were further incubated for 15 minutes at 37°C in a 5% CO_2 humidified atmosphere, cells were then harvested by scraping and aspirated into 1.5ml centrifuge tubes. Tubes were then centrifuged at 6600 x g for 1.5 minutes in an Eppendorf Centrifuge 5415D. Prior to visualisation under the microscope the

supernatants were aspirated with a Pasteur pipette and the pellets were resuspended into Propidium Iodide solution (10μl of 1mg/ml in PBS). The pellet was resuspended by aspiration (4 times), before being transferred to a glass slide. A glass cover slip was then placed on top and the slides viewed, employing an UV wavelength light source attached to the microscope to visualise the dyes. Slides were viewed using the x 40 objective lens and with the x 10 objective giving a total magnification of x 400. Photographs were taken using a 10 (or 20 for fields with a high percentage of PI stained cells) second exposure by means of a manual shutter release button. After E6 film processing colour reversal prints were produced.

The number of cells that had taken up each dye was scored by eye to calculate the percentage of cells that had stained positively with propidium iodide versus total staining.

2.2.4 Flow Cytometry

2.2.4.1 Propidium Iodide Staining

Cells ($2x10^5$ per ml) were harvested and centrifuged at 6600 x g for 1.5 minutes. Supernatants were removed using Pasteur pipettes, then the cell pellets were washed with PBS prior to centrifugation at 6600 x g for 1.5 minutes. PBS was removed and propidium iodide (PI) solution (200μl) was added to the cell pellets. Tubes were foil wrapped and left at 0 - 4°C for 16 hours before being agitated with a Gilson pipette and transferred to a flow cytometry tube. Samples were then immediately run through a flow cytometer with the intensity of light scatter and the FL3 fluorescence emitted between 605 and 635nm. Following excitation at 488nm (argon laser) the number of events and their fluorescence were recorded for individual nucleoids. The median was

calculated for 17,000 nucleoid events unless otherwise stated. The histograms were then gated to determine the position in the cell cycle nucleoids. Apoptotic nucleoids were calculated as a percentage of the total nucleoids measured.

2.2.4.2 DCFDA staining

Cells ($2x10^5$ per ml, 2ml) were incubated with test agents in 35mm well plates. 30 minutes before the end of incubation DCFDA solution (200µl of 7.5mM diluted from a 75mM stock in PBS) was added to the plates. After exactly 30 minutes cells were immediately harvested with a Gilson pipette and a rubber policeman and transferred to a flow cytometry tube. Samples were then immediately run through a Coulter EPICS flow cytometer with the intensity of light scatter and the FL1 fluorescence emitted between 505 and 535nm. Following excitation at 488nm (argon laser) the fluorescence were recorded for individual nucleoids. After positive analysis of control untreated cells, positive analysis was removed and the median X was calculated for 10,000 nucleoid events.

2.2.5 Glutathione Assays

2.2.5.1 Glutathione (GSH) Assay

Glutathione (GSH), reduced standards were freshly prepared for each experiment from a stock (100mM in sterile distilled water) and prepared as shown in table 2.1. Cells ($2x10^5$) were then harvested and centrifuged in a 1.5ml eppendorf tube in an Eppendorf Centrifuge 5415D for 6600 x g for 1.5 minutes. Supernatants were then removed and PBS (1ml) added to wash the pellet. Tubes were recentrifuged at 6600 x g for 1.5 minutes and the PBS was then removed, making sure to leave the pellet dry. SSA (3.33µl of 1% made up in distilled water) was then added to precipitate the protein and the tubes were immediately centrifuged at 13000 x g for 1.5 minutes. Stock buffer

(96.6µl of 125mM sodium phosphate, 6.3mM disodium EDTA, pH 7.5 autoclaved) was then added to each tube. Standards and samples (25µl) were then aliquoted into a flat bottomed plates (96 well) in triplicate, the remaining aliquot was immediately frozen at -70°C for later use in the GSSG assay. Daily buffer (150µl of 0.3mg NADPH/ml stock buffer) and DTNB solution (50µl of 6mM DTNB in daily buffer) was then added to all wells. The plate was then loaded onto the carriage of a 96 well plate reader and glutathione reductase solution (25µl of 20U/ml) was then added as quickly as possible to initiate the reaction. The OD was then recorded every minute for 5 minutes at 410nm.

Concentration GSH/well (µM)	**Amount GSH (nmols/well)**	**Volume added GSH (µl) (100mM stock)**	**Volume added SSA (µl) (1%)**	**Volume added Stock Buffer (µl)**
0	0	0	33.3	967
20	0.5	0.2	33.3	966.8
40	1.0	0.4	33.3	966.6
60	1.5	0.6	33.3	966.4
80	2.0	0.8	33.3	966.2
100	2.5	1.0	33.3	966

Table 2.1 Reduced glutathione standard composition

2.2.5.2 Glutathione (GSSG) Assay

Oxidised glutathione (GSSG) standards were freshly prepared for each experiment from an oxidised glutathione stock (1.5µM in sterile distilled water) as shown in table 2.2.

Std. name	Conc. (nmol/well)	Volume added GSSG Stock (1.5μM) or other standard as stated	Volume added SSA (1%) (μl)	Volume added d.H_2O (μl)
A	0	0μl	33.3	967
B	0.0009375	50μl of C	3.3	46.7
C	0.001875	50μl of D	3.3	46.7
D	0.00375	50μl of E	3.3	46.7
E	0.0075	50μl of F	3.3	46.7
F	0.015	10μl of H	3.3	46.7
G	0.075	50μl of H	3.33	46.7
H	0.15	100μl	33.3	867

Table 2.2 Oxidised glutathione standard composition

The remaining 25μl aliquot from the GSH assay was employed for this assay. To the frozen aliquot and standards (25μl), 2-VP (0.5μl) and TEA (0.5μl) were added. Samples and standards were then vortexed and centrifuged for 30 seconds at 13000 x g. Aliquots of standards and samples (10μl) were then plated out into a microtitre plate (96 well plate). Daily buffer (75μl of 0.3mg NADPH/ml stock buffer) and DTNB solution (25μl of 6mM DTNB in daily buffer) were added to the wells. The plate was then loaded onto the carriage of a 96 well plate reader and glutathione reductase solution (12.5μl of 20U/ml) was then added as quickly as possible to initiate the reaction. The OD was then recorded every minute for 5 minutes at 410nm.

2.2.6 Estimation of Protein Concentration

Protein concentrations were assessed according to a modified version of Sigma Procedure No. TPRO-562, based on the method of Smith *et al.*, (1985). Protein standards of six concentrations were prepared from the protein standard solution (bovine serum albumin, 1mg/ml) diluted in coating buffer (15mM sodium carbonate, 35mM sodium hydrogen carbonate, pH 9.2) as stated in Table 2.3.

Standard Number	Volume added of Coating Buffer (µl)	Volume added of Protein Standard Solution (µl)	Protein Concentration (µg/well) (µg/10µl)
1	10	0	0
2	8	2	2
3	6	4	4
4	4	6	6
5	2	8	8
6	0	10	10

Table 2.3 Composition of BCA standards

Each standard (10µl) was plated out in triplicate into a 96 well flat bottomed microtitre plate. Unknown samples (10µl) were also plated out in triplicate. Samples were prepared by harvesting cells, and centrifuging the cell suspensions at 6600 x g for 1.5 minutes in an Eppendorf Centrifuge 5415D the supernatants were then removed and 1ml PBS added to wash the cell pellets, the cell pellets were then recentrifuged at 6600 x g for 1.5 minutes, the PBS removed and the pellets were fully resuspended in coating buffer (200µl).

Bicinchoninic acid solution (200µl) containing copper (II) sulphate pentahydrate 4% solution (50:1) was then added to all wells (samples and standards), the plate was then incubated at 37°C for 30 minutes. The absorbance of the plate was then measured at 570nm in a 96 well plate reader.

Unknowns were calculated from a standard curve prepared by plotting the absorbances of the standards against protein concentration using the software package GraphPad PRISM. Then employing linear regression conducted by GraphPad PRISM, the equivalent protein concentration of the unknowns were calculated by cross-reference to the standard curve generated.

2.2.7 Protein Carbonyl determination by Enzyme Linked Immunosorbent Assay (ELISA)

2.2.7.1 Preparation of Carbonyl Standards

For reduced BSA, BSA (10mg/ml) in PBS (50ml) was reduced for 16 hours at 4°C with sodium borohydride (1g), any foam was reduced to solution with acetone (0.5ml). The pH of the solution was then adjusted with concentrated hydrochloric acid to 7.4, with foaming reduced by addition of acetone. For oxidised BSA, BSA (10mg/ml) in PBS (50ml) was oxidised with AAPH (50mM) for 16 hours at 37°C.

Reduced and oxidised BSA solutions were then desalted through PD10 columns to remove any excess reducing and oxidising agents. The protein concentrations of both oxidised and reduced BSA solutions were assessed by the BCA assay and both were sterile filtered and diluted to 2mg/ml. The solutions were then mixed in ratios to give a range of samples (10ml reduced and 0ml oxidised, 9ml reduced and 1ml oxidised etc.)

Each sample (500µl) was then added to DNPH (500µl of 10mM) and left for 1 hour on a sample mixer at 22 - 25°C. Controls were also set up consisting of sample (500µl) and HCl (500µl of 2N) instead of DNPH. TCA (500µl of 20%) was then added to each sample and control and vortexed for 30 seconds, the samples and controls were then centrifuged at 13000 x g for 3 minutes. The supernatants were then discarded and the pellet washed 3 times with ethanol: ethyl acetate solution (1:1) until the final wash was colourless. The pellets were left 5 minutes in each wash. After washing, the pellets were then resuspended fully in guanidine HCl (1ml of 6M) and after vortexing the tubes were incubated at 37°C for 20 minutes, tubes were revortexed and incubated for a further 10 minutes at 37°C. The solutions were then assessed and if the pellets were fully resuspended the absorbance of the solutions (both samples and controls) were read at 360nm by a spectrophotometer. The molarity of the solution was calculated by taking the OD of the sample – OD of the corresponding blank divided by 22000 (extinction coefficient). The amount of carbonyl in nmol per mg protein was then determined by dividing by the initial concentration of protein employed in the carbonyl standards in mg/ml.

Figure 2.4 Worked example of carbonyl determination of a newly prepared Standard

Oxidised (1ml) and reduced (9ml) protein solutions (2mg/ml) were mixed after preparation. The OD of the standard and the blank were measured at 360nm giving values of 0.106 and 0.006 respectively.

The corrected OD was divided by the extinction coefficient to give the molarity of the solution.

$$0.100 \div 22000 = 0.000004545 \text{ M}$$

$$= 4.545 \text{ µmol/l}$$

$$= 4.545 \text{ nmol/ml}$$

The solution was at a protein concentration of 2mg/ml, therefore the carbonyl value has to be divided by 2 to give a carbonyl value in nmol/mg protein.

4.545 ÷ 2 = 2.2725 nmol carbonyl / mg protein

2.2.7.2 Protein Carbonyl Enzyme Linked ImmunoSorbent Assay (ELISA)

Standards and samples were diluted to 0.02mg/ml with coating buffer (15mM sodium carbonate, 35mM sodium hydrogen carbonate, pH9.2), plated out into separate microtitre plate wells in triplicate (50µl per well) and the plates covered. Plates were then incubated for 1 hour at 37°C. Plates were washed three times by means of a plate washer containing PBS and (v/v) 0.05% Tween-20. Plates were then agitated to remove any remaining liquid. 2,4-dinitrophenylhydrazine (50µl of 1mM in 2N HCl) was then added for 1 hour at 22 - 25°C to all wells. Plates were then washed as above, agitated and then blocked for 16 hours at 0 - 4°C with blocking buffer (250µl of 1% (v/v) Tween-20 in PBS). Plates were then washed as above, agitated and primary antibody, (mouse-anti-DNP antiserum) diluted 1:1000 in blocking buffer (50µl) was added to each well and incubated for 2 hours at 37°C. Plates were then washed as above, agitated and peroxidase labelled secondary antibody, (rat anti mouse IgE) diluted 1:5000 in blocking buffer (50µl) was added to each well and incubated for 1 hour at 37°C. Plates were washed as above, agitated and the substrate was added (50µl of 10ml 0.15M citrate-phosphate buffer, pH 5.0, 8µl H_2O_2 and 20mg of o-phenyldiamine as a tablet) to each well and plates were incubated in the dark for 15 minutes at 22 - 25°C. The colour reaction was stopped in each well by the addition of H_2SO_4 (50µl of 2M). Absorbance was read at 490nm in a micro plate reader.

2.2.8 Gene Expression Studies

2.2.8.1 mRNA EXTRACTION

DEPC treatment of glassware; glassware was thoroughly washed and then soaked in a 10% solution of heavy duty household bleach for 30 minutes. The bleach solution was then removed and the glassware was filled with distilled water, DEPC was then added at concentration of 0.1%, glassware was then foil covered and left for 24 hours at 22 - 25°C. The DEPC treated water was then sent for autoclaving to break down DEPC to facilitate disposal, and the foil covered glassware autoclaved.

Sterile conditions were employed throughout, consisting of the following measures - Only RNase and DNase free filter tips and double gloves were used. All work areas were wiped down with 70% ethanol, and all 1.5ml centrifuge tubes and PCR tubes were autoclaved in DEPC sterilized glassware.

Cells ($2x10^5$) were harvested into a RT grade centrifuge tube (1.5ml). Cells were centrifuged for 1.5minutes at 13000 x g in an Eppendorf Centrifuge 5415D. Supernatants were removed and PBS (1ml) added, cells were centrifuged for another 1.5minutes at 13000 x g and the PBS removed. The extraction was carried out using the Dynal mRNA direct kit protocol. Pellets were resuspended into 200µl Dynal lysis/binding buffer (100mM Tris-HCl, pH 7.5, 500mM LiCl, 10mM EDTA, pH8.0, 1% LiDS and 5mM DTT) and aspirated twenty times to fully resuspend each pellet with fresh tips being used for each tube. The solution was then aspirated five times using 1ml sterile syringes and sterile 21 gauge needles to shear the DNA. This was then repeated using 1ml sterile syringes and sterile 25 gauge needles. Tubes were then centrifuged for 1 minute at 13000 x g in an Eppendorf Centrifuge 5415D. Resuspended

Dynal Oligo $(dT)_{25}$ beads (30µl) were washed in Dynal lysis/binding buffer twice before being added to each tube of lysed cells. The tubes were then mixed on a Dynal sample mixer for 5 minutes at 22-25°C. Tubes were then magnetised on the Dynal MPC®-E magnet (Magnetic particle concentrator for microtubes of Eppendorf type (1.5ml)) and the colourless solution removed. Dynal wash buffer A (200µl of 10mM Tris-HCl, pH 7.5, 0.15M LiCl, 1mM EDTA, 0.1% LiDS) was then added to the pellet and the cells resuspended in it. The tubes were then remagnetised the colourless solution removed and Dynal wash buffer A added (200µl) and the cells resuspended. The process was then repeated using Dynal wash buffer B (200µl of 10mM Tris-HCl, pH 7.5, 0.15M LiCl, 1mM EDTA). After two washes with wash buffer B the cell pellet was resuspended in DEPC treated water (30µl of 0.1%). This was then transferred to a fresh tube (1.5ml), and master mix was added (39µl of 10mM DTT (7.5µl of 100mM), 1mM dNTPs (7.5µl dNTP mix), 25U RNAsin (1.8µl), 1U (3µl) RQ1 RNase-free DNase, 0.1% DEPC treated water (4.2µl) and Expand buffer (15µl)). Each tube was aspirated twice and incubated at 37°C for 60 minutes. DNase was heat inactivated at 70°C for 10 minutes in a preheated dry heating block. Samples were then centrifuged at 13000 x g for 1 minute in an Eppendorf centrifuge 5415D.

2.2.8.2 RT-PCR

Two RT grade PCR tubes were labelled for each sample, one positive and one negative. RNAsin 15U (1µl) was added to the negative tubes and 30U (2µl) to the positive tubes, mRNA extraction product (46µl) was added to the positive tubes and mRNA extraction product (23µl) was added to the negative tubes. Expand RT 50U, (1µl) was then added to the positive tubes. For reverse transcription mRNA was incubated at 37°C for 1 hour

in Expand RT buffer containing 10mM DTT, 1mM dNTPs, 25U RNAsin, 1U RQ1 RNase-free DNase. DNase was heat inactivated at 70°C for 10 minutes. The samples were then incubated at 42°C for 1 hour before being stored in the short term at 0 - 4°C, and at -20°C in the long term.

2.2.8.3 Primers

The primers (50nmol of each) as stated in table 2.4 were synthesised by Gibco/BRL, Life Technologies, Paisley, Scotland. Each primer was diluted to 100 pmol/µl in sterile 1 x TE buffer (10mM Tris, 1mM EDTA, pH 8.0), and then further diluted tenfold in 1 x TE buffer and stored as 10µl aliquots at -20°C.

2.2.8.3.1 Primer Sequences

Primer	Forward primer sequence (5' – 3')	Reverse primer sequence (5'-3')	Reference
GAPDH	AGA ACA TCA TCC CTG CCT C	GCC AAA TTC GTT GTC ATA CC	Hall et al., 1998
β- Actin	GTG GGG CGC CCC AGG CAC CA	CTC CTT AAT GTC ACG CAC GAT TTC	Ray et al, 2000
BAX	GCA GGG AGG ATG GCT GGG GAG A	TCC AGA CAA GCA GCC GCT CAC G	Ray et al, 2000
GCS	CCT TCT GGC ACA GCA CGT TG	TAA GAC GGC ATC TCG CTC CT	El Mouatassium et al., 2000
GPX	CCT CAA GTA CGT CCG ACC TG	CAA TGT CGT TGC GGC ACA CC	El Mouatassium et al., 2000

Table 2.4 Sequences of the primers used

2.2.8.4 Polymerase Chain Reactions

PCR was performed in PCR buffer with sterile water, 200mM dNTPs and 10pmol of each primer. All reactions were covered in a drop of mineral oil and hot start conditions were used, full details of each PCR as stated in table 2.5. Reactions were initiated with 2.5U (0.5µl) Taq DNA Polymerase. All liquid handling was conducted using filter tips.

2.2.8.4.1 Optimal PCR Conditions

PRIMER	CONDITIONS	CYCLES
GAPDH	98°C 3 minutes + Taq 60°C 2 minutes 72°C 2 minutes ..... 94°C 30 seconds 60°C 30 seconds 72°C 30 seconds ..... 94°C 30 seconds 60°C 30 seconds 72°C 4 minutes	1 cycle 26 cycles 1 cycle
GPX	94°C 1 minute 94°C 45 seconds + Taq 56°C 1 minute 72°C 2 minutes ..... 94°C 45 seconds 56°C 1 minute 72°C 1 minute ..... 72°C 10 minutes	1 cycle 27 cycles 1 cycle
GCS	94°C 1 minute 94°C 45 seconds + Taq 56°C 1 minute 72°C 1 minute ..... 94°C 45 seconds 56°C 1minute 72°C 1minute ..... 72°C 10 minutes	1 cycle 31 cycles 1 cycle

PRIMER	CONDITIONS	CYCLES
BAX	94°C 4 minutes 94°C 1 minute +Taq 65°C 1 minute 72°C 1 minute ..... 94°C 1 minute 65°C 1 minute 72°C 1 minute ..... 72°C 10 minutes	1 cycle 29 cycles 1 cycle
β-ACTIN	94°C 1 minute 94°C 45 seconds + Taq 67°C 1 minute 72°C 1 minute ..... 94°C 45 seconds 67°C 1 minute 72°C 1 minute ..... 72°C 10 minutes	1 cycle 35 cycles 1 cycle

Table 2.5 Optimal PCR Conditions for PC12 derived RT products

2.2.8.5 Agarose gel electrophoresis of PCR products

Gel loading solution (2.5µl of 0.05% w/v bromophenol blue, 40% w/v sucrose, 0.1M EDTA, pH 8.0) was added to the PCR reaction products (10µl). Samples were loaded onto 1.5% agarose gels made up in 1 x TBE (89mM Tris, 89mM boric acid, 2.5mM EDTA, pH 8.0, 100ml Gel). Gels were electrophoresed at 80V for 2 hours in 350ml 1 x TBE. Post staining was achieved with ethidium bromide (10µl of a 10mg/ml solution) dissolved into 100ml of distilled water for 15 minutes in the dark at 22 - 25°C. Gels were visualised on an U.V. transilluminator table at 312nm. Photographs were taken using both a Polaroid Gel Cam with a 0.8 x electrophoresis hood and Polaroid 667 film using an aperture setting of 4.5 and a shutter speed of ¼. Expression levels were quantitated using the software package Phoretix 1D Advanced, Version 4.01 (Non

Linear Dynamic Limited) and normalised to GAPDH. Gels were all loaded with a size ladder, usually a 123bp DNA ladder prepared according to manufacturer's instructions.

2.2.9 Preparation of stock solutions

2.2.9.1 Retinoic acid for SH-SY5Y differentiation

RA (100mg) was reconstituted into 33.26ml of DMSO. This stock solution was then stored as 200µl aliquots at -20°C. A fresh aliquot was used for each differentiation experiment.

2.2.9.2 Amyloid β peptide, fragment 25-35

Aβ (1mg) was dissolved into 1ml DMSO giving a stock solution of 940µM. This was stored at -20°C. For aging, the peptide was incubated at 37°C for 24 hours.

2.2.9.3 Amyloid β peptide, fragment 1-42

Aβ (0.1mg) was dissolved into 100µl of sterile distilled water giving a stock of 221.5µM. This was stored at -20°C. For aging the peptide was incubated at 37°C for 24 hours.

2.2.9.4 Ascorbic Acid (Vitamin C)

A stock was made up fresh each time for an experiment. The working stock made up each time was 0.08805g dissolved into 50ml autoclaved 0.02M PBS. The stock was then sterile filtered and diluted accordingly in 0.02M PBS.

2.2.9.5 Nerve Growth Factor (NGF)

On reconstitution 1 vial of NGF (100μg) was dissolved into 10ml of 10% (v/v) FBS in PBS giving a stock solution of 10μg/ml. This stock solution was then aliquoted (200μl) and stored at -20°C. A new aliquot was employed in each NGF experiment, aliquots were not refrozen. NGF working solutions were diluted in 10% (v/v) FBS in PBS.

2.2.9.6 Human Brain Derived Neurotrophic Factor (hBDNF)

hBDNF (1μg) was reconstituted in sterile distilled water and then aliquoted (10μl) and stored at -70°C for a maximum of six weeks

2.2.9.7 Deferoxamine mesylate

Deferoxamine mesylate was reconstituted in sterile 0.02M PBS to 100mM and stored at -20°C in working aliquots.

2.2.10 Ascorbic Acid Uptake

2.2.10.1 Preparation of Ascorbic Acid

^{14}C radiolabelled ascorbic acid was dissolved at 1mg/ml with a specific activity of 1.85MBq/ml. Unlabelled ascorbic acid was dissolved at 10.75mg/ml. Through calculation it was determined for every 250μl, 50μl of radiolabelled ascorbate was required to achieve a radiolabelled 2.2mg solution of ascorbate.

Unlabelled cold AA	10.75 mg/ml	200 μl	2.15 mg
^{14}C labelled AA	1 mg/ml	50 μl	0.05 mg
		250 μl	2.2 mg

Therefore in 1ml there will be 8.8mg of ascorbic acid, this is at a concentration of 50mM, which represents a 100x stock solution, termed 'A' in Table 2.6. Solutions were then prepared as in table 2.6, in order for 10µl to be added to each well as in table 2.7.

Solution Name	^{14}C labelled	PBS
A	Only stock solution used	-
B	125µl of solution A	292µl
C	280µl of solution B	140µl
D	250µl of solution C	250µl
E	300µl of solution D	200µl

Table 2.6 ^{14}C ascorbic acid solution preparation

Final concentration required (µM)	Actual concentration to be added (mM)	Solution Name
30	3	E
50	5	D
100	10	C
150	15	B
500	50	A

Table 2.7 ^{14}C ascorbic acid solutions added to cells

2.2.10.2 Assay of uptake of ascorbic acid into cells

Cells ($2x10^5$ cells per ml, 1ml) were seeded into a 12 well plate and incubated at 37°C, 5% CO_2 for 4 hours. Radiolabelled ascorbic acid was then added to cells, and plates

were then incubated for a further 4 and 24 hours at 37°C, 5% CO_2 as stated in Table 2.7. Labelled ascorbic acid standards (0, 30, 50, 150 and 500μM) were also prepared. At the end of the experiment, wells were aspirated with all the contents of the well, were transferred to a centrifuge tube (1.5ml) and centrifuged at 2000 x g for 5 minutes. The supernatants were then aspirated and PBS added to wash the pellet, cells were recentrifuged at 2000 x g for 5 minutes before lysis buffer was added (1ml of 1% Triton in 0.02M PBS). The lysate was then transferred to a counting vial containing optiphase (10ml) for scintillation counting. For the SH-SY5Y cells, the supernatants were aspirated from the wells and lysis buffer was added (1ml of 1% Triton in 0.02M PBS). The wells were then scraped with a cell scraper and the lysate was then transferred to a counting vial containing optiphase (10ml) for scintillation counting. A standard curve was constructed of ascorbic acid against counts per minute (CPM) with the CPM of the unknowns read off the standard curve to equate to the concentration of ^{14}C-ascorbic acid taken up.

2.2.11 Effect of nitroxybutyl ester of flurbiprofen (NO-FB) & novel compounds on PC12 cells

2.2.11.1 Cell culture

PC12 cells were maintained in RPMI 1640 with Glutamax I, with penicillin (0.5U/ml) streptomycin (0.5mg/ml), horse serum (10% v/v) and foetal bovine serum (5% v/v) and cultured as stated previously in section 2.2.1.1.

2.2.11.2 Collagen coating of tissue culture plastics

Collagen, type 1 solution (0.01% in 0.1M glacial acetic acid) was prepared at 22-25°C and then sterilised with chloroform overnight. Collagen solution was added to tissue culture plates (24 well, 1ml per well) and plates were incubated for 6 hours at 37°C, 5%

CO_2. Excess solution was then removed and plates were allowed to air dry at 37°C with loose lids. Prior to the addition of cells plates were washed three times with PBS.

2.2.11.3 Crystal violet assay

Experiments for this assay were plated out into 12 well plates. At harvest culture medium was removed and crystal violet solution added (500µl of 0.4mg/ml in 30% methanol) to each well. Plates were then incubated for 20 minutes at 22-25°C. The stain was then removed and the wells washed three times with H_2O (3 times), plates were then allowed to dry. The stain was then released from the cells by incubation with agitation for 30 minutes at 22-25°C with sodium dodecyl sulphate (400µl of 0.01g/ml) in each well. Aliquots (150µl) were then transferred to a 96 well flat microtitre plate for measurement of absorbance at 570nm on a microtitre plate reader.

2.2.11.4 Caspase activity assay

At harvest, plates were placed on ice, culture medium was removed and PBS (1ml of 0.02M) was added to each well. Cells were then removed from plates with a cell scraper and transferred to microfuge tubes. Tubes were then centrifuged for 20 seconds at 12000 x g. Pellets were then rinsed with ice cold PBS (1ml of 0.02M) and then resuspended by pipetting up and down ten times in homogenisation buffer (110µl of 100mM HEPES, 140mM NaCl, 1mM EDTA (pH7.4), containing 0.5mM phenylmethylsulphonyl fluoride (PMSF), 5µg/ml aprotinin, 5µg pepstatin and 10µg leupeptin). Extracts were then frozen in liquid nitrogen and stored at -70°C. Before assay homogenates were thawed and refrozen twice, before a final thaw and centrifugation at 12000 x g for 20 minutes at 4°C. Supernatants (25µl) were incubated at 37°C with assay buffer (175µl of 100mM HEPES (pH7.4), 20% v/v glycerol, 0.5mM

PMSF, 5μg/ml aprotinin, 5μg pepstatin and 10μg leupeptin and the caspase 3-like activity substrate Ac-Asp-Glu-Val-Asp-7-amido-4-methylcoumarin (15μM). Formation of fluorescent product was measured on a Victor multilable counter. Dithiothreitol (DTT) 5mM was added to the assay buffer to stabilise the activity of recombinant caspase 3. DTT was not included in the assay of tissue homogenates since concentrations up to 20mM had no effects on activity.

2.2.11.5 Protein carbonyl determination by ELISA

Standards and samples were diluted to 0.02mg/ml with coating buffer (15mM sodium carbonate, 35mM sodium hydrogen carbonate, pH9.2), plated out into separate microtitre plate wells in triplicate (50μl per well) and the plates covered. Samples were then processed as stated in section 2.2.7.2.

2.2.11.6 Flow cytometry

Cells ($2x10^5$ per ml) were harvested and centrifuged at 6600 x g for 1.5 minutes. Supernatants were removed using Pasteur pipettes, then the cell pellets were washed with PBS prior to centrifugation at 6600 x g for 1.5 minutes. PBS was removed and propidium iodide (PI) solution (200μl) was added to the cell pellets. Samples were then processed as stated in section 2.2.4.1.

CHAPTER THREE

EFFECTS OF OXIDANTS ON NEURONAL CELL VIABILITY and MORPHOLOGY

3. TOXICITY

It has been reported that the neurotoxicity of Aβ *in vitro* depends on the Aβ preparation and the culture conditions, and therefore its neurotoxicity may not be based on a single mechanism (Gschwind & Huber, 1995).

Induction of neurotoxicity has been observed using synthetic Aβ peptides containing the 29-35 residues in many cell types including PC12 cells (Yallampalli *et al.*, 1998; Mazziotti & Perlmutter, 1998; Schubert *et al.*, 1995; Pike *et al.*, 1993). H_2O_2 has also been shown to be toxic towards PC12 cells, markedly decreasing MTT activity (Jang & Surh, 2001; Xiao *et al.*, 1999). Many groups have proposed that Aβ in cultured cells and neurons induces apoptosis (Yallampalli *et al.*, 1998; Forloni *et al.*, 1993), however, other groups have shown Aβ to be toxic to nerve cells via a necrotic manner (Behl *et al.*, 1994a). The toxicity of agents against SY5Y cells have also been investigated; $A\beta_{1-42}$, $A\beta_{25-35}$, UV radiation and H_2O_2 and have been shown to be cytotoxic, however whether this is by apoptosis or necrosis is a contentious issue (Olivieri *et al.*, 2001; Misonou *et al.*, 2000; Li *et al.*, 1996).

The neurotoxicity of Aβ and H_2O_2 have been assessed in PC12 and SY5Y cells, using a variety of methods including the MTT assay, caspase assays, DNA fragmentation analysis, viable cell counting, cell staining and the lactate dehydrogenase (LDH) assay (Ekinci *et al.*, 2000; Lindenboim *et al.*,1995; Hansen *et al*, 1989). Shearman *et al.*, (1994) have shown that PC12 cells are more sensitive to Aβ25-35 than SY5Y cells.

Cytotoxicity was measured by the MTT assay. The MTT assay is an indicator of cell viability, it measures early metabolic changes within cells when exposed to stimuli. It

reflects, in part, activity of the mitochondria respiratory chain. MTT is a water soluble tetrazolium salt, which dissolves to a yellowish solution when prepared in a salt solution. Dissolved MTT is converted to an insoluble purple formazan product by cleavage of the tetrazolium ring only by active mitochondrial dehydrogenase enzymes in living cells. In particular, MTT is reduced at the ubiquinone and cytochrome b and c sites of the mitochondrial electron transport system to yield an insoluble purple product, and is the result of succinate dehydrogenase activity (Supino, 1995). The water insoluble formazan is then solubilised using an organic solvent and the dissolved material is measured spectrophotometrically yielding an absorbance, which is a function of mitochondrial activity. However, although it is assumed that MTT is reduced by active mitochondria, recently it was suggested that MTT is taken up by cells through endocytosis and reduced by a N-methylmaleimide-sensitive flavin oxidase (Liu *et al.*, 1997). MTT has been used for a variety of uses such as an indication of cell number, cytotoxicity and as a measure of cell proliferation. The MTT assay has been reported to be a specific, early indicator of Aβ-mediated dysfunction of the cell redox activity in PC12 cells (Shearman *et al.*, 1994).

Several versions of the MTT assay have been published (Isobe *et al.*, 1999; Shearman *et al.*, 1995; Hansen, *et al.*, 1989). However many authors have alluded to technical problems with MTT assays giving rise to great variation. The method of Hansen *et al.*, (1989) gave rise to far less variation. Reasons for this greater reliability/ reproducibility include: a) the inclusion of SDS in the assay; it has been reasoned to be advantageous since it dissolves the lipid layers and proteins in the cells, permitting the intracellular formazan-dye grains to be liberated and to dissolve in the watery/organic phase, and, b) other MTT assays involve washing steps where there is always a risk of losing cells and

formazan during washing procedures. Herein, the MTT assay has been optimised for the cell lines and agents investigated.

The MTT methodology has been used to define the kinetics, which equates to the dose dependency of oxidant and Aβ induced toxicity, together with the cytoprotective effects of specified agents.

There is a debate whether Aβ (and oxidant) cell death is via an apoptotic or necrotic means: the MTT assay does not define the mode of cell death, only that there has been a reduction in cell viability. Determination of the mode of cell death can be achieved by cell staining with specific fluorochromes. For example, propidium iodide will stain cells following membrane disruption (e.g.necrosis) whereas Hoechst will stain nuclear material in living cells, where the structure of chromatin stained gives an indication as to the mode of death as employed in section 3.3 (Darzynkiewicz & Li, 1997).

3.1 MTT ASSAY

3.1.1 MTT Optimisation

3.1.1.1 Comparison of two methods for measuring cell viability via the formation of a MTT formazan product

The original MTT assay involved addition of MTT (25μl of 5mg/ml) to cells for 4 hours before solubilisation with DMSO (100μl) prior to reading the OD of the plate at test and reference wavelengths of 550 and 620nm respectively. The modified assay involved the addition of MTT (25μl of 5mg/ml) to cells for 2 hours before solubilisation with a solution of SDS, DMF and distilled water, see methods section 2.2.2. The OD of the solubilised formazan was subsequently read at test wavelength 570nm. The results

show the modified assay to be the better of the two methods as this produced the smallest coefficient of variations.

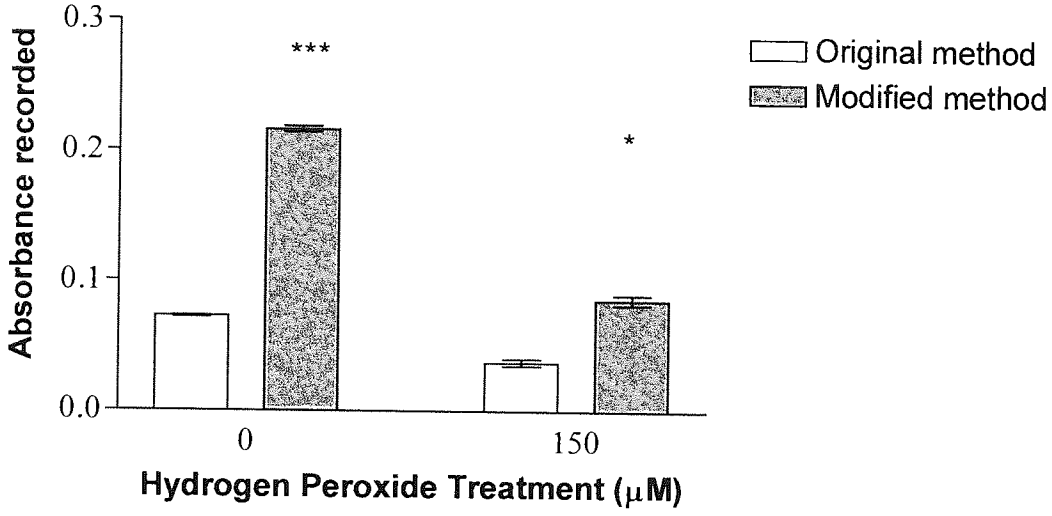

Figure 3.1.1 Comparison of two MTT assays for determination of H_2O_2 toxicity. PC12 cells (2 x 10^5) were incubated with H_2O_2 (150μM) for 8 hours at 37°C, 5% CO_2. Data represents the mean absorbance of formazan produced ± SEM of 12 replicates. * represents P value < 0.0001 compared to the original method, * represents P value 0.016 compared to the original method (Unpaired t test).**

3.1.1.2 Relationship between cell number and MTT reductive activity

In order to investigate the effects of cell number on MTT product formation, four cell concentrations were employed in the modified assay. Figure 3.1.2 shows a dose relationship between formazan product produced and cell number. Increasing cell numbers causes increased formazan product formation, the average OD recorded changed from 0.06 for $5x10^3$ cells/ml through to 0.134 for $5x10^5$ cell/ml. The results produced with 2 and $5x10^5$ cells per ml were both greater, compared to results generated with $5x10^3$ cells per ml. To prevent problems of overconfluency with SY5Y cells, $2x10^5$ cells per ml were subsequently adopted for future MTT assays

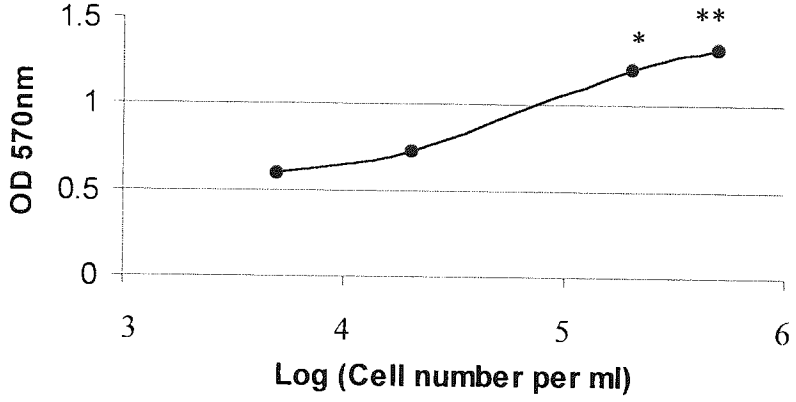

Figure 3.1.2 The effects of cell number on formazan production in the modified MTT assay. PC12 cells (100µl) were plated out into a 96 well plate at 5 x 10^3, 2 x 10^4, 2 x 10^5 and 5 x 10^5 cell per ml . Plates were incubated for 24 hours at 37°, 5% CO_2. Cells were then subject to the modified MTT assay as stated in section 2.2.2. Data shown are the mean absorbance of formazan produced ± SEM of 6 replicates. * represents P value <0.05 and ** represents P value <0.01 (Dunnett's test).

3.1.1.3 Effect of medium on MTT reductive activity of PC12 cells

In order to investigate the effects of cell culture on PC12 MTT reductive capacity, a comparison was made between the use of serum containing (15%) and serum free medium.

Untreated PC12 cells in complete medium (15%) yielded higher absorbances of formazan product, compared to those for serum free medium. A t-test, (unpaired) was conducted on the data, which showed the significant differences ($P<0.0001$), where MTT reduction was greater in complete medium. Subsequent experiments were undertaken in complete medium for two reasons: firstly the basal absorbance was very low in the serum free medium cells, (these cells would have been at their optimum and under no challenge). Secondly challenged cells would have produced less reductive capacity, making any MTT changes very hard to quantify.

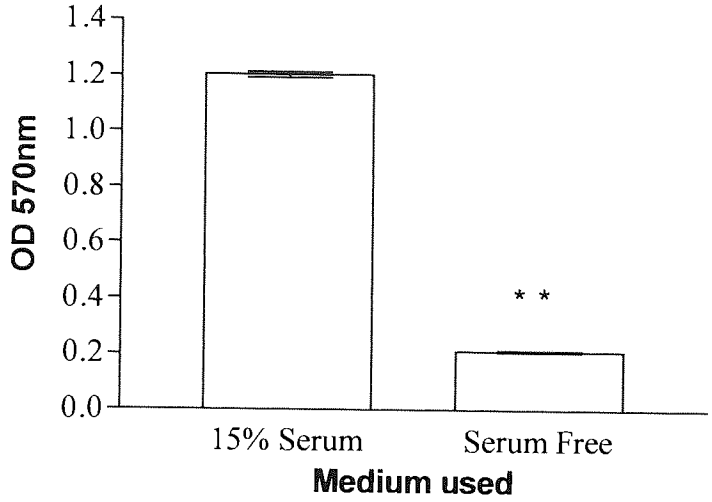

Figure 3.1.3 The effects of growth medium on the results produced in the modified MTT assay. PC12 cells (2 x 10^5) were incubated for 24 hours at 37°C, 5% CO_2 in the two media described. Data represents the mean absorbance ± SEM of 16 replicates for each medium. ** represents P < 0.0001 (Unpaired two sample t-test).

After optimisation, all MTT assays were conducted as stated in section 2.2.2, using the modified method, in complete medium (15% serum) and at a concentration of 2 x 10^5 cells per ml (100µl per well). All plates were incubated at 37°C, 5% CO_2 for four hours after seeding to ensure the effects observed were due to the agents/treatments employed and not the effects of seeding.

3.1.2 PC12 Cell Line MTT Results

3.1.2.1 Effect of hydrogen peroxide on MTT reductive activity

The effects of H_2O_2 on PC12 cell reductive capacity were investigated. Figure 3.1.4 shows that increases in H_2O_2 concentration causes decreases in the OD recorded, indicative of lower MTT reductive activity, and therefore viable cell numbers.

A Dunnett's post test was conducted on the results comparing H_2O_2 treatments to control, which showed there were significant decreases in formazan absorbance with increasing H_2O_2 treatments, $P<0.01$.

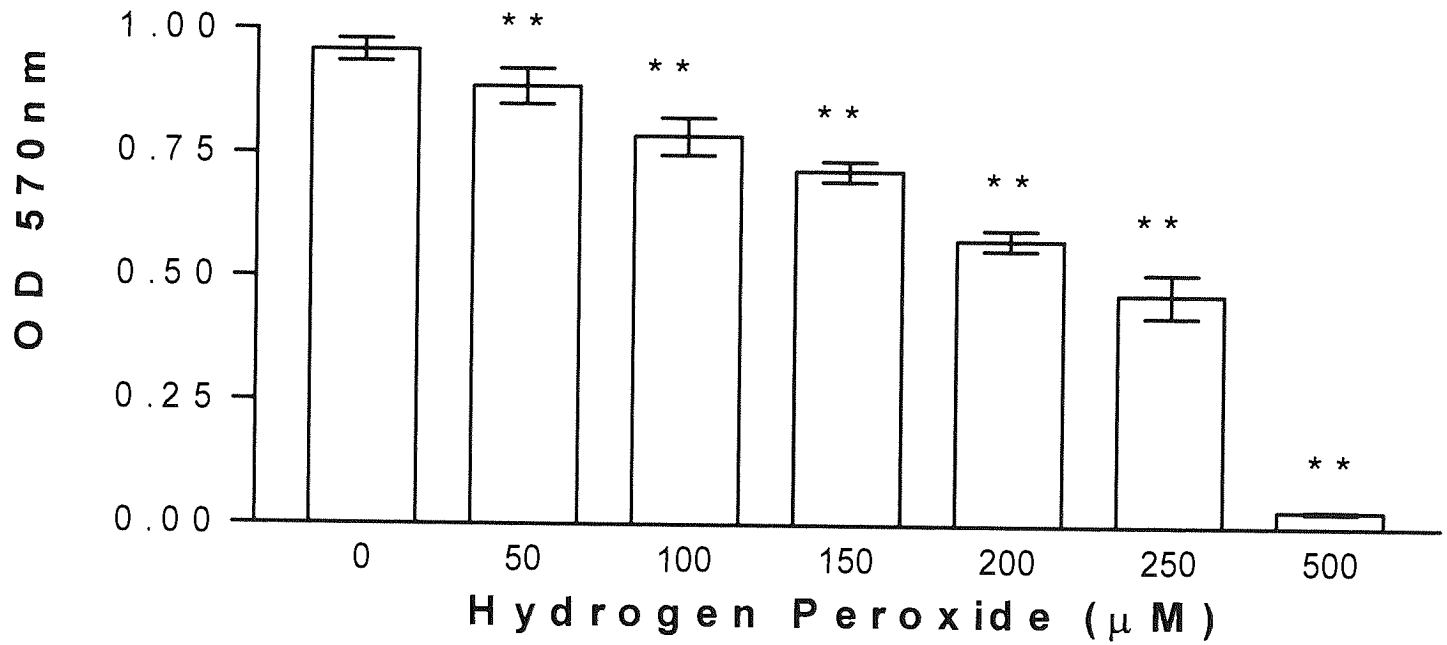

Figure 3.1.4 The effect of hydrogen peroxide on PC12 cell viability using the MTT assay. PC12 cells (2×10^5) were incubated for 4 hours at 37°C, 5% CO_2 before the addition of H_2O_2 (50, 100, 150, 200, 250 and 500μM) for 24 hours at 37°C, 5% CO_2. Cells were then subject to the standard MTT assay as stated in section 2.2.2. Data shown are the mean absorbance of formazan produced ± SEM of 6 replicates for each treatment. ** represents P values of <0.01 (Dunnett's test).

3.1.2.2 Effect of Amyloid β on MTT reductive activity

3.1.2.2.1 Effect of Amyloid β peptide, fragment 25–35

The effects of increasing concentrations of Aβ peptide fragment 25-35 (Aβ) on PC12 cell viability were investigated. Figure 3.1.5 shows a dose dependent relationship between increasing Aβ dose, and decreasing MTT product formation, where at 100μM Aβ a 91.1% loss of reductive capacity was recorded. A Dunnett's post test was used to compare the effects of Aβ at increasing concentrations to controls. At 10-100μM Aβ, the differences were significant, $P<0.01$.

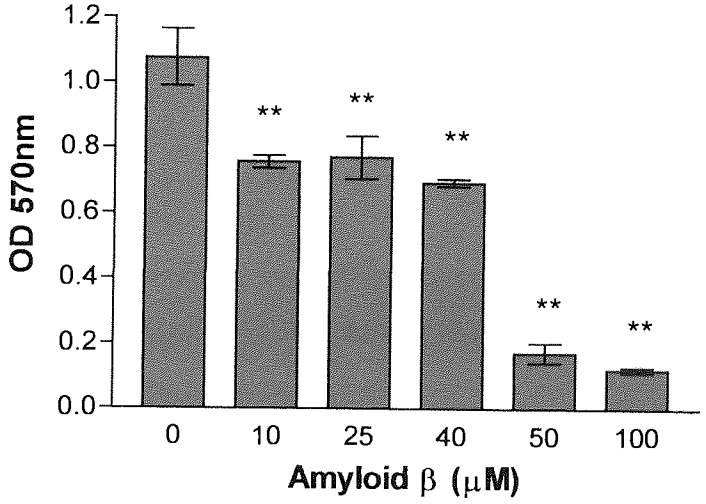

Figure 3.1.5 The effects of amyloid β (25-35) toxicity on PC12 cells. PC12 cells ($2x10^5$) were incubated with aged Aβ (10, 25, 40, 50 and 100μM) for 24 hours at 37°C, 5% CO_2. Cells were then subject to the standard MTT assay as stated in section 2.2.2. Graph shows the mean absorbance of formazan produced ± SEM for at least 3 replicates. * represents $P<0.05$ and ** represents $P<0.01$ (Dunnett's test).

3.1.2.2.2 Effect of Amyloid β peptide, fragment 1-42

The effect of increasing concentrations of Aβ peptide, fragment 1-42 (Aβ) on PC12 cells were investigated. Figure 3.1.6 showed no significant effects up to and including 10.1μM of Aβ 1-42 of both newly solubilised and aged peptides.

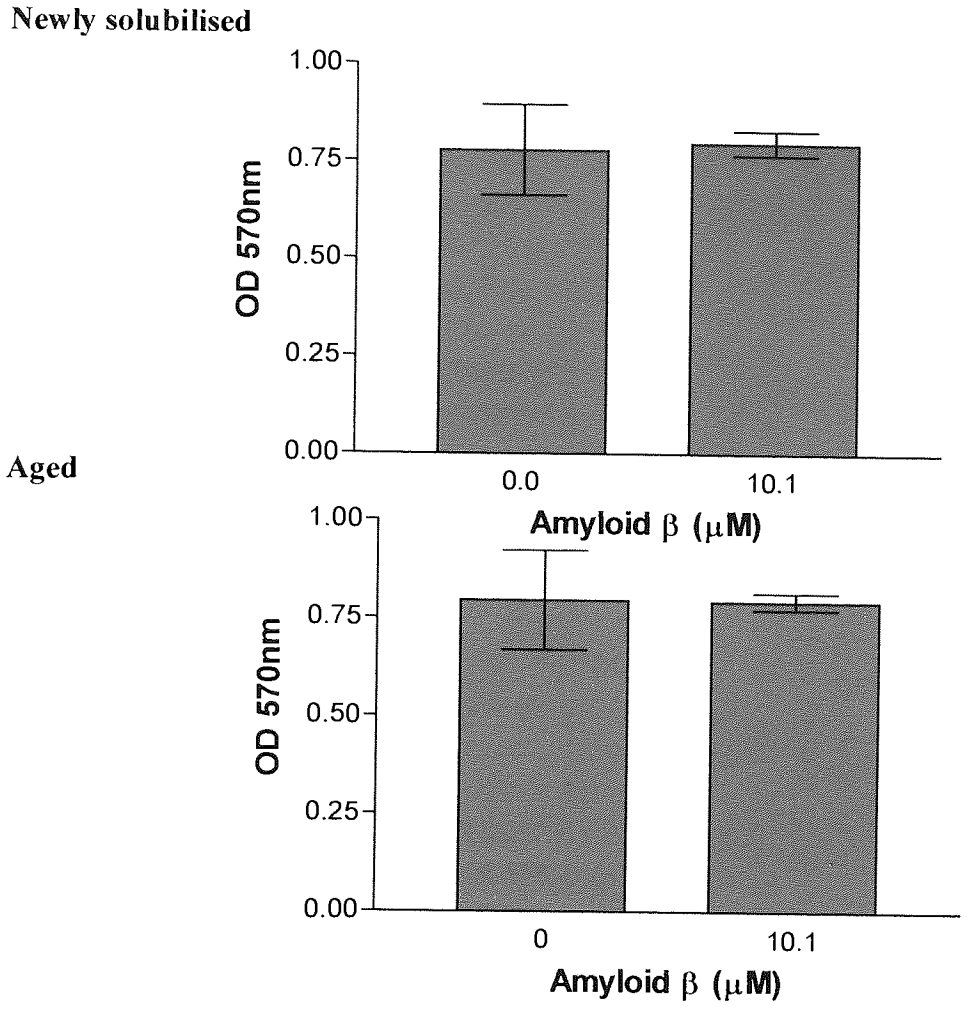

Figure 3.1.6 The effects of amyloid β (1-42) toxicity on PC12 cells. PC12 cells ($2x10^5$) were incubated with Aβ (10.1μM) for 24 hours at 37°C, 5% CO_2. Cells were then subject to the standard MTT assay as stated in section 2.2.2. Graph shows the mean absorbance of formazan produced ± SEM for 6 replicates.

3.1.2.3 Effect of Nerve Growth Factor on hydrogen peroxide toxicity as assessed by MTT reductive activity

The effects of NGF on the percentage changes in MTT reductive capacity produced by increasing concentrations of H_2O_2 were assessed using three concentrations of NGF versus control treated cells. Figure 3.1.7 shows that NGF has no significant effects on basal levels (unchallenged cells) of MTT reductive activity, however in cells challenged with low H_2O_2 doses (50-250μM) NGF (10ng/ml) did have a significant protective effects of at least $P<0.05$ (Dunnett's post test).

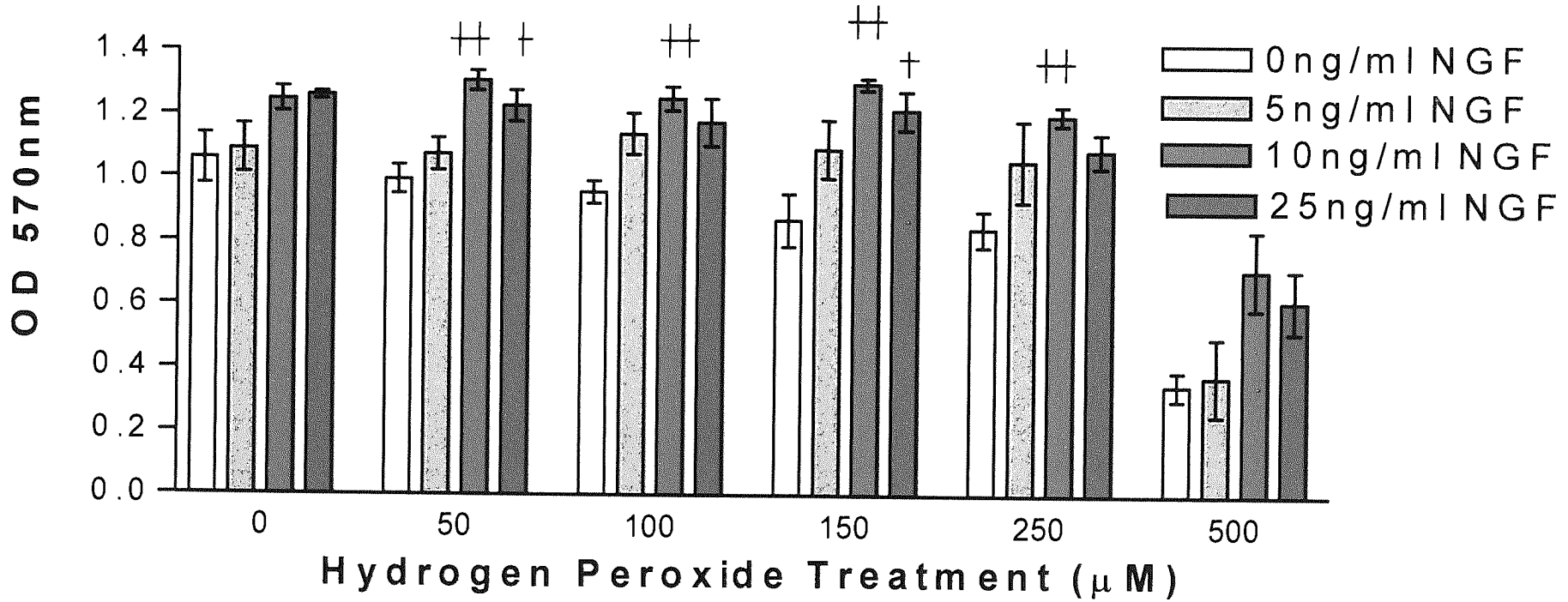

Figure 3.1.7 The effects of nerve growth factor on PC12 cell viability in the presence or absence of H_2O_2. PC12 cells (2×10^5) were incubated with NGF (5, 10 and 25ng/ml) for 24 hours at 37°C, 5% CO_2. H_2O_2 (50, 100, 150, 250 and 500μM) were then added for a further 24 hours at 37°C, 5% CO_2. Cells were then subject to the standard MTT assay as stated in section 2.2.2. Graph shows the mean absorbance of formazan produced ± SEM for at least 4 replicates. ┼ represents $P<0.05$, ┼┼ represents $P<0.01$ when compared to treatment in the absence of NGF at each H_2O_2 concentration.

3.1.2.3.1 Effect of nerve growth factor on amyloid β peptide, fragment 25-35 toxicity as assessed by MTT reductive activity

The effects of NGF on the percentage changes in MTT reductive capacity produced by increasing concentrations of Aβ peptide, fragment 25-35 were assessed using two concentrations of NGF versus control treated cells. Figure 3.1.8 shows decreases in MTT absorbance with increasing Aβ concentration, and that only at 10ng/ml NGF in control treated cells was there some significant protection offered by NGF.

3.1.2.4 Effect of ascorbic acid on MTT reductive activity

The effect of AA on cell viability as measured by MTT reductive activity was assessed using two concentrations of AA (50 and 100μM) versus control. Figure 3.1.9 shows 50μM AA to exert significant increases in MTT reductive activity and therefore cell viability compared to control; 50μM AA caused a significant 20.3% increase in the MTT activity ($P<0.01$, Dunnett's), whilst 100μM AA caused an insignificant 5.2% reduction in activity.

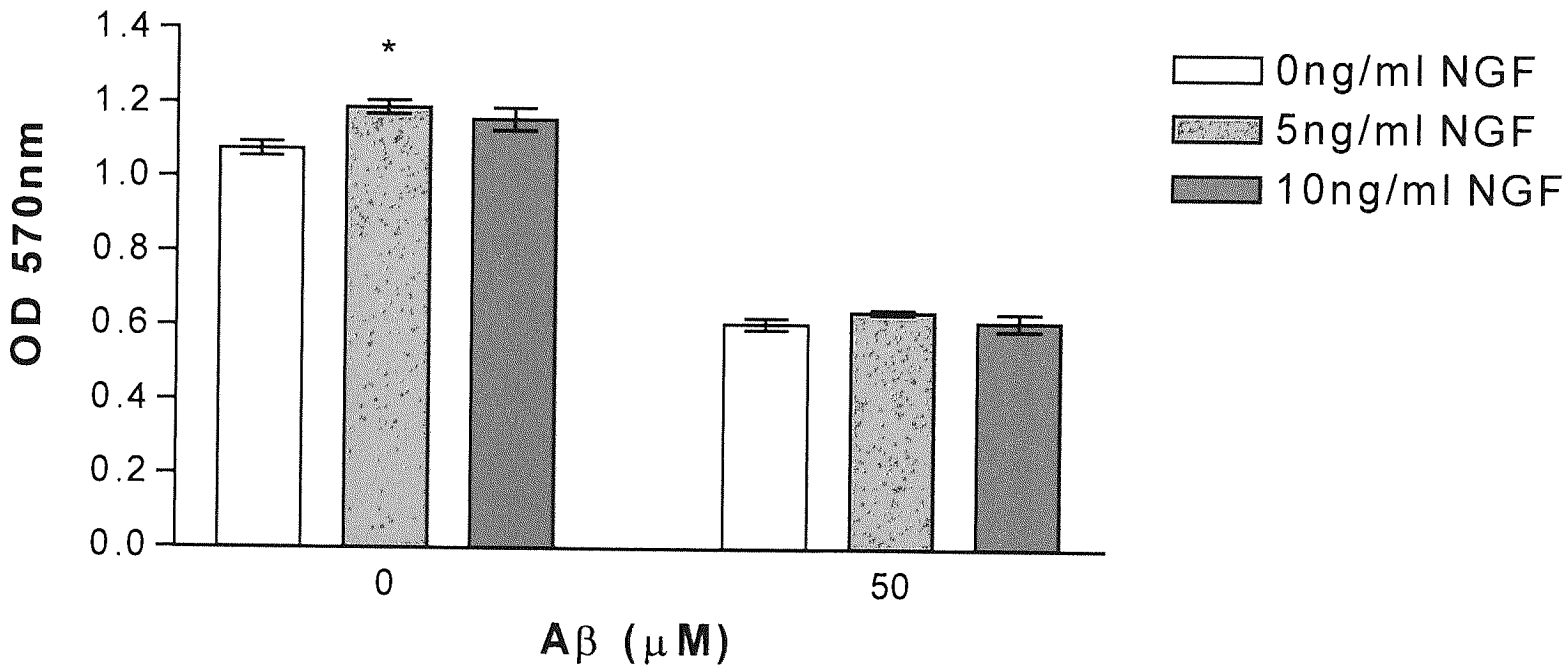

Figure 3.1.8 The effects of nerve growth factor on PC12 cell viability in the presence or absence of Aβ (fragment 25-35). PC12 cells (2 x 10^5) were incubated with NGF (5, 10, 25 and 50ng/ml) for 24 hours at 37°C, 5% CO_2. Amyloid β peptide (50μM) were then added for a further 24 hours at 37°C, 5% CO_2. Cells were then subject to the standard MTT assay as stated in section 2.2.2. Graph shows the mean absorbance of formazan product ± SEM for at least 4 replicates. * represents $P<0.05$, where compared to untreated cells.

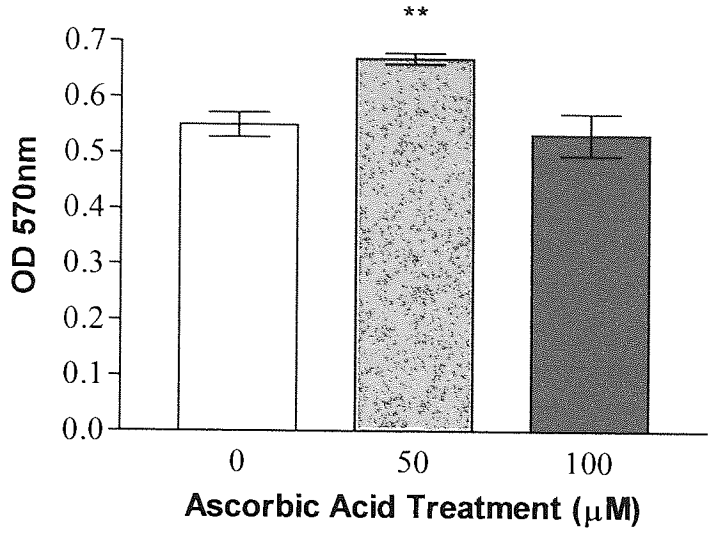

Figure 3.1.9 The effect of ascorbic acid on MTT reductive activity in PC12 cells. PC12 cells (2 x 10^5) were incubated with AA (50 and 100μM) for 24 hours at 37°C, 5% CO_2. Cells were then subject to the standard MTT assay as stated in section 2.2.2. Figure 3.1.8 shows the mean absorbance of formazan produced ± SEM for 16 replicates. ** represents P value < 0.01 (Dunnett's test)

3.1.2.4.1 Effect of ascorbic acid on hydrogen peroxide toxicity as assessed by MTT reductive activity

The effect of AA on MTT reductive capacities of PC12 cells under H_2O_2 challenge was assessed using two AA concentrations (50 and 100μM) versus control treated cells. Figure 3.1.10, shows that against H_2O_2 challenge (0-150μM), cells treated with AA showed dose dependent losses of viability. In the absence of AA pre-treatment, there was an overall 36.77% loss in MTT activity whereas in 50μM AA pre-treated cells 57.69% loss in MTT activity was observed and following 100μM AA treatment there was 40% loss in activity, comparing OD values recorded at 0μM H_2O_2 and 150μM H_2O_2. At each H_2O_2 dose including basal levels (0, 50, 100 and 150μM) AA pre-treatment caused a significant decrease ($P<0.01$, $n=6$). However, comparison between toxicity observed by 150μM peroxide, in the presence or absence of 100μM AA, showed AA to protect from further oxidative damage.

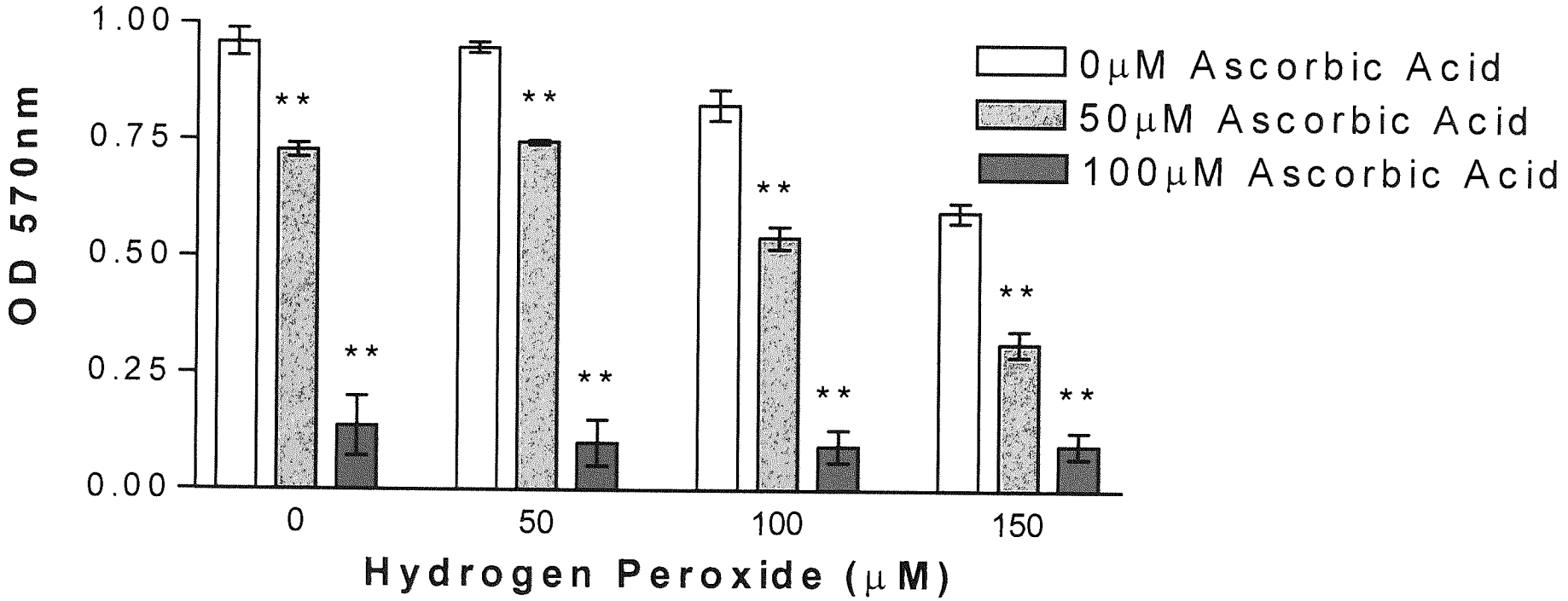

Figure 3.1.10 The effects of ascorbic acid on hydrogen peroxide induced toxicity in PC12 cells. PC12 cells (2 x 10^5) were incubated with AA (50 and 100μM) for 24 hours at 37°C, 5% CO_2. H_2O_2 (50, 100 and 150μM) were then added for a further 24 hours at 37°C, 5% CO_2. Cells were then subject to the standard MTT assay as stated in section 2.2.2. Graph shows the mean absorbance of formazan produced ± SEM for 6 replicates. ** represents $P < 0.01$ (Dunnett's test).

3.1.3 SH-SY5Y Cell Line MTT Results

3.1.3.1 Effects of hydrogen peroxide on MTT reductive activity

The effects of increasing concentrations of H_2O_2 on SY5Y cells were investigated. Figure 3.1.11 shows a dose dependent relationship between increasing H_2O_2 concentration and decreases in MTT absorbance, up to and including 50μM H_2O_2. Furthermore reductions in MTT activity were also seen at higher H_2O_2 doses. In the absence of H_2O_2, cells were recorded as having a MTT reductive capacity of 100%. With increasing H_2O_2 concentrations, this reduced significantly and dose dependently to 59.0% at 40μM H_2O_2 and 3.8% MTT reductive capacity at 500μM ($P<0.01$, Dunnett's).

3.1.3.2 Effect of Amyloid β on MTT reductive activity

3.1.3.2.1 Effect of Amyloid β peptide, fragment 25-35

The effects on SY5Y cell viability as determined using the MTT assay of increasing concentrations of Aβ peptide, fragment 25-35 were investigated. Figure 3.1.12 shows Aβ to cause significant decreases in the MTT reductive activity ($P<0.01$, Dunnett's test), where the effects were not dose dependent.

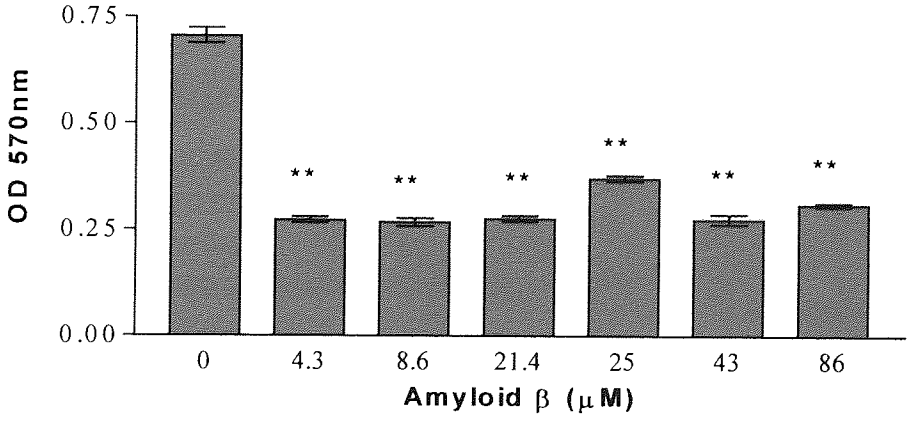

Figure 3.1.12 The effects of amyloid β (25-35) induced toxicity on SY5Y cells. SY5Y cells ($2x10^5$) were incubated with aged Aβ (4.3, 8.6, 21.4, 25, 43 and 86μM) for 24 hours at 37°C, 5% CO_2. Cells were then subject to the standard MTT assay as stated in section 2.2.2. Graph shows the mean absorbance of formazan produced ± SEM for 4 replicates. ** represents $P < 0.01$ (Dunnett's test)

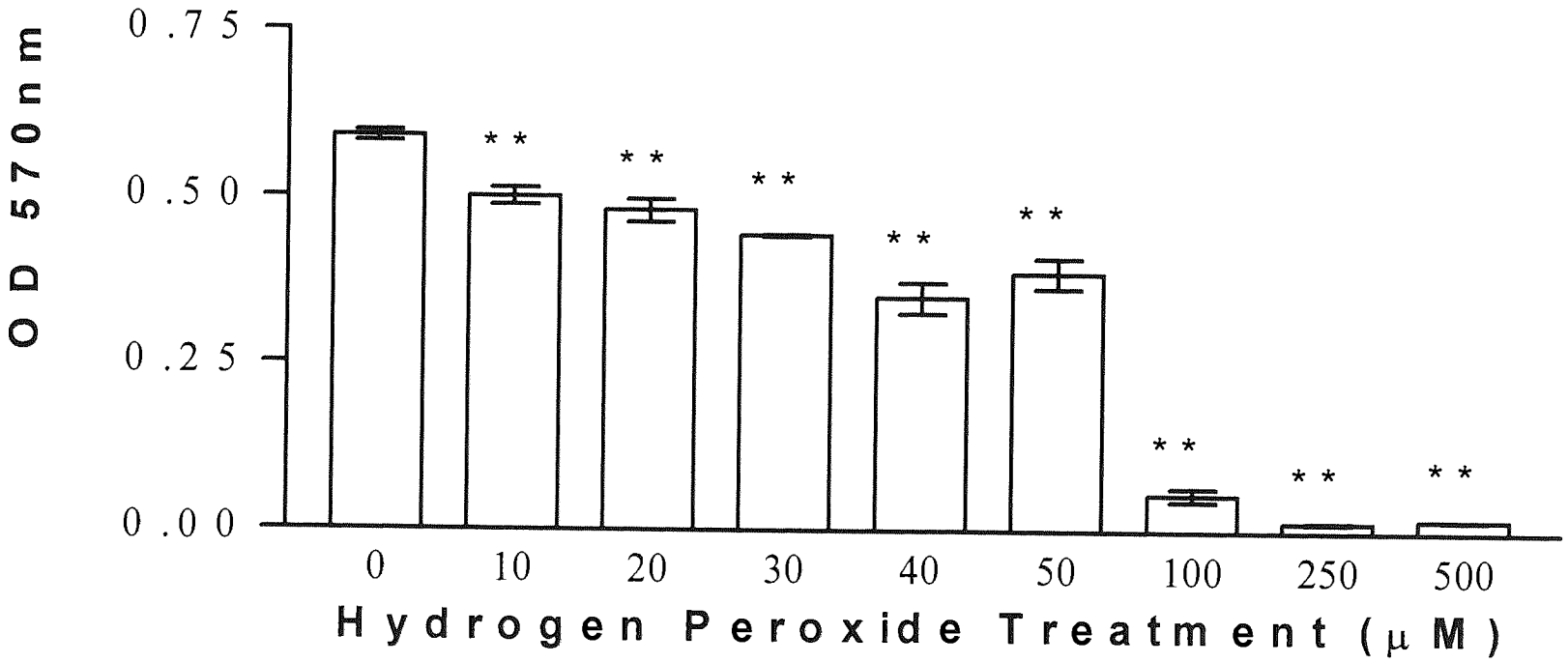

Figure 3.1.11 The effects of hydrogen peroxide toxicity on SY5Y cell viability using the MTT assay. SY5Y cells ($2x10^5$) were incubated for 4 hours at 37°C, 5% CO_2 before the addition of H_2O_2 (10, 20, 30, 40, 50, 100, 250 and 500μM) for 24 hours at 37°C, 5% CO_2. Cells were then subject to the standard MTT assay as stated in section 2.2.2. Data shown are the mean absorbance of formazan produced ± SEM of 6 replicates. ** represents $P< 0.01$ (Dunnett's test).

3.1.3.2.2 Effect of Amyloid β peptide, fragment 1-42

The effect of increasing concentrations of Aβ peptide fragment 1-42 on SY5Y cell viability were examined. Figure 3.1.13 shows significant decreases in MTT reductive capacity at each Aβ dose by both newly solubilised ($P<0.01$, Dunnett's) and aged peptides ($P<0.0001$, unpaired t test). However, the responses seen were not dose dependent. **Newly solubilised**

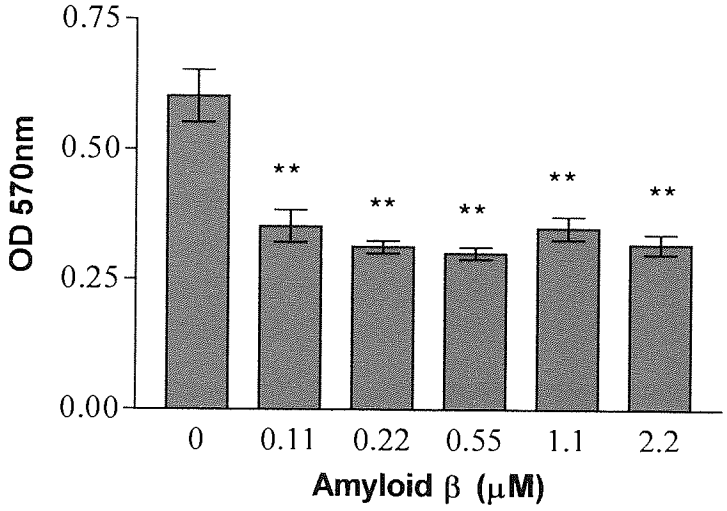

Aged

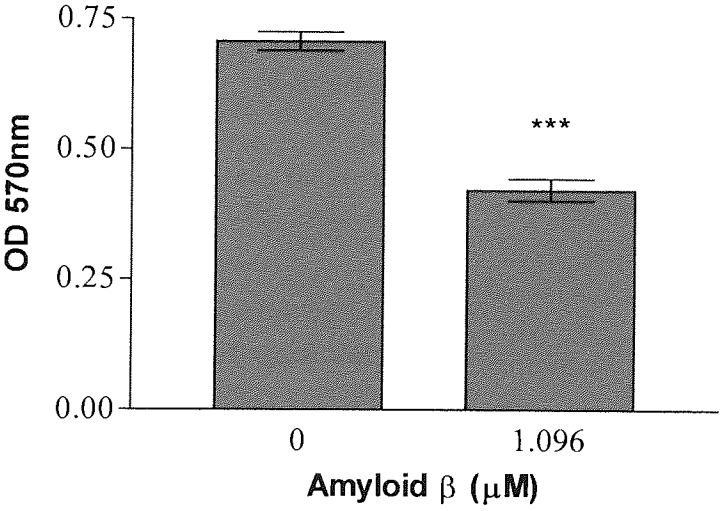

Figure 3.1.13 The effects of amyloid β (1-42) toxicity on SY5Y cells. SY5Y cells (2 x 10^5) were incubated with Aβ (0.1, 0.22, 0.55, 1.1 and 2.2μM) for 24 hours at 37°C, 5% CO_2. Cells were then subject to the standard MTT assay as stated in section 2.2.2. Graph shows the mean absorbance of formazan produced ± SEM for at least 3 replicates. ** P<0.01 (Dunnett's test) *** P<0.0001 (Unpaired t-test).

3.1.3.3 Effect of Nerve Growth Factor on MTT reductive activity in SY5Y cells

The effects of NGF on cell viability as measured by MTT reductive activity were assessed using four concentrations of NGF versus control. Figure 3.1.14 shows a general trend of increasing NGF concentration, causing an increase in MTT reductive activity, of which some effects were significant. All NGF concentrations caused increases in absorbances, however, only the 10ng/ml and 50ng/ml treatments were shown to be significant at $P<0.05$ and $P<0.01$ respectively, using a Dunnett's post test.

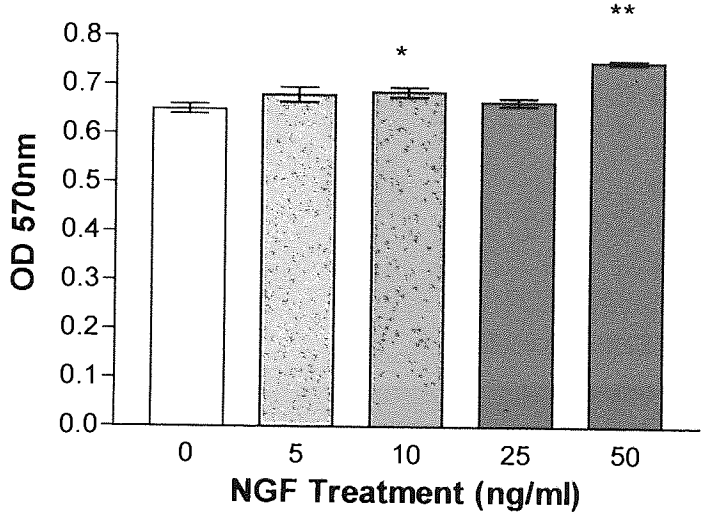

Figure 3.1.14 The effects of nerve growth factor on SY5Y cells. SY5Y cells (2 x 10^5) were incubated for 4 hours at 37°C, 5% CO_2 before the addition of NGF (5, 10, 25 and 50ng/ml) for 24 hours at 37°C, 5% CO_2. Figure shows the mean absorbance of formazan produced ± SEM for 6 replicates. * represents $P<0.05$, ** represents $P<0.01$ (Dunnett's test).

3.1.3.3.1 Effect of Nerve Growth Factor on hydrogen peroxide toxicity as assessed by MTT reductive activity

The effects of NGF on the percentage of MTT reductive capacity under H_2O_2 challenge were assessed using two NGF concentrations (10 and 25ng/ml) versus control cells. Figure 3.1.15 shows that increasing H_2O_2 concentration caused dose dependent decreases in MTT absorbance at each NGF concentration. In the absence of H_2O_2 the increases in absorbance in cells pre-treated with 25ng/ml NGF were shown to be significant $P<0.01$ compared to controls (Dunnett's test). At 100μM H_2O_2 the increases

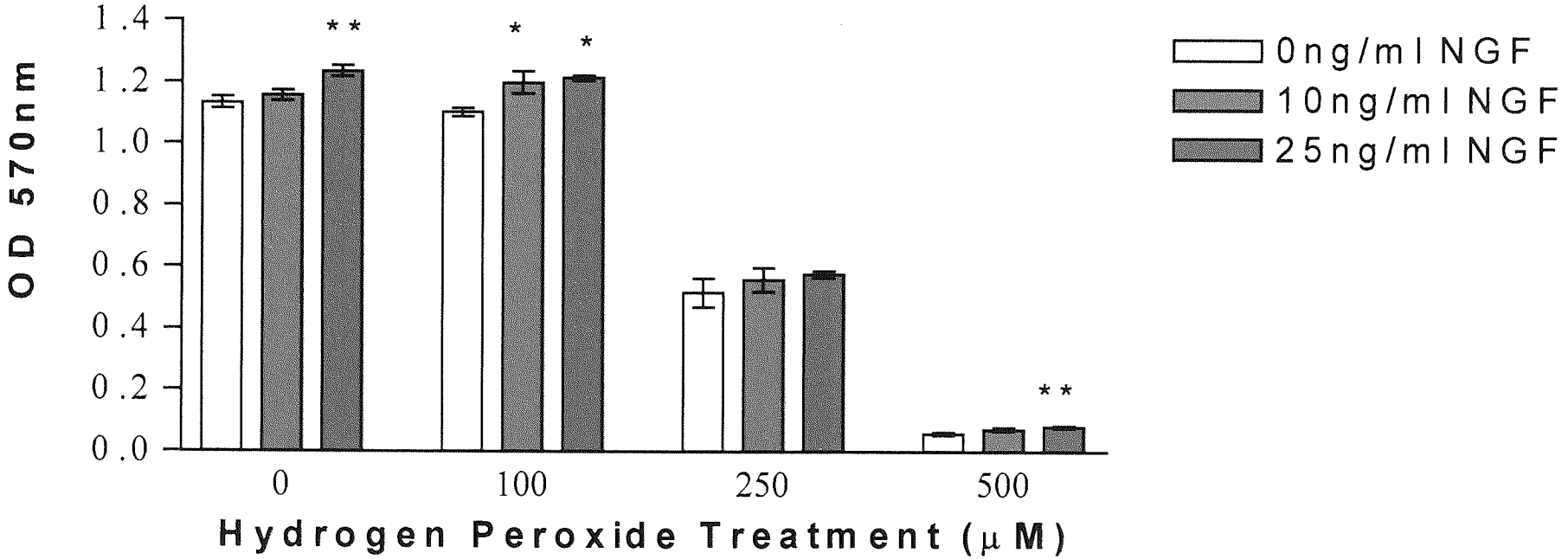

Figure 3.1.15 The effects of nerve growth factor on SY5Y cell viability in the presence and absence of H_2O_2. SY5Y cells ($2x10^5$) were incubated with NGF (10 and 25ng/ml) for 24 hours at 37°C, 5%CO_2. H_2O_2 (100, 250 and 500μM) were then added for a further 24 hours at 37°C, 5% CO_2. Cells were then subject to the standard MTT assay as stated in section 2.2.2. Graph shows the mean absorbance of formazan produced ± SEM for 4 replicates. ┼ represents P<0.05, ┼┼ represents P<0.01 (Dunnett's test) when compared to treatment in the absence of NGF.

in mitochondrial activity in cells pre-treated with 10 and 25ng/ml NGF were also significant ($P<0.05$) compared with peroxide treatment alone. Again at 500μM H_2O_2, MTT reduction recorded in cells pre-treated with 25ng/ml NGF was greater than for control cells, $P<0.01$.

3.1.3.4 Effect of ascorbic acid on MTT reductive activity

The effect of AA on cell viability as measured by MTT reductive activity was assessed using two concentrations of AA (50 and 100μM). Figure 3.1.16 shows that none of the AA concentrations had significant effects on viability. However, there was a general trend recorded for increasing AA concentration, to increase mitochondrial activity.

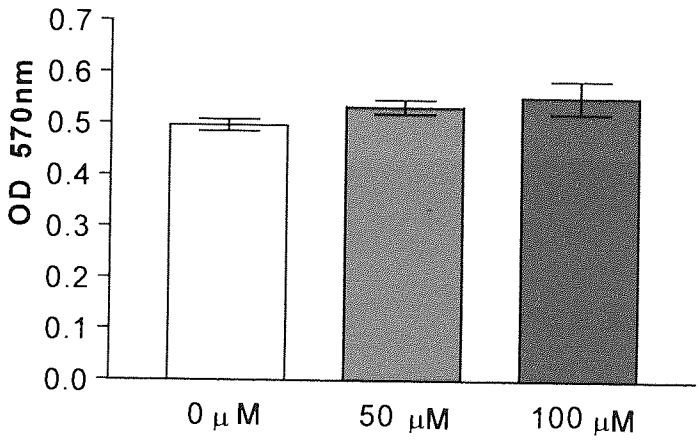

Figure 3.1.16 The effects of ascorbic acid on SY5Y cells. SY5Y cells ($2x10^5$) were incubated with AA (50 and 100μM) for 24 hours at 37°C, 5%CO_2. Cells were then subject to the standard MTT assay and results are expressed as mean absorbance of formazan produced ± SEM.

3.1.3.4.1 Effects of ascorbic acid on hydrogen peroxide toxicity as assessed by MTT reductive activity

The effect of AA on MTT reductive capacities under H_2O_2 challenge was assessed using two AA concentrations (50 and 100μM). Figure 3.1.16 had previously shown no significant effects of AA on unchallenged cells. However, against H_2O_2 challenge, AA

showed a protective effect (see figure 3.1.17), where pre-incubation with 100μM AA offered significant protection against 500μM peroxide ($P<0.05$, Dunnett's).

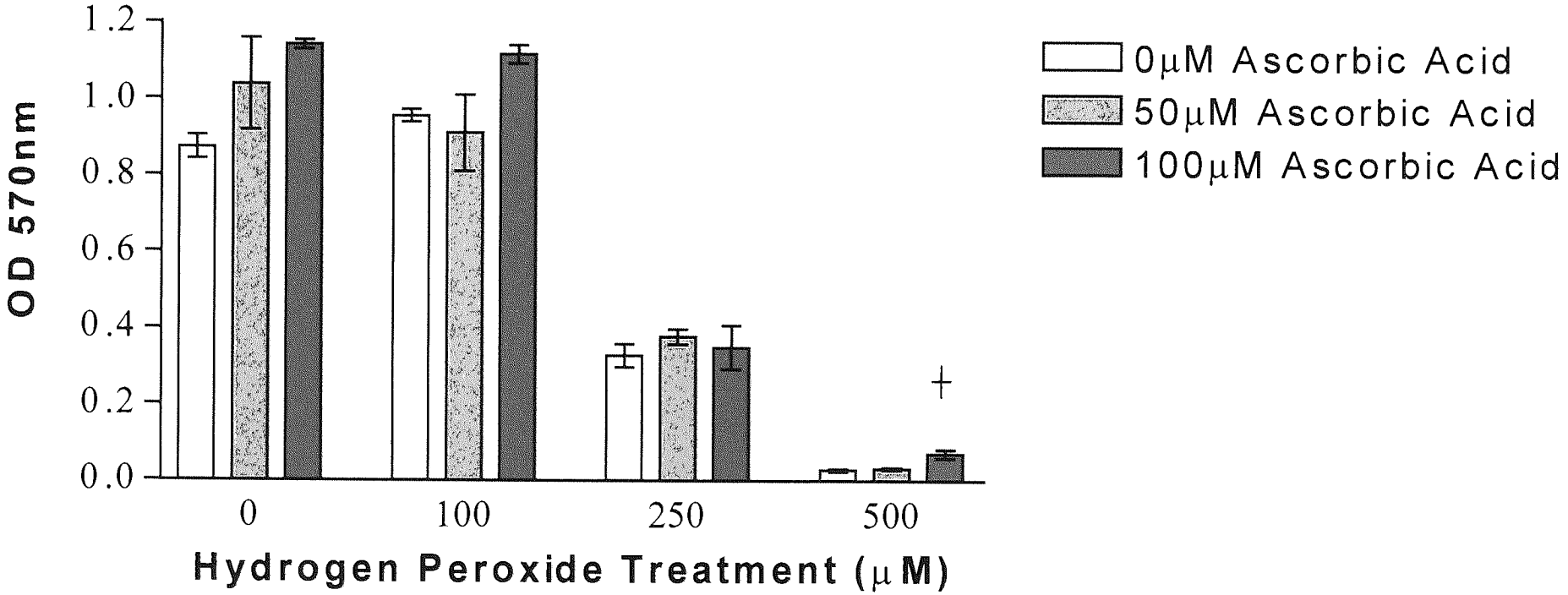

Figure 3.1.17 The effects of ascorbic acid on hydrogen peroxide induced toxicity in SY5Y cells. SY5Y cells (2×10^5) were incubated with AA (50 and 100μM) for 24 hours at 37°C, 5% CO_2. H_2O_2 (100, 250 and 500μM) were then added for a further 24 hours at 37°C, 5% CO_2. Cells were then subject to the standard MTT assay as stated in section 2.2.2. Graph shows the mean absorbance of formazan produced ± SEM for 4 replicates. + represents $P<0.05$, when compared to treatment in the absence of AA (Dunnett's test).

3.1.4 SY5Y DIFFERENTIATION RESULTS

In order to assess whether SY5Y cells were differentiated, before being employed, cells were observed for their morphology and also a small aliquot was tested for expression of the *trk B* receptor. Morphological changes and positive *trk B* receptor expression would confirm successful differentiation.

3.1.4.1 Video Microscopy

Video microscopy images were taken of cells undergoing differentiation treatment as described in 2.2.1.7. Differentiation with retinoic acid (RA) is known to cause changes in the neuronal biochemistry and morphology of cells.

Results showed there to be no distinct differences between the two cells types morphologically. RA differentiated cells often tend to have marked extensive neurite outgrowths, however although outgrowths were seen as shown in figure 3.1.18 there were not clear distinctions between the two cell treatments. Other groups including Kaplan *et al.*, (1993) have also previously noted this, where SY5Y cells treated with RA alone resulted in cells that were more substrate adherent yet exhibited only limited neurite outgrowth responses.

3.1.4.2 *trk B* ELISA

To evaluate whether SY5Y cells had differentiated and were expressing the specific neurotrophic factor receptor, an ELISA was developed to probe for expression of *trk B*. *trk* B was determined as it encodes an essential component of a functional receptor for BDNF (Squinto *et al.*, 1991). Figure 3.1.19 shows that differentiated cells treated for 7 days with 10μM RA showed significantly enhanced expression of *trk B*.

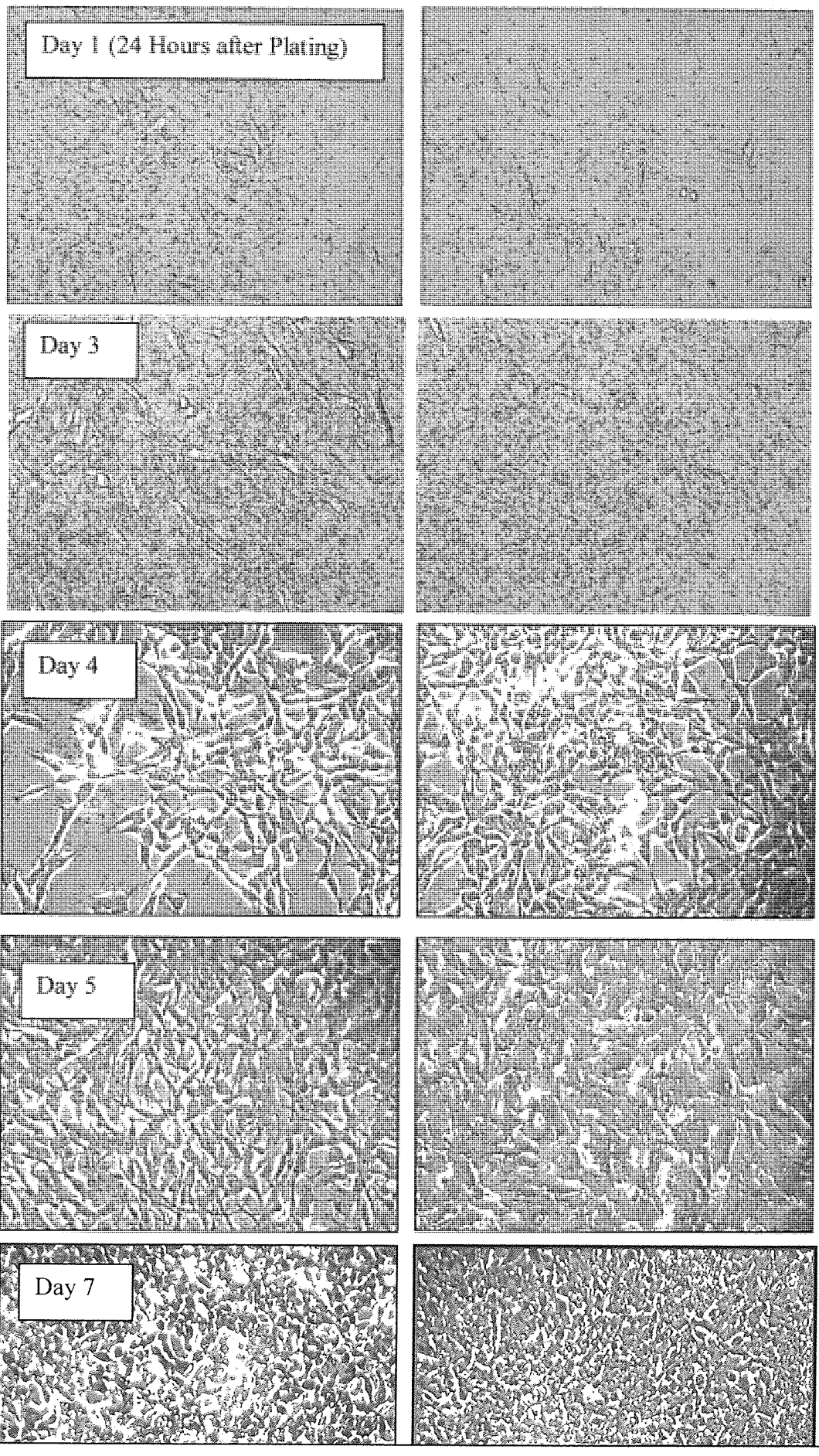

Figure 3.1.18 Video microscopy images of SY5Y cells undergoing differentiation treatment. SY5Y ($1x10^5$) were incubated for 7 days in 1% medium with either the presence of RA or DMSO, with the media changed every 48 hours.

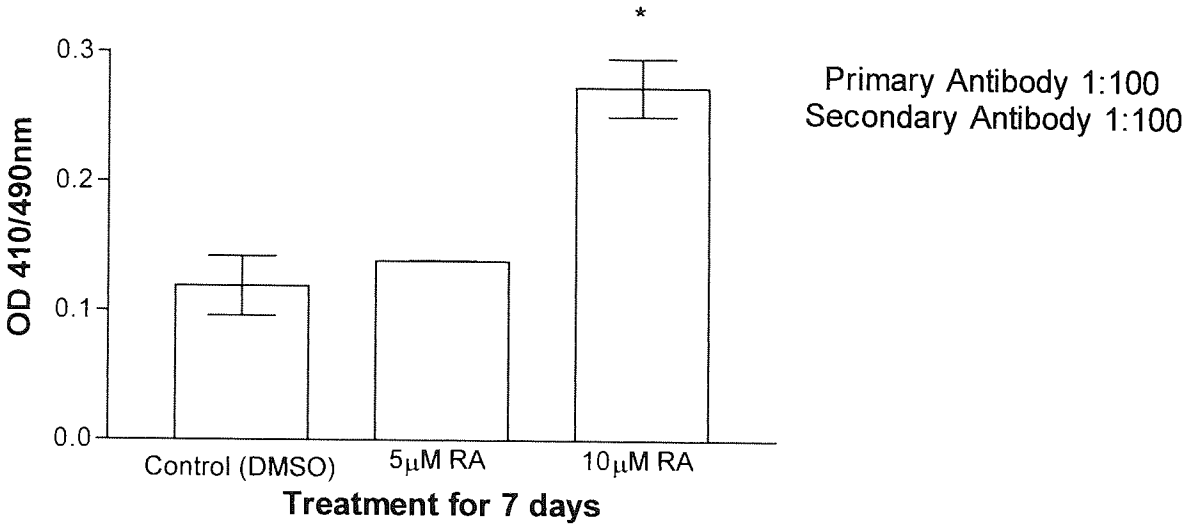

Figure 3.1.19 ***trk*** **B ELISA of differentiated and undifferentiated SY5Y cells. SY5Y ($2x10^5$) cells were differentiated as stated in section 2.2.1.7, after harvest and protein estimation, samples were diluted to 0.15mg/ml before plating out for a Trk B ELISA as described in section 2.2.1.7.1. Graph shows mean OD ± SEM for 4 replicates. * represents P<0.05 (Single factor ANOVA).**

10μM RA was subsequently employed for all differentiation.

3.1.5 Differentiated SH-SY5Y Cell Line MTT Results

3.1.5.1 Effects of hydrogen peroxide on MTT reductive activity

The effects of increasing concentrations of H_2O_2 on differentiated and control SY5Y cell viability were investigated. Figure 3.1.20 shows a dose dependent relationship in both differentiated and control cells with increases in H_2O_2 concentration causing a decrease in the MTT reductive activity. These results show the differentiated cells are more resistant to H_2O_2 toxicity, however the actual MTT formazan basal levels in differentiated cells were less that half (47.8%) those of undifferentiated cells. Dunnett's post tests conducted showed the effects seen at each H_2O_2 dose in undifferentiated cells and at 40 and 100μM H_2O_2 in differentiated cells to be significant, P<0.01.

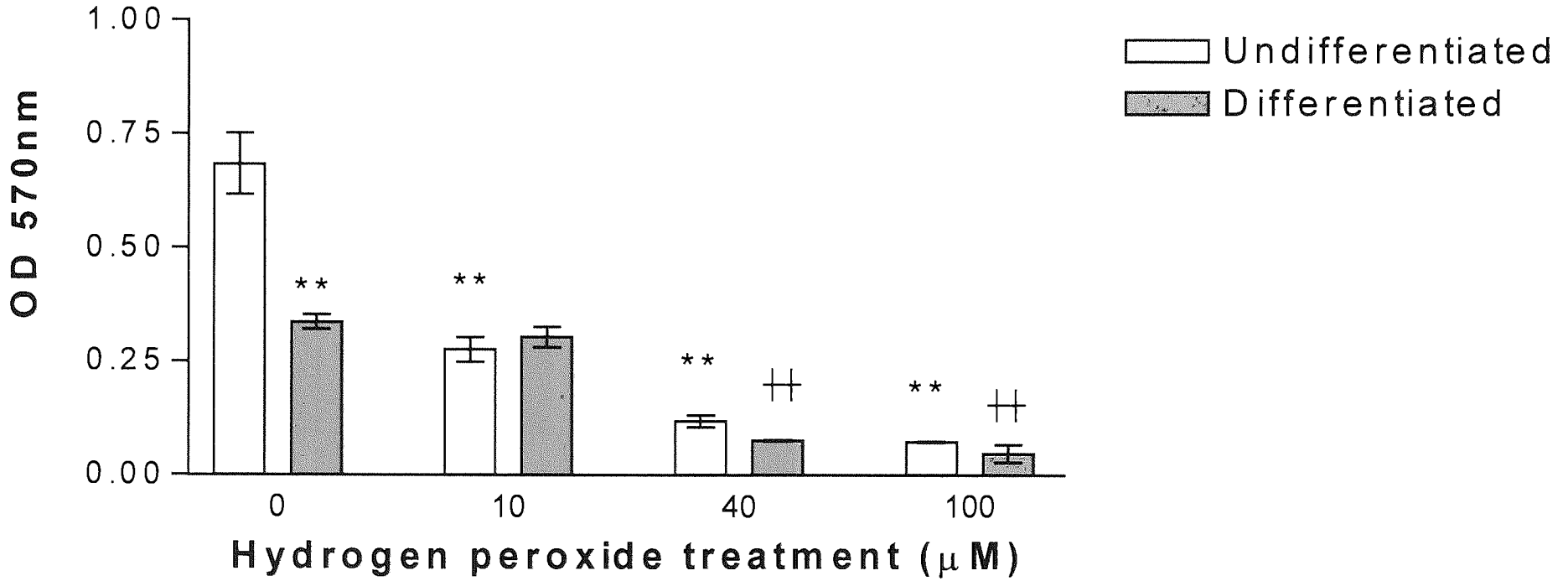

Figure 3.1.20 The effects of hydrogen peroxide on differentiated SY5Y cell viability using the MTT assay. Differentiated SY5Ys and their appropriate controls ($2x10^5$) were incubated with H_2O_2 (10, 40 and 100μM) for 24 hours at 37°C, 5% CO_2. Cells were then subject to the standard MTT assay and data expressed as the mean absorbance of formazan produced ± SEM of 16 replicates.
**** represents P<0.01 (Dunnett's test) when compared to 0μM H_2O_2 in undifferentiated cells.**
++ represents P<0.01 when compared to 0μM H_2O_2 in differentiated cells.

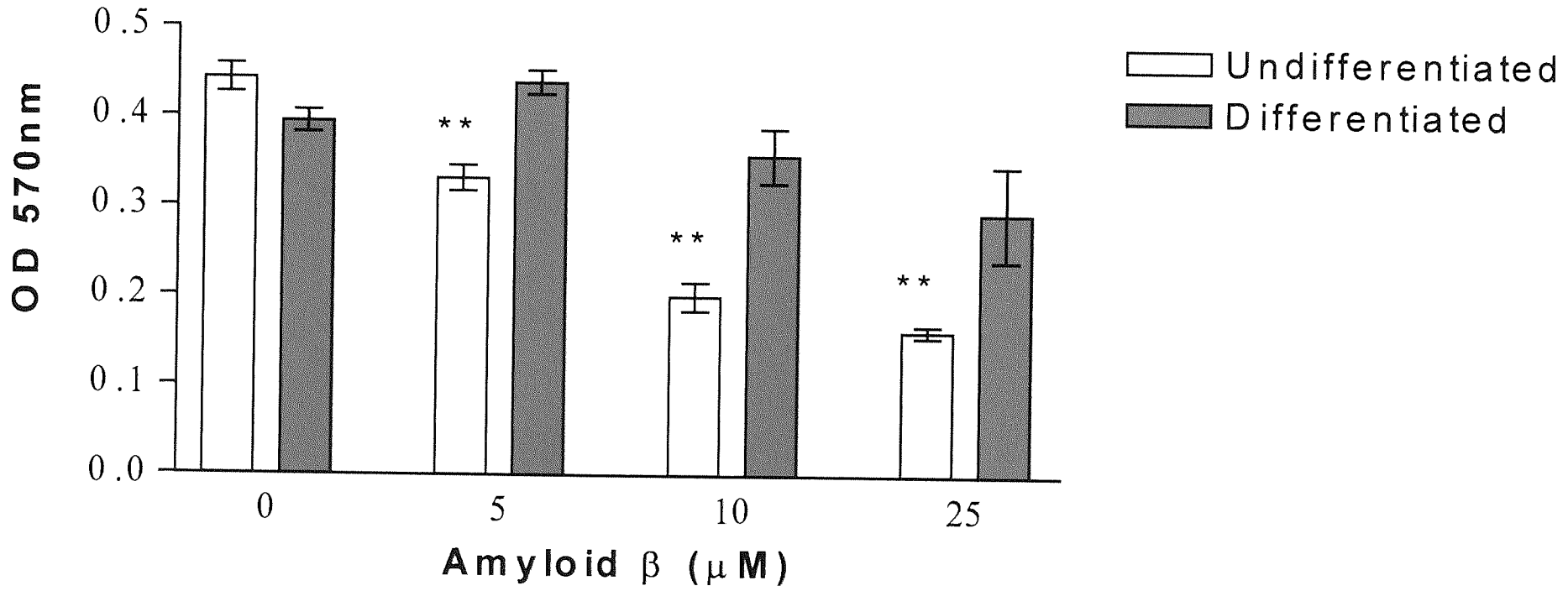

Figure 3.1.21 Amyloid β (25-35) (Aβ) induced toxicity on SY5Y cells. Differentiated SY5Y cells and their appropriate controls (2×10^5) were incubated with Aβ (5, 10 and 25μM) for 24 hours at 37°C, 5% CO_2. Cells were then subject to the standard MTT assay where results are expressed as the mean absorbance of formazan produced ± SEM of 4 replicates. ** represents $P < 0.01$ (Dunnett's test) when compared to 0μM Aβ in undifferentiated cells.

3.1.5.2 Effect of Amyloid β on MTT reductive activity

3.1.5.2.1 Effect of Amyloid β peptide, fragment 25-35

The effect of increasing concentrations of aged Aβ peptide, fragment 25-35, on differentiated and undifferentiated SY5Y cell viability were investigated. Figure 3.1.21 shows a dose dependent relationship between increasing Aβ dose and decreasing MTT product formation in undifferentiated cells, where differentiated cells are more resistant to Aβ toxicity. Dunnett's post tests conducted, showed the effects seen at each Aβ dose to only be significant only in undifferentiated cells, $P<0.01$.

3.1.5.3 Effects of nerve growth factor on MTT reductive activity

The effects of NGF on SY5Y differentiated and undifferentiated cell viability as measured by MTT reductive activity were assessed using three concentrations of NGF (5, 10 and 25ng/ml) versus control. Figure 3.1.22 no effect of increasing NGF concentration in both cell types (differentiated and undifferentiated).

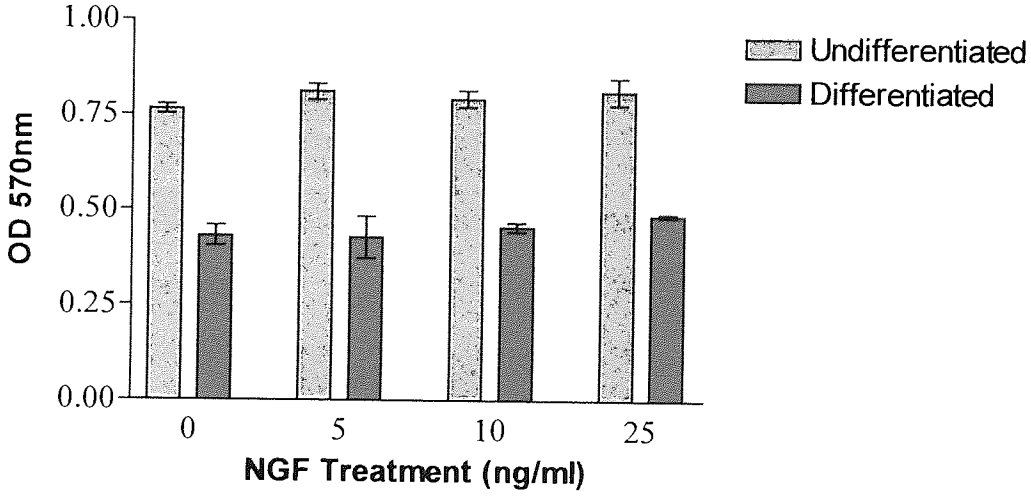

Figure 3.1.22 The effect of nerve growth factor on differentiated SY5Ys and undifferentiated SY5Y cells. Differentiated SY5Ys and their appropriate controls ($2x10^5$) were incubated with NGF (5, 10 and 25ng/ml) for 24 hours at 37°C, 5% CO_2. Cells were then subject to the standard MTT assay. Figure shows the mean absorbance of formazan produced ± SEM for 4 replicates.

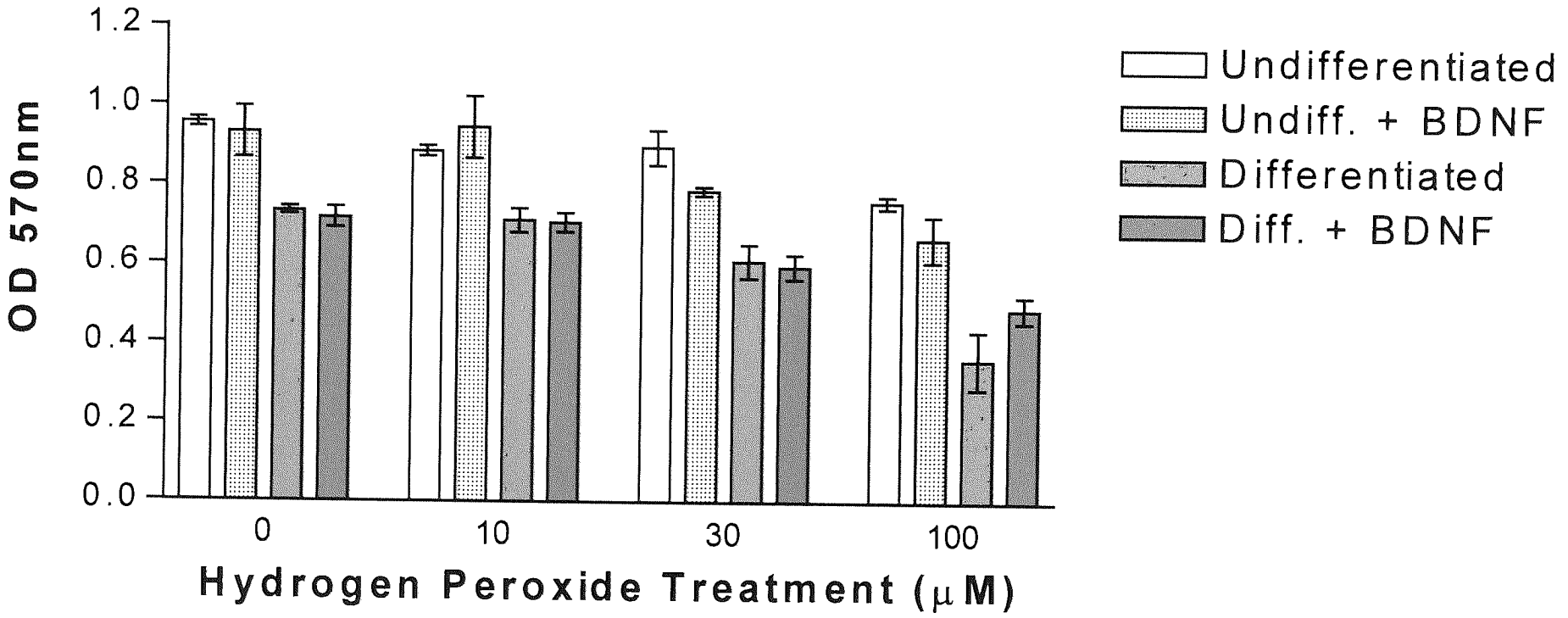

Figure 3.1.23 The effect of brain derived growth factor on protection of differentiated SY5Ys and control SY5Y cells from peroxide toxicity. Differentiated SY5Ys and their appropriate controls ($2x10^5$) were incubated with BDNF (10ng/ml) for 24 hours at 37°C, 5% CO_2. Cells were then subject to the standard MTT assay as stated in section 2.2.2. Graph shows the mean absorbance of formazan produced ± SEM for 3 replicates.

3.1.5.4 Effects of brain derived growth factor on hydrogen peroxide toxicity

The effects of BDNF on cell viability following peroxide treatment as measured by MTT reductive activity were assessed using 10ng/ml BDNF versus control. Figure 3.1.23 shows a general trend for a dose dependent loss in viability or toxicity with increasing H_2O_2 concentrations in both cell types, however, no significant effects of BDNF on cell viability were recorded in either undifferentiated or differentiated cells.

3.1.6 DISCUSSION

Results show OS, whether induced by H_2O_2 or Aβ, causes a decrease of MTT activity. These data also demonstrate that sensitivity to OS is influenced by culture conditions, where maintaining cells in culture for a 24 hour pre-incubation period reduced their sensitivity to oxidant induced cytotoxicity. Studies undertaken using increasing cell densities confirm that cell number is an important factor.

On a molar basis, Aβ caused significantly greater loss of mitochondrial activity than H_2O_2. Possible explanations are that Aβ targets the mitochondria, Aβ could redox cycle and generated ROS continuously or it acts via a peroxide independent process.

NGF was used at a range of 0-50ng/ml. It has recently been reported that optimal NGF protective activity is achieved at concentrations of 10ng/ml (Shooter, 2001). In the results presented 10ng/ml produced consistently protective effects in agreement with Shooter. The lack of any effect by BDNF pre-treatment contradicts other reports – therefore from a lack of correlation with the work of other groups, the uptake of BDNF needs to be checked by radio labelling, to ensure the BDNF is actually being taken up.

AA was used at 50μM as this represents the average serum level for healthy subjects, and it had been reported that concentrations above this cause OS and apoptosis to neuronal cells in culture (Puskas *et al.*, 2000). In both cell lines treated with 100μM AA, no significant increases in apoptosis were recorded in unchallenged cells. However, in peroxide challenged PC12 cells a significant decrease in cell viability was recorded in the presence of AA. Therefore AA was exerting a pro-oxidant effect in culture, and generally did not cause inhibition of cell death in PC12 cells. However, AA was slightly protective in SY5Y cells, although the levels of protection were low and the relevance of this protection remains unclear. AA can exert different effects due to its two mechanisms of uptake, reduced via an Na+ -dependent ascorbate transporters (SVCT1 and SVCT2) and glutamate-ascorbate heteroexchange ion channel, and oxidised dehydroascorbate (DHA) via GLUT, a glucose transporter (Song *et al.*, 2001). As cells were cultured in different media it is important to note that when agents when added to cells in culture can undergo chemical reactions with constituents of cell culture media, some of which lead to H_2O_2 generation. Ascorbate can also be oxidised easily in certain cell culture media to generate H_2O_2, and it has been reported that the cytotoxic effects of ascorbate on cells in culture could be entirely due to the generation of H_2O_2 in the culture media (Halliwell *et al.*, 2000). It has been hypothesized that ascorbate is oxidised to DHA by oxygen (O_2) in solution (Culture medium or plasma), and the dehydroascorbate is transported by a 'dehydroascorabte transporter (GLUT) where it is reduced back to the ascorbate generating oxidative stress. The oxidative stress, in turn, triggers apoptosis (Song *et al.*, 2001).

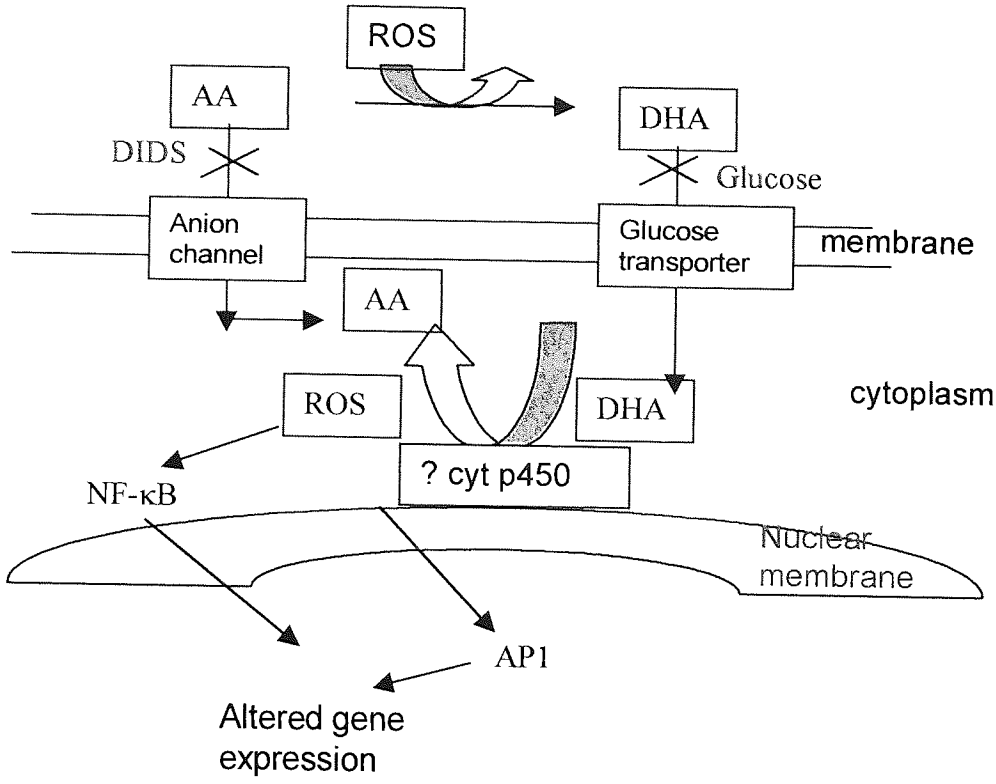

Figure 3.1.24 The mechanism for uptake of AA and DHA , adapted from Griffiths & Lunec, 2001) DIDS – selective anion channel inhibitor

SY5Y cells were more susceptible than PC12 cells, there could be many reasons for this. Various groups have reported differences between the toxicity of agents to different cells lines (Davis *et al.*, 2001; Dudek *et al.*, 2001; Gschwind & Huber, 1995). Reasons that have been proposed for these differences in vulnerability, include that different cells contain the AOX glutathione at varying concentrations. It has also been suggested that differences between cell types can often be due to the mode of induced cell death, either necrotic or apoptotic. This shows a limitation of the systems available as deposition of Aβ may play a causal role in AD pathogenesis, these data show that different toxicity mechanisms can occur depending on cell type, and therefore which cell type is showing the equivalent *in vivo* result?. Therefore further development of this data is needed, to be able to finally evaluate the toxic mechanisms of Aβ by *in vivo* studies with either chronic or acute peptide applications into animal brains or by performing *in situ* analysis of neuronal cell death in transgenic brains exhibiting severe

amyloidosis (Gschwind & Huber, 1995). Also as most cells in culture exposed to 95% air/5% CO_2 are essentially in a hyperoxic environment compared to the *in vivo* situation. Therefore the cells that can tolerate, or adapt to, such conditions to allow them to grow and proliferate may behave very differently from cells *in vivo* (Halliwell & Gutteridge, 1999).

Yao *et al.,* (2001) have demonstrated that AOX inhibited Aβ induced ROS production but not Aβ induces apoptosis and cell death. They suggested that the Aβ induced free radical, mediated neurotoxicity may not be the cause of AD, although it may participate in the progression of the disease. However, the experiments included in this section did not show the mode of cell death, whether it was apoptotic or necrotic. Previous groups have alluded to both forms of cell death by Aβ and H_2O_2. Li *et al.,* (1996) provided the initial evidence that apoptosis was the major mechanism of Aβ neurotoxicity. However MTT is only a reflection of cell viability and therefore further morphological analysis was conducted on both cell types, to determine whether apoptosis was occurring under these conditions.

3.2 Morphological effects of H_2O_2 toxicity recorded by video microscopy

The morphology of cells undergoing treatment with H_2O_2 was investigated using an inverted microscope attached to a digital camera. PC12 cells are a non-adherent line, which normally form spherical clusters of cells under optimal conditions. SY5Y cells are an adherent cell line with neuroblast morphology. Addition of H_2O_2, AA and NGF did show some effects on morphology, however the quality of PC12 images were low.

Images shown in figure 3.2.4 show that the addition of increasing amounts of H_2O_2 caused changes in SY5Y morphology; within the field of view, densely covered areas of adherent neuroblasts were lost following H_2O_2 treatment, with cells rounding up, and clumps of cells forming which appear condensed. Figure 3.2.5 shows clear effects of NGF on H_2O_2 toxicity, where a greater number of SY5Y cells of a normal morphology can be observed after 25ng/ml NGF in the presence of 250μM H_2O_2 compared to cells treated with 250μM H_2O_2 in the absence of NGF. Figure 3.2.6 shows some effects of AA on H_2O_2, following treatment with 100μM AA, at 250 and 500μM H_2O_2 there were a greater number of cells and more cells displaying a normal morphology, however these effects were not as clear as those recorded with NGF.

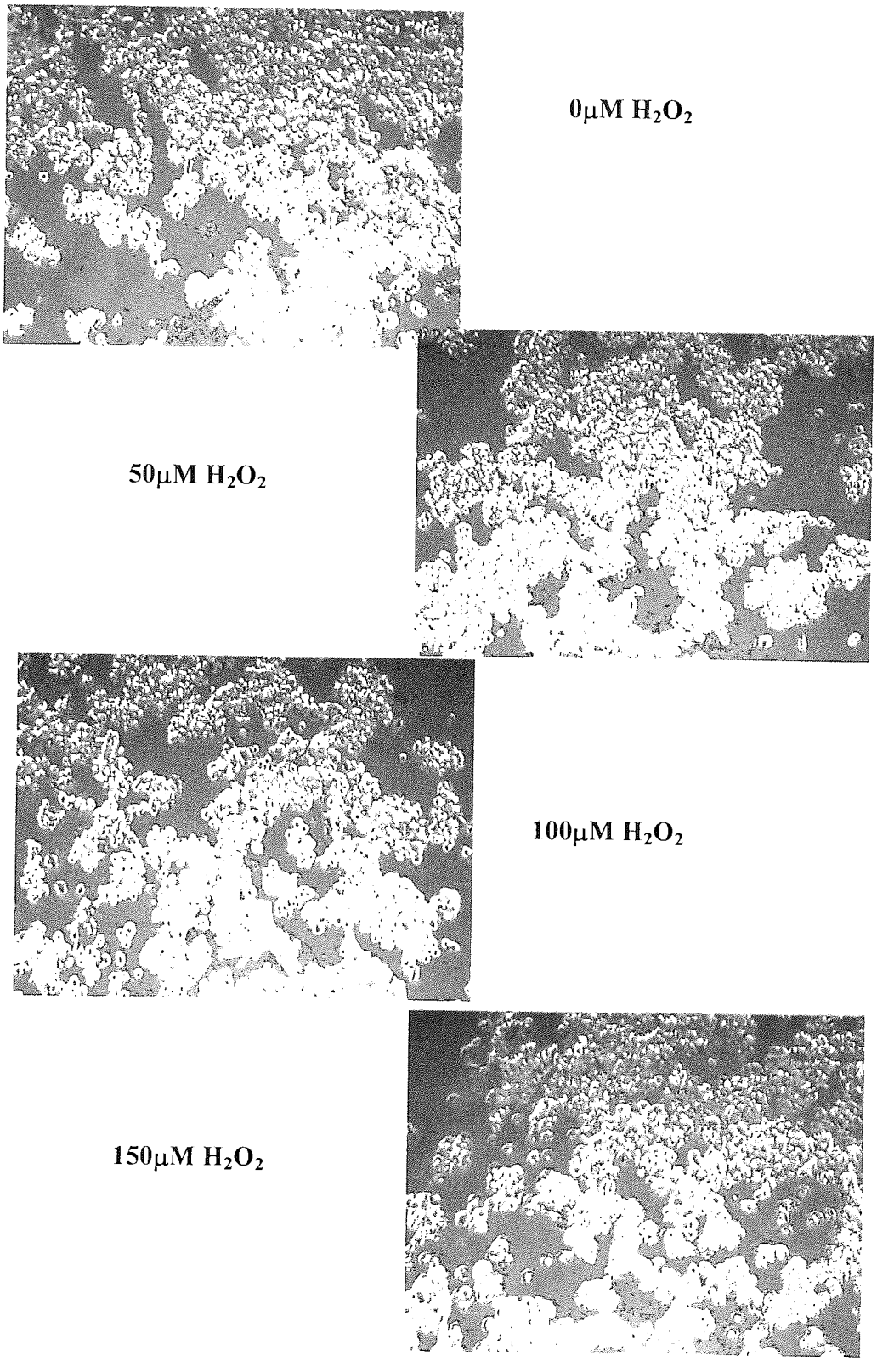

Figure 3.2.1 Representaive video microscopy stills of PC12 cells treated with hydrogen peroxide (0, 50, 100 and 150μM) for 24 hours at 37°C, 5% CO_2., stills were taken of at least 5 fields, only 1 field is shown for each treatment.

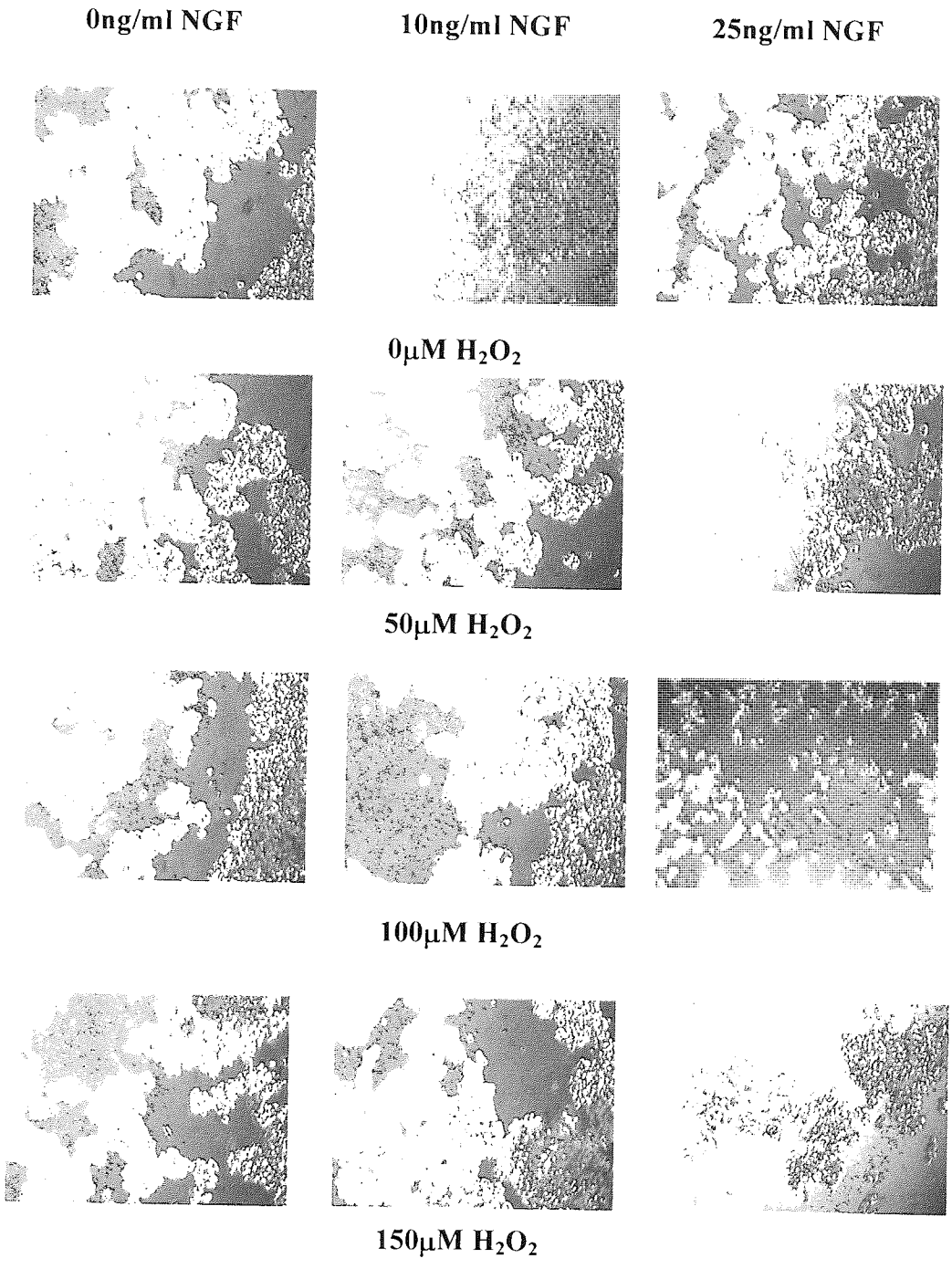

Figure 3.2.2 Representative video microscopy stills of PC12 cells (1ml) pre-treated with NGF (0, 10 and 25ng/ml) for 24 hours at 37°C, 5% CO_2 then treated with hydrogen peroxide (0, 50, 100 and 150μM) for 24 hours at 37°C, 5% CO_2., stills were taken of at least 5 fields, only 1 field is shown for each treatment.

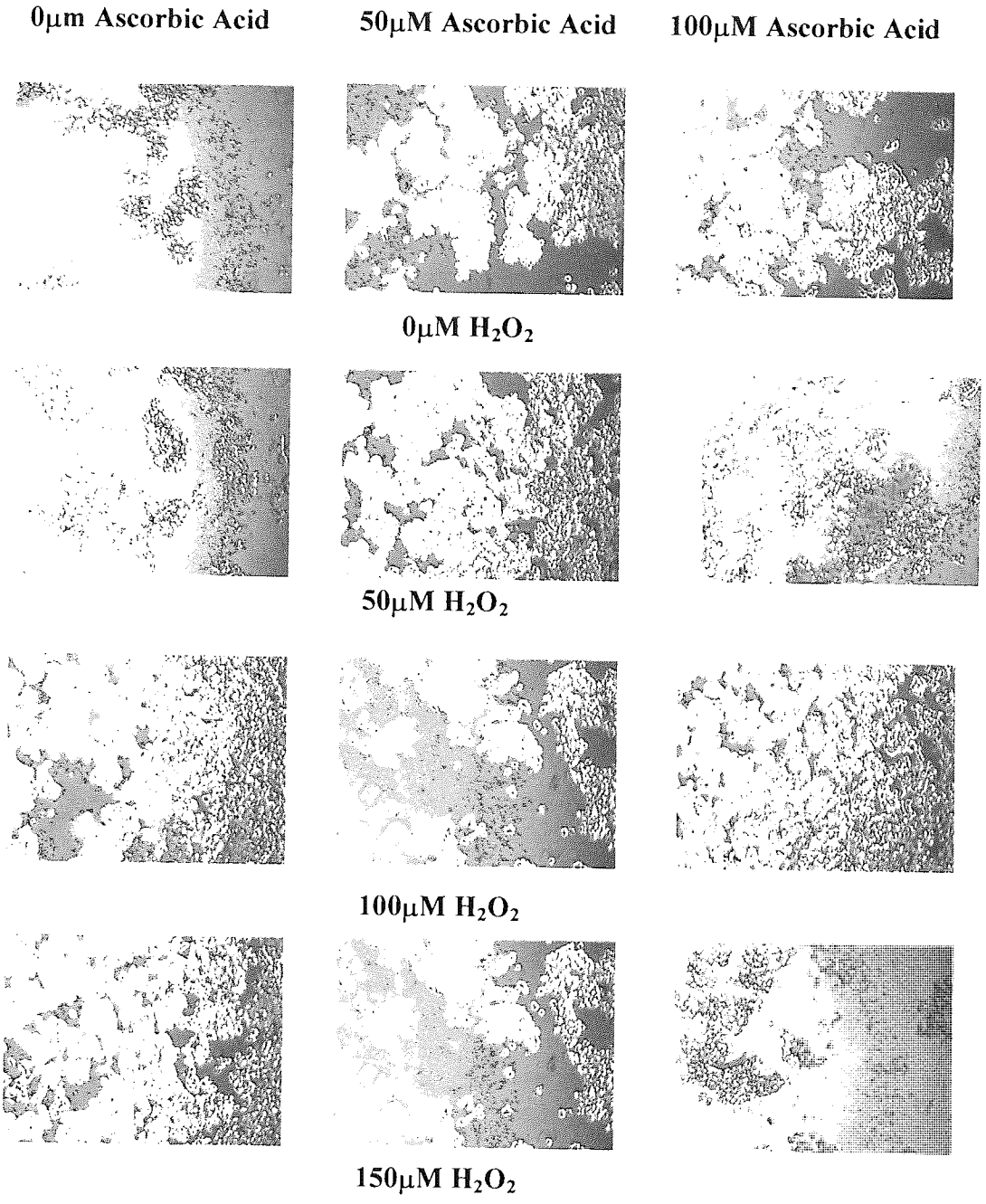

Figure 3.2.3 Representative video microscopy stills of PC12 cells pre-treated with ascorbic acid (0 and 100μM) for 24 hours at 37°C, 5% CO_2 then treated with hydrogen peroxide (0, 50, 100 and 150μM) for 24 hours at 37°C, 5% CO_2., stills were taken of at least 5 fields, only 1 field is shown for each treatment.

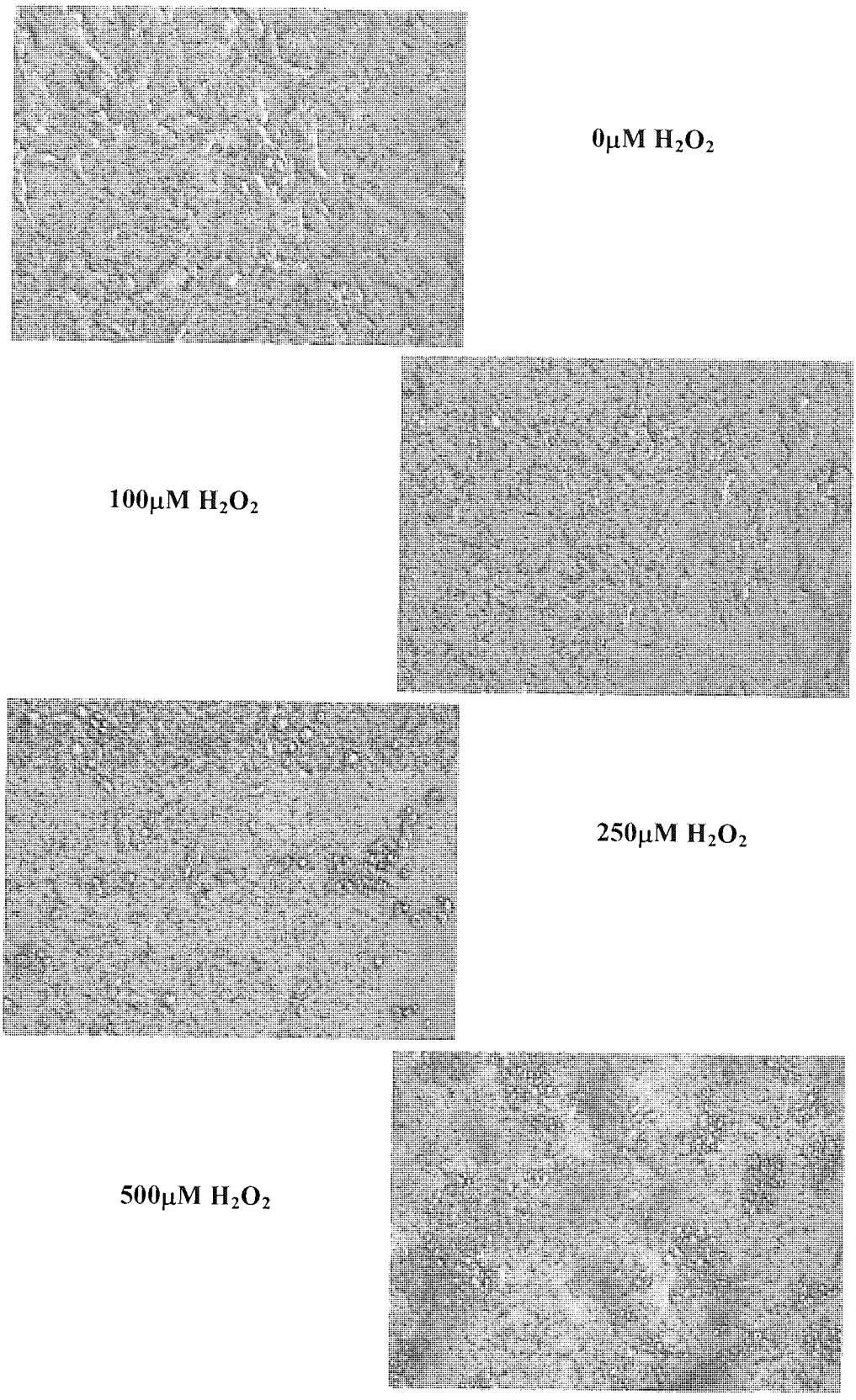

Figure 3.2.4 Representative video microscopy stills of SH-SY5Y cells treated with hydrogen peroxide (0, 100, 250 and 500μM) for 24 hours at 37°C, 5% CO_2., stills were taken of at least 5 fields, only 1 field is shown for each treatment.

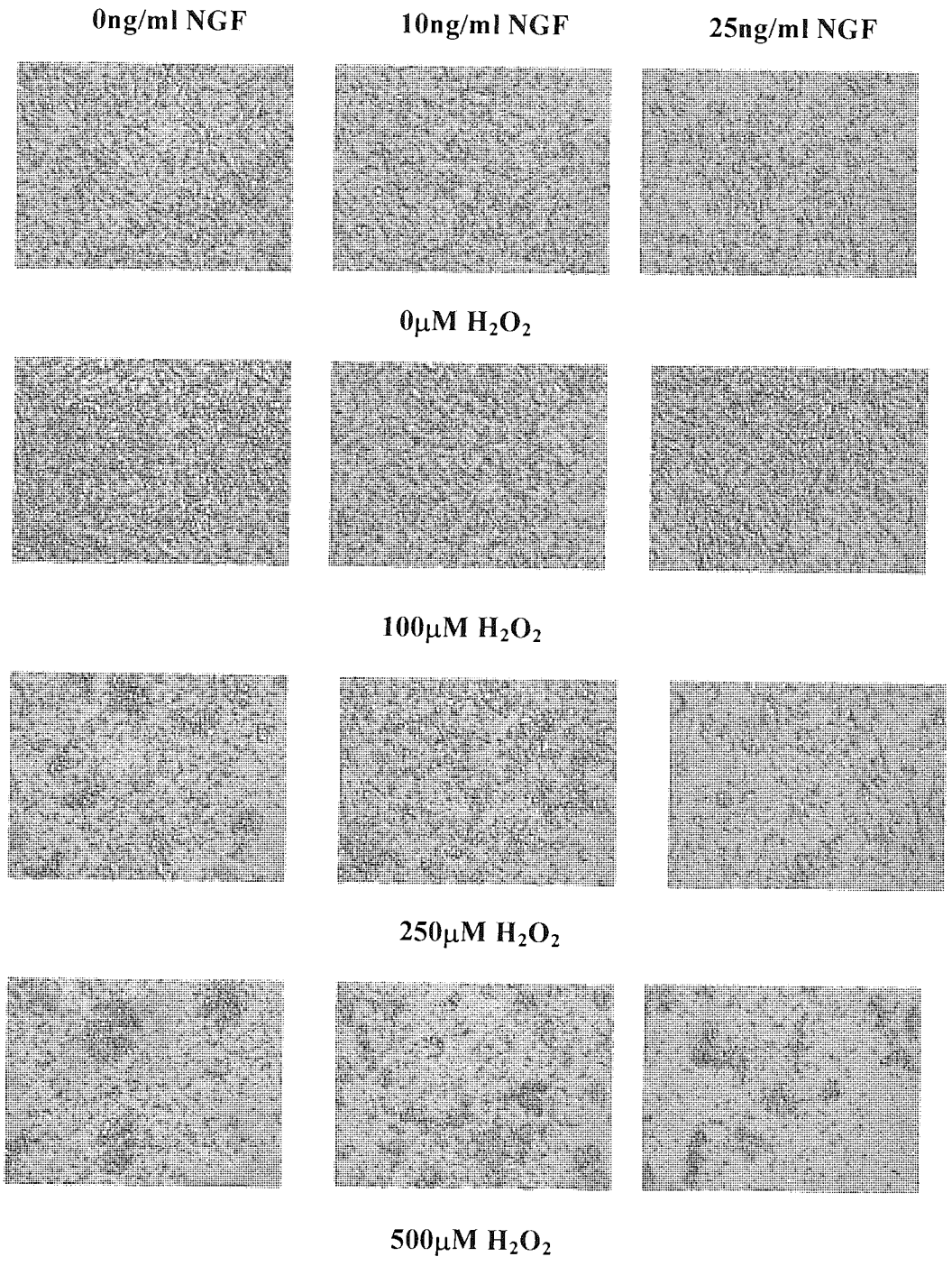

Figure 3.2.5 Representative video microscopy stills of SH-SY5Y cells (1ml) pre-treated with NGF (0, 10 and 25ng/ml) for 24 hours at 37°C, 5% CO_2 then treated with hydrogen peroxide (0, 100, 250 and 500μM) for 24 hours at 37°C, 5% CO_2., stills were taken of at least 5 fields, only 1 field is shown for each treatment.

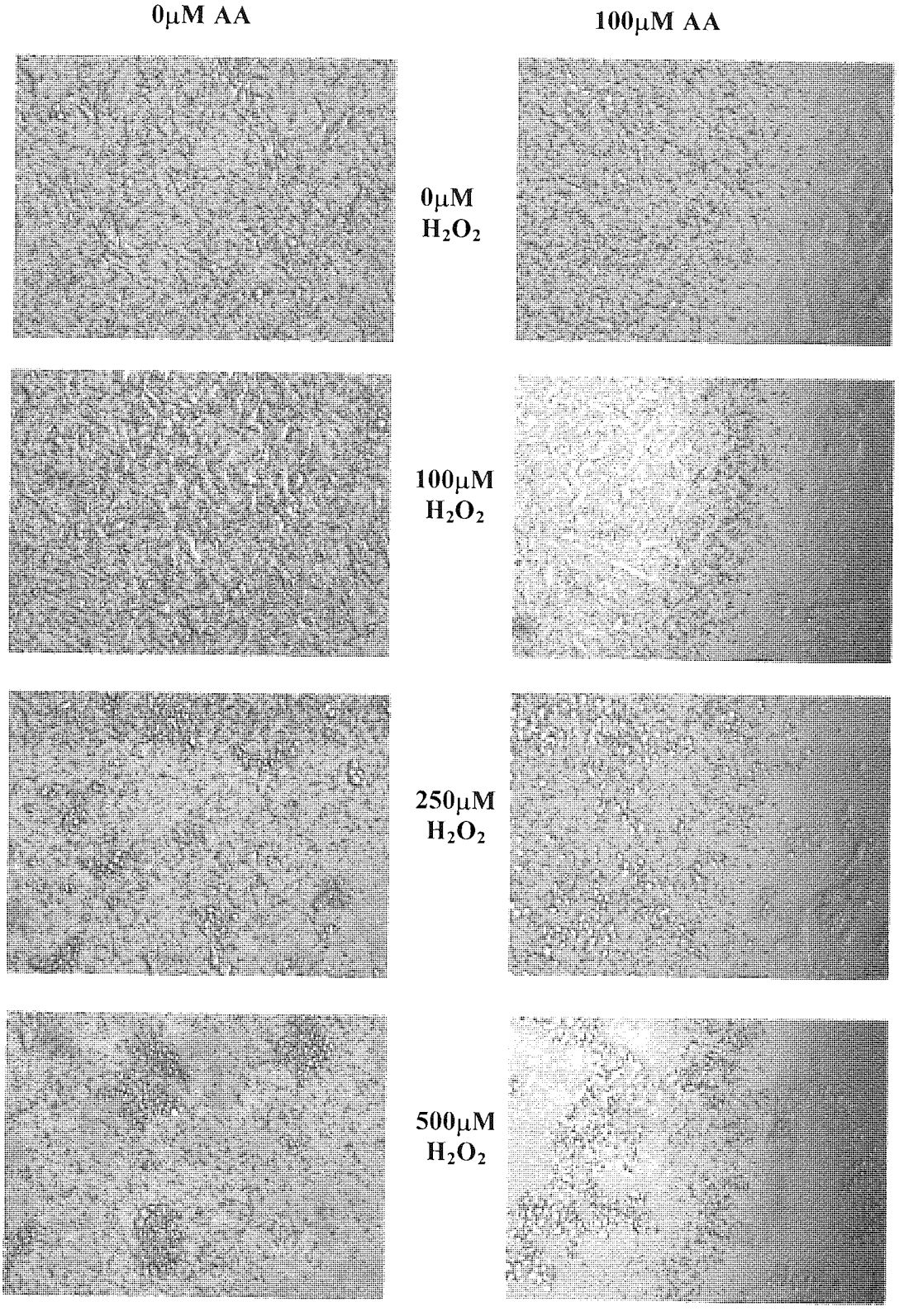

Figure 3.2.6 Representative video microscopy stills of SH-SY5Y cells pre-treated with ascorbic acid (0 and 100μM) for 24 hours at 37°C, 5% CO_2 then treated with hydrogen peroxide (0, 100, 250 and 500μM) for 24 hours at 37°C, 5% CO_2., stills were taken of at least 5 fields, only 1 field is shown for each treatment.

3.3 Fluorescence microscopy to determine nuclear condensation and cellular viability

Viable (intact plasma membrane) and dead (damaged plasma membrane) cells can be discriminated by differential staining. Hoechst 33342 (Hoechst) is a specific DNA stain that is membrane permeable and binds to the AT base pairs in the DNA, thereby staining the DNA in cells (without permeabilization). All viable and apoptotic cells take up the dye; nuclear morphology defines viable 'normal' cells from apoptotic cells. In contrast to normal cells which are uniformly stained, the nuclei of apoptotic cells exhibit highly condensed chromatin that is stained by Hoechst; this either takes the form of crescents around the periphery of the nucleus, or the entire nucleus appears to be one or a group of featureless, bright spherical beads. Co-staining of the cells with propidium iodide (PI) allows the discrimination of non-viable dead cells from apoptotic cells.

PI intercalates into the DNA helix through damaged plasma membranes and fluoresces strongly orange –red under 405-490nm wavelengths. Positively PI stained cells are indicative of non-viable cells that have expired in a necrotic manner.

Results

Cells were dual stained with Hoechst and PI, and then counted according to the stain they had taken up. The percentages of PI containing cells of the total cells were calculated. Differential staining with these two agents was optimised to enable the visualisation of the morphology of cells alongside actual staining. This facilitated transfer of the images seen down the microscope, onto film. Various film products were employed to achieve high definition reproducible and analysable images.

Different film speeds along with shutter speeds were employed, alongside different film types including monochrome, colour and tungsten. The optimal requirements for high definition images were Tungsten colour reversal film, with a film speed of 64, and a shutter speed of 10 seconds. However, when the PI cells were those of interest a speed of 20 seconds was required as cells fluoresce red with a very low light intensity. The percentage of PI cells was counted in four fields for each treatment. All blue cells (positively Hoechst stained) represent cells that are either viable cells or those undergoing apoptosis and excluding non-viable cells. All red cells (positively PI stained) represent non-viable cells, the number of PI stained cells were then converted into a percentage of the total cell number.

Dual Hoechst / PI staining analysis by other investigators have revealed that both $A\beta_{25-35}$ and $A\beta_{1-42}$ treated PC12 cells are predominantly stained with PI, and do not show any nuclear damage, such as condensation and/or fragmentation of nuclei. In contrast Aβ untreated cells were not stained with PI. Results suggest that Aβ treatment induces an abnormality in cell membrane permeability, because PI is an impermeable compound. It has already been reported that cells undergoing necrotic cells death are predominantly stained with PI without showing DNA damage (Suzuki, 1997). H_2O_2 has also been shown to cause morphological alterations characteristic of apoptosis such as cell shrinkage and blebbings (Zhang *et al.*, 1997).

N.B. Photographs included should be considered as qualitative only, due to the uneven number of cells in each of the fields.

3.3.1 Effect of hydrogen peroxide on PC12 cell viability

The effects of increasing concentrations of H_2O_2 on PC12 cell viability were investigated. Cells were dual stained with PI and Hoechst to examine whether H_2O_2 caused changes in cell viability, and whether the changes in viability were via an apoptotic or necrotic means.

Figure 3.3.1 shows that increasing H_2O_2 concentrations caused increases in the percentage of PI stained cells indicative of reductions in cell viability. The basal level of PI (non viable) cells recorded was 18.6% at 0μM H_2O_2, this rose significantly to 52.4% at 150μM H_2O_2, 40.9% at 200μM H_2O_2 to 86.4% at 250μM H_2O_2. ($P<0.01$, Dunnett's post test, n=4).

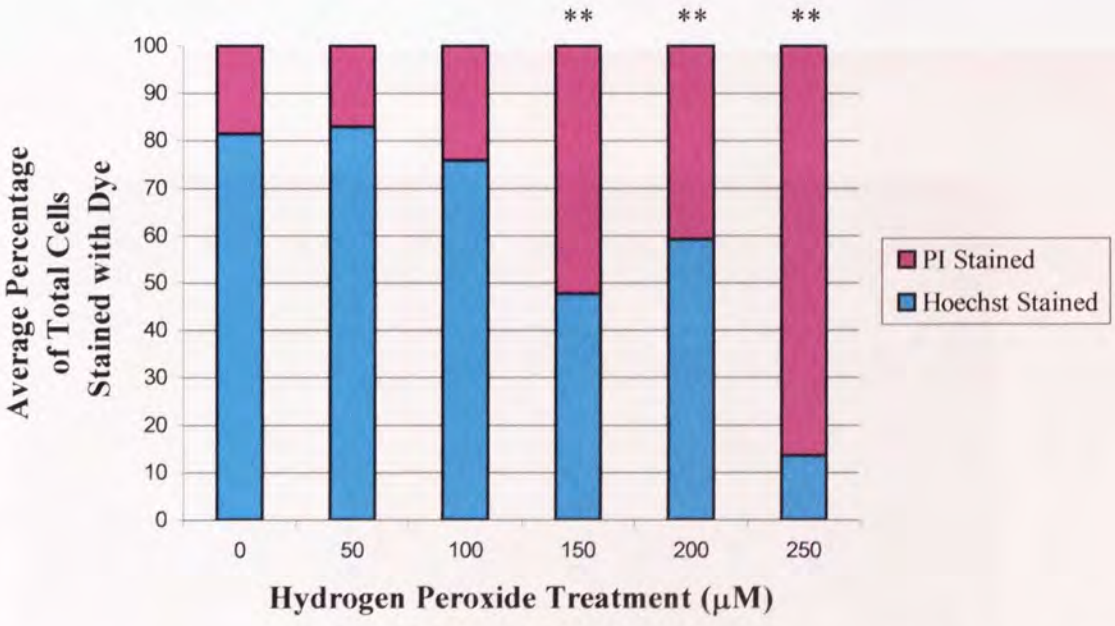

Figure 3.3.1 The effects of hydrogen peroxide on PC12 cells. PC12 cells ($2x10^5$) were incubated with H_2O_2 (50, 100, 150, 200 and 500μM) for 24 hours at 37°C, 5% CO_2. Graph shows the mean percentage of propidium stained (non-viable) cells and Hoechst stained (viable) cells as a percentage of total cells stained, n=4.

Photographs of PI/Hoechst staining investigating the effects of H_2O_2 on PC12 cells are included as figures 3.3.2 and 3.3.3.

A

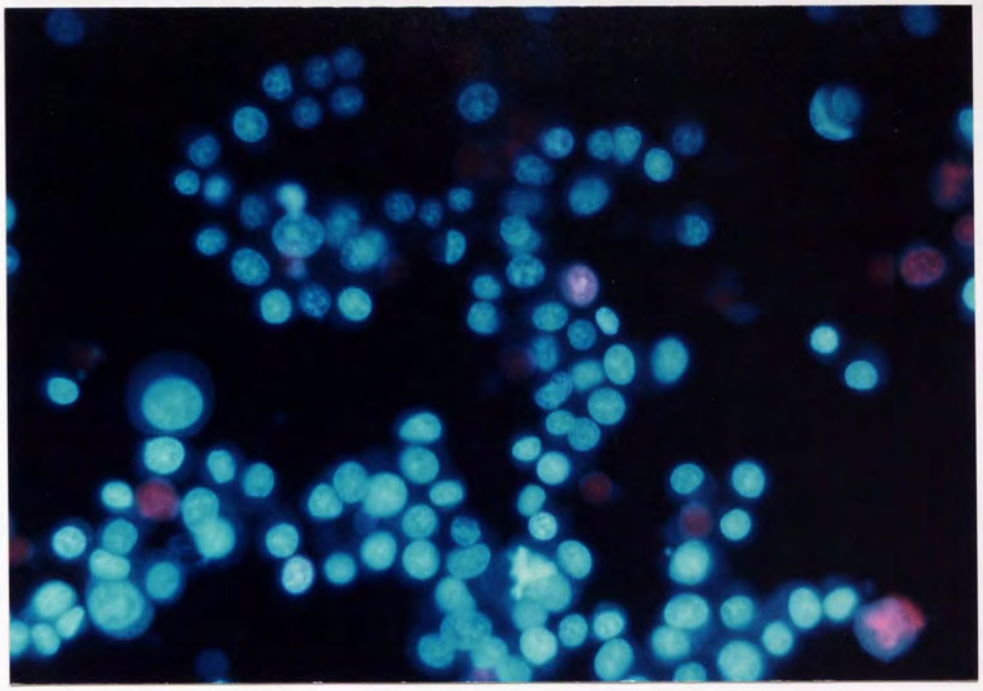

B

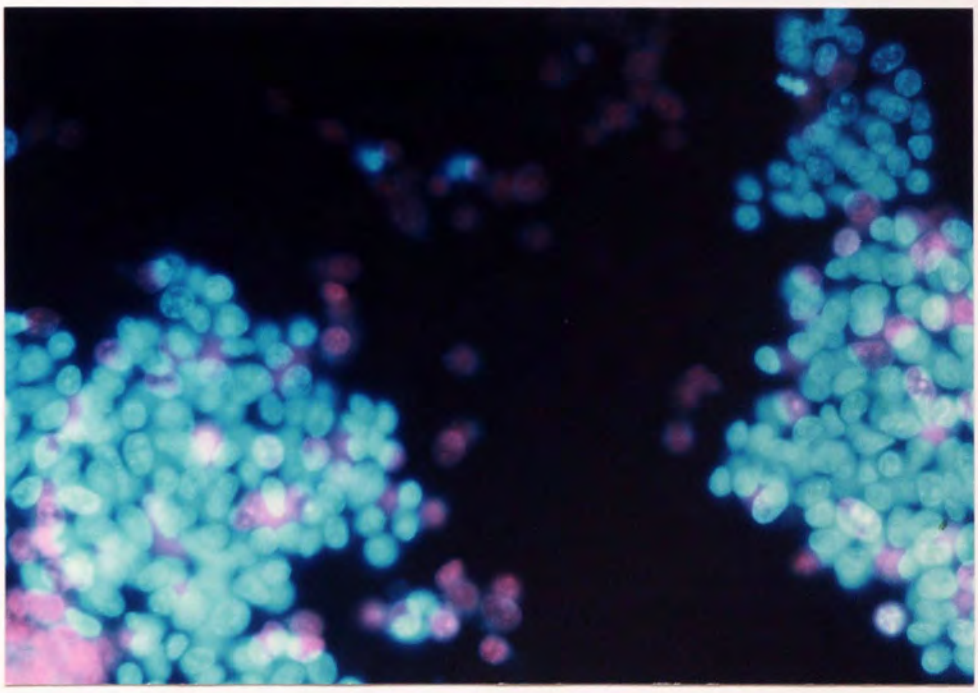

Figure 3.3.2 Photographs of Hoechst/PI staining of PC12 cells exposed to H_2O_2 for 24 hours. A represents 0μM, B represents 100μM.

C

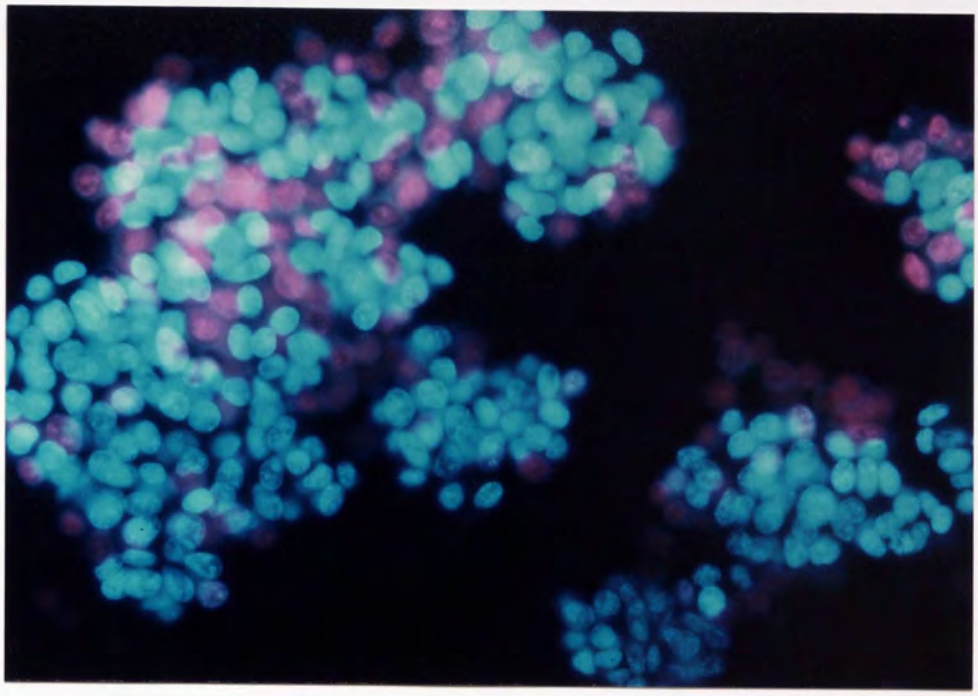

D

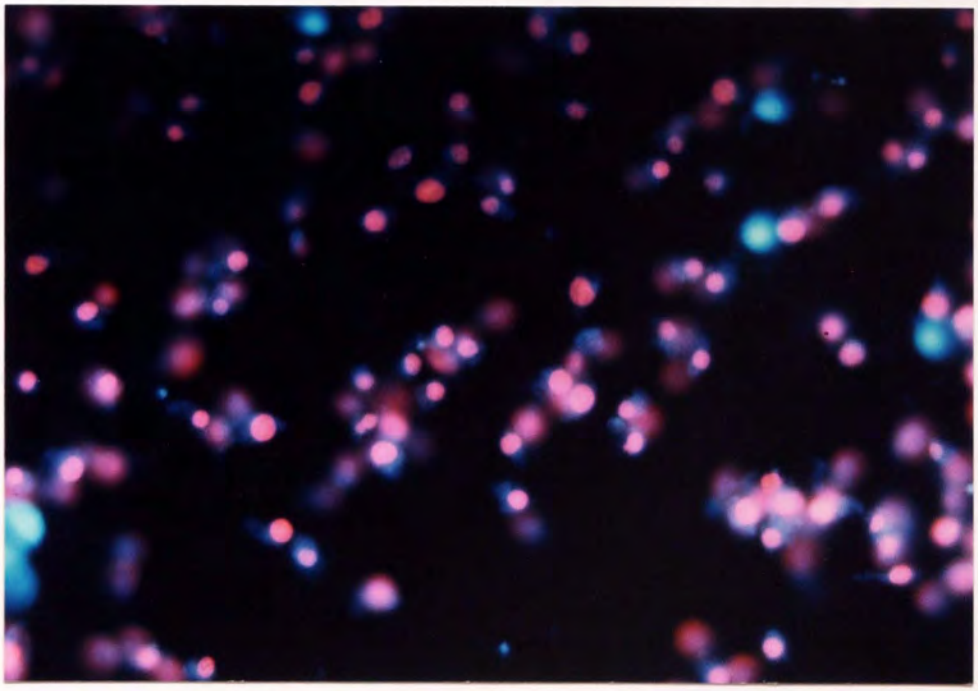

Figure 3.3.3 Photographs of Hoechst/PI staining of PC12 cells exposed to H_2O_2 for 24 hours. C represents 200μM, D represents 500μM.

3.3.1.1 Effect of Nerve Growth Factor on hydrogen peroxide toxicity as assessed by fluorescence microscopy

The effects of NGF on PC12 cell viability were also investigated to examine whether NGF caused any significant protection against H_2O_2 challenge to PC12 cells. Cells were pre-treated for 24 hours with two concentrations of NGF (10 and 25ng/ml), and then subsequently challenged with increasing concentrations of H_2O_2 (150, 300μM) for 24 hours.

Figure 3.3.4 shows that increasing H_2O_2 concentrations caused dose dependent decreases in cell viability as represented by increases in the percentage of PI stained cells. The basal level of non viable cells recorded was 5.7% in the absence of H_2O_2, this rose through 10.8% at 150μM H_2O_2 ($P<0.001$) to 94.4% at 300μM H_2O_2.($P<0.001$).

NGF had two distinct effects, at low H_2O_2 concentrations (0 and 150μM), it promoted an increase in PI staining and thus reduced cell viability. However, at high H_2O_2 (300μM) concentrations NGF prevented the increase in PI staining and thus maintained the number of viable cells. NGF was shown to reduce cell viability or protect against toxicity depending on H_2O_2 dose. In the absence of H_2O_2 (0μM), the effects of NGF were compared, the mean percentage of PI stained cells were 5.8%, 7.0% and 26.2% for 0ng/ml, 10ng/ml and 25ng/ml NGF respectively, where NGF (25ng/ml) caused a significant increase in cell death in unchallenged cells compared to control non-NGF pre-treated cells (Dunnett's post test, $P<0.01$, $n=4$).

In the presence of peroxide (150μM), the mean percentage of PI stained cells were 10.8%, 9.0% and 53.8% for 0ng/ml, 10ng/ml and 25ng/ml NGF respectively. NGF

(25ng/ml) caused a significant increase in cell death compared to non pre-treated cells (Dunnett's post test, $P<0.01$, $n=4$).

At 300μM H_2O_2 the mean percentage of PI stained cells were 94.4%, 14.2% and 25.6% for 0ng/ml, 10ng/ml and 25ng/ml NGF respectively, where NGF (10ng/ml and 25ng/ml) exerted significant protection against cell death induced by H_2O_2 (300μM) compared to non pre-treated cells where $P<0.01$, $n=4$ (Dunnett's post test).

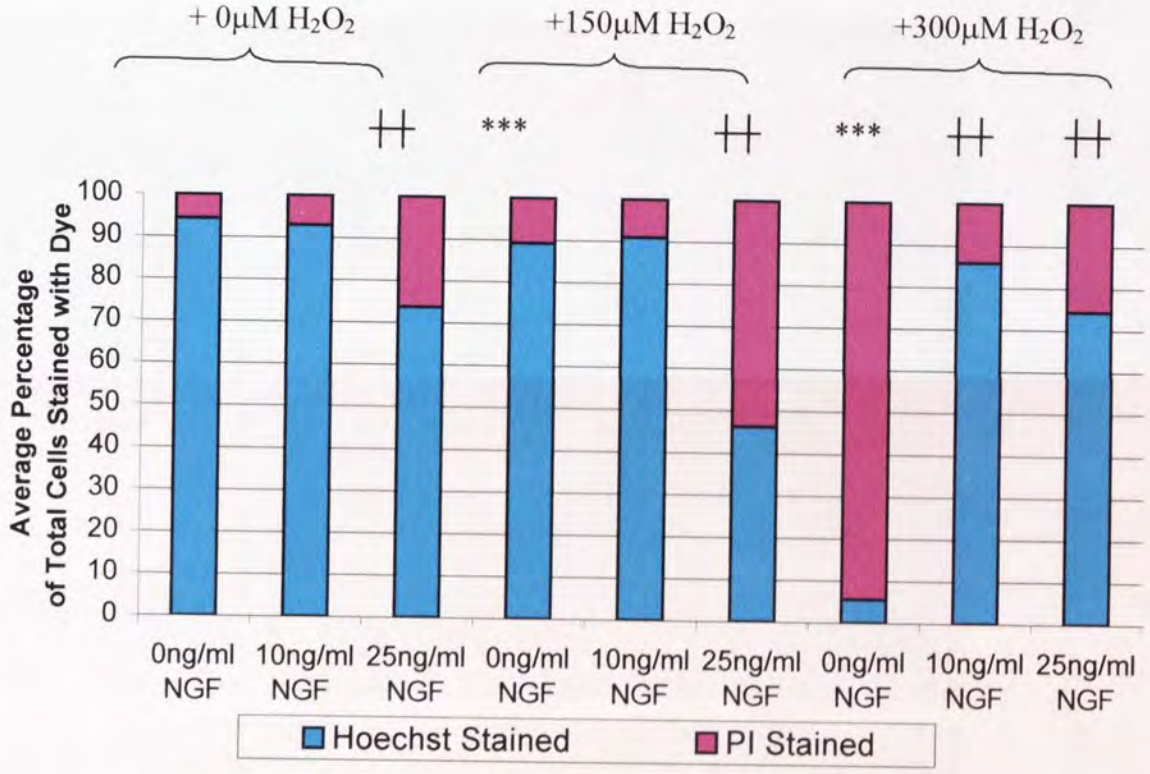

Figure 3.3.4 The effects of nerve growth factor on hydrogen peroxide toxicity on PC12 cell viability. PC12 cells ($2x10^5$) were incubated with NGF (10 and 25ng/ml) for 24 hours at 37°C, 5%CO_2. Data are expressed as the mean percentage of propidium stained (non-viable) cells as a percentage of total cells stained ± SEM.
***** represents $P<0.001$ (Dunnett's test) versus control, $n=4$.**
++ represents $P<0.01$ (Dunnett's test) versus 0ng/ml NGF pre-treatment, $n=4$.

Photographs of PI/Hoechst staining investigating the effects of NGF on 300μM H_2O_2 on PC12 cells are included as figure 3.3.5.

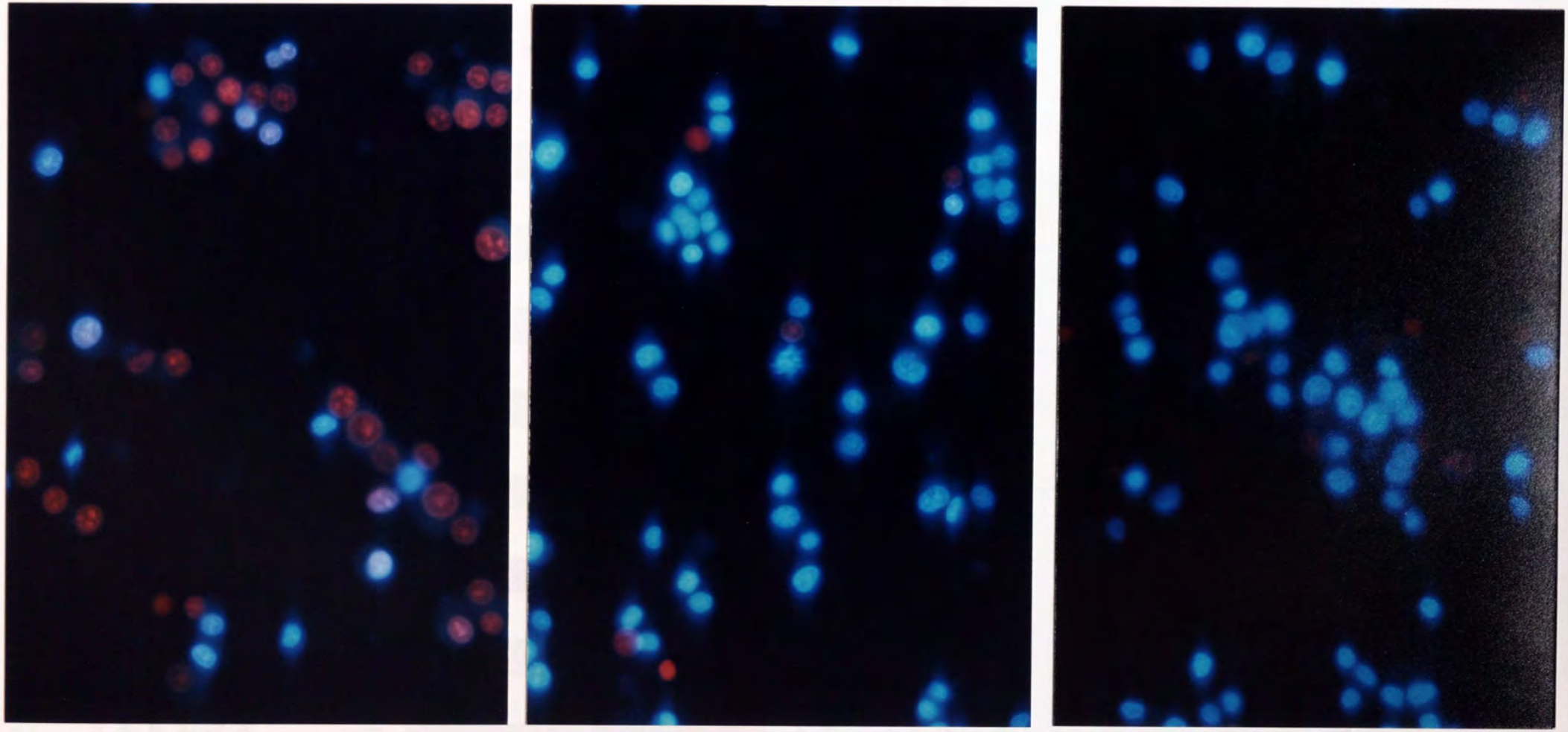

A B C

Figure 3.3.5 Photographs of Hoechst/PI staining of PC12 cells pretreated with A 0ng/ml NGF, B 10ng/ml NGF,C 25ng/ml NGF then subsequently exposed to 300μM H_2O_2

3.3.1.2 Effects of ascorbic acid on hydrogen peroxide toxicity as assessed by fluorescence microscopy

The effects on AA pre-treatment against H_2O_2 challenge on PC12 cells were investigated. Cells were pre-treated for 24 hours with two concentrations of AA (50 and 100μM), then subsequently challenged with increasing concentrations of H_2O_2 (150 and 300μM) for 24 hours.

Figure 3.3.6 shows that increasing H_2O_2 concentrations caused a decrease in cell viability as represented by increases in the percentage of PI stained cells. The basal level of non viable cells recorded was 9.1%, this rose through 45.2% at 150μM H_2O_2 ($P<0.01$) to 38.4% at 300μM H_2O_2.($P<0.01$).

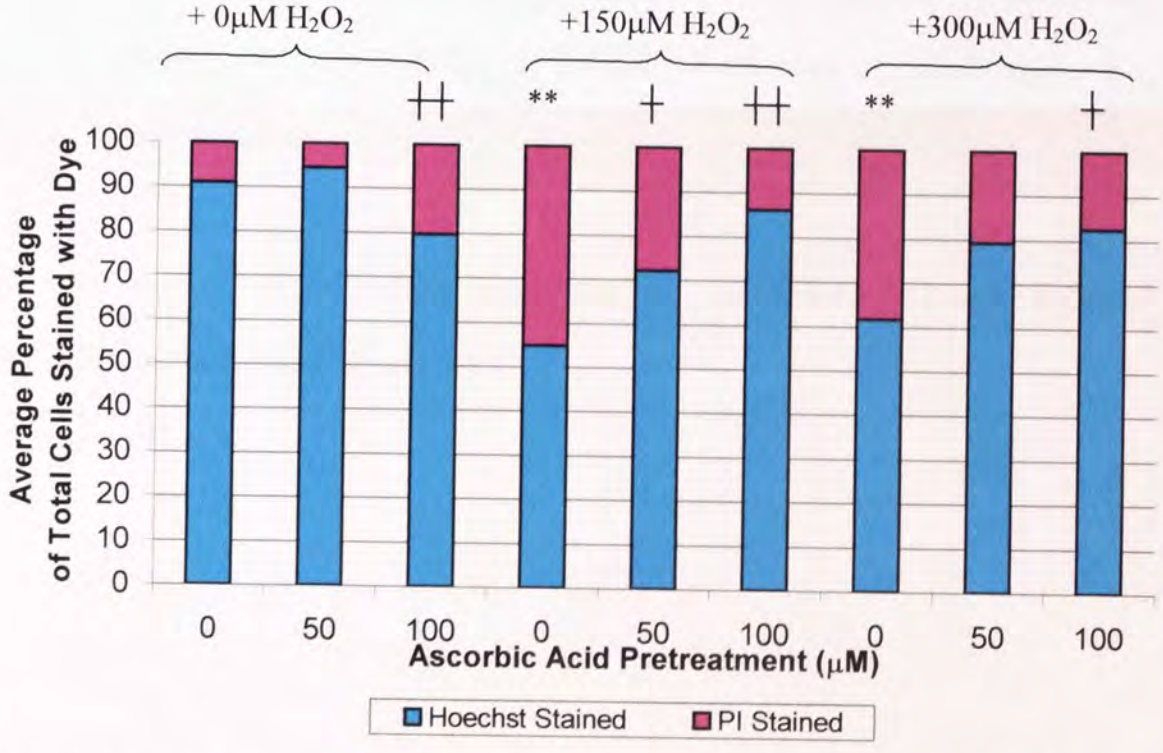

Figure 3.3.6 The effects of ascorbic acid on hydrogen peroxide toxicity on PC12 cell viability. PC12 cells ($2x10^5$) were incubated with AA (50 and 100μM) for 24 hours at 37°C, 5% CO_2. H_2O_2 was then added (150 and 300μM) for 24 hours at 37°C, 5% CO_2. Graph shows the mean percentage of propidium stained (non-viable) cells as a percentage of total cells stained ± SEM of 4 replicates. represents $P<0.01$ (Dunnett's test) versus 0μM H_2O_2. + represents $P<0.05$, ++ represents $P<0.01$ (Dunnett's test) versus 0μM AA pre-treatment, n=4.**

AA had two distinct effects, in control cells it promoted a increase in PI staining and thus a reduced cell viability. Results show AA (100μM) to cause a significant decrease in cell viability in unchallenged cells compared to cells not treated with AA ($P<0.01$, Dunnett's test, n=4). However in challenged cells (150 and 300μM H_2O_2), AA prevented the increase in PI staining due to peroxide, and thus caused a protection of cell viability.

In the presence of H_2O_2 the opposite effects were recorded with AA. At 150μM H_2O_2 the mean percentage of PI stained cells were 45.2%, 27.9% and 13.9% for 0μM, 50μM and 100μM AA respectively. Results show AA (50 and 100μM) significantly protects against loss of viability as PI stained cells,($P<0.05$ and $P<0.01$ respectively) induced by 150μM peroxide. At 300μM H_2O_2 only 100μM AA afforded significant protection $P<0.05$ (Dunnett's test).

Photographs of PI/Hoechst staining investigating the effects of AA on 300μM H_2O_2 on PC12 cells are included as figures 3.3.7.

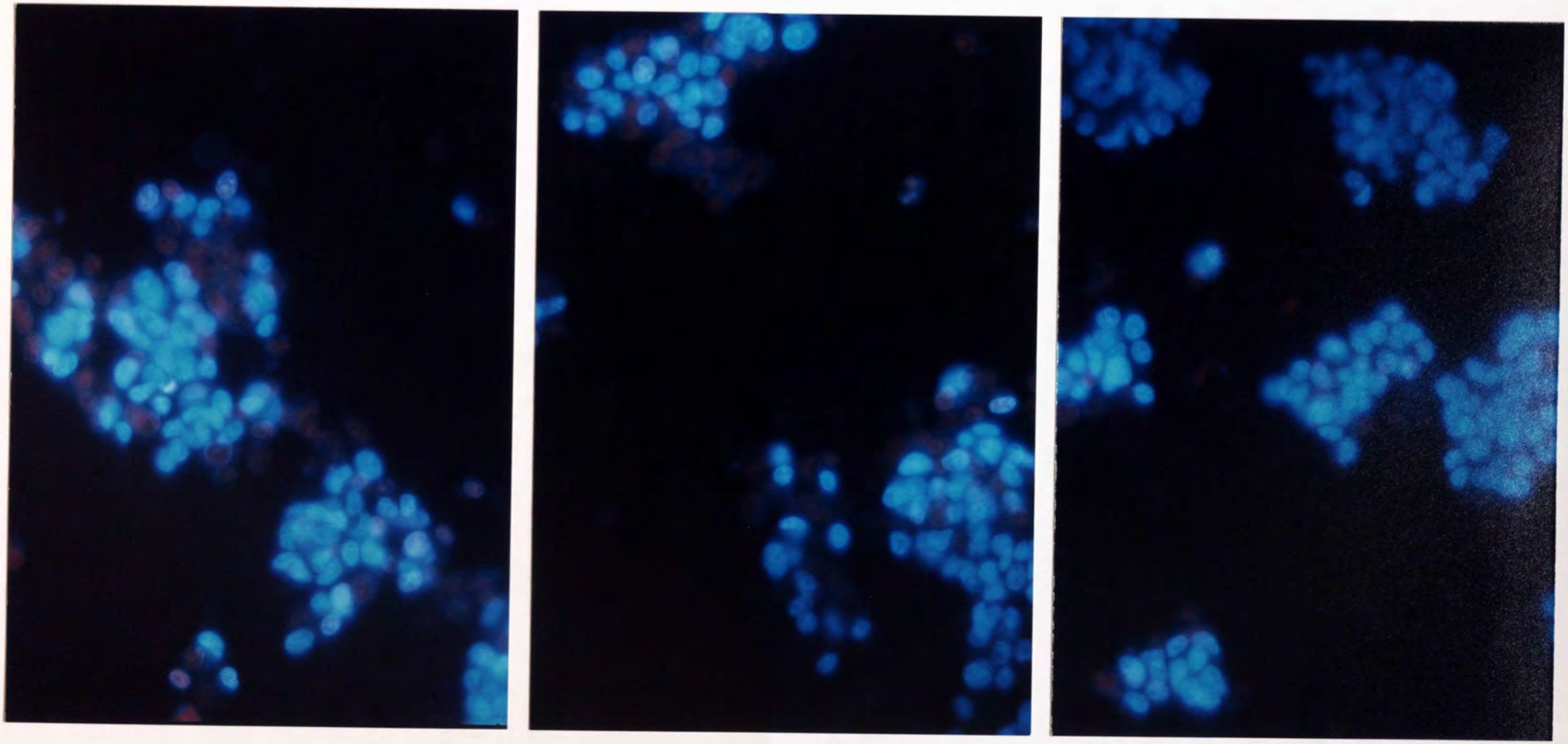

A B C

Figure 3.3.7 Photographs of Hoechst/PI staining of PC12 cells pretreated with A 0μM AA, B 50μM AA, C 100μM AA then subsequently exposed to 300μM H_2O_2

3.3.2 Effect of hydrogen peroxide on SH-SY5Y cell viability

The effects of peroxide on SY5Y cell DNA were investigated using increasing concentrations of H_2O_2. Figure 3.3.8 shows a dose dependent relationship between increasing H_2O_2 concentrations and increases in the percentage of PI (non-viable) stained cells. The basal level of non viable cells recorded was 38.1%, this rose significantly to 87.8% at 100μM H_2O_2, 98.3% at 250μM H_2O_2, to 99.5% at 500μM H_2O_2 (Dunnett's test, $P<0.001$, $n=4$ for all treatments).

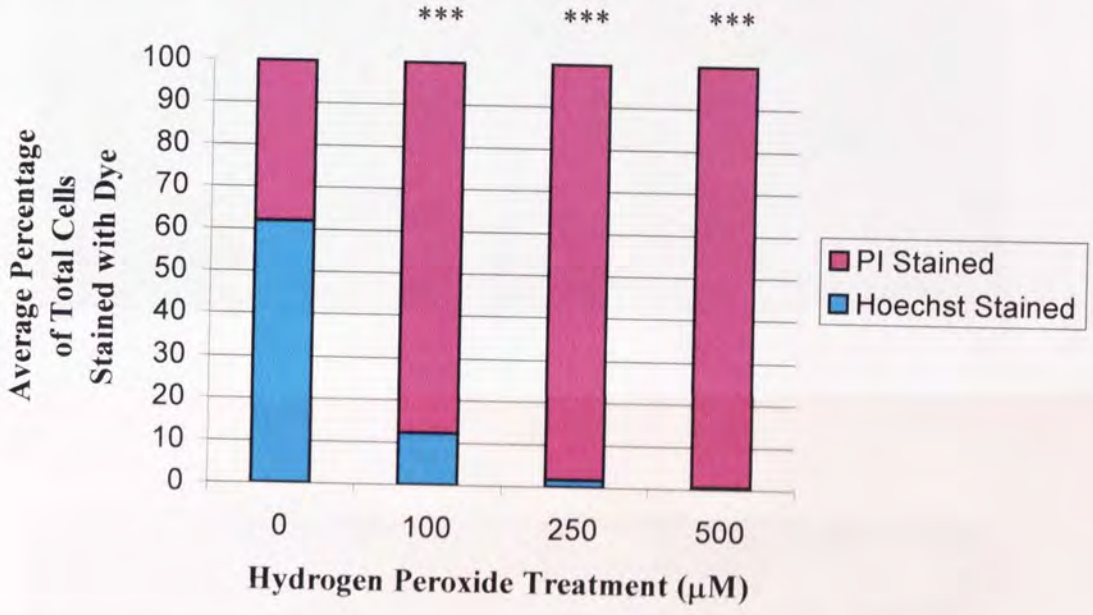

Figure 3.3.8 The effects of hydrogen peroxide on SY5Y cells. SY5Y cells ($2x10^5$) were incubated with H_2O_2 (100, 250 and 500μM) for 24 hours at 37°C, 5% CO_2. Graph shows the mean percentage of propidium stained (non-viable) cells as a percentage of total cells stained ± SEM of 4 replicates. * represents $P<0.001$ (Dunnett's test).**

Photographs of PI/Hoechst staining investigating the effects of H_2O_2 on SY5Y cells are included as figures 3.3.9 and 3.3.10.

A

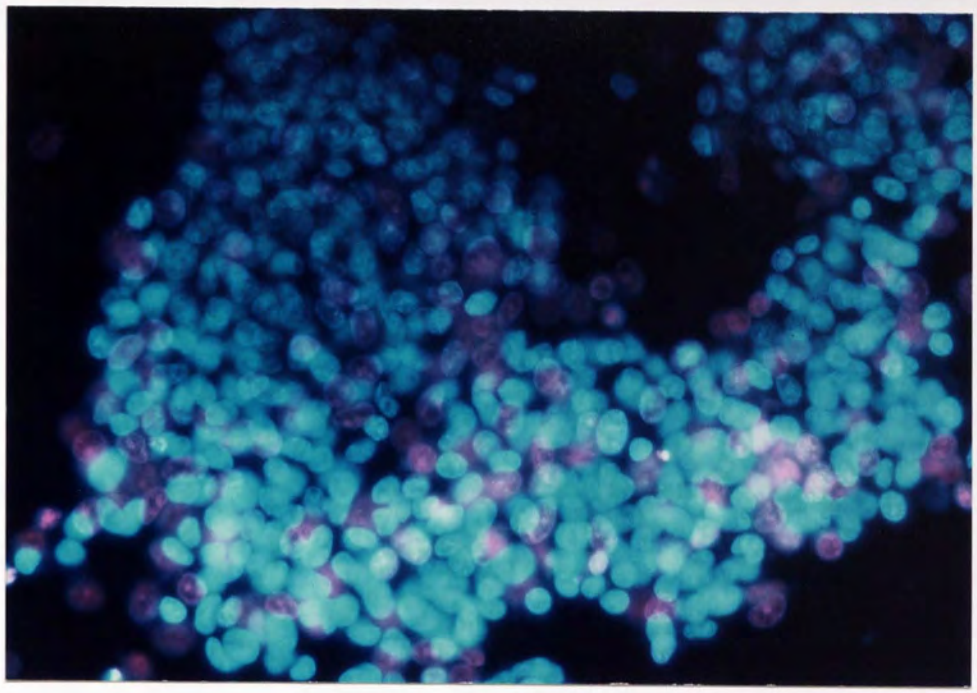

B

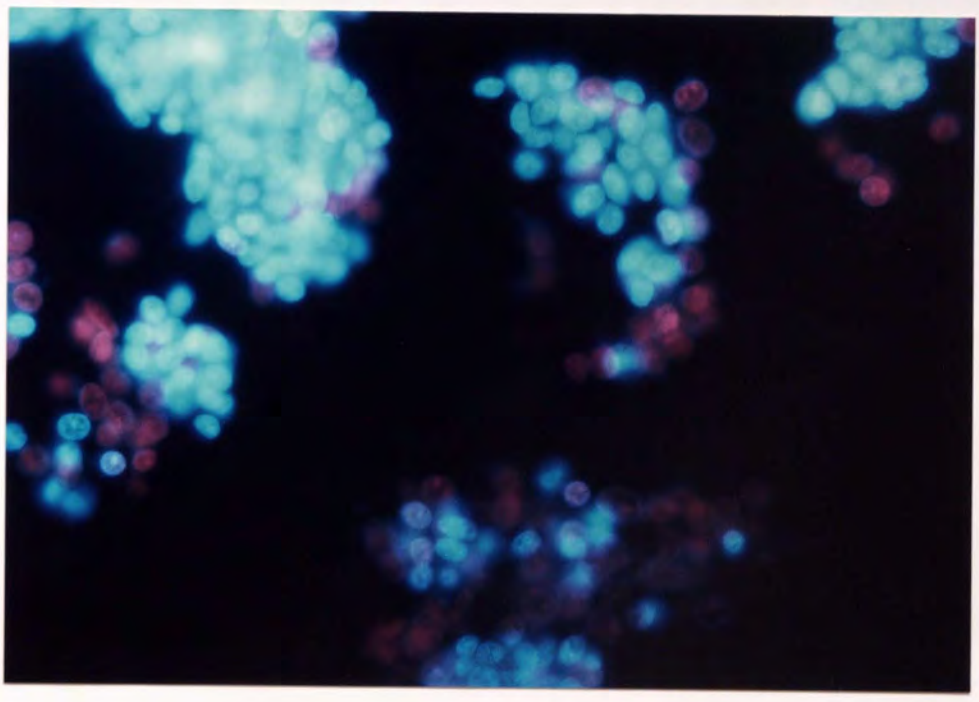

Figure 3.3.9 Photographs of Hoechst/PI staining of SY5Y cells exposed to H_2O_2 for 24 hours. A represents 0μM, B represents 100μM.

C

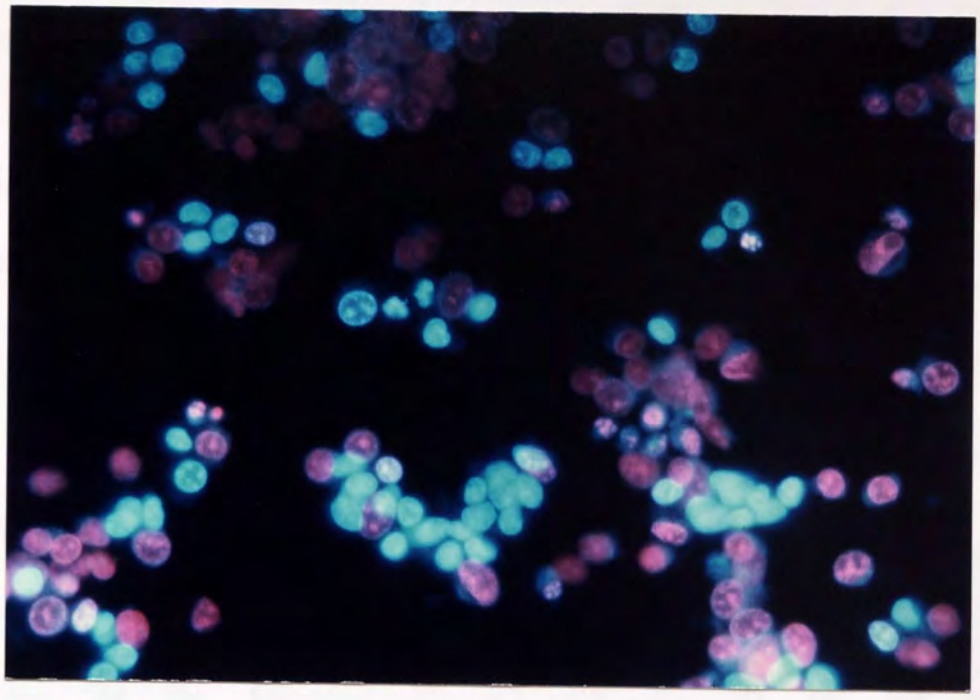

D

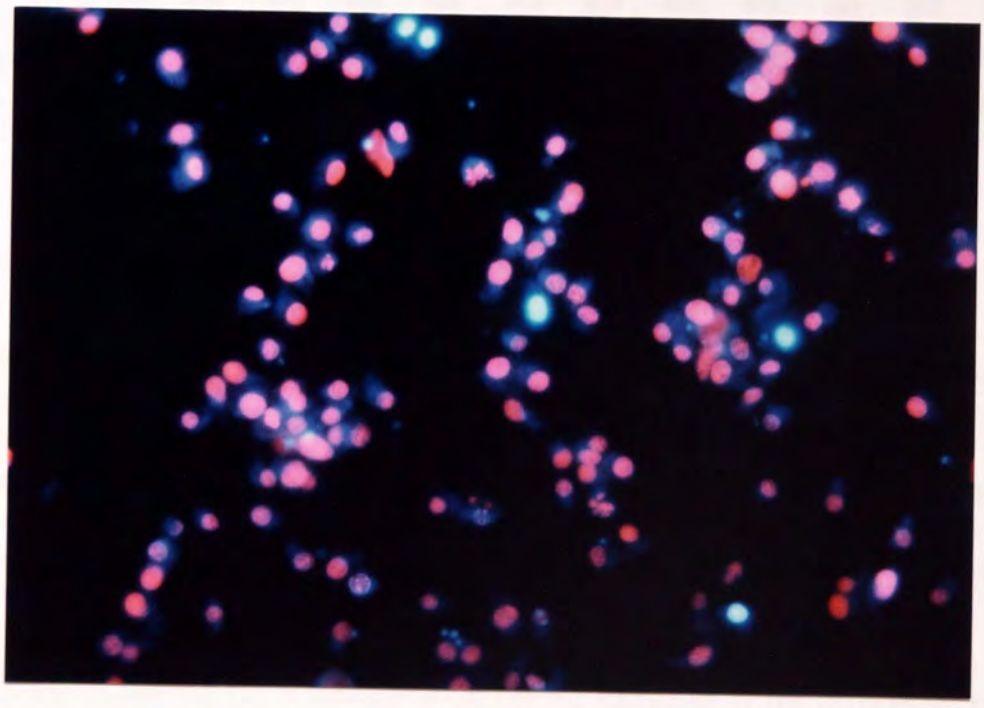

Figure 3.3.10 Photographs of Hoechst/PI staining of SY5Y cells exposed to H_2O_2 for 24 hours. C represents 250μM, D represents 500μM.

3.3.2.1 Effect of Nerve Growth Factor on hydrogen peroxide toxicity as assessed by fluorescence microscopy

The effects on NGF on SY5Y cell viability were investigated in the presence and absence of H_2O_2. Cells pre-treated for 24 hours with two concentrations of NGF (10 and 25ng/ml), were subsequently challenged with increasing concentrations of H_2O_2 (100, 250 and 500μM) for 24 hours.

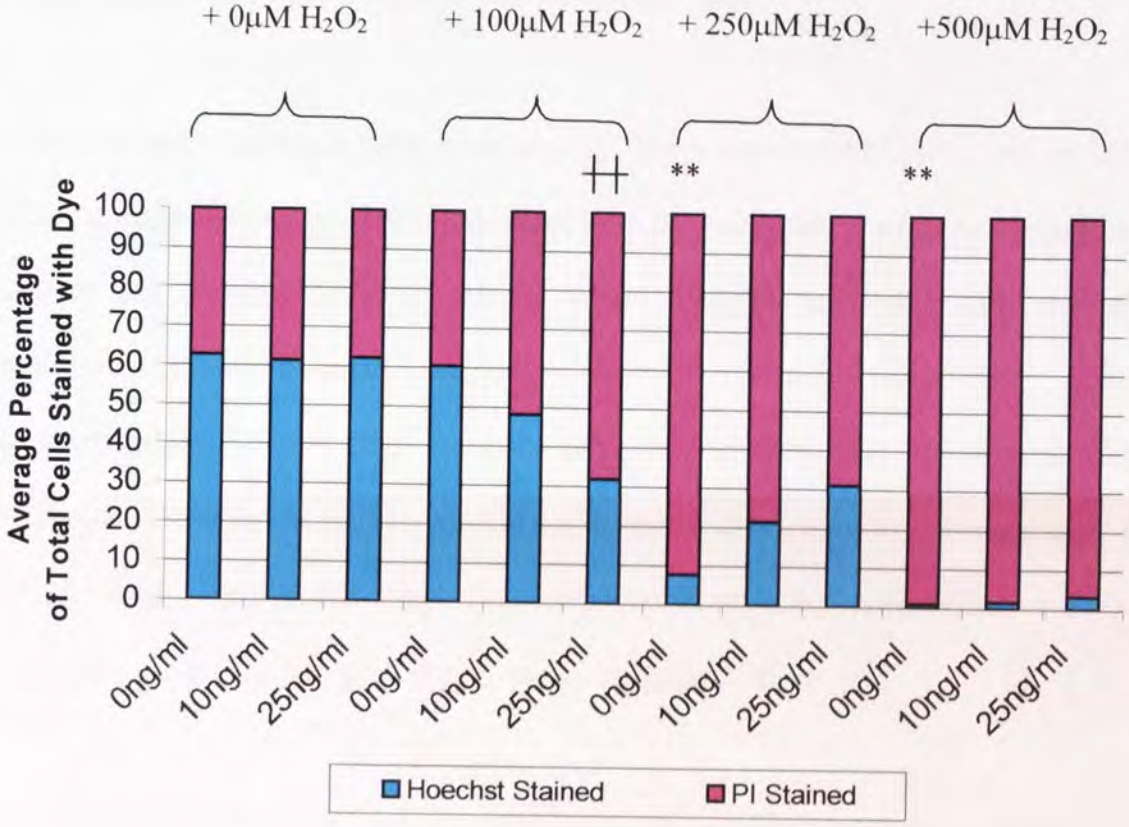

Figure 3.3.11 The effects of nerve growth factor on hydrogen peroxide toxicity on SY5Y cell viability. SY5Y cells ($2x10^5$) were incubated with NGF (10 and 25ng/ml) for 24 hours at 37°C, 5% CO_2. H_2O_2 was then added (100, 250 and 500μM) for 24 hours at 37°C, 5% CO_2. Graph shows the mean percentage of propidium stained (non-viable) cells as a percentage of total cells stained ± SEM of 4 replicates. ** represents P<0.01 (Dunnett's test) versus 0μM H_2O_2. ++ represents P<0.01 (Dunnett's test) versus 0ng/ml NGF.

Results show increasing H_2O_2 concentration caused increases in the percentage of PI stained cells. This is indicative of a reduction in cell viability in a dose dependent relationship up to 250μM in control (0ng/ml NGF) cells. The basal level of non viable

cells recorded was 37.3%, this rose through 39.7% at 100μM H_2O_2, 92.3% at 250μM H_2O_2, to 99.0% at 500μM H_2O_2 showing very significant decreases in cell viability at 250 and 500μM H_2O_2 ($P<0.01$, n=4 for each treatment).

NGF was shown to reduce or increase cell viability depending on H_2O_2 dose. In the absence of H_2O_2 (0μM H_2O_2) NGF had no significant effects on cell viability in unchallenged cells compared to non NGF pre-treated cells.

In the presence of peroxide there were varying effects recorded with NGF. At 100μM H_2O_2 the mean percentage of PI stained cells were 39.7%, 52.0% and 68.2% for 0ng/ml, 10ng/ml and 25ng/ml NGF respectively where 25ng/ml pre-treated cells showed significantly greater cell death compared to non-NGF treated controls ($P<0.05$, n=4). In the presence of 250μM H_2O_2 the mean percentage of PI stained cells were 92.3%, 78.6% and 69.0% for 0ng/ml, 10ng/ml and 25ng/ml NGF respectively. Results show a trend for NGF (10ng/ml and 25ng/ml) to maintain cell viability, however, this was not significant. At 500μM H_2O_2, NGF also had no significant effect.

Photographs of PI/Hoechst staining investigating the effect of NGF pre-treatment on exposure of SY5Y cells to 250μM H_2O_2 are included as figure 3.3.12.

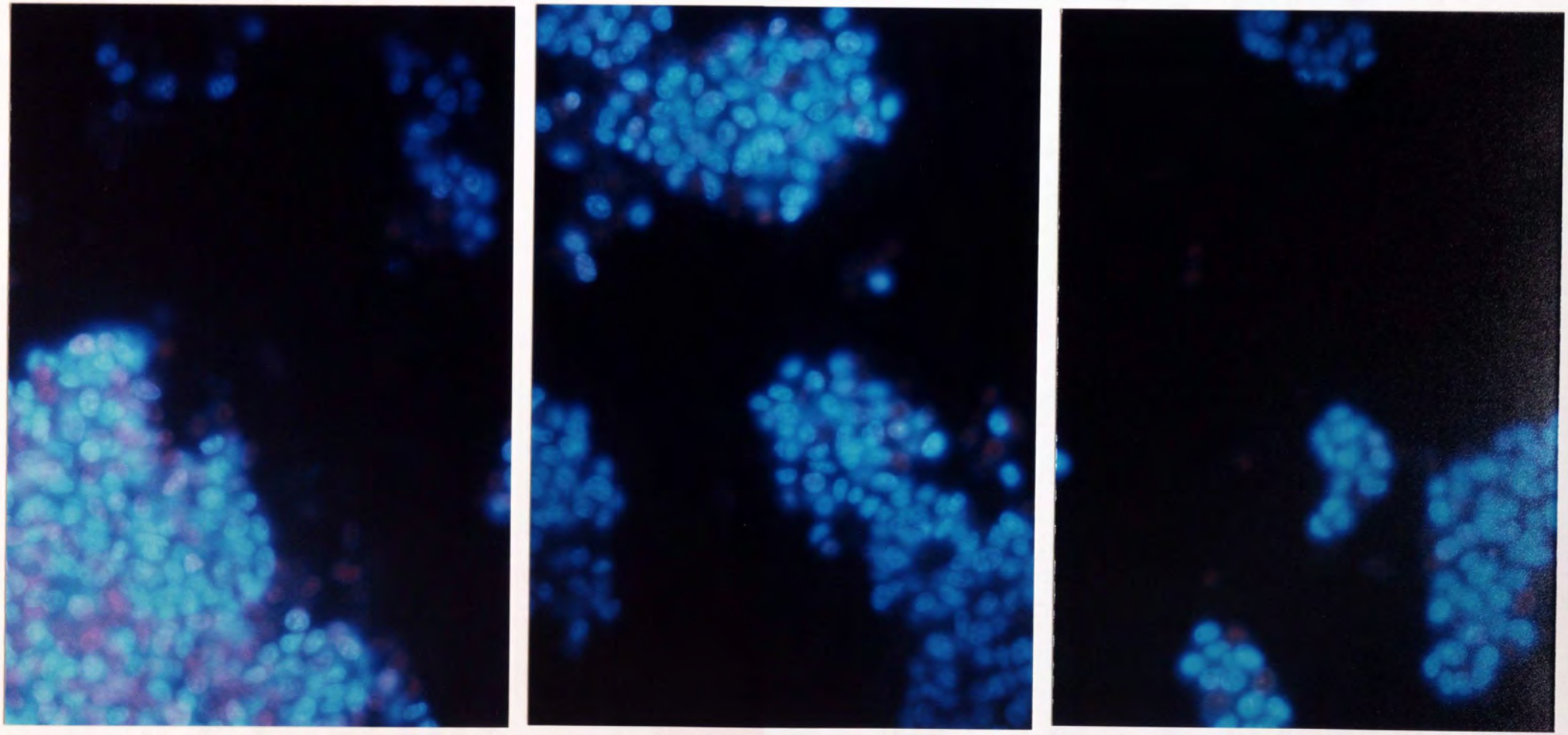

A B C

Figure 3.3.12 Photographs of Hoechst/PI staining SY5Y cells pretreated with A 0ng/ml NGF, B 10ng/ml NGF,C 25ng/ml NGF and subsequently treated with 250μM H_2O_2

3.3.2.2 Effects of ascorbic acid on hydrogen peroxide toxicity as assessed by fluorescence microscopy

The effects on AA on SY5Y cells in the presence and absence of H_2O_2 were investigated. Cells were pre-treated for 24 hours with two concentrations of AA (50 and 100μM), were subsequently challenged with increasing concentrations of H_2O_2 (100, 250, 500μM) for 24 hours. Figure 3.3.13 shows increasing H_2O_2 causes decreases in cell viability as represented by increases in the percentage of PI stained cells.

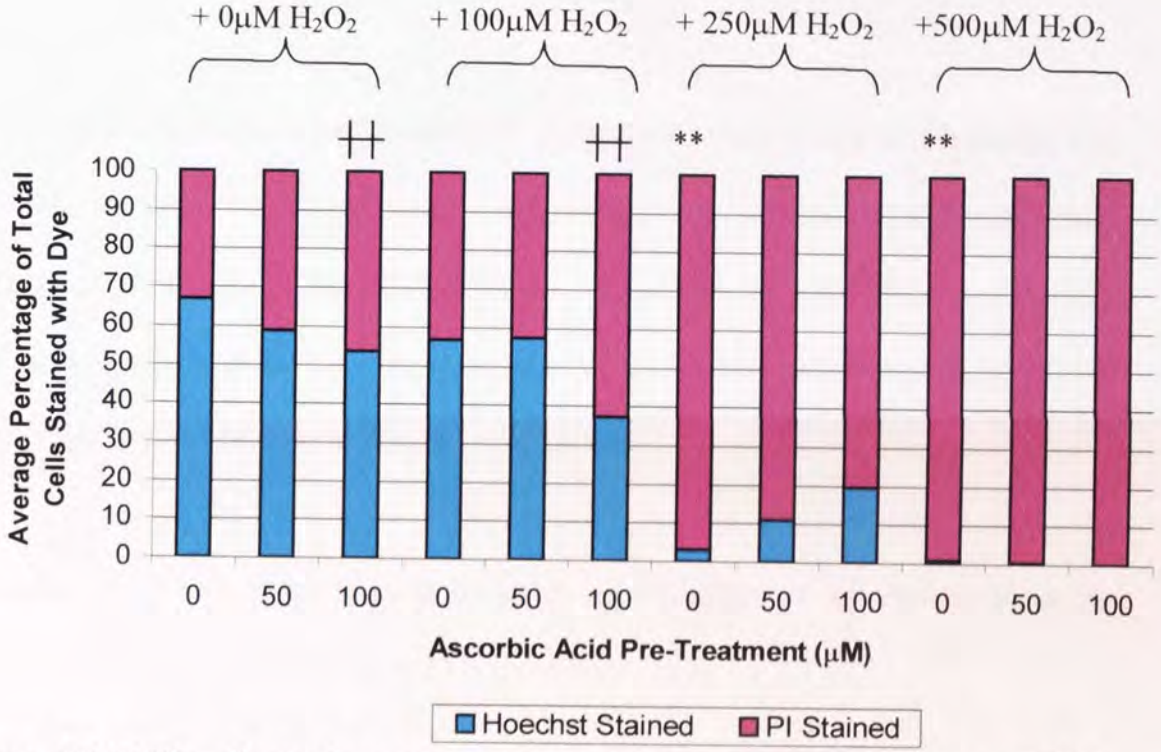

Figure 3.3.13 The effects of ascorbic acid on hydrogen peroxide toxicity on SY5Y cell viability. SY5Y cells ($2x10^5$) were incubated with AA (50 and 100μM) for 24 hours at 37°C, 5% CO_2. H_2O_2 was then added (100, 250 and 500μM) for 24 hours at 37°C, 5% CO_2. Graph shows the mean percentage of propidium stained (non-viable) cells as a percentage of total cells stained ± SEM of 4 replicates. ** represents P<0.01 (Dunnett's test) versus 0μM H_2O_2 treatment, ++ represents P<0.01 (Dunnett's test) versus 0μM AA.

Increasing H_2O_2 concentrations caused increases in the percentage of PI stained cells. This was indicative of reductions in cell viability in a dose dependent relationship up to 250μM in the absence of AA treatment where the effects were significant at 250 and 500μM H_2O_2 (P<0.01) (Dunnett's post test).

AA had dose distinct effects, at low H_2O_2 concentrations and in unchallenged cells (0 and 100μM) it promoted an increase in PI staining and thus a reduction in cell viability. AA was shown to reduce viability or protect against toxicity depending on H_2O_2 dose. In the absence of H_2O_2, the mean percentage of PI stained cells were 33.1%, 41.3% and 46.5% for 0μM, 50μM and 100μM AA respectively, where the effects of AA (100μM) were to cause a significant decrease in cell viability in unchallenged cells, $P<0.01$ (Dunnett's, n=4).

At 100μM H_2O_2 the mean percentage of PI stained cells were 43.2%, 42.5% and 62.8% ($p<0.01$) for 0μM, 50μM and 100μM AA respectively. At 250μM H_2O_2 the mean percentage of PI stained cells were 96.9%, 89.0% and 80.5 for 0μM, 50μM and 100μM AA respectively, however these were not significant. AA also had no significant effects on toxicity induced by 500μM H_2O_2.

Photographs of PI/Hoechst staining investigating the effect of AA pre-treatment on exposure of SY5Y cells to 250μM H_2O_2 are included as figure 3.3.14.

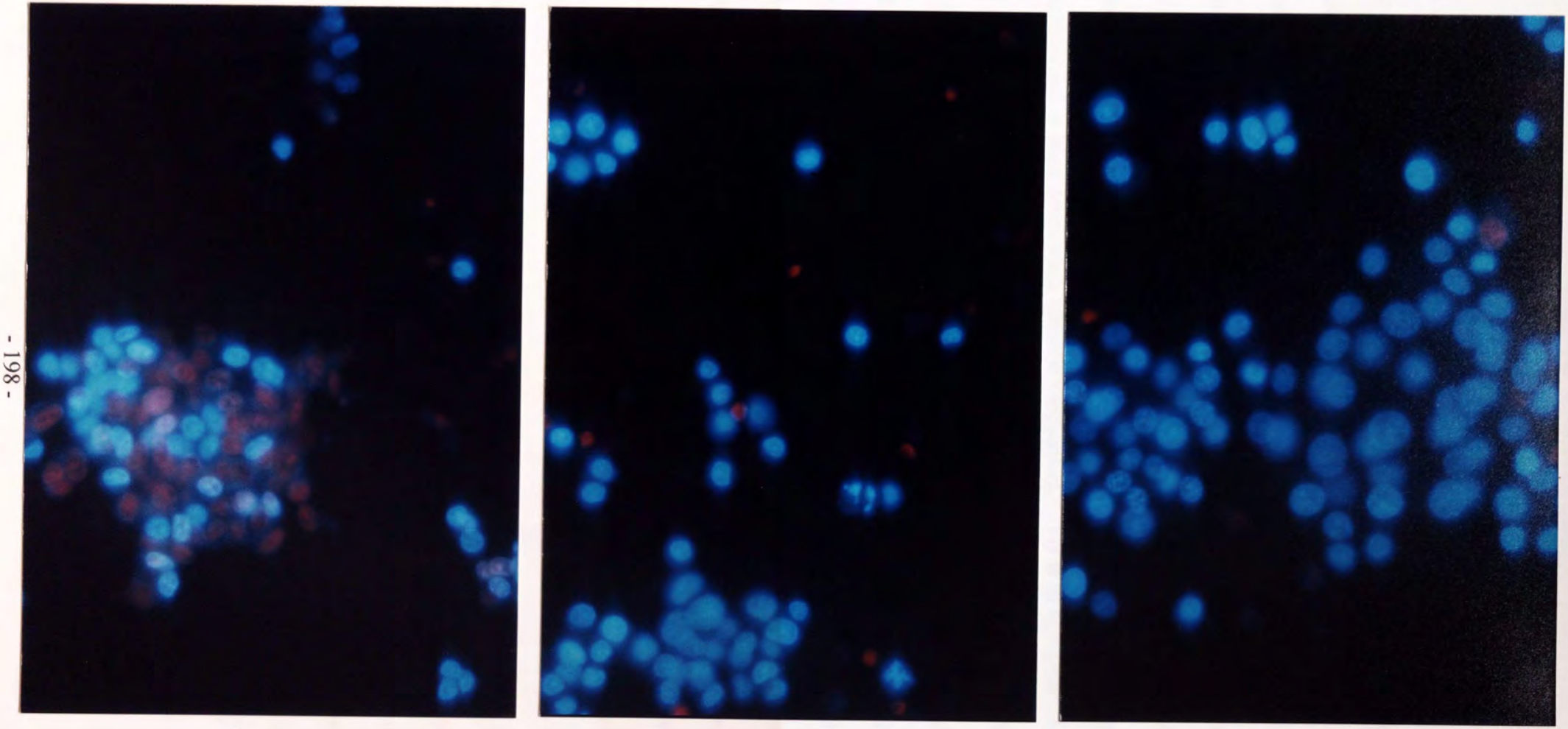

A B C

Figure 3.3.14 Photographs of Hoechst/PI staining of SY5Y cells and pretreated with A 0μM AA, B 50μM AA, C 100μM then subsequently exposed to 250μM H_2O_2

3.3.3 Discussion

There are discrepancies between the results obtained from the MTT assay and those of Hoechst staining, however, Misonou *et al.*, (2000) have suggested that this may be due to cell washing and fixing. Results have shown in both cell lines, with high H_2O_2 doses (500μM) cell die via a necrotic manner as indicated by PI staining. With increasing H_2O_2 dose, the staining changed from mainly Hoechst positive to mostly Propidium iodide positive. This shows at lower H_2O_2 doses cell death occurs via an apoptotic mechanism and at high doses via a necrotic mechanism. This is in agreement with the work published by Jang & Surh (2001) and Satoh *et al.*, (1997) who have also shown at high H_2O_2 doses (250μM) that PC12 cells exhibit apoptotic morphologies. Ray *et al.*, (2000) have also published work showing moderate H_2O_2 doses (100μM) cause apoptotic death. Typical examples of apoptotic cells are shown in figure 3.3.5 B which clearly shows an apoptotic cell showing blebbs in the centre of the photograph, another example is in figure 3.3.14B which shows shrunken cells and blebbed cells in the centre field of this photograph. Data produced with NGF showed clear protection in both cell lines at 250/300μM H_2O_2 causing reductions in positive PI staining and apoptotic morphologies in figures 3.3.4 and 3.3.11. This is interesting as Connor *et al.*, (1996) has suggested that apoptosis may be caused by a reduction in neurotrophic growth factors and has suggested that a loss of growth factors may be responsible for DNA fragmentation and perhaps apoptosis in AD brains. Therefore addition of NGF causing protection agrees with this hypothesis. AA protection was clearly apparent in the PC12 cells, as shown in figure 3.3.6 but not in the SY5Y cells, as little change was evident as shown in figure 3.3.13. These data suggest that low concentrations of H_2O_2 cause death via an apoptotic means, which can be retarded by treatment with NGF and in PC12 cells also by AA.

3.4 FLOW CYTOMETRY

In addition to changes in nuclear morphology, loss of DNA integrity also characterizes apoptosis. When DNA extracted from apoptotic cells is analysed using gel electrophoresis, a characteristic internucleosomal "ladder" of DNA fragments is often found. Larger DNA fragments can also be seen at earlier times in apoptotic cell cultures. These gel results are often used as a hallmark of apoptosis detection. However, such analysis requires the extraction of DNA from large numbers of cells. In addition, the apoptosis must be relatively synchronous for this analysis, a synchrony that is not always present. It has also not been directly demonstrated that DNA fragments in this way in intact cells. Regardless of the specific methods used, the change in nuclear morphology often does not coincide with the appearance of detectable strand breaks in every cell. Although many cytochemical methods are based on the detection of strand breaks or on the appearance of DNA fragments in gel electrophoresis, there is no reason to assume that nuclear morphological changes and detectable DNA strand breaks occur at the same time (Willingham, 1999).

Flow cytometry is an established methodology that allows rapid and very accurate measurement of a variety of parameters attributed to cell structure, phenotype and function. Changes in cell size and gross structure, in plasma membrane permeability or physical integrity, as well as in chromatin and DNA structure, which occur during cell death can be analysed by flow cytometry

Most, but not all cells, cut nuclear DNA at the linker regions between nucleosomes during apoptosis, giving rise to a range of DNA fragments that are oligmers of about 180 base pairs.

In flow cytometry, after suitable fixation or permeabilizing of cells, in this case with Triton – X100, packets of nucleoids are released and low molecular weight fragments of DNA may be extracted, including an extra 'sub G_1' peak indicative of apoptotic cells. These are shown in the DNA histogram (Ormerod, 1998) in figure 3.4.

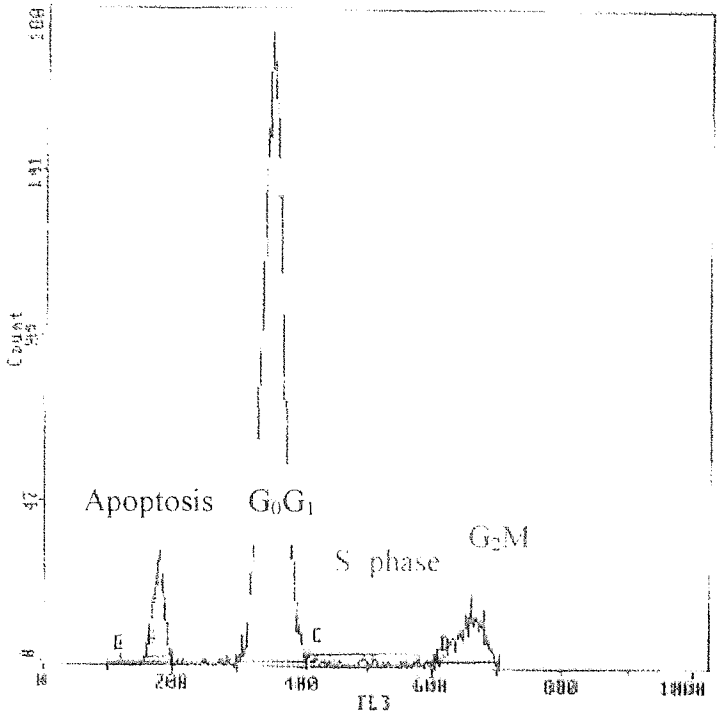

Figure 3.4 A typical flow cytometry DNA profile showing the proportion of cells in each aspect of the cell cycle.

The presence of nucleoids with low DNA staining capacity, lower than that of G_0G_1 (sub G_1) nucleoids in cultures treated with various cytotoxic agents, is considered a marker of cell death by apoptosis (Nicoletti *et al.*, 1991). Therefore apoptotic nucleoids have a decreased PI fluorescence compared with the nucleoids in the main peak G_0G_1 (Darzynkiewicz & Li, 1997).

In order to quantitate the apoptosis induced, flow cytometric analysis of sub-diploid DNA was undertaken following neuronal cell treatment with, H_2O_2 and Aβ, and the 'protective' ~~ag~~ents NGF, AA and BDNF for various time periods.

3.4.1 PC12 CELLS

3.4.1.1 Evaluation of time course of hydrogen peroxide action as assessed by flow cytometry

In order to investigate the time course of H_2O_2 induced PC12 toxicity, cells were harvested after the addition of H_2O_2 at 0, 4 and 24 hours as shown in figure 3.4.1. At 4 hours there was only one significant effect seen, this was at the highest dose, 150μM H_2O_2, where the number of apoptotic nucleoids recorded had increased to 15.8%, this was considered significantly different to the other three treatments 6.8% at 0μM H_2O_2, 5.9% at 50μM H_2O_2, and 9.6% at 100μM H_2O_2, $P<0.01$ (Dunnett's test). At 24 hours, both 100 and 150μM H_2O_2 treatments caused significant apoptosis. At 24 hours the percentage of apoptotic nucleoids were 6.1% in control cells, 14.7% at 50μM H_2O_2, 33.6% at 100μM H_2O_2 and 50.1% at 150μM H_2O_2 respectively, where the effects of 100 and 150μM H_2O_2 on inducing apoptosis were considered significant $P<0.01$ (Dunnett's test). Therefore in all subsequent experiments flow cytometry samples were analysed after 24 hours of treatment.

3.4.1.2 Effect of hydrogen peroxide as assessed by flow cytometry

The effects of H_2O_2 on PC12 cell viability were investigated using increasing concentrations of H_2O_2. Figure 3.4.2 showed that increases in H_2O_2 concentration caused increases in the percentage of nucleoids classified as apoptotic. In control PC12 populations, only 6.1% apoptotic nucleoids were recorded, this rose to 80.2% recorded for 250μM H_2O_2, and was considered significant, $P<0.01$ at 100, 150, 200 and 250μM H_2O_2 (Dunnett's post test, n=4).

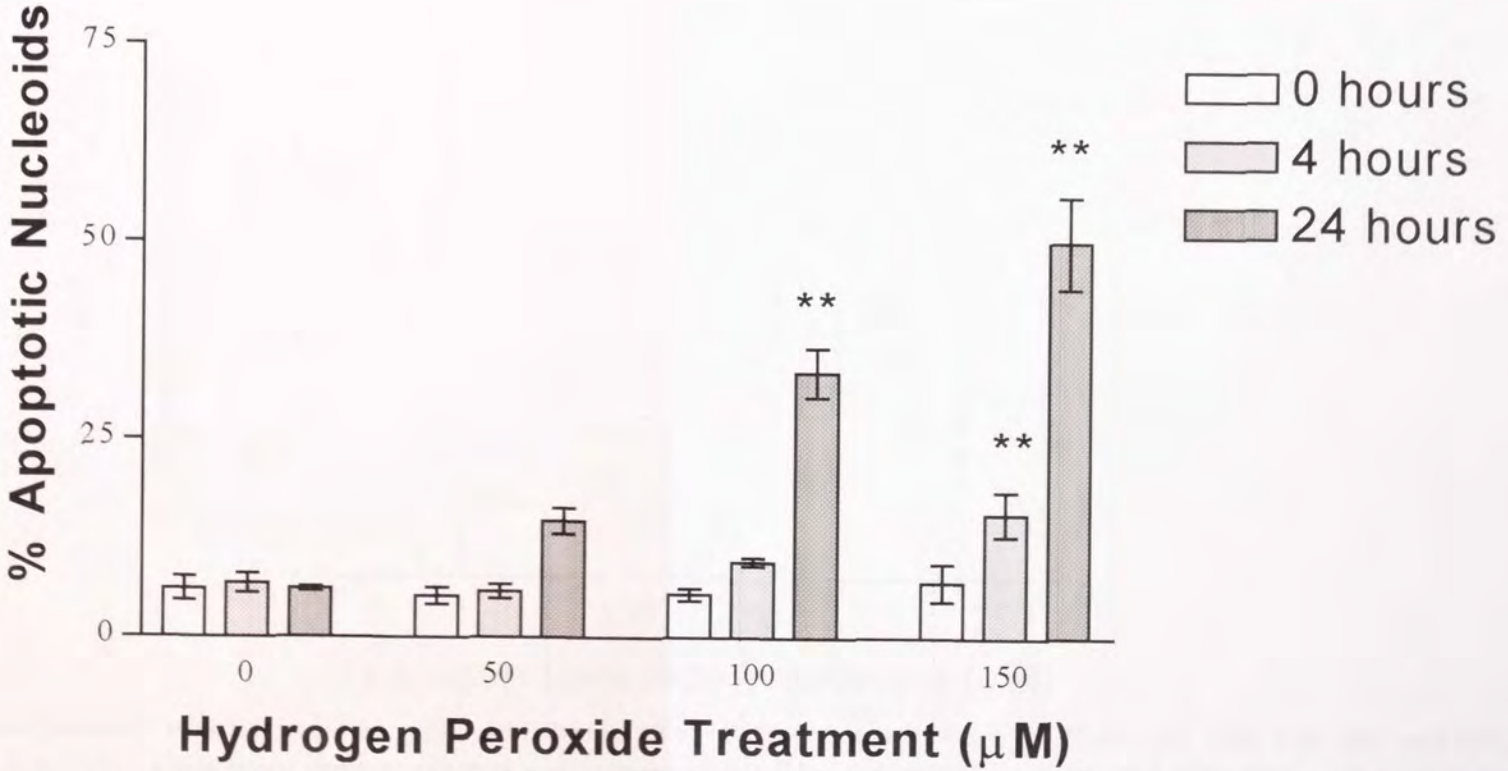

Figure 3.4.1 Time course of hydrogen peroxide toxicity in PC12 cells. PC12 cells (2 x 10^5) were incubated with H_2O_2 (50, 100 and 150μM) for 0-24 hours at 37°C, 5% CO_2. Cells were harvested and prepared for flow cytometry where data are expressed as the mean percentage apoptotic events of the nucleoids analysed ± SEM of 6 replicates. ** represents P<0.01 (Dunnett's test).

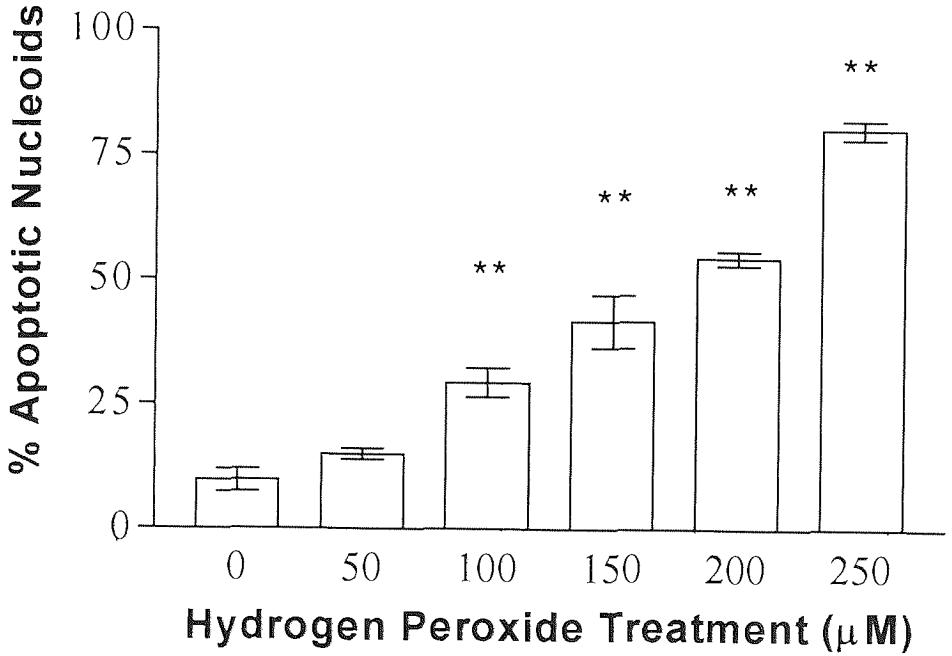

Figure 3.4.2 Hydrogen peroxide toxicity in PC12 cells. PC12 cells (2 x 10^5) were incubated with H_2O_2 (50, 100, 150, 200 and 250μM) for 24 hours at 37°C, 5% CO_2. Cells were then harvested and prepared for flow cytometry in method 2.2.4. Figure shows the mean percentage of apoptotic events of the nucleoids analysed ± SEM of 4 replicates. ** represents P <0.01 (Dunnett's test).

3.4.1.3 Effect of aged amyloid β peptide, fragment 25-35 as assessed by flow cytometry

The effects of Aβ on PC12 cell apoptosis were investigated. Figure 3.4.3 showed that aged Aβ (25-35) caused significant increases in the percentage of nucleoids classed as apoptotic after 24 hours ($P<0.01$, Dunnett's test).

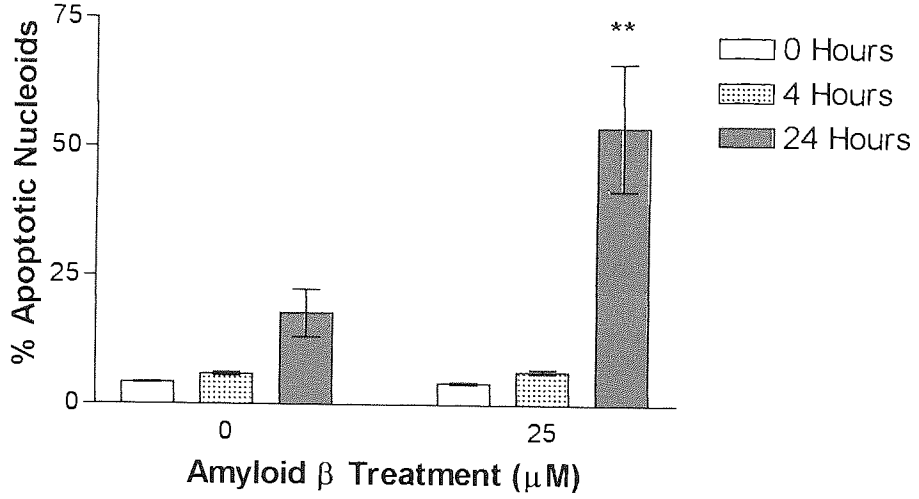

Figure 3.4.3 Time course of amyloid β peptide toxicity in PC12 cells. PC12 cells ($2x10^5$) were incubated with Aβ (25μM) for 0-24 hours at 37°C, 5% CO_2. Cells were harvested and prepared for flow cytometry as stated in method 2.2.4. Figure shows the mean percentage apoptotic events of the nucleoids analysed ± SEM of 3 replicates. ** represents P value < 0.01 (Dunnett's test).

3.4.1.4 Effect of nerve growth factor as assessed by flow cytometry

In order to investigate any protective effects of NGF on PC12 cell viability, experiments were set up with three concentrations of NGF. Cells were incubated with NGF for 24 hours before harvest for determination of apoptotic nucleoids as a percentage of total events. Figure 3.4.4 shows that NGF had no significant effects on the levels of apoptotic nucleoids in unchallenged PC12 cells versus controls.

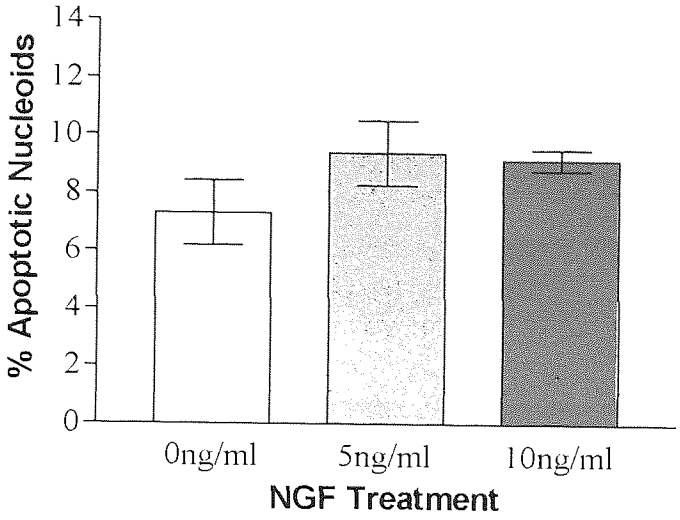

Figure 3.4.4 The effects of nerve growth factor on PC12 cells. PC12 cells (2 x 10^5) were incubated with NGF (5, 10ng/ml) for 24 hours at 37°C, 5% CO_2. Cells were then harvested and prepared for flow cytometry as stated in method 2.2.4. Graph shows the mean percentage apoptotic events of the nucleoids analysed ± SEM, n=9.

3.4.1.4.1 Effects of nerve growth factor on hydrogen peroxide action as assessed by flow cytometry

The effects of NGF on the percentage of apoptotic nucleoids produced by increasing concentrations of H_2O_2 were assessed using two concentrations of NGF versus control treated cells. Figure 3.4.4 had previously shown that NGF has no significant effects on basal apoptotic nucleoid levels, and this was confirmed in figure 3.4.5 in unchallenged cells. Figure 3.4.5 show that increasing H_2O_2 treatment caused significant increases in the percentage of apoptotic nucleoids recorded. Both 5ng/ml and 10ng/ml NGF caused significant decreases in the percentage of apoptotic nucleoids recorded following 50μM H_2O_2 treatment, $P<0.05$ for 5ng/ml NGF and a $P<0.01$ for 10ng/ml NGF (Dunnett's post test). At 100μM H_2O_2, both NGF treatments protected against the increase in the percentage of apoptotic nucleoids recorded, however, these effects were only significant at 10ng/ml NGF, $P<0.05$. At 150μM H_2O_2, 5ng/ml had no significant effect in the percentage of apoptotic nucleoids, however 10ng/ml caused a significant decrease in the percentage of apoptotic nucleoids, $P<0.05$.

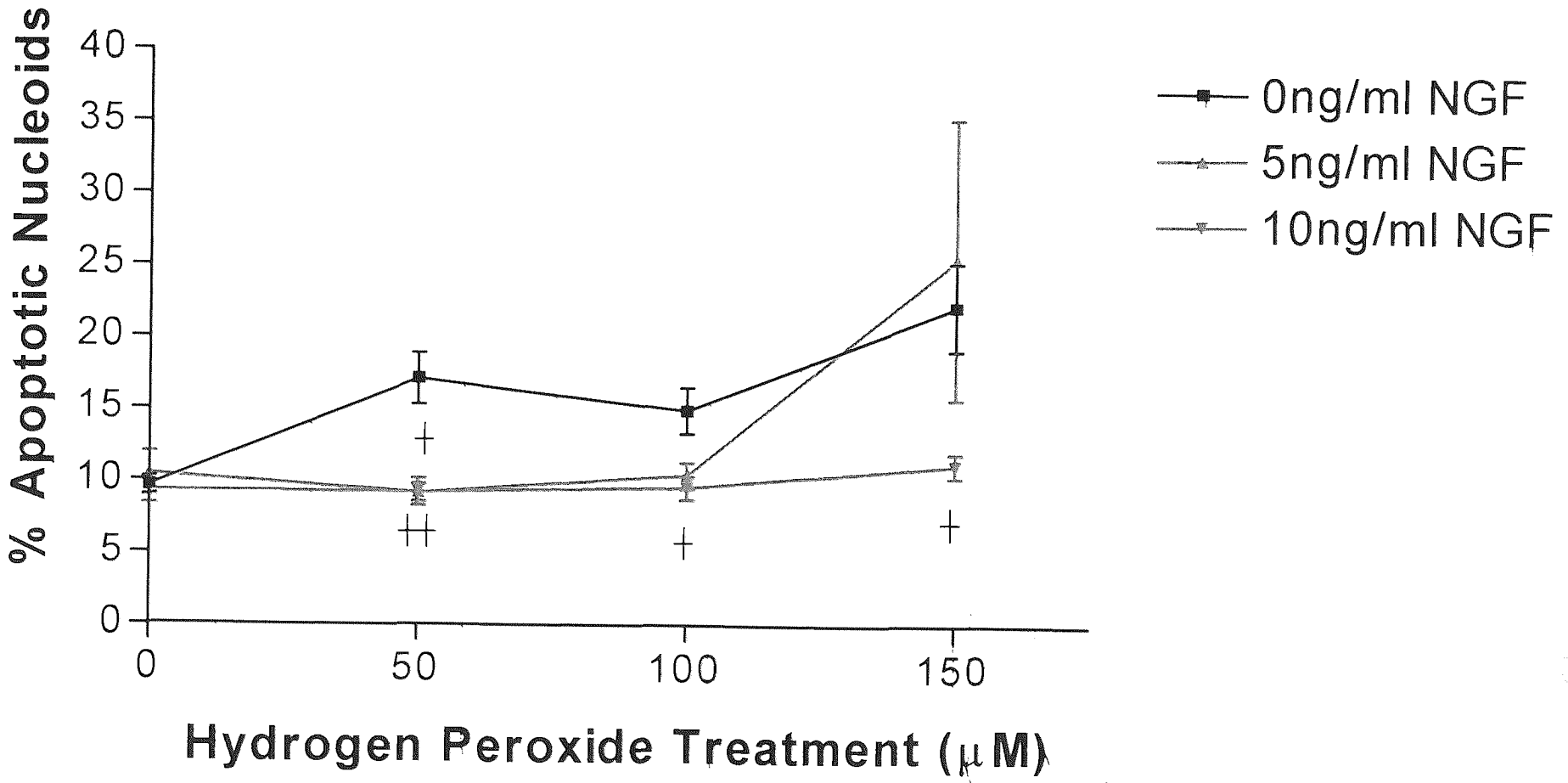

Figure 3.4.5 Overview of the effects of nerve growth factor on hydrogen peroxide toxicity in PC12 cells. PC12 cells (2 x 10^5) were incubated with NGF (5 and 10ng/ml) for 24 hours at 37°C, 5%CO_2, then further incubated with H_2O_2 (50, 100 and 150μM) for 24 hours at 37°C, 5%CO_2. Cells were then harvested and prepared for flow cytometry as stated in method 2.2.4. Graph shows mean percentage apoptotic events of the nucleoids analysed ± SEM for 9 replicates for 0 and 10ng/ml and 3 replicates for 5ng/ml. + represents $P < 0.05$ and ++ represents $P < 0.01$ when compared to 0ng/ml NGF (Dunnett's test).

3.4.1.5 Effect of ascorbic acid on DNA fragmentation as assessed by flow cytometry

Potential protective effects of AA on PC12 DNA fragmentation were investigated. Cells incubated with two concentrations of AA (50 and 100μM) showed no significant effects on the basal level of apoptotic nucleoids in cells as shown in Figure 3.4.6.

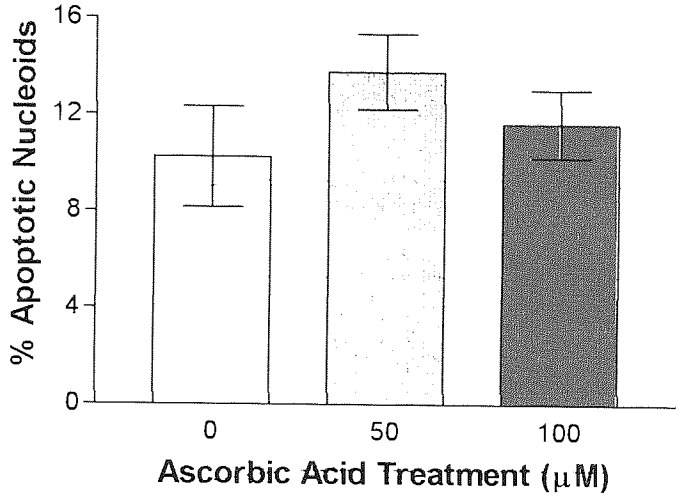

Figure 3.4.6 The effects of ascorbic acid on PC12 cells. PC12 cells ($2x10^5$) were incubated with ascorbic acid (50 and 100μM) or 24 hours at 37°C, 5%CO_2. Cells were then harvested and prepared for flow cytometry as stated in method 2.2.4. Graph shows the mean percentage of apoptotic events of the nucleoids analysed ± SEM for 4 replicates.

3.4.1.5.1 Effect of ascorbic acid on hydrogen peroxide action as assessed by flow cytometry

The ability of AA to exert a protective effect on the percentage of apoptotic nucleoids produced by increasing concentrations of H_2O_2 was investigated using 100μM AA versus control treated cells. Figure 3.4.7 shows that AA has no significant effect on the percentage of apoptotic nucleoid levels. Cells treated with 100μM AA in the presence and absence of 100μM H_2O_2 produced 23.9% and 11.1% apoptotic nucleoids respectively. This was compared to cells challenged with 0 and 100μM H_2O_2 in the absence of AA, which yielded 11.4% and 23.2% apoptotic nucleoids respectively.

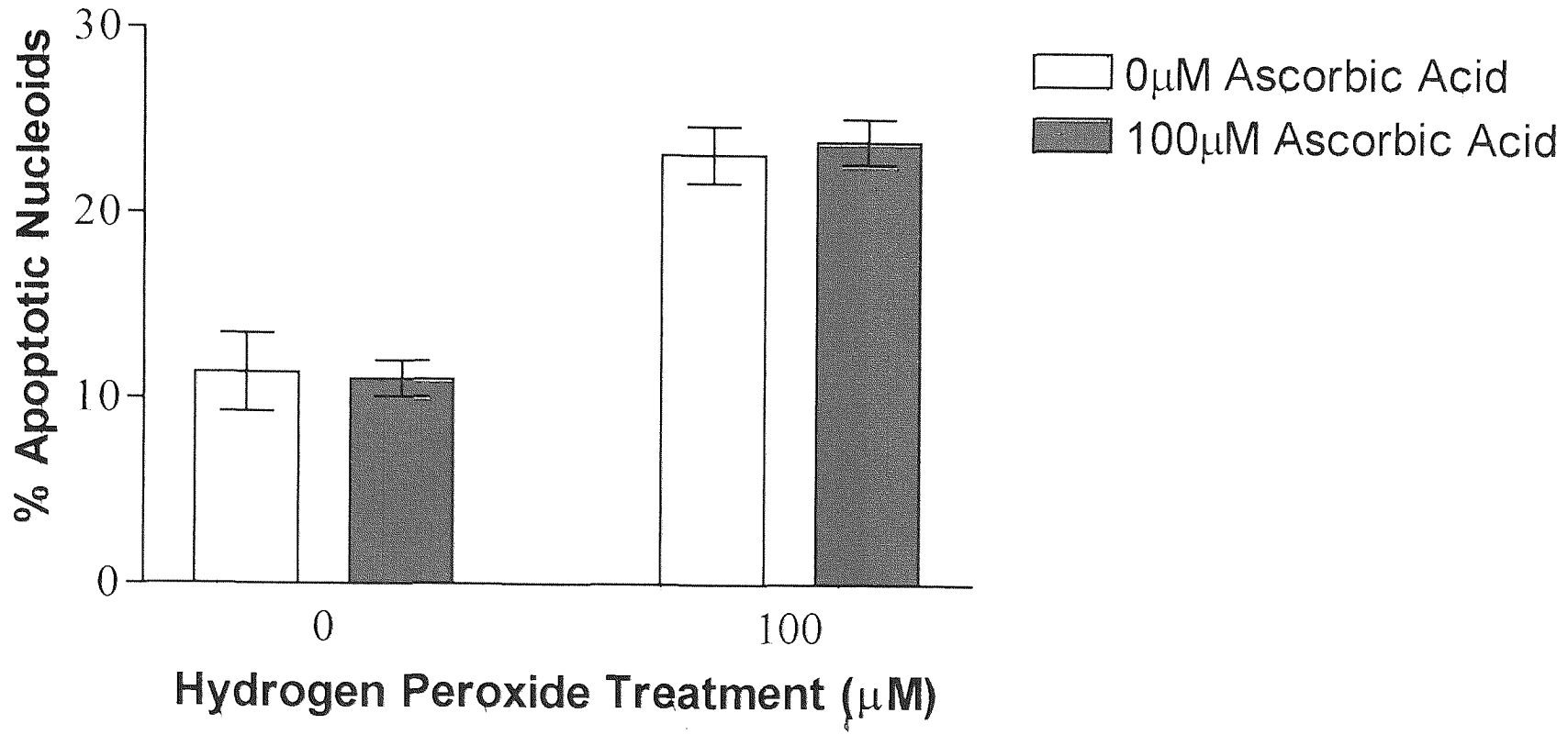

Figure 3.4.7 The effects of ascorbic acid on hydrogen peroxide toxicity in PC12 cells. PC12 cells (2×10^5) were incubated with AA (100μM) for 24 hours at 37°C, 5% CO_2. H_2O_2 treatment was then added (100μM) versus control) for 24 hours at 37°C, 5% CO_2. Cells were then harvested and prepared for flow cytometry, as stated in method 2.2.4. Graphs show the mean percentage apoptotic events of the nucleoids analysed ± SEM for 6 replicates.

3.4.2 SY5Y cells

3.4.2.1 Effects of hydrogen peroxide on DNA fragmentation as assessed by flow cytometry

The effects of H_2O_2 on SY5Y cell apoptosis were investigated using increasing concentrations of H_2O_2. Figure 3.4.8 shows that increases in H_2O_2 concentrations caused increases in the percentage of nucleoids classed as apoptotic. Under control conditions only 3.1% apoptotic nucleoids were recorded, this rose to 67.1% apoptotic nucleoids recorded for 500μM H_2O_2, and was significant for all doses tested, $P<0.01$ (Dunnett's post test, n=4).

3.4.2.2 Effect of nerve growth factor on DNA fragmentation as assessed by flow cytometry

In order to investigate any effects of NGF on SY5Y cell apoptosis, experiments were set up with three concentrations of NGF. Cells were incubated with NGF for 24 hours before harvest for determination of apoptotic nucleoids by flow cytometry. Figure 3.4.9 shows that NGF has no significant effects on basal levels of apoptotic nucleoids in untreated SY5Y cells. However as the graph shows there is a general trend of increasing NGF concentration, causing an increase in the percentage of apoptotic nucleoids recorded.

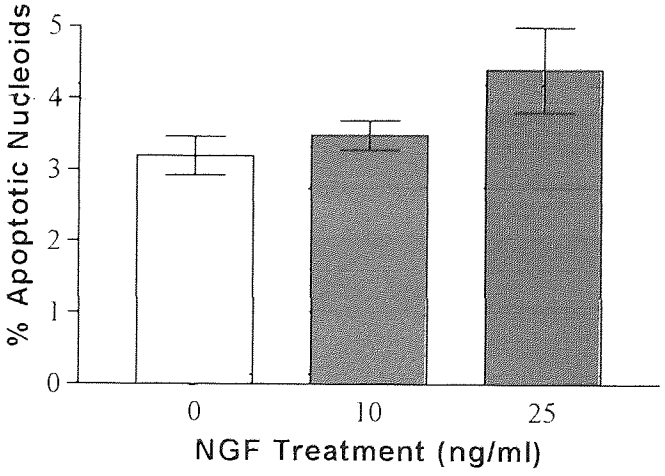

Figure 3.4.9 The effects of nerve growth factor on SY5Y cells. SY5Y cells (2x 10^5) were incubated with NGF (10 and 25ng/ml) for 24 hours at 37°C, 5% CO_2. Graph show the mean percentage of apoptotic events of the nucleoids analysed ± SEM for 6 replicates.

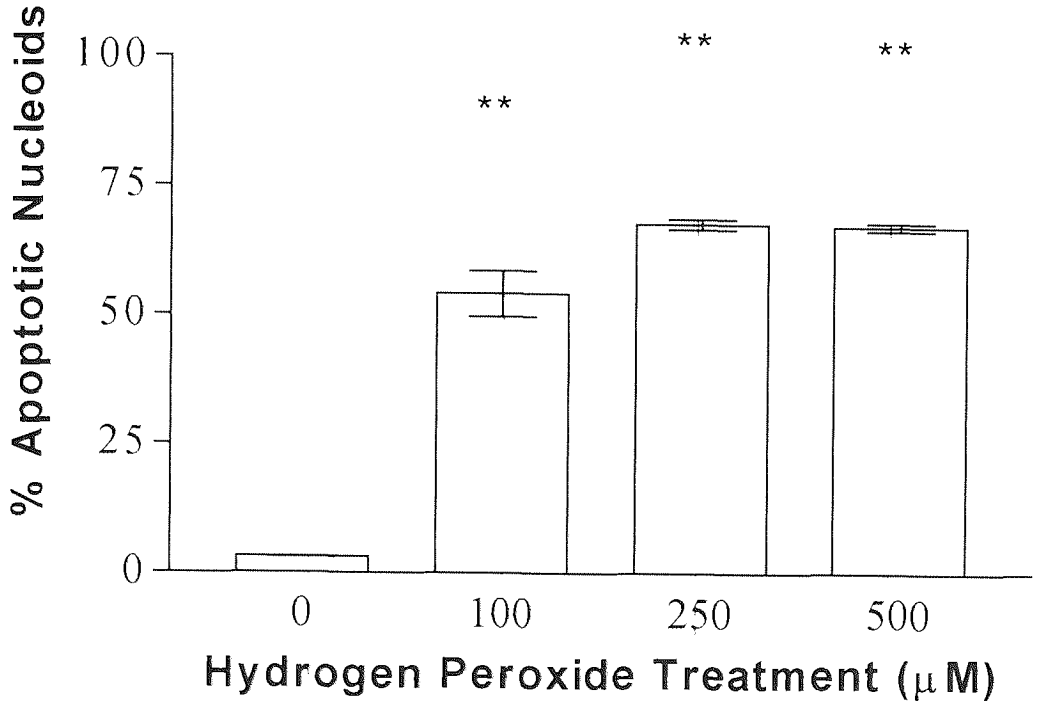

Figure 3.4.8 The effects of hydrogen peroxide toxicity on SY5Y cells. SY5Y cells (2 x 10^5) were incubated with H_2O_2 (100, 250, and 500μM) for 24 hours at 37°C, 5% CO_2. Cells were then harvested and prepared for flow cytometry as stated in method 2.2.4. Figure show the mean percentage of apoptotic events of the nucleoids analysed ± SEM of 4 replicates.
** represents P value < 0.01 (Dunnett's test).

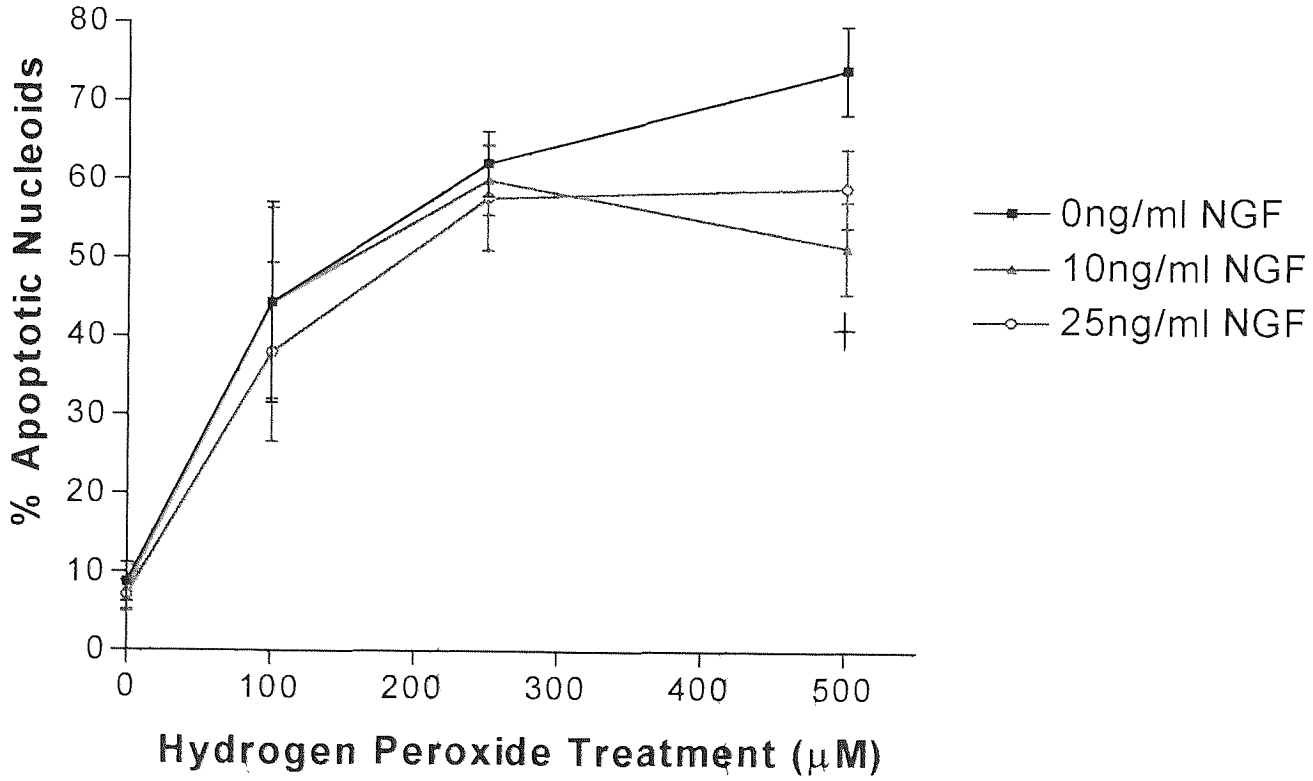

Figure 3.4.10 Overview of the effects of nerve growth factor on hydrogen peroxide toxicity in SY5Y cells. SY5Y cells (2 x 10^5) were incubated with NGF (10 and 25ng/ml) for 24 hours at 37°C, 5%CO_2, then further incubated with H_2O_2 (100, 250 and 500μM) for 24 hours at 37°C, 5%CO_2. Cells were then harvested and prepared for flow cytometry as stated in method 2.2.4. Graph shows mean percentage apoptotic events of the nucleoids analysed ± SEM for 6 replicates. + represents P value < 0.05 (Dunnett's test) versus 0ng/ml NGF

3.4.2.2.1 Effect of nerve growth factor on hydrogen peroxide induced apoptosis as assessed by flow cytometry

The effects of NGF on the percentage of apoptotic nucleoids produced by increasing concentrations of H_2O_2 were assessed using two concentrations of NGF versus control treated cells. Figure 3.4.9 had previously shown that NGF had no significant effects on basal apoptotic nucleoid levels, this was reproduced here (Figure 3.4.10) At 100 and 250μM H_2O_2 there were also no significant protective effects of NGF on apoptosis of SY5Y cells recorded. However, 25ng/ml NGF significantly prevented the increase in the percentage of apoptotic nucleoids recorded by 500μM H_2O_2, $P<0.05$ (Dunnett's test, n=6).

3.4.2.3 Effect of ascorbic acid on DNA fragmentation as assessed by flow cytometry

The effects of two concentrations of AA on SY5Y cell apoptosis were investigated. Cells were incubated with AA for 24 hours before harvest. Figure 3.4.11 shows that AA had no significant effects on basal levels of apoptotic nucleoids in untreated SY5Y cells

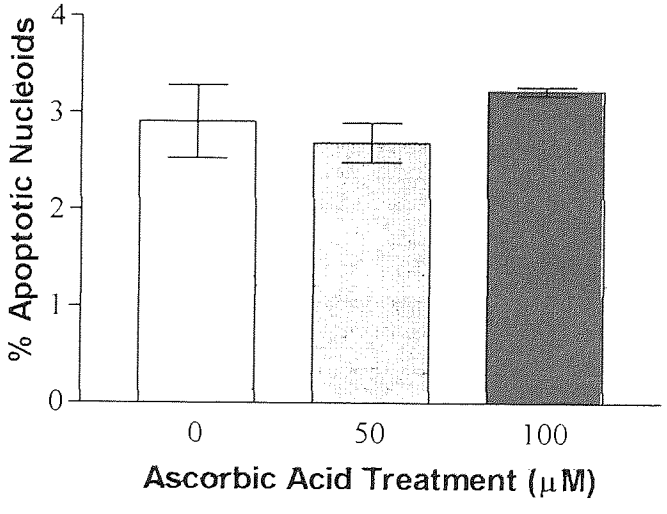

Figure 3.4.11 The effects of ascorbic acid on SY5Y cells. SY5Y cells (2 x 10^5) were incubated with ascorbic acid (50 and 100μM) for 24 hours at 37°C, 5% CO_2. Cells were then harvested and prepared for flow cytometry as stated in method 2.2.4. Graphs show the mean percentage of apoptotic events of the nucleoids analysed ± SEM for 4 replicates.

3.4.2.4 Effect of ascorbic acid on hydrogen peroxide induced DNA fragmentation as assessed by flow cytometry

In order to determine whether AA has any protective effects against peroxide challenge on SY5Y apoptosis, two concentrations of AA pre-treatment were compared to peroxide treated cells alone. Previously, AA has been shown to have no significant effects on basal apoptotic nucleoid levels (as shown in figure 3.4.11) and this was reconfirmed in the results recorded with no peroxide challenge in figure 3.4.12.

In the presence of 100μM H_2O_2, there were no significant effects on the percentages of apoptotic nucleoids recorded with each AA treatment. At higher H_2O_2 concentrations (250 and 500μM), there were significant increases in the percentage of apoptotic nucleoids with increasing AA pre-treatment ($P<0.01$, Dunnett's post test, n=9) In the absence of AA and in the presence of 250μM H_2O_2, the percentage of apoptotic nucleoids was 62.5% this rose to 81.5% for 50μM AA and 87.0% for 100μM AA respectively. In the presence of 500μM H_2O_2, the percentage of apoptotic nucleoids was 74.8%, this rose to 91.7% for 50μM AA and 92.3% for 100μM AA in the presence of 500μM H_2O_2 ($P<0.01$, Dunnett's test, n=9).

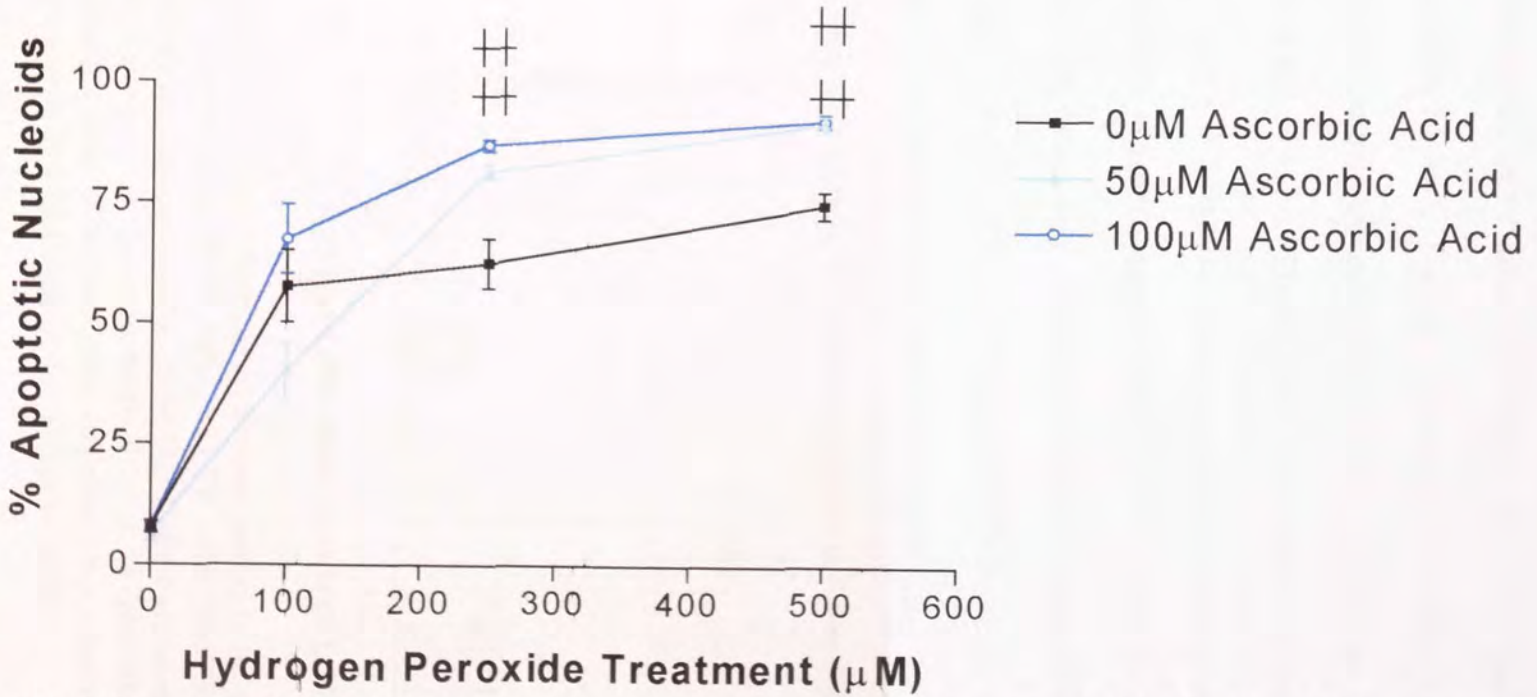

Figure 3.4.12 Overview of the effects of ascorbic acid on hydrogen peroxide toxicity in SY5Y cells. SY5Y cells (2 x 10^5) were incubated with AA (50 and 100μM) for 24 hours at 37°C, 5%CO_2, then further incubated with H_2O_2 (100, 250 and 500μM) for 24 hours at 37°C, 5%CO_2. Cells were then harvested and prepared for flow cytometry as stated in method 2.2.4. Graph shows mean percentage apoptotic events of the nucleoids analysed ± SEM for 9 replicates. ++ represents P value < 0.01 (Dunnett's test).

3.4.3 DIFFERENTIATED SY5Y CELLS

3.4.3.1 Effect of hydrogen peroxide and evaluation of time course of action on DNA fragmentation as assessed by flow cytometry

In order to investigate the time course of action of H_2O_2 on both undifferentiated and differentiated SY5Y cells, experiments were set up harvesting cells at 4 and 24 hours post H_2O_2 addition. Figures 3.4.13 and 3.4.14 show that in both cell types increasing H_2O_2 concentrations caused increases in the percentage of apoptotic nucleoids recorded after 4 and 24 hours. Figure 3.4.13, shows after 4 hours there were differences in both cell types with increasing H_2O_2 concentrations causing significant increases in apoptosis ($P=0.0141$ in undifferentiated cells, and $P=0.0263$ in differentiated cells, unpaired t-tests, n=3, two-tailed). Figure 3.4.14 shows after 24 hours there were also significant changes in both cell types. Figure 3.4.14 also shows differentiated cells to be more resistant to 100μM H_2O_2 induced apoptosis after 24 hours when compared to the response after 4 hours of treatment as shown in figure 3.4.13.

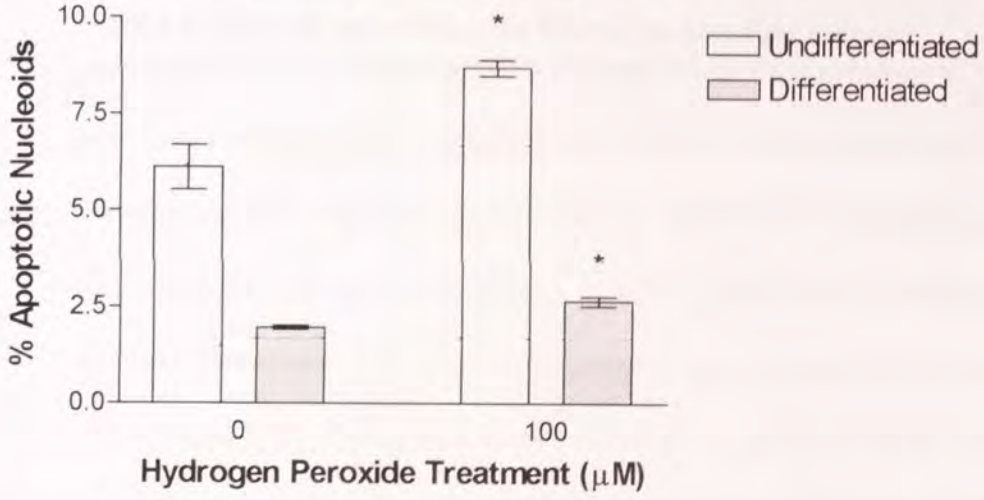

Figure 3.4.13 The effects of hydrogen peroxide on apoptosis in undifferentiated and differentiated SY5Y cells. SY5Y cells ($2x10^5$) were incubated with H_2O_2 (100μM) for 4 hours at 37°C, 5%CO_2. Cells were then harvested and prepared for flow cytometry as stated in method 2.2.4. Figure shows the mean percentage of apoptotic events of the nucleoids analysed after 4 hours ± SEM of 3 replicates. * represents $P<0.05$ (Unpaired t-test, two tailed).

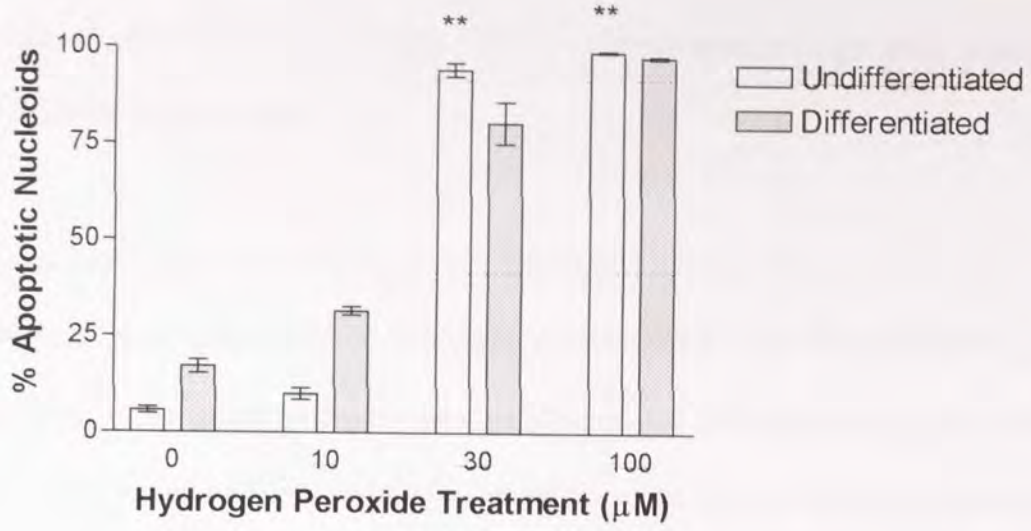

Figure 3.4.14 The effects of hydrogen peroxide on apoptosis in undifferentiated and differentiated SY5Y cells. SY5Y cells ($2x10^5$) were incubated with H_2O_2 (10, 30 and 100μM) for 24 hours at 37°C, 5%CO_2. Cells were then harvested and prepared for flow cytometry as stated in method 2.2.4. Figure shows the mean percentage of apoptotic events of the nucleoids analysed after 24 hours ± SEM of 3 replicates. ** represents P<0.01 (Dunnett's test) when compared to 0μM H_2O_2 in undifferentiated cells. + represents P<0.05 and ++ represents P<0.01 when compared to 0μM H_2O_2 in differentiated cells (Dunnett's test).

3.4.3.2 Effect of nerve growth factor on hydrogen peroxide induced apoptosis on DNA fragmentation as assessed by flow cytometry

In order to determine whether NGF (10ng/ml) exerted an effect against peroxide challenge in differentiated cells, cells were pre-treated with NGF for 24 hours before the addition of H_2O_2. Figure 3.4.15 shows the effects of NGF against H_2O_2 challenge in differentiated and undifferentiated cells. In undifferentiated, unchallenged cells (Figure 3.4.15a), in the absence of NGF there was a basal level of 9.1% apoptotic nucleoids, in differentiated cells (Figure 3.4.15c) this was significantly increased, with cells having a basal level of 18.1% apoptotic nucleoids (P=0.0019, unpaired t-test). Undifferentiated cells unchallenged treated with 10ng/ml (Figure 3.4.15b) had a basal level of 9.3% apoptotic nucleoids, which was significantly different to differentiated

cells treated with 10ng/ml NGF (Figure 3.4.15d) (basal level of 20.3% apoptotic nucleoids (P=0.0165, unpaired t-test)). However, there were no significant effects of NGF alone in each cell type.

Increases in H_2O_2 caused increases in apoptosis for all four experimental paradigms. At the highest H_2O_2 concentration, (100μM), differentiated cells showed significantly lower levels of apoptotic nucleoids than undifferentiated cells challenged with 100μM H_2O_2. Undifferentiated cells had 67.0% apoptotic nucleoids, and undifferentiated cells treated with 10ng/ml NGF and challenged with 100μM had 75.1% apoptotic nucleoids (P=0.0038, unpaired t-test, two tailed, n=3). Differentiated cells challenged with 100μM had 56.0% apoptotic nucleoids, and differentiated cell treated with 10ng/ml NGF challenged with 100μM had 60.3% apoptotic nucleoids, a significant difference (P=0.0017, unpaired t-test, two-tailed, n=3).

The results show that increasing H_2O_2 treatment caused increases in the percentage of apoptotic cells in a dose dependent manner up to and including 30μM H_2O_2 in undifferentiated untreated cells. All H_2O_2 doses produced significant increases in the number of apoptotic nucleoids ($P<0.01$, Dunnett's post test). Undifferentiated cells treated with 10ng/ml NGF also produced significant increases in the percentage of apoptotic cells in a dose dependent manner up to and including 30μM H_2O_2.

The results also show increases in the percentage of apoptotic cells after 10μM H_2O_2 treatment in differentiated untreated cells, but higher H_2O_2 treatment had no further effects. All H_2O_2 doses produced significant changes compared to untreated controls, $P<0.01$ (Dunnett's test). Differentiated cells treated with peroxide and 10ng/ml NGF

also showed significant increases in the percentage of apoptotic cells, $P<0.01$, (Dunnett's test) compared with controls, and no evidence of cytoprotection was observed. In both differentiated and undifferentiated cells there were no significant effects of 10ng/ml NGF in the absence of H_2O_2.

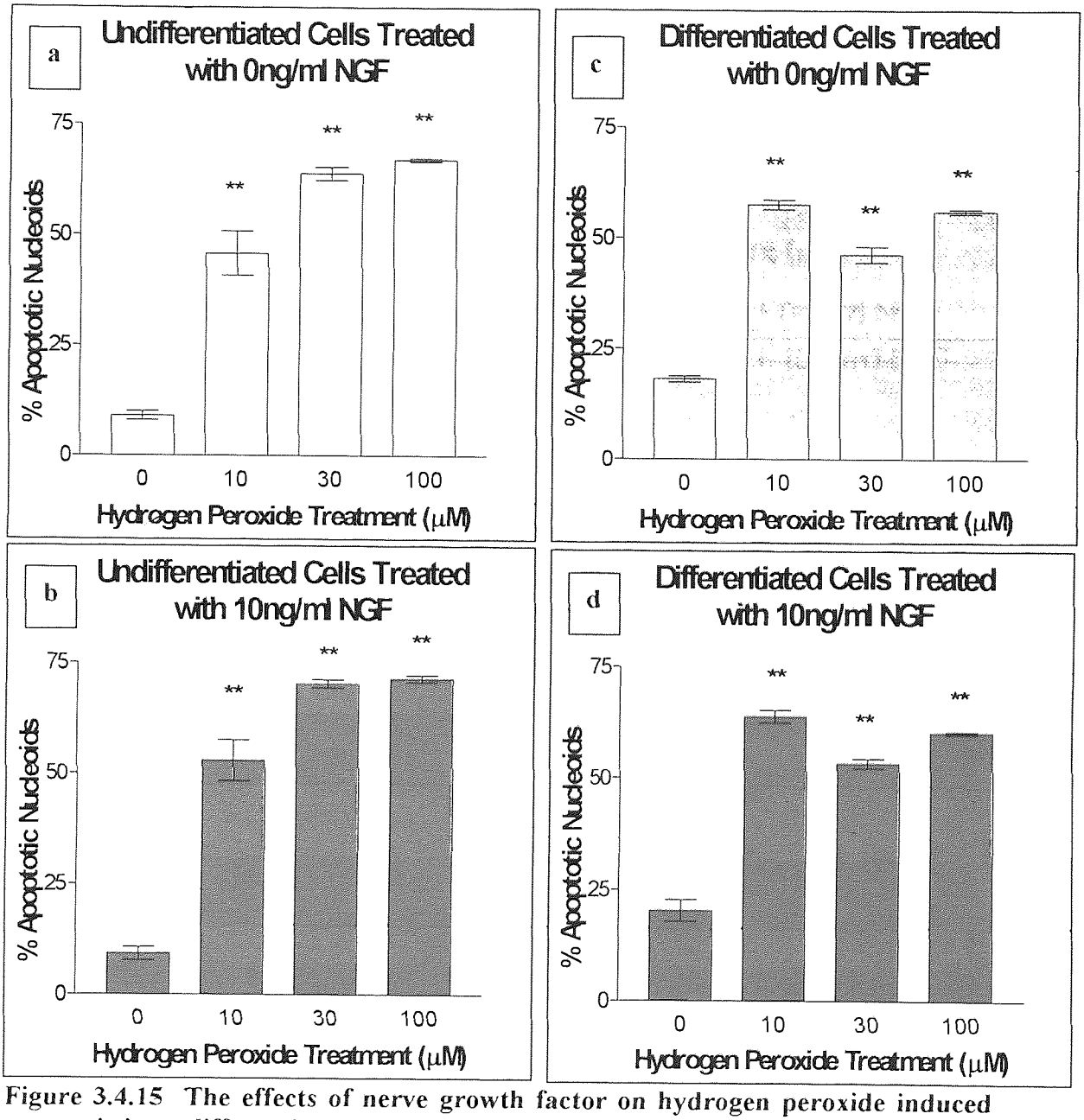

Figure 3.4.15 The effects of nerve growth factor on hydrogen peroxide induced apoptosis in undifferentiated and differentiated SY5Y cells. Undifferentiated and differentiated SY5Y cells described in method 2.2.1.7 ($2x10^5$) were incubated with NGF (10ng/ml) for 24 hours at 37°C, 5%CO_2. H_2O_2 (10, 30 and 100μM) was then added for a further 24 hours at 37°C, 5%CO_2. Cells were then harvested and prepared for flow cytometry as stated in method 2.2.4. Graphs show the mean percentage of apoptotic events of the nucleoids analysed ± SEM for 3 replicates. ** represents $P<0.01$ (Dunnett's test) compared to control.

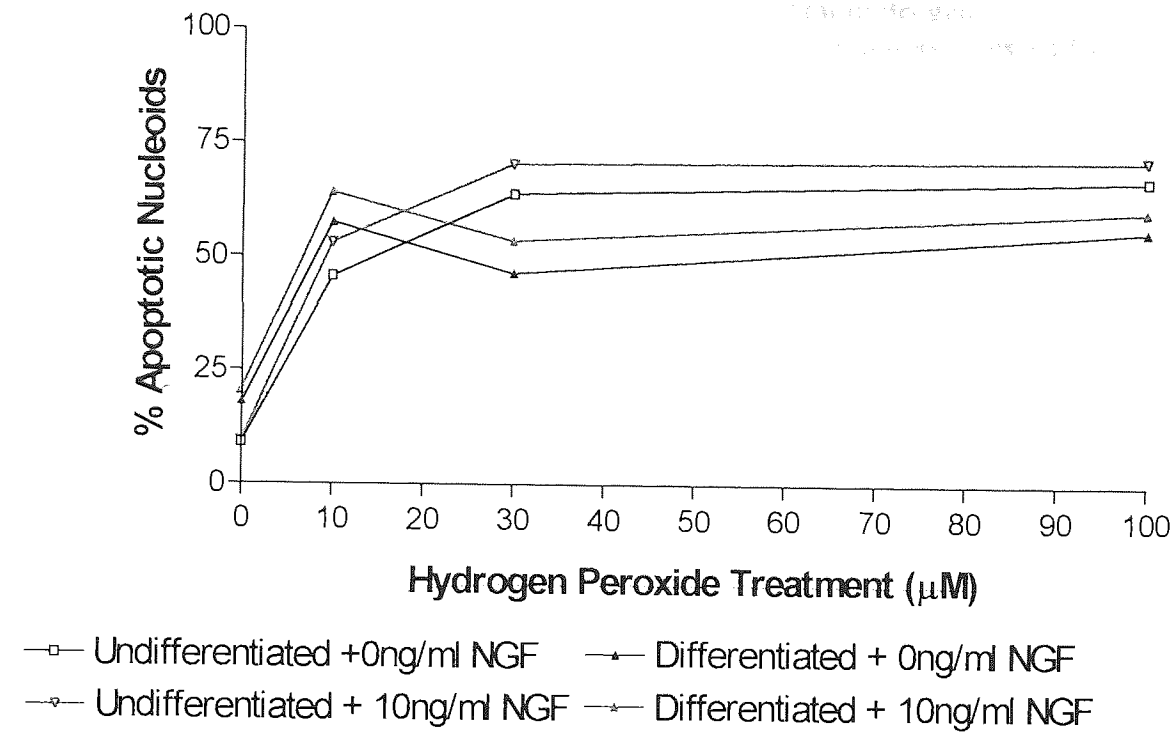

Figure 3.4.16 Overview of the effects of NGF on hydrogen peroxide induced apoptosis in undifferentiated and differentiated SY5Y cells.

Statistical analysis showed that NGF actually caused significant increases in the percentage of apoptotic nucleoids with NGF pre-treatment at 30 and 100μM H_2O_2 when comparing 10ng/ml NGF treated cells to 0ng/ml NGF treated cells in undifferentiated cells($P<0.05$, Dunnett's test, n=6). In differentiated cells, NGF also caused significant increases in the percentage of apoptotic nucleoids with NGF pre-treatment at 10, 30 and 100μM H_2O_2 when comparing 10ng/ml NGF treated cells to 0ng/ml treated cells ($P<0.05$, Dunnett's test, n=6).

3.4.3.3 Effect of brain derived neurotrophic factor on hydrogen peroxide induced apoptosis on DNA fragmentation as assessed by flow cytometry

The effects of BDNF on the percentage of apoptotic nucleoids produced by increasing concentrations of H_2O_2 were assessed using 5 and 10ng/ml BDNF versus control. Figures 3.4.17 a-c and 3.4.18 a-c show the effects of BDNF against H_2O_2 toxicity in both differentiated and undifferentiated cells.

In undifferentiated cells there were increases in the percentage of apoptotic nucleoids, following BDNF treatment. In the absence of BDNF (figure 3.17a), the percentage of apoptotic nucleoids rose from 5.4% at 0μM H_2O_2 through 4.9%, 5.9% to 35.4% at 100μM H_2O_2. BDNF treatment (5ng/ml) (figure 3.17b) caused the percentage of apoptotic nucleoids to rise from 5.8% in the absence of H_2O_2 to 27.7%, and from 4.7% to 63.8% in the presence of 100μM H_2O_2. However, at 10ng/ml BDNF (figure 3.17c), BDNF prevented the increase in the percentage of apoptotic nucleoids rose induced by 100μM H_2O_2.

In differentiated cells in the absence of BDNF (figure 3.17d), the percentage of apoptotic nucleoids rose from 12.0% (no challenge) to 50.4% at 100μM H_2O_2. In the presence of BDNF (5ng/ml) (figure 3.17e), the percentage of apoptotic nucleoids rose from 12.4% at no H_2O_2 challenge through 18.9% at 10μM H_2O_2, 20.0% at 30μM H_2O_2 to 47.4% at 100μM H_2O_2. In the presence of BDNF (10ng/ml) (figure 3.17f), the percentage of apoptotic nucleoids was not changed by H_2O_2 titration.

Results show a greater sensitivity of differentiated cells to BDNF, which subsequently caused reductions in the percentage of apoptotic nucleoids recorded Differentiated cells

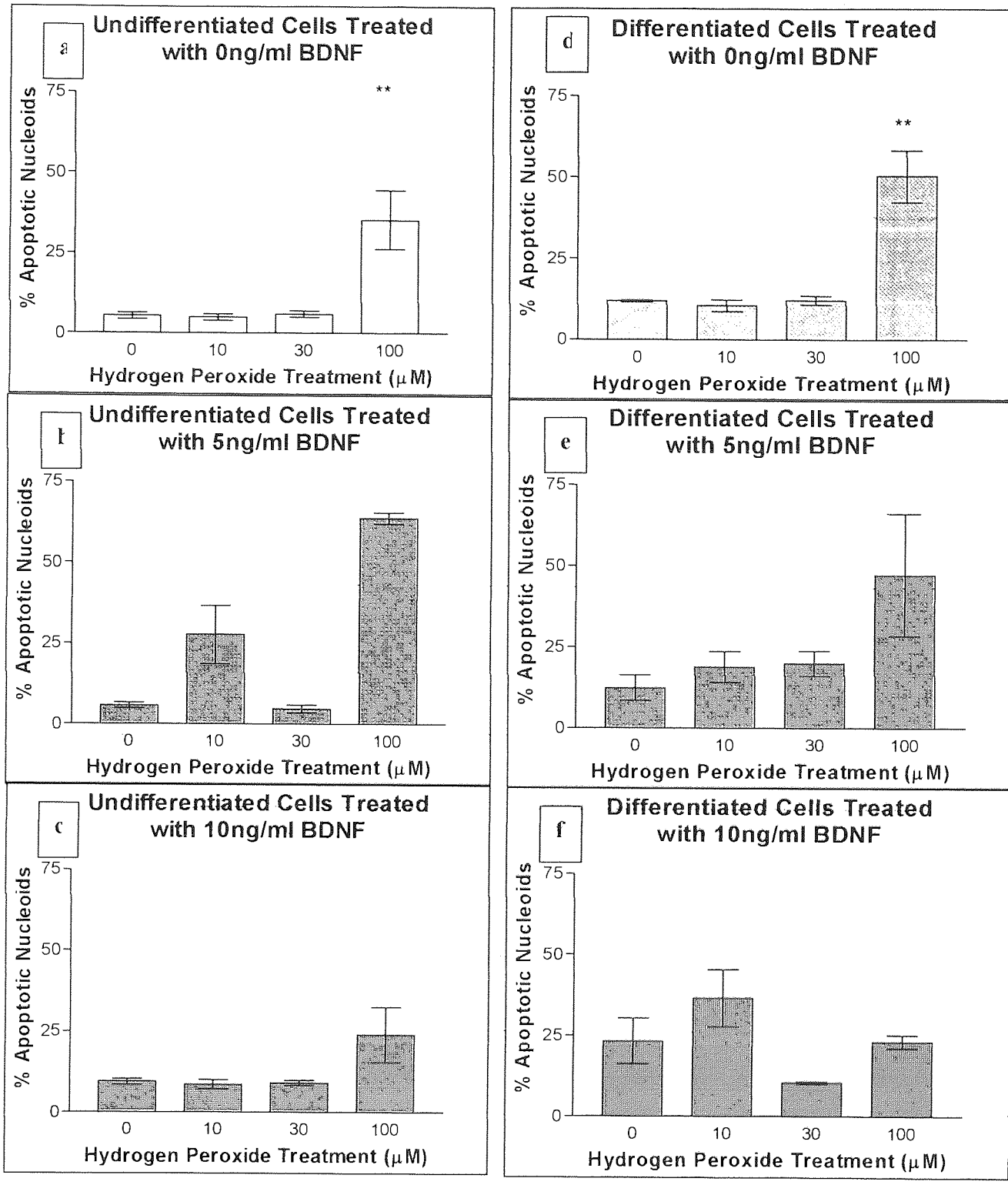

Figure 3.4.17 The effects of brain derived neurotrophic factor on hydrogen peroxide induced apoptosis in undifferentiated cells and differentiated. Undifferentiated and differentiated SY5Y cells described in method 2.2.1.7 ($2x10^5$) were incubated with NGF (10ng/ml) for 24 hours at 37°C, 5%CO_2. H_2O_2 (10, 30 and 100μM) was then added for a further 24 hours at 37°C, 5%CO_2. Cells were then harvested and prepared for flow cytometry as stated in method 2.2.4. Graphs show the mean percentage of apoptotic events of the nucleoids analysed ± SEM for 3 replicates. ** represents $P<0.01$ (Dunnett's test) compared to control.

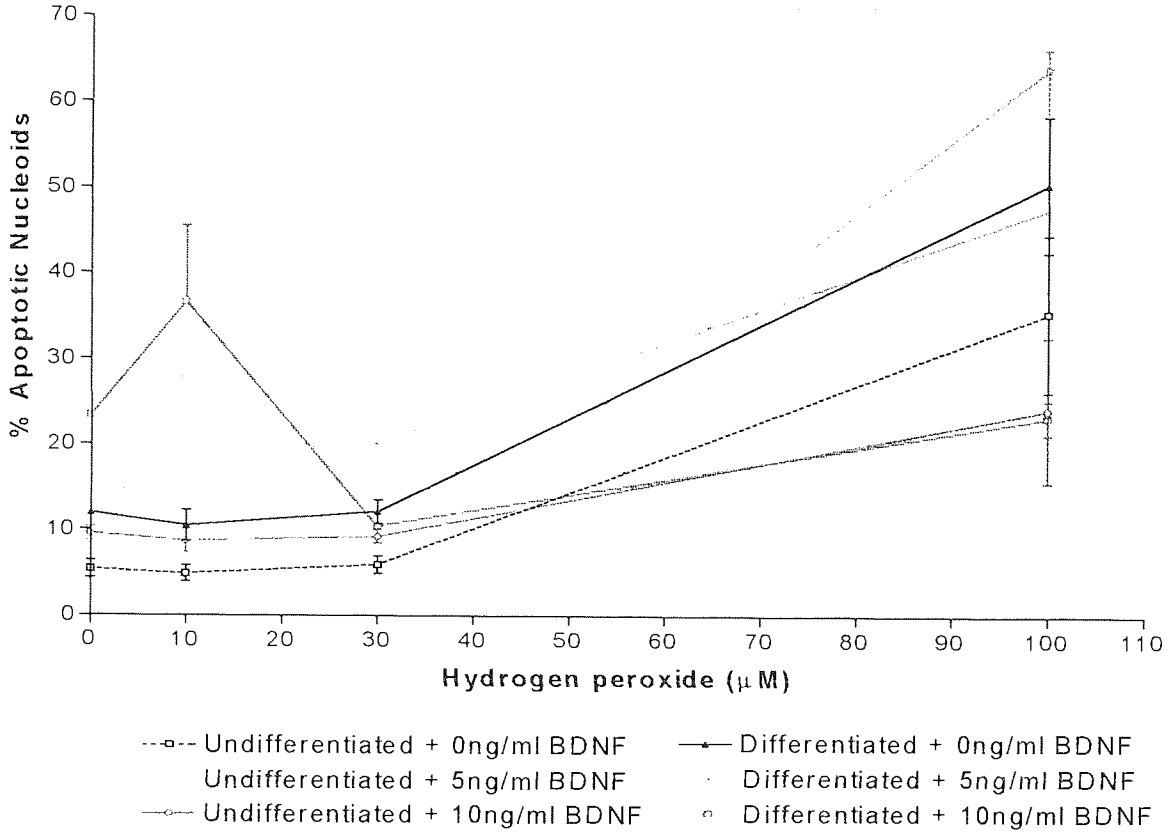

Figure 3.4.18 Summary overview of the effects of brain derived factor shown in figure 3.4.17 a-f.

The effects of BDNF on the percentage of apoptotic nucleoids produced by H_2O_2 on each cell type (undifferentiated and differentiated) were statistically analysed, to investigate whether any of the effects of BDNF on each cell type were significantly different to that cell type treated with 0ng/ml BDNF at each H_2O_2 concentration tested. Tests showed that in undifferentiated cells, 10ng/ml BDNF pre-treatment caused significant increases in the percentage of apoptotic nucleoids compared to non pre-treated cells at 0, 10 and 30μM H_2O_2 ($P<0.01$ at 0 and 10μM H_2O_2, $P<0.05$ at 30μM, Dunnett's test). There was also a signifcant increase in apoptotic nucleoids with 5ng/ml BDNF at 10μM H_2O_2 ($P<0.01$, Dunnett's test). In differentiated cells, tests showed that the only significant effect was at 10μM H_2O_2, where pre-treatment with 10ng/ml BDNF caused an increase in apoptotic nucleoids compared to controls ($P<0.05$, Dunnett's test, n=6), although there was a trend of BDNF pre-treatment causing reductions.

treated with BDNF showed only reductions in the percentage of apoptosis recorded. At 5ng/ml BDNF (figure 3.17e), a 6% reduction in the percentage of apoptotic nucleoids was recorded at 100μM H_2O_2 compared to at 0ng/ml BDNF. At 10ng/ml BDNF (figure 3.17f), a 54.2% reduction in the percentage of apoptotic nucleoids was recorded at 100μM H_2O_2 compared to 0ng/ml BDNF.

3.4.3.4 Effects of ascorbic acid on hydrogen peroxide induced apoptosis as assessed by flow cytometry

The effects of AA on the percentage of apoptotic nucleoids produced by increasing concentrations of H_2O_2 were assessed using 50 and 100μM AA. Figures 3.4.19 and 3.4.20 show the effects of AA against H_2O_2 induced apoptosis in both differentiated and undifferentiated cells.

In undifferentiated cells (figure 3.4.19) there were dose dependent increases in the percentage of apoptotic nucleoids following peroxide treatment in each AA treatment. In the absence of AA the percentage of apoptotic nucleoids rose from 7.3% at control through 49.5% at 10μM H_2O_2, 55.0% at 30μM H_2O_2 to 67.0% at 100μM H_2O_2. In the presence of 50μM AA the percentage of apoptotic nucleoids rose from 8.3% at 0μM H_2O_2 through 43.9% at 10μM H_2O_2, 87.2% at 30μM H_2O_2 to 96.4% at 100μM H_2O_2. However, in the presence of 100μM AA the percentage of apoptotic nucleoids rose from 5.2% at 0μM H_2O_2 though 70.8% at 10μM H_2O_2, 92.7% at 30μM H_2O_2 to 96.3% at 100μM H_2O_2.

In differentiated cells (figure 3.4.20) there were dose dependent increases in the percentage of apoptotic nucleoids in each AA treatment. In the absence of AA the

percentage of apoptotic nucleoids rose from 8.0% in the absence of H_2O_2 through 40.4% at 10μM H_2O_2, 43.9% at 30μM H_2O_2 to 48.8% at 100μM H_2O_2. Following 50μM AA pre-treatment for 24 hours before peroxide challenge, the percentage of apoptotic nucleoids rose from 5.4% in controls through 39.2% at 10μM H_2O_2, 47.7% at 30μM H_2O_2 to 53.9% at 100μM H_2O_2. However, following 100μM AA, the percentage of apoptotic nucleoids increased from 8.1% in controls though 65.3% at 10μM H_2O_2, 68.4% at 30μM H_2O_2 to 74.5% at 100μM H_2O_2.

Undifferentiated cells

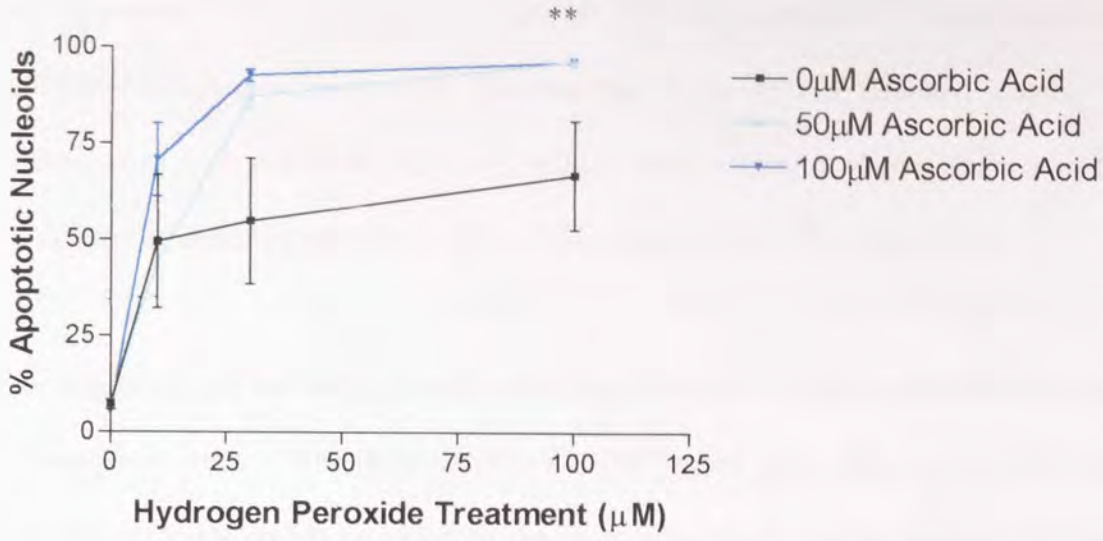

Figure 3.4.19 The effect of ascorbic acid on hydrogen peroxide induced apoptosis in undifferentiated cells. Cells ($2x10^5$) were incubated with AA (50 and 100μM) for 24 hours at 37°C, 5%CO_2. H_2O_2 (10, 30, and 100μM) for 24 hours at 37°C, 5%CO_2. Graphs show the mean percentage of apoptotic events of the nucleoids analysed ± SEM for 6 replicates for 0 and 100μM AA treatments and 3 replicates for 50μM AA treatments. ** represents P<0.01 (Dunnett's test).

Differentiated cells

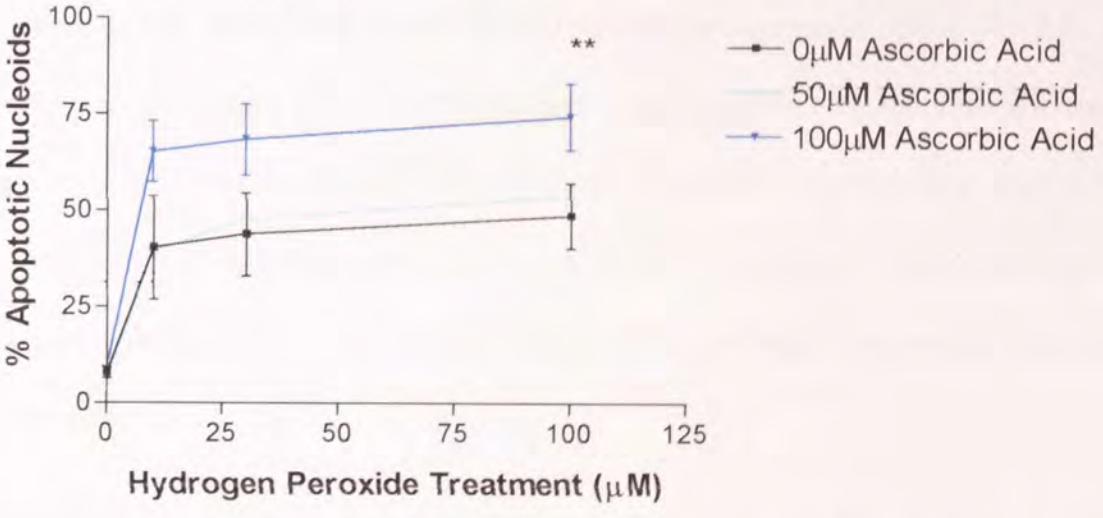

Figure 3.4.20 The effect of ascorbic acid on hydrogen peroxide induced apoptosis in differentiated cells. Cells ($2x10^5$) were incubated with AA (50 and 100μM) for 24 hours at 37°C, 5%CO_2. H_2O_2 (10, 30, and 100μM) for 24 hours at 37°C, 5%CO_2. Graphs show the mean percentage of apoptotic events of the nucleoids analysed ± SEM for 6 replicates for 0 and 100μM AA treatments and 3 replicates for 50μM AA treatments. ** represents P<0.01 (Dunnett's test).

The effects of H_2O_2 on both undifferentiated and differentiated cells were assessed. In undifferentiated cells in the absence of AA, 100μM H_2O_2 caused a 59.7% increase in the percentage of apoptotic nucleoids, this was significant $P<0.01$ (Dunnett's test). In differentiated cells untreated with AA, 100μM H_2O_2 caused a 40.8% increase in the percentage of apoptotic nucleoids, this was significant $P<0.01$ (Dunnett's test).

The effects of AA on H_2O_2 toxicity were also assessed in both undifferentiated and differentiated cells. Undifferentiated cells pre-treated with AA showed differing responses to H_2O_2, which depended on the dose of the insult. In the presence of 50μM AA, a 43.9% increase in the percentage of apoptotic nucleoids was recorded following 100μM H_2O_2 challenge compared with peroxide challenge in the absence of AA. Similarly, at 100μM AA a 43.7% increase in the percentage of apoptotic nucleoids was recorded following 100μM H_2O_2 challenge compared with peroxide challenge in the absence of AA. Differentiated cells showed the same pro-apoptotic effects with AA. In the presence of 50μM AA, a 10.5% increase in the percentage of apoptotic nucleoids was recorded following 100μM H_2O_2 challenge compared to peroxide challenge in the absence of AA. Similarly, at 100μM AA, a 52.7% increase in the percentage of apoptotic nucleoids was recorded at 100μM H_2O_2 challenge compared to peroxide challenge.

3.4.4 Discussion

Flow cytometric analysis showed in all cells types that increasing doses of H_2O_2 caused increases in the percentage of apoptotic nucleoids, indicative that H_2O_2 is exerting its toxic effect at least in part via an apoptotic means. As H_2O_2 insult increased in each cell type, it took longer to process the sample. The analysis of each sample is based on

analysis of light scatter of cells, at higher doses there was a decline in the number of events in each sample.

Aβ was also shown to cause increases in the percentage of sub diploid nucleoids; indicative also that it is exerting a toxic effect via an apoptotic process. This confirms the earlier work of Li *et al.*,(1996) and Kuner *et al.*, (1998) among others who have shown Aβ to induce apoptosis in human neuroblastoma cells and SH-SY5Y cells. Mazziotti & Perlmutter (1998) have also shown Aβ to induce apoptosis in PC12 cells.

NGF (10ng/ml) pre-treatment was shown to have a significant effect in reducing the percentage of apoptotic nucleoids in PC12 cells. NGF (10 and 25ng/ml) was also shown to be protective in SY5Y where a majority of cells were lost. This observation is important in the context of AD, where reduced numbers of cells are recorded. A treatment that can rescue any remaining vulnerable cells has great potential.

It is believed that the cellular responses to NGF are elicited through binding and activation of its receptors, TrkA and $p75^{NTR}$ (Bothwell, 1995). Numerous intracellular signalling cascades are triggered by NGF receptor activation, and there is evidence for convergence of, and direct interactions between, NGF signalling and signalling triggered by other molecules. PC12 cells treated with NGF have been shown to cause a sustained activation of the MAP kinase pathway (Muroya *et al.*, 1992). Convergence of control over the MAP kinase pathway may also occur between Ras, PKC, and Src. Src is a member of a large family of non receptor protein tyrosine kinases that share significant sequence homology. Src kinases regulate a wide range of cellular events including survival. It has been proposed that signalling through Src, PI3 kinase, PKC

and JNK may play a role in cell survival signalling. Therefore it has been suggested that survival signalling may be controlled in part by a signalling unit that includes Src, PI3 kinase and PKC (Sofroniew *et al.*, 2001).

In contrast AA, showed no protective effects against H_2O_2, however it did show some pro-oxidant effects some of which were significant. This pro-oxidant effect may be due to redox cycling in different media – other workers have suggested that AA has an anti-oxidant effect. This pro-oxidant effect is real and may actually prime cells to respond to further oxidative challenge through an adaptive response, by induction of repair genes, detoxifying enzymes and other defence systems.

Differentiated SY5Y cells were used to represent a more physiological post-mitotic model, however, these cells showed significant pro-oxidant effects of NGF, and general pro-oxidant effects with AA. However BDNF was show at 10ng/ml to cause a significant reduction in apoptotic nucleoids compared to untreated controls.

Differentiation of the SY5Y cells was considered to successful however perhaps not totally completely. Morphological observations show the cells to not look post-mitotic, and as they were still growing as prolifically as normal cells, but their trk B expression levels has increased, which was shown to be very important.

BDNF is known to have trophic effects on various neurons, throughout the brain and spinal cord, via its high-affinity tyrosine kinase receptor trk B. It has been reported that the mRNA for this neurotrophin is reduced in AD. This has been proposed as having important consequences for the neurotrophic support of vulnerable neurons in AD.

More recently BDNF protein levels have been shown, by immunohistochemical techniques, to be reduced in neurons in the hippocampus and temporal cortex (Connor *et al.*, 1997) It has been suggested that decreased levels of BDNF may be associated with lack of trophic support and may contribute to the degeneration of specific neuronal subpopulations in the AD-affected brain, including the basal forebrain cholinergic system (Hock *et al.*, 2000). There is also accumulating evidence to show, that in addition, neurons expressing the BDNF receptor trk B may also be affected in AD. One of the roles of BDNF is to rescue and protect cell loss centrally (Allen *et al.*, 1999).

An anomalous result was obtained in the study of BDNF effects in SY5Y cells, where undifferentiated cells showed protective benefit against OS from co-incubation with BDNF. Therefore there may be a basal trk B expression in SY5Y cells, which is subsequently up-regulated with RA treatment. The ELISA results presented in figure would agree with this, as undifferentiated cells shows a small positive absorbance reading after background subtractions.

CHAPTER FOUR

OXIDANTS and PROTEIN CARBONYL FORMATION

4.1 Intracellular peroxide production in cells

H_2O_2 has previously been suggested to mediate Aβ cytotoxicity through antioxidant inhibition and production of lipid peroxidation in treated cells (Behl *et al.,* 1994b). This may be due to a redox cycling mechanism. The levels of intracellular peroxide can be quantitated using the nonfluorescent fluorochrome 2',7'-dichlorofluorescin diacetate (DCFDA) which is freely permeable to cells. Inside cells it is de-esterified by endogenous esterases to the ionised free acid, 2',7'-dichlorofluorescin (DCF). This becomes trapped within cells and accumulated DCF is able to interact with peroxides and hydroperoxides in the cell to form the fluorescent compound 2',7'-dichlorofluorescein (Pereira *et al.*, 1999, Behl *et al.*, 1994a; Tsuchiya *et al.,* 1994).

In order to confirm whether generation of ROS occurs in the models employed and whether these levels could be modulated by exogenous agents, the effects of H_2O_2 and Aβ on kinetics of intracellular peroxide levels were investigated in neuronal cells in the presence and absence of NGF.

4.1.1 PC12 Cells

4.1.1.1 Intracellular peroxide production in hydrogen peroxide treated cells

In order to validate methodology for determination of the intracellular production of peroxides, PC12 cells were co-incubated with H_2O_2 (0 and 150μM) and the fluorochrome DCFDA. Cells were harvested after exactly 30 minutes, and immediately analysed through a flow cytometer.

Figure 4.1 shows that incubation with H_2O_2 causes an increase in the median fluorescence (Md X) values indicative of an increase in intracellular peroxide

concentrations. The Md X increased significantly from 0.607 to 2.690 with 150μM H_2O_2 concentration (P=0.0008, Unpaired t-test).

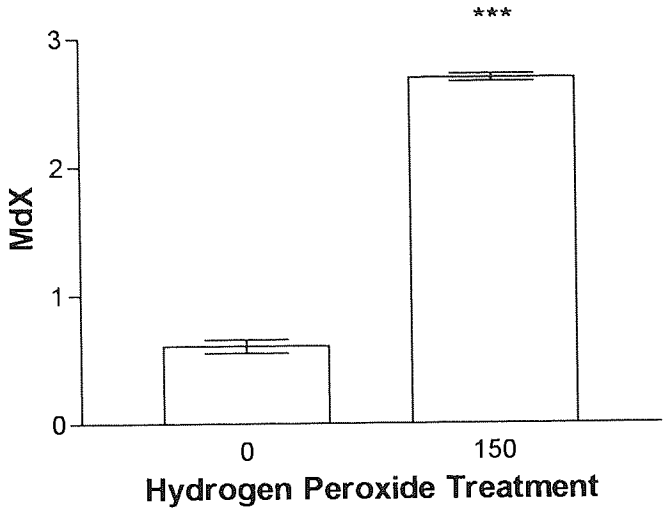

Figure 4.1 Intracellular peroxide levels in PC12 cells following incubation with hydrogen peroxide. PC12 cells ($2x10^5$) were incubated for 4 hours at 37°C, 5%CO_2 before the co-addition of H_2O_2 (150μM) and DCFDA (75μM) for 30 minutes at 37°C, 5%CO_2. Cells were then harvested and analysed by flow cytometry. Figure shows the average median X ± SEM, where n=12 replicates. * represents P < 0.001 (Unpaired t-test)**

4.1.1.2 Intracellular peroxide production in amyloid β peptide, fragment 25-35, treated cells

It has been proposed that Aβ may exert its toxicity through either independent or metal dependent peroxide generation. Huang *et al.*, (1999) published data to show that Aβ directly produced H_2O_2 through metal ion reduction. The effects of Aβ, fragment 25-35 on intracellular peroxide production were therefore assessed using DCFDA in association with the metal chelator (iron) desferoxamine mesylate (DFX), in order to corroborate/rebut the findings of Huang *et al.*(1999)

Figure 4.2 shows that 25μM Aβ peptide caused an increase in the Md X value compared to PBS treated cells. A 30% increase in Md X to 0.799 was observed for Aβ treated cells compared with 0.607 for control cells, indicative of an increase in

intracellular peroxide concentrations in the presence of Aβ. The iron chelator DFX caused a 40% decrease in the median X recorded. Pre-treatment of cells with DFX before the administration of Aβ caused a further reduction in the median X by 70%.

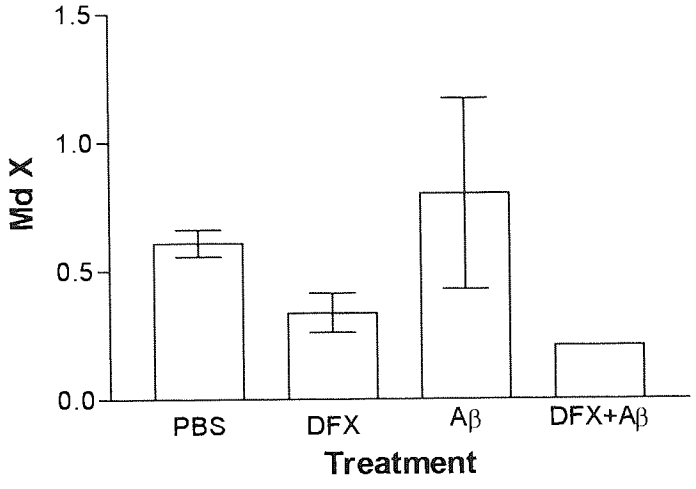

Figure 4.2 Intracellular peroxide levels in PC12 cells following incubation with amyloid β peptide in the presence or absence of deferoxamine mesylate. PC12 cells ($2x10^5$) were incubated for 4 hours at 37°C, 5%CO_2 before the addition of PBS, DFX (100μM) or Aβ (25μM) for 24 hours at 37°C, 5%CO_2. Cells were also pre-treated with DFX (100μM) for 24 hours before the addition of Aβ (25μM). For the last 30 minutes of each incubation DCFDA (75μM) was added. Cells were then harvested and analysed by flow cytometry. Figure shows the mean median X ± SEM, where n=6.

4.1.1.3 Intracellular peroxide production in nerve growth factor treated cells challenged with hydrogen peroxide

The effects of NGF on intracellular peroxide levels were also assessed using DCFDA. PC12 cells were incubated with NGF (5 and 10ng/ml) versus control for 24 hours at 37°C, 5% CO_2 before the addition of H_2O_2 (150μM, or PBS control) and the fluorochrome DCFDA. Figure 4.3 shows increasing NGF concentrations cause a basal 20% increase in the Md X values indicative of an increase in intracellular peroxide concentrations, however these were not significant. No significant protective effects of NGF were recorded against peroxide challenge. Increasing NGF concentrations increased MdX DCF fluorescence from 2.690 to 3.135 (P value 0.0011, Single factor

ANOVA). When peroxide challenge was compared to unchallenged cells, there were also significant increases in peroxide levels ($p<0.01$).

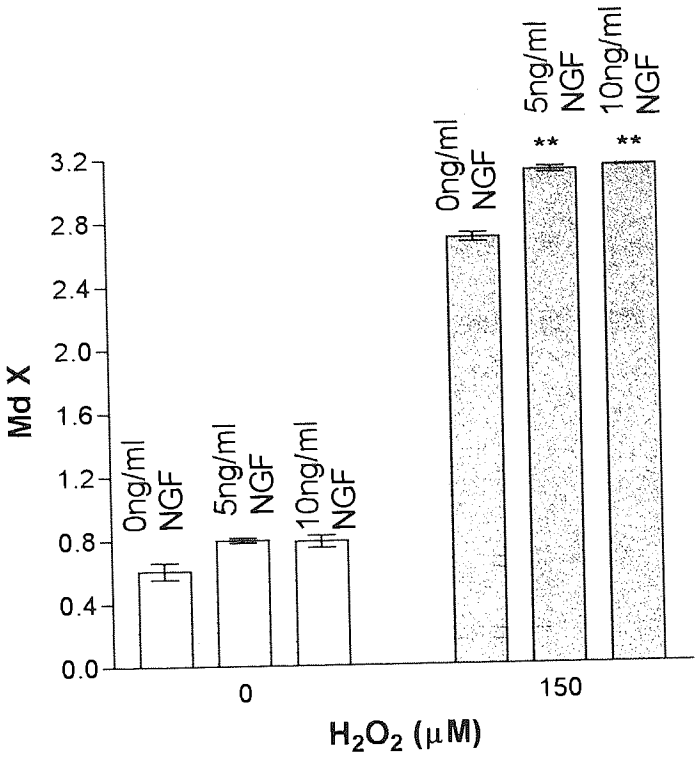

Figure 4.3 Intracellular peroxide levels in PC12 cells following incubation with nerve growth factor (NGF). PC12 cells ($2x10^5$) were incubated for 4 hours at 37°C, 5%CO_2 before the addition of NGF (5 and 10ng/ml) for 24 hours at 37°C, 5%CO_2. H_2O_2 (0 and 150μM) and DCFDA (75μM) were then added for 30 minutes. Cells were then harvested and analysed by flow cytometry. Figure shows the mean median X ± SEM of 3 replicates. ** represents $P<0.01$ when compared to 0ng/ml NGF at 150μM H_2O_2 ,(Single factor ANOVA).

4.1.1.4 Intracellular peroxide production in nerve growth factor treated cells challenged with amyloid β peptide, fragment 25-35

Investigations were conducted into the intracellular production of peroxides by Aβ in the presence of NGF. PC12 cells were incubated with NGF (5 and 10ng/ml) for 24 hours at 37°C, 5%CO_2 before the addition of Aβ (25μM) and the fluorochrome DCFDA. Cells were harvested and immediately analysed through a flow cytometer.

Figure 4.4 shows some protective effects of NGF against Aβ induced peroxide generation. In the absence of NGF, cells treated with Aβ had a Md X value of 0.799 compared to PBS treatment with a Md X value of 0.607. Pre-treatment with 5ng/ml NGF prior to Aβ showed a decrease in the Md X value for DCF fluorescence to 0.300, indicative of a decrease in intracellular peroxide concentration. Pre-treatment of PC12 cells with 10ng/ml NGF prior to Aβ showed a trend of decreases in the Md X value to 0.549, compared to PBS treatment with a Md X value of 0.785.

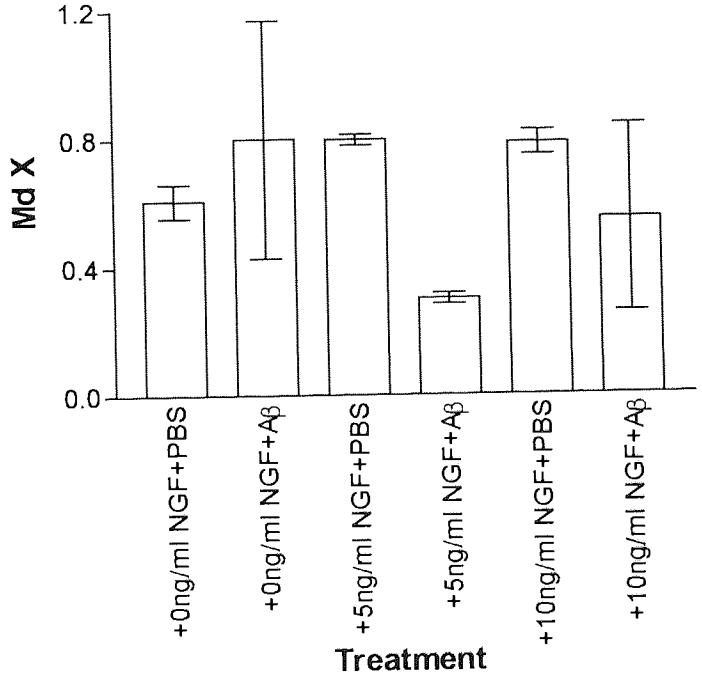

Figure 4.4 Intracellular peroxide levels in PC12 cells following pre-treatment with nerve growth factor (NGF) before challenge with amyloid β peptide(Aβ). PC12 cells ($2x10^5$) were incubated for 4 hours at 37°C, 5%CO_2 before the addition of NGF (5 and 10ng/ml) for 24 hours at 37°C, 5%CO_2. Aβ (25μM) was then added for 4 hours at 37°C, 5%CO_2. For the final 30 minutes of incubation, DCFDA (75μM) was added. Cells were then harvested and analysed by flow cytometry. Figure shows the average median X ± SEM of 3 replicates.

4.1.2 SY5Y Cells

4.1.2.1 Effects of hydrogen peroxide

In order to establish the methodology for determination of intracellular production of peroxides in neuroblasts, SY5Y cells were co-incubated with H_2O_2 (0 and 150μM) and the fluorochrome DCFDA. Cells were harvested and immediately analysed through a flow cytometer.

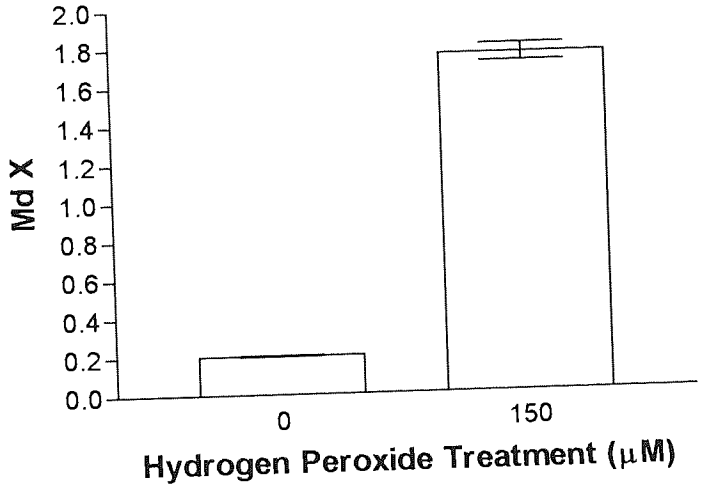

Figure 4.5 Intracellular production of peroxides in SY5Y cells caused by incubation with hydrogen peroxide. SY5Y cells ($2x10^5$) were incubated for 4 hours at 37°C, 5%CO_2 before the co-addition of H_2O_2 (150μM) and DCFDA (75μM) for 30 minutes at 37°C, 5%CO_2. Cells were then harvested and analysed by flow cytometry. Results are recorded as the median X of 10,000 events, where n=3.

Figure 4.5 shows 150μM H_2O_2 causes an increase in the Md X values indicative of an increase in intracellular peroxide concentrations, where the Md X increased 8 fold, from 0.198 to 1.710.

4.1.2.2 Intracellular peroxide production in nerve growth factor treated cells

The effects of NGF on intracellular peroxide production were also assessed using the fluorochrome DCFDA.

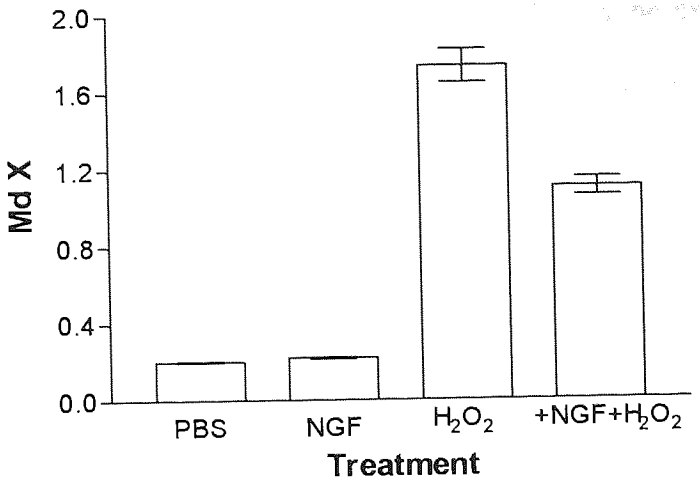

Figure 4.6 Effect of NGF on intracellular peroxide levels in SY5Y cells. SY5Y cells ($2x10^5$) were incubated for 4 hours at 37°C, 5%CO_2 before the addition of NGF (10ng/ml) or H_2O_2 (150μM) for 24 hours at 37°C, 5%CO_2. Samples were also set up of NGF (10ng/ml) treatment for 24 hours and H_2O_2 (150μM) treatment for 30 minutes. For the last 30 minutes of each incubation DCFDA (75μM) was added. Cells were then harvested and analysed by flow cytometry. Figure shows the median X ± SEM, where n=3.

NGF had no effect on intracellular peroxide levels in the absence of any stressors. H_2O_2 caused an increase in the Md X value from 0.198 to 1.710 with 150μM H_2O_2 in PBS treated cells. However, following 24 hours of NGF pre-treatment the shift in fluorescence was reduced to 1.040.

4.1.3 Discussion

DCFDA staining has previously been shown to increase with ROS production (Satoh *et al.*, 1997). Results show H_2O_2 increased intracellular peroxide levels in both cell lines; this is in agreement with the work of other groups (Jang & Surh, 2001).

These data have shown that NGF pre-treatment in unchallenged cells did not cause any significant lowering of intracellular peroxide levels in both cell lines. However, in NGF pretreated H_2O_2 challenged cells two different trends were seen. In PC12 cells no trend was recorded, however in SY5Y cells there was a trend towards lowering of peroxide

production with increasing NGF pre-treatment. NGF may be exerting its protective action on H_2O_2 toxicity by lowering intracellular peroxide levels directly thereby stopping chain reactions and resultant toxicity on cells. However it has been suggested that an increased rate of DCF oxidation could be interpreted as an indication of general OS due to a variety of reasons, including depletion of AOX, rather than as a specific proof of augmented ROS formation (Jakubowski & Bartosz, 2000). Therefore, differences between cells may reflect differences in metabolic/mitochondrial generation of ROS, levels of AOX protection or changes in NO production as peroxynitrite is measured by DCF.

Results add credance to the suggestion that Aβ increases intracellular peroxides, this further reinforces the hypothesis that Aβ directly produces H_2O_2 as shown by increased DCFDA fluorescence levels. The inclusion of the iron chelator DFX further supported this, and also alludes to the fact that Aβ cannot exert its toxicity without the bioavailability of iron. This supports the work of Monji *et al.*, (2001) who have demonstrated that Aβ (25-35)-associated free radical generation is iron dependent and strongly influenced by the aggregational state of the peptide.

At low NGF concentrations (5ng/ml), NGF shows a trend towards a decrease in peroxide production versus control in Aβ treated cells – however the n number is small and further replicates are necessary. In addition, the time course of peroxide needs to be investigated to determine whether there is cumulative generation of ROS with time.

4.2 PROTEIN OXIDATION

Proteins are organic compounds composed of polymers of amino acids, which contain carbon, nitrogen, hydrogen, oxygen, phosphorus and occasionally sulphur. They form 17% of body weight and approximately 50% of all the organic material in the body, and are very important biological components. The name protein is derived from the Greek word *proteios*, which means 'of first importance', they are indispensable components of all living things, where they play crucial roles in all biological processes (Sherwood, 1993).

Amino acids have a general structure with a carboxyl group –COOH and an amino group $-NH_2$ at either end of the molecule. The typical structure of an amino acid is shown in Figure 4.7.

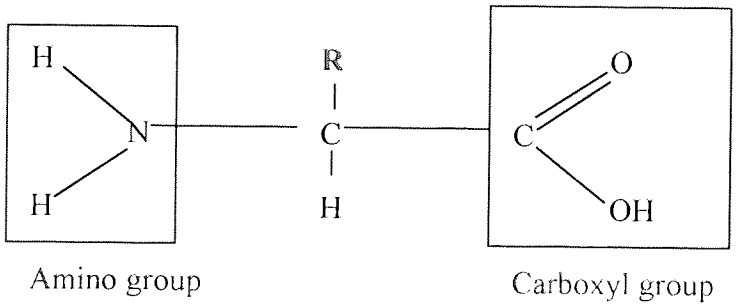

Figure 4.7 Typical structure of an amino acid
R = side chain which can be aliphatic, aromatic, acid, base or neutral.

Oxidised proteins can contain a carbonyl group $-C(=O)-$. The carbonyl group is one of the most important and reactive groups both in cells and in organic chemistry generally. Measuring the levels of protein carbonyls is an accepted index of OS (Buss *et al.*, 1997). Detection of ROS damage to amino acid residues (particularly histidine, arginine, lysine and proline) in proteins producing carbonyl moieties relies on the reaction with 2,4-dinitrophenylhydrazine (DNPH) (Evans *et al.*, 1999). The reaction

produces hydrazone derivatives in acidic media, which are then determined, either spectrophotometrically or via anti-DNP and ELISA means.

(Reaction 19)

Protein carbonylation represents non-enzymic damage that can result from a number of different pathways. Carbonyl groups may be introduced into proteins by reactions with aldehydes (4-hydroxy-2-nonenal, malondialdehyde) produced during lipid peroxidation or with reactive carbonyl derivatives (ketoamines, ketoaldehydes, deoxyosomes) generated as a consequence of the reaction of reducing sugars or their oxidation products with lysine residues of proteins (Wondrak *et al.*, 2000).

As assessed by the presence of carbonyl groups, it has been established that protein oxidation is associated with aging, OS and a number of diseases (Berlett & Stadtman, 1997). However, the current protein carbonyl measurements detect an incompletely characterised range of products, and have been shown by many groups to not be straightforward especially in tissue samples (Smith *et al.*, 1998; Shaw *et al.*, 1995, Bowling *et al.*, 1993). Tissue levels of around 1 nmol/mg protein have been recorded, suggesting that 5% of proteins contain a carbonyl function, which is roughly one carbonyl group per 10-20,000 parent amino acids. Carbonyl levels differ due to non-standardised procedures so they are not directly comparable, however, they all do show a general trend. Higher carbonyl levels have been recorded in post-mortem brain tissue from AD patients and control patients. Carbonyl levels were higher in AD patients, in fact they were shown to be significantly higher in the parietal lobe, average values

recorded were 12.59±1.2 nmol/mg protein in AD patients and 8.79±0.53 nmol/mg protein in control patients (Lyras *et al.*, 1997) Higher carbonyl levels have also been recorded with OS. Evans *et al.*, (1999) have shown that after 10 minutes of OS in gerbil brains, significant increases in carbonyl levels are evident. Increased protein carbonyls have also been recorded in plasma during disease. In plasma from normal adults a mean carbonyl value of approximately 0.1 nmol/mg protein has been recorded, with higher levels of up to 4 nmol/mg protein measured in plasma from critically ill patients (Winterbourn & Buss, 1999). Similarly, higher carbonyl values have also been recorded with advancing age. Kasapoglu & Őzben, (2001) have shown increases in an age-related pattern with significantly higher levels in a 60-69 age group compared to 20-29 and 30-39 age groups, this is in contrast to the results of Lyras *et al.*,(1997) who showed no correlation between age and protein carbonyls. However Lyras' group investigated levels in different brain areas and Kasapoglu & Őzben investigated serum levels.

Oxidative damage to proteins may be of particular importance *in vivo*, since the loss of protein function may affect the activity of enzymes, receptors, and membrane transporters, among others. Moreover, oxidatively modified proteins may contain very reactive chemical groups that could contribute to secondary damage to other biomolecules. As a result of free radical exposure, many changes can occur in proteins, including amino acid modification, fragmentation, and a decrease or loss of biological function (Salvi *et al.*,2001).

Damaged proteins have two potential fates involving either proteolyic breakdown by the proteasome or the enzymic repair of selected amino acids (i.e. cystine) (Squier, 2001).

The cells ability to repair protein damage, however, seems rather limited and most forms of protein damage appear to be irreversible. The only mechanism cells have to deal with irreversibly damaged proteins is to replace them through protein turnover. The decrease in protein turnover with age could therefore be a major cause of the increased concentration of damaged proteins (Ryazanov & Nefsky, 2002).

ROS are known to oxidise biological macromolecules, with proteins being an important target (Linton *et al.*, 2001), particularly in ageing. Therefore protein damage has been assessed by measuring the levels of protein carbonyls in PC12 and undifferentiated and differentiated SY5Y cells exposed to OS induced by H_2O_2 and Aβ, and the protective effects of AOX such as AA, NGF and BDNF have also been investigated.

4.2.1 Protein determination

The BCA assay detects cuprous ions generated from cupric ions by reaction with protein under alkaline conditions (Brenner & Harris, 1995), and was the assay of choice as other procedures are affected by detergents leading to artificially high values. Reactions 20 and 21 show the basis for the BCA assay (Smith *et al.*, 1985).

$$\textbf{Protein} + \textbf{Cu}^{2+} \longrightarrow \textbf{Cu}^{1+} \qquad \text{(Reaction 20)}$$

$$\textbf{Cu}^{1+} + \textbf{BCA} \longrightarrow \textbf{BCA-Cu}^{1+}\ \textbf{complex} \qquad \text{(Reaction 21)}$$

The BCA assay was examined for interference by coating buffer, (15mM sodium carbonate, 35mM sodium hydrogen carbonate, pH 9.2), in which samples were harvested in for carbonyl ELISAs. Coating buffer was used to produce a set of protein standards tested alongside a set of protein standards made up in water.

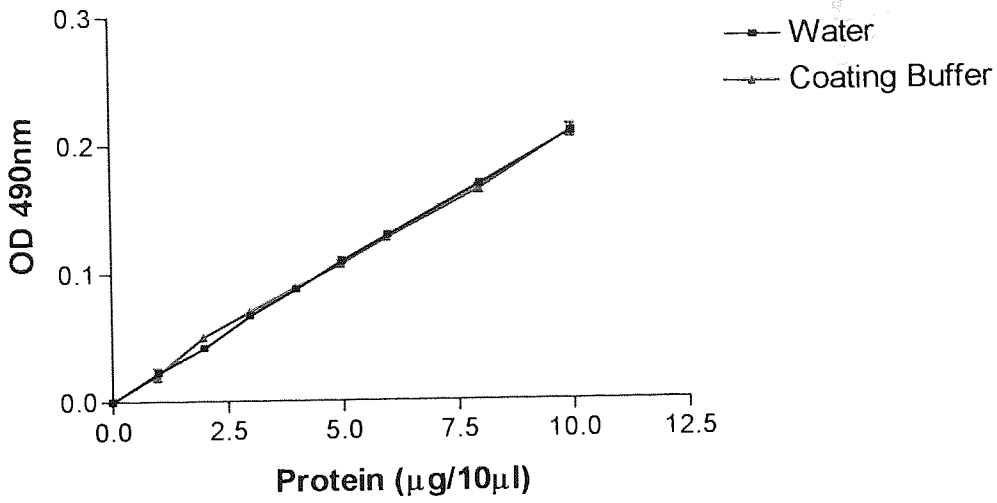

Figure 4.8 Comparison of protein solutions diluted in either water or carbonate buffer. Graph shows mean absorbance ± SEM of 4 replicates.

Results show coating buffer to have no significant effect on protein concentrations recorded using the BCA assay when compared to water. Therefore all protein concentration measurements were made in coating buffer. After analysis samples were diluted to 0.02mg/ml in coating buffer for ELISA.

It has been reported that the BCA assay is susceptible to interference with H_2O_2 and reducing agents such as glutathione by reducing the cupric ions to cuprous ions resulting in artifactually high values (Brown *et al.*, 1989). Therefore in all treatments, cells were washed, and resuspended in coating buffer to alleviate this potential problem.

4.2.2 PC12 CELLS

4.2.2.1 Evaluation of time course of hydrogen peroxide action on protein carbonyl levels

In order to investigate the time course action of H_2O_2 on PC12 cells, cells were set up with increasing H_2O_2 concentrations and harvested after 0, 4 and 24 hours of peroxide treatment. Figure 4.9 showed carbonyl levels increasing with increasing H_2O_2

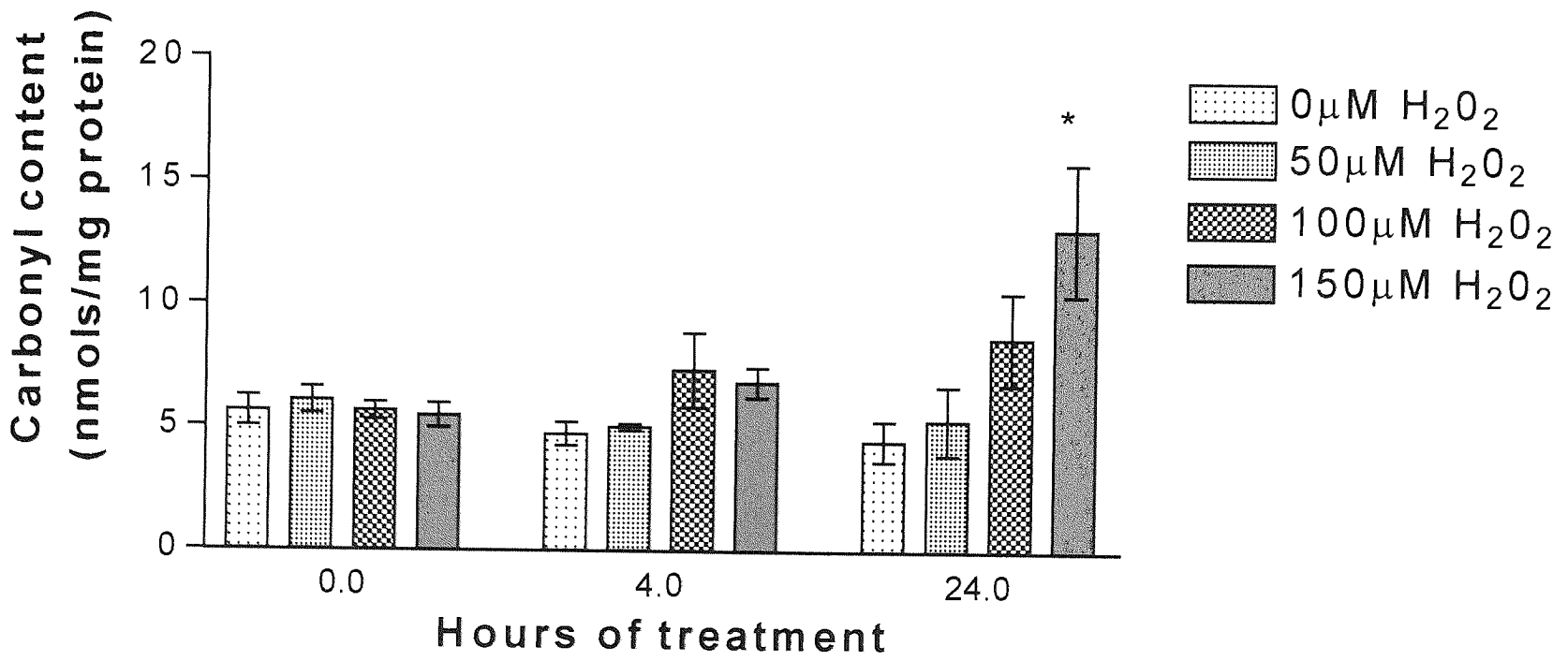

Figure 4.9 The effects of hydrogen peroxide on protein carbonyl levels over 24 hours. PC12 cells ($2x10^5$) were incubated with H_2O_2 (50, 100 and 150μM for 0 – 24 hours at 37°C, 5%CO_2. Cells were harvested and prepared for carbonyl ELISAs as stated in method 2.2.7. Figure shows the mean carbonyl content ± SEM for 4 replicates. * represents $P<0.05$ (Dunnett's test).

concentrations at 4 and 24 hours. After 4 hours of treatment there was a general trend of increasing H_2O_2 concentration, increasing carbonyl content, however, the increases were not significant. After 24 hours increasing H_2O_2 concentrations caused significant increases in carbonyl levels from 4.5 nmol/mg protein in controls, to 5.3 nmol/mg protein at 50μM H_2O_2, 8.6 nmol/mg protein at 100μM H_2O_2 to 13.1 nmol/mg protein at 150μM H_2O_2 ($P<0.05$, Dunnett's test).

4.2.2.2 Effect of amyloid β peptide, fragment 25-35 on protein carbonyl levels

The effect of Aβ peptide (fragment 25-35) on protein carbonyl levels in PC12 cells were investigated over 24 hours of treatment. Figure 4.10 shows Aβ has no significant effects on carbonyl levels, however, an increasing trend was observed. After 24 hours of Aβ treatment the level of carbonyls recorded had increased to 6.5 nmols/mg protein compared to untreated cells with a level of 4.6 nmols/mg protein.

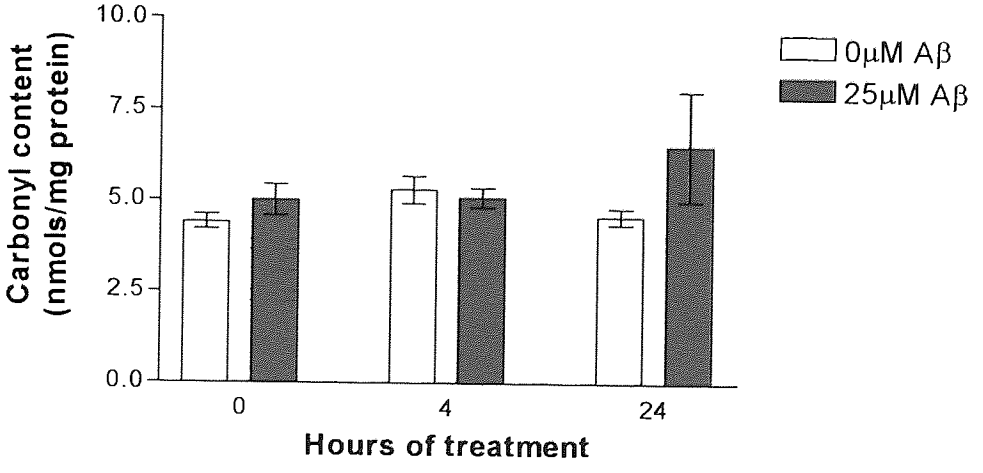

Figure 4.10 The effects of $A\beta_{25-35}$, on protein carbonyl levels in PC12 cells over 24 hours. PC12 cells ($2x10^5$) were incubated with Aβ (25μM) for 0-24 hours at 37°C, 5%CO_2. Figure shows the mean carbonyl content ± SEM for 4 replicates.

4.2.2.3 Effect of nerve growth factor on protein carbonyl levels

The effects of NGF on PC12 cells were investigated, cells were incubated with 10ng/ml NGF and harvested over a period of up to and including 24 hours as shown in figure 4.11. None of the effects recorded were significant, however there was a general trend after 2 hours which was sustained until 24 hours, where NGF treated cells showed lower carbonyl levels than untreated cells.

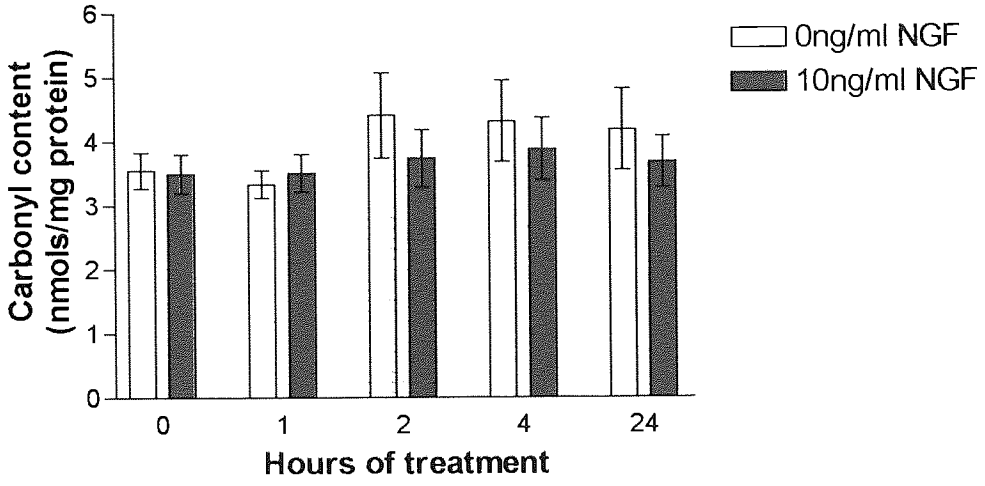

Figure 4.11 The effects of NGF on protein carbonyl levels in PC12 cells over 24 hours. PC12 cells ($2x10^5$) were incubated with NGF (10ng/ml) for 0-24 hours at 37°C, 5%CO_2. Figure shows the mean carbonyl content ± SEM for 6 replicates.

4.2.2.3.1 Effect of nerve growth factor on the actions of hydrogen peroxide as assessed by protein carbonyl levels

The effects of NGF on the actions of H_2O_2 on protein carbonyl levels were investigated. Figures 4.9 had previously shown H_2O_2 to significantly increase levels of protein carbonyls, and figure 4.11 had shown NGF to cause a decrease in protein carbonyls. Therefore, the effect on carbonyl levels of pre-treatment with NGF before peroxide insult was investigated. Figure 4.12 shows a general trend of two opposite effects of NGF against peroxide challenge. At a low dose (5ng/ml) NGF in all but one of the H_2O_2 doses (150μM) shows a pro-oxidant effect, with increases in carbonyl levels compared to controls, and at 10ng/ml NGF an anti-oxidant effect, was observed with

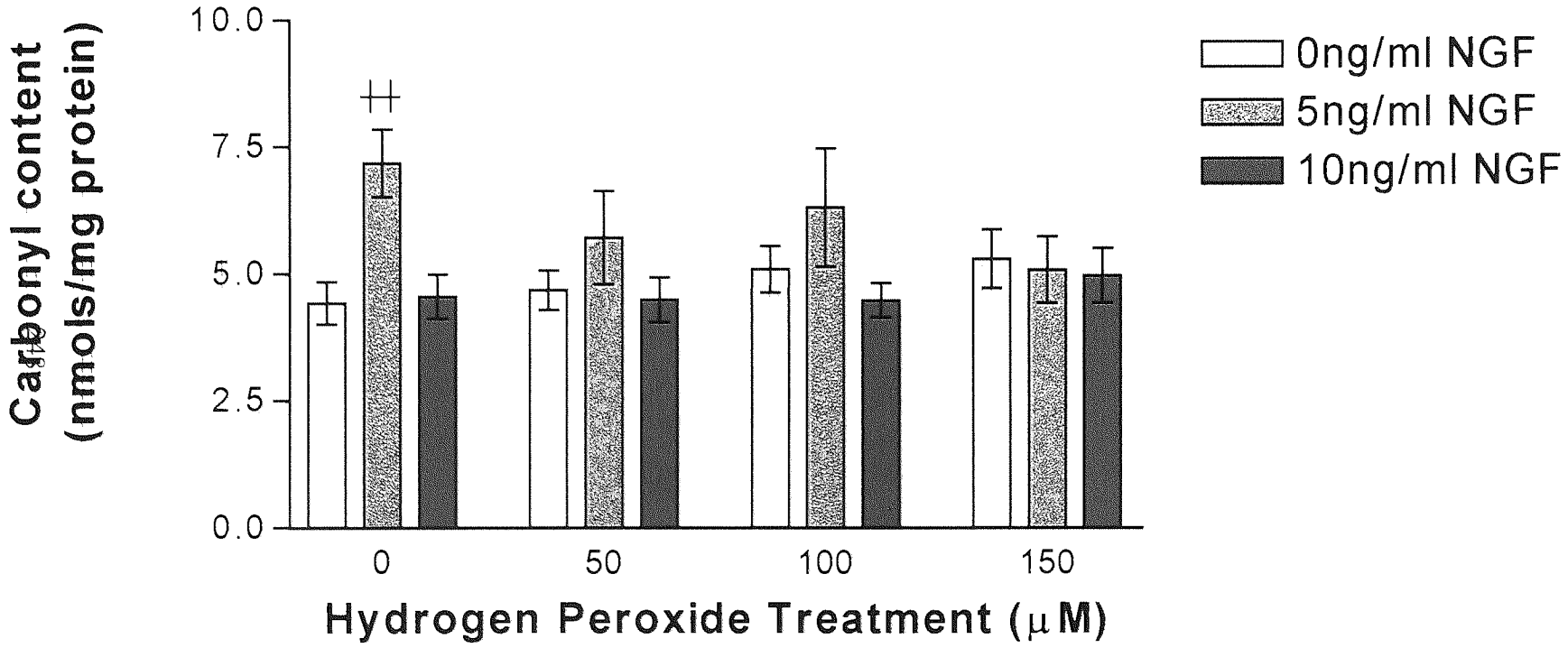

Figure 4.12 The effects of nerve growth factor (NGF) and hydrogen peroxide on protein carbonyl levels in PC12 cells. PC12 cells ($2x10^5$) were incubated with NGF (5 and 10ng/ml) for 24 hours at 37°C, 5%CO_2, before H_2O_2 treatment (50, 100, 150μM). Cells were harvested and prepared for carbonyl ELISA's as stated in method 2.2.7. Figure shows the mean carbonyl content ± SEM for 6 replicates. ++ represents $P<0.01$ (Dunnett's test) when compared to the same treatment in the absence of NGF.

decreases in carbonyl levels compared to controls. However none of the effects were significant.

In untreated cells challenged with H_2O_2 slight increases in the amounts of carbonyl were recorded, with carbonyl levels of 4.4 nmols/mg protein at 0μM H_2O_2 ranging to 5.3 nmols/mg protein at 150μM H_2O_2. This is in contrast to figure 4.9 where there was an increase from 4.5 nmols/mg protein in controls to 13.1 nmols/mg protein following 150μM H_2O_2 treatment for 24 hours. However in this paradigm cells had been allowed a further 24 hours of growth due to the period of pre-treatment with 0ng/ml NGF, before the addition of H_2O_2 doses.

Pre-treatment with 5ng/ml NGF caused significant increases in the recorded basal carbonyl content from 4.4 nmols/mg protein in 0ng/ml NGF cells to 7.2 nmols/mg protein ($P<0.01$ Dunnett's test), in contrast to figure 4.11. However, cells had been cultured for an additional 24 hours. Pre-treatment with 10ng/ml NGF caused no significant effects with a carbonyl content of 4.6 nmols/mg protein.

4.2.2.4 Effect of ascorbic acid as assessed by protein carbonyl levels

The effects of AA on carbonyl levels in PC12 cells were investigated. Cells were incubated with AA (50 and 100μM) for 24 hours and protein carbonyl levels compared to controls. Figure 4.13 shows AA to have no significant effects on protein carbonyl levels, although there was a general decrease with increasing AA treatment.

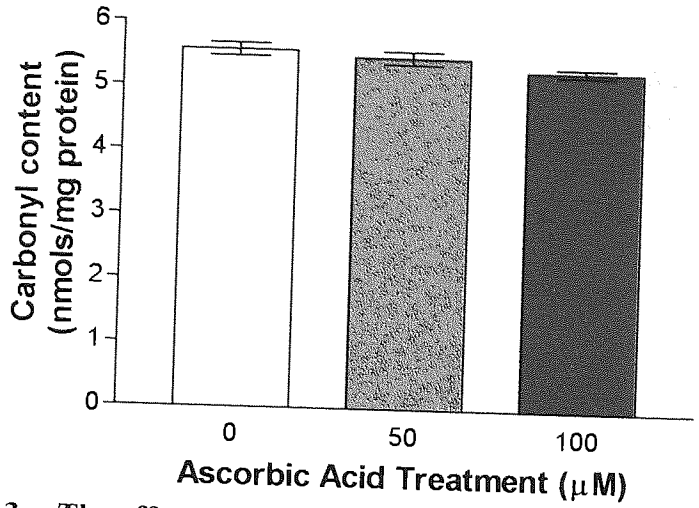

Figure 4.13 The effects of ascorbic acid (AA) on protein carbonyl levels in PC12 cells over 24 hours. PC12 cells ($2x10^5$) were incubated with AA (50 and 100μM) for 24 hours at 37°C, 5%CO_2. Cells were harvested and prepared for carbonyl ELISA's as stated in method 2.2.7. Figure shows the mean carbonyl content ± SEM for 6 replicates.

4.2.2.4.1 Effect of ascorbic acid on the actions of hydrogen peroxide as assessed by protein carbonyl levels

The effects of AA on protein carbonyl levels against unchallenged cells and against the actions of H_2O_2 were also assessed. Figure 4.14 shows both AA concentrations investigated to act in a pro-oxidant manner to cause increases in basal carbonyl levels, ($P<0.05$ Dunnett's test), the opposite to figure 4.13. There were also small increases in carbonyls in all treatments against H_2O_2 challenge, however the changes were smaller with AA treatment when compared to the respective control levels, however none of the effects were significant.

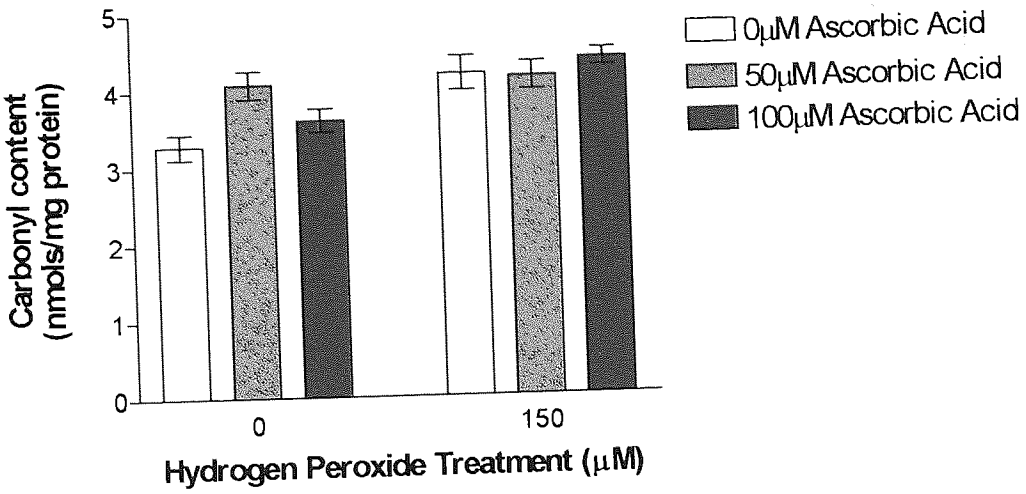

Figure 4.14 The effects of ascorbic acid (AA) and hydrogen peroxide on protein carbonyl levels in PC12 cells. PC12 cells ($2x10^5$) were incubated with AA (50 and 100μM) for 24 hours at 37°C, 5%CO_2, before H_2O_2 treatment (150μM). Cells were harvested and prepared for carbonyl ELISA's as stated in method 2.2.7. Figure shows the mean carbonyl content ± SEM for 6 replicates.

4.2.3 SY5Y CELLS

4.2.3.1 Evaluation of time course of action of hydrogen peroxide induction in protein cabonyl levels

The time course of carbonyl induction is SY5Y cells was investigated at 0, 4 and 24 hours after the addition of H_2O_2. Figure 4.15 shows at 4 hours there were increases in carbonyl levels, however none were significant, however, at 24 hours there were further increases in carbonyl levels, which were significant only at 500μM when compared to levels at 0μM H_2O_2 ($P<0.01$, Dunnett's test).

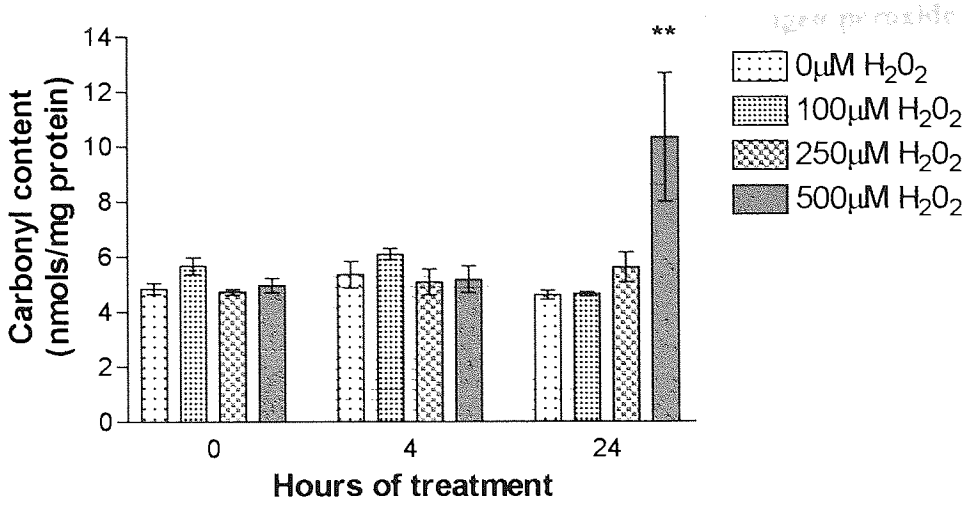

Figure 4.15 The effects of hydrogen peroxide on protein carbonyl levels in SY5Y cells over 24 hours. SY5Y cells ($2x10^5$) were incubated with H_2O_2 treatment (100, 250 and 500μM). Cells were harvested and prepared for carbonyl ELISA's as stated in method 2.2.7. Figure shows the mean carbonyl content ± SEM for 6 replicates. * represents P<0.05, ** represents P<0.01 (Dunnett's test).

4.2.3.2 Effect of nerve growth factor on protein carbonyl levels

SY5Y cells were incubated with NGF for 24 hours to investigate the effects of NGF on protein carbonyl levels. Figure 4.16 shows that various concentrations of NGF have no significant effects on carbonyl levels in unchallenged cells.

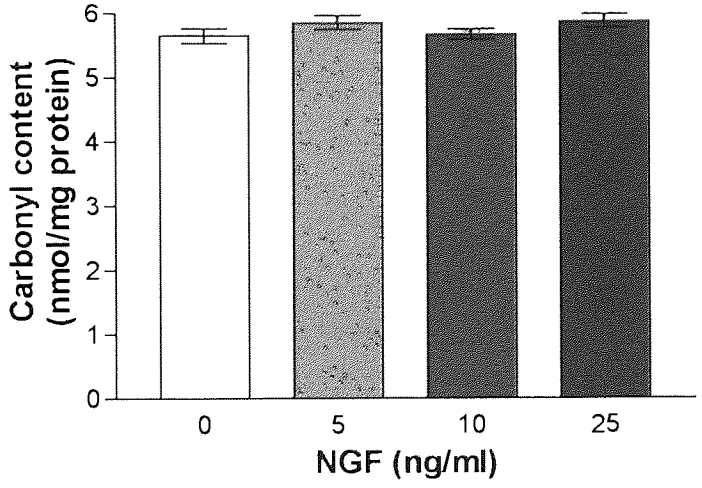

Figure 4.16 The effects of nerve growth factor (NGF) on protein carbonyl levels in SY5Y cells. SY5Y cells ($2x10^5$) were incubated with NGF (5, 10 and 25ng/ml) for 24 hours at 37°C, 5%CO_2. Cells were harvested and prepared for carbonyl ELISA's as stated in method 2.2.7. Figure shows the mean carbonyl content ± SEM for 6 replicates.

4.2.3.3 Effect of nerve growth factor on the actions of hydrogen peroxide as assessed by protein carbonyl levels

The effects of NGF on H_2O_2 induced protein carbonyl levels were investigated. Figure 4.17 shows the effect of NGF on peroxide challenge, at each H_2O_2 concentration the effects of NGF treatment were compared to controls, which showed there were no significant differences. However, NGF (25ng/ml) treatment showed consistently a trend of lower carbonyl values than 0ng/ml controls.

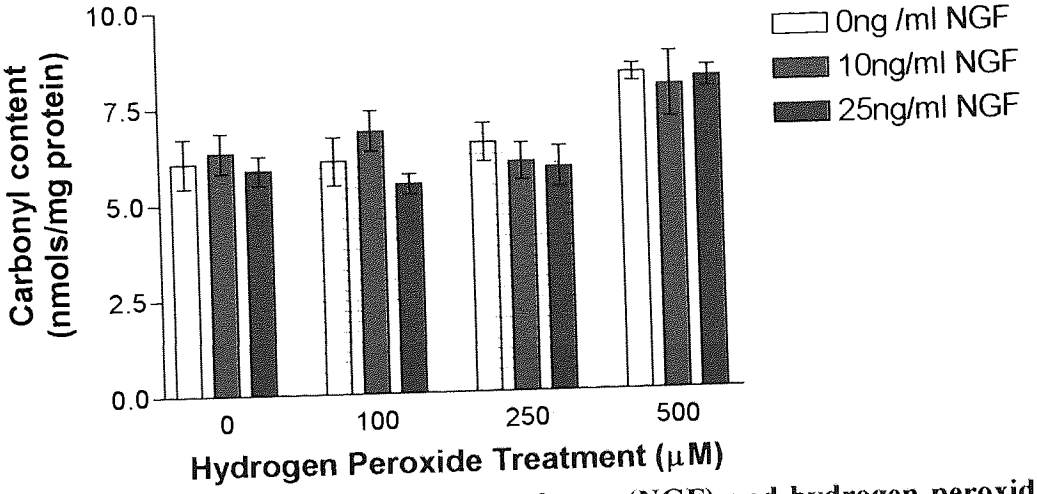

Figure 4.17 The effects of nerve growth factor (NGF) and hydrogen peroxide on protein carbonyl levels in SY5Y cells. SY5Y cells ($2x10^5$) were incubated with NGF (10 and 25ng/ml) for 24 hours at 37°C, 5%CO_2 before H_2O_2 treatment (100, 250 and 500μM). Cells were harvested and prepared for carbonyl ELISA's as stated in method 2.2.7. Figure shows the mean carbonyl content ± SEM for 6 replicates.

4.2.3.4 Effect of ascorbic acid on the actions of hydrogen peroxide as assessed by protein carbonyl levels

The effects of AA on protein carbonyl levels after H_2O_2 challenge were assessed after 4 and 24 hours pre-treatment with 50 and 100μM AA in SY5Y cells as shown in figure 4.18. After 4 hours of treatment there were no significant effects recorded although decreases were apparent in AA pre-treated cells. However significant decreases in protein carbonyl levels due to AA were recorded after 24 hours, where after 250μM and

500μM H_2O_2, there were significant reductions with both 50 and 100μM AA pre-treatment ($P<0.05$ and $P<0.01$ respectively, Dunnett's test).

4 Hours of Ascorbic Acid Pre-treatment

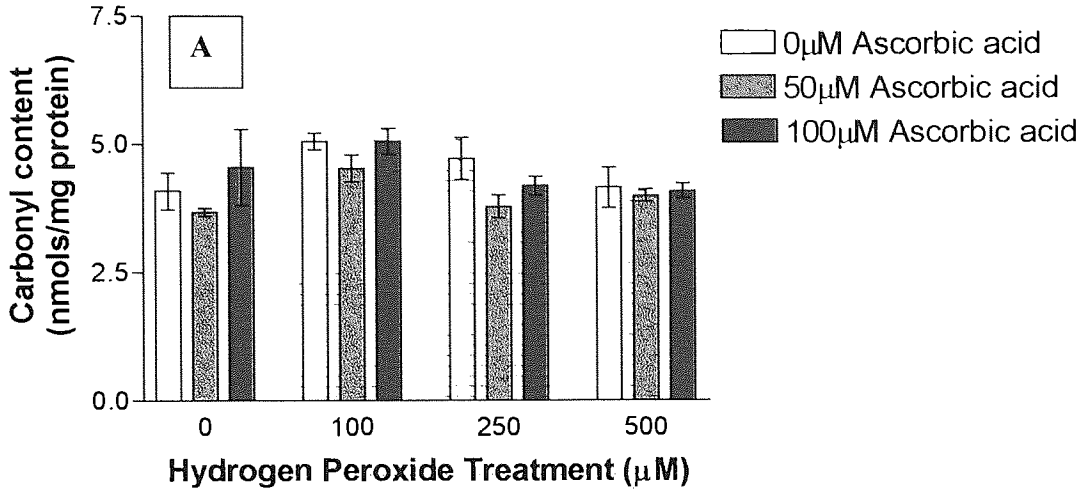

24 hours of Ascorbic Acid Pre-treatment

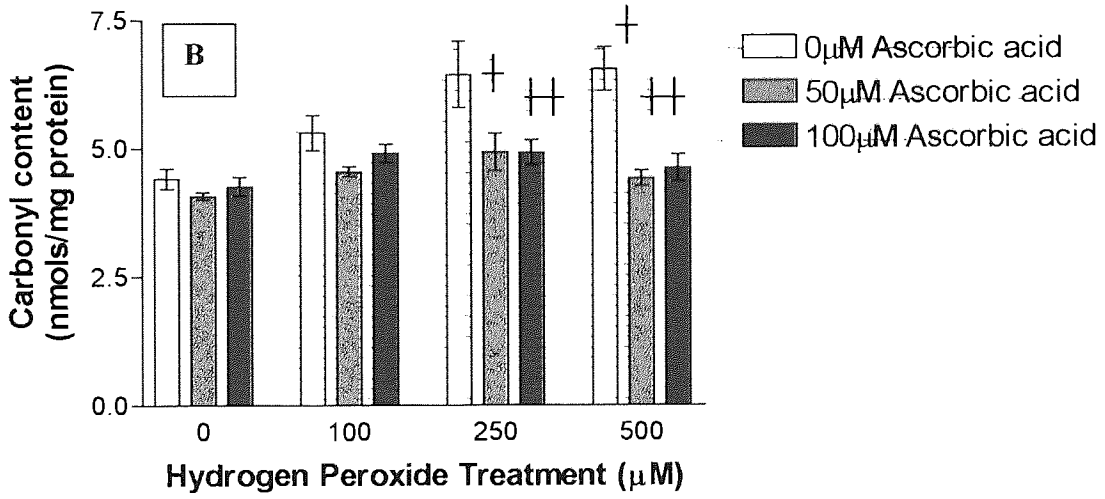

Figure 4.18 The effects of ascorbic acid (AA) pre-treatment on the effects of hydrogen peroxide on protein carbonyl levels in SY5Y cells. SY5Y cells ($2x10^5$) were incubated with AA (50 and 100μM) for 4 hours (Figure A) and 24 hours (Figure B) at 37°C, 5%CO_2 before addition of H_2O_2 (100, 250 and 500μM). Cells were then harvested and prepared for a carbonyl ELISA as stated in method 2.2.7. Figure shows the mean carbonyl content ± SEM for 6 replicates. ┼ represents $P<0.05$, ┼┼ represents $P<0.01$ when compared to the same treatment in the absence of AA

4.2.4 DIFFERENTIATED SY5Y CELLS

4.2.4.1 Effect of differentiation on protein carbonyl levels

The effect of differentiation on protein carbonyl levels was investigated. Cells harvested after 7 days of differentiation as stated in section 2.2.1.7 were subject to a carbonyl ELISA. Figure 4.19 shows a trend towards lower basal levels in differentiated cells, however this was not significant.

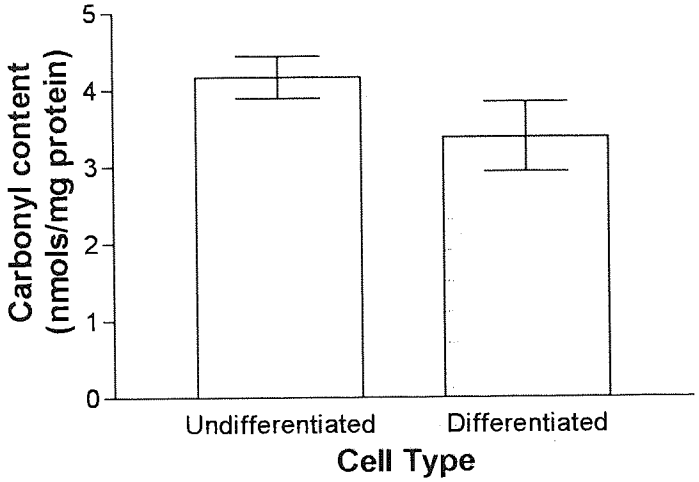

Figure 4.19 The effect of differentiation on basal protein carbonyl levels. Differentiated SY5Y cells ($2x10^5$) as stated in section 2.2.1.7 were subject to a carbonyl ELISA as stated in method 2.2.7. Figure shows the mean carbonyl content ± SEM for 5 replicates.

4.2.4.2 Effect of hydrogen peroxide on protein carbonyl levels

The effects of H_2O_2 in both undifferentiated cells and differentiated cells were investigated. In both cell types H_2O_2 caused a general trend of increasing the amount of protein carbonyls with increasing H_2O_2 concentration as shown in figure 4.20. However, there were no significant differences between differentiated cells and undifferentiated cells.

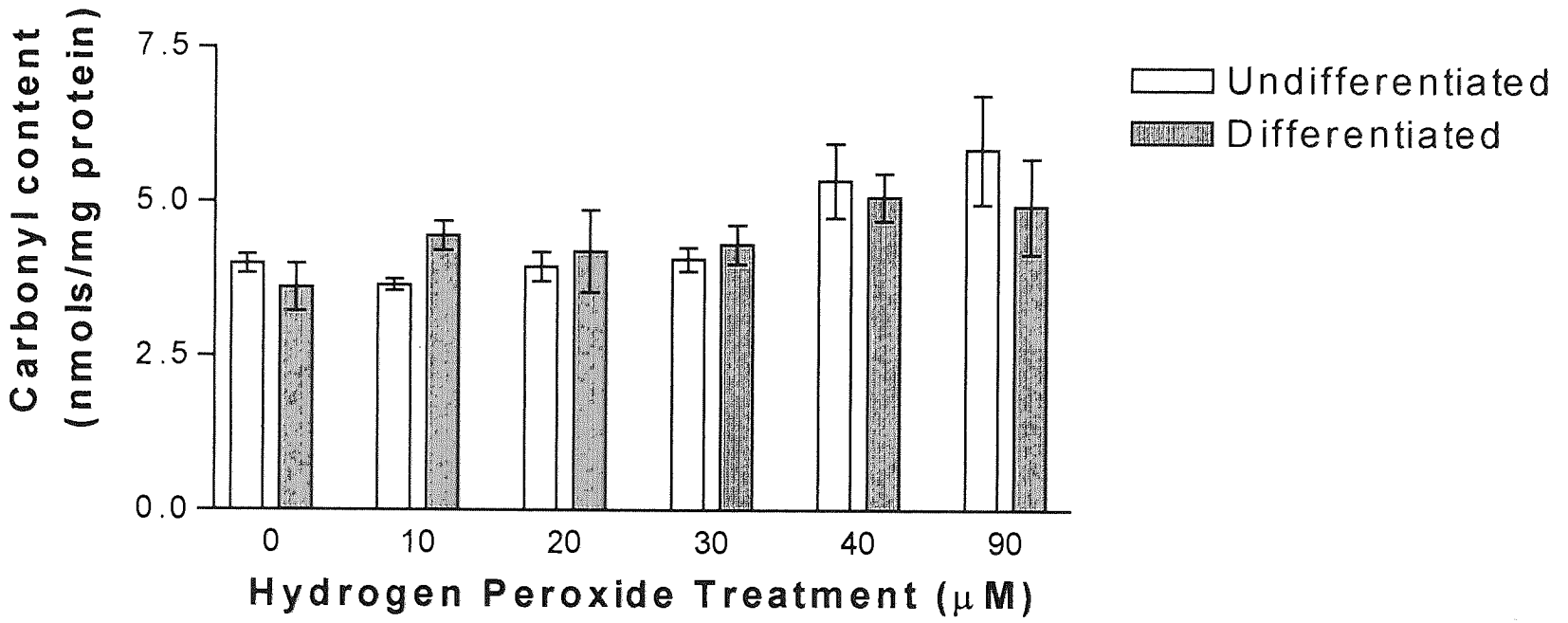

Figure 4.20 The effects of hydrogen peroxide on differentiated and undifferentiated SY5Y cells on protein carbonyl levels. SY5Y cells ($2x10^5$) were incubated with hydrogen peroxide (10, 20, 30, 40 and 90μM) at 37°C, 5%CO_2 for 24 hours. Cells were then harvested and prepared for a carbonyl ELISA as state in method 2.2.7. Figure shows the mean carbonyl content ± SEM for 6 replicates.

4.2.4.3 Effect of nerve growth factor on hydrogen peroxide toxicity as assessed by protein carbonyl levels

The effects of NGF on H_2O_2 toxicity as assessed by protein carbonyl levels, in both undifferentiated cells and differentiated cells were investigated. Figure 4.21 shows differences in carbonyl formation between the two cell types, at 10, 30 and 100μM H_2O_2. Undifferentiated cells challenged with H_2O_2 and pre-treated with NGF had lower carbonyl values compared to untreated cells of the same type, whereas differentiated cells pre-treated with NGF and challenged with H_2O_2 showed an increase.

Cells pre-treated with NGF had significantly lower carbonyl values ($P=0.0118$, $n=3$, unpaired t-test, two tail) than untreated cells after challenge with 30μM H_2O_2. Cells pre-treated with NGF had significantly higher carbonyl levels following challenge with 10μM H_2O_2 ($P=0.0029$, $n=3$, unpaired t-test two tail) than untreated cells.

4.2.4.4 Effect of ascorbic acid on hydrogen peroxide toxicity on protein carbonyl levels

The effects of AA on H_2O_2 toxicity in both undifferentiated cells and differentiated cells were investigated by assessing protein carbonyl levels. Figure 4.22 showed increases in carbonyl levels recorded with increasing H_2O_2 in both cell types, however these were only significant for differentiated cells. Comparing carbonyl levels in each cell type at each H_2O_2 concentration, significant differences were recorded at 100μM H_2O_2($P=0.0124$, unpaired t-test, $n=6$) where greater protein oxidation was observed.

Results showed AA pre-treatment exerted significant protective effects against carbonyl induction following peroxide challenge. In undifferentiated cells significant reductions were seen at 30 and 100μM H_2O_2 in carbonyl levels when comparing untreated cells to

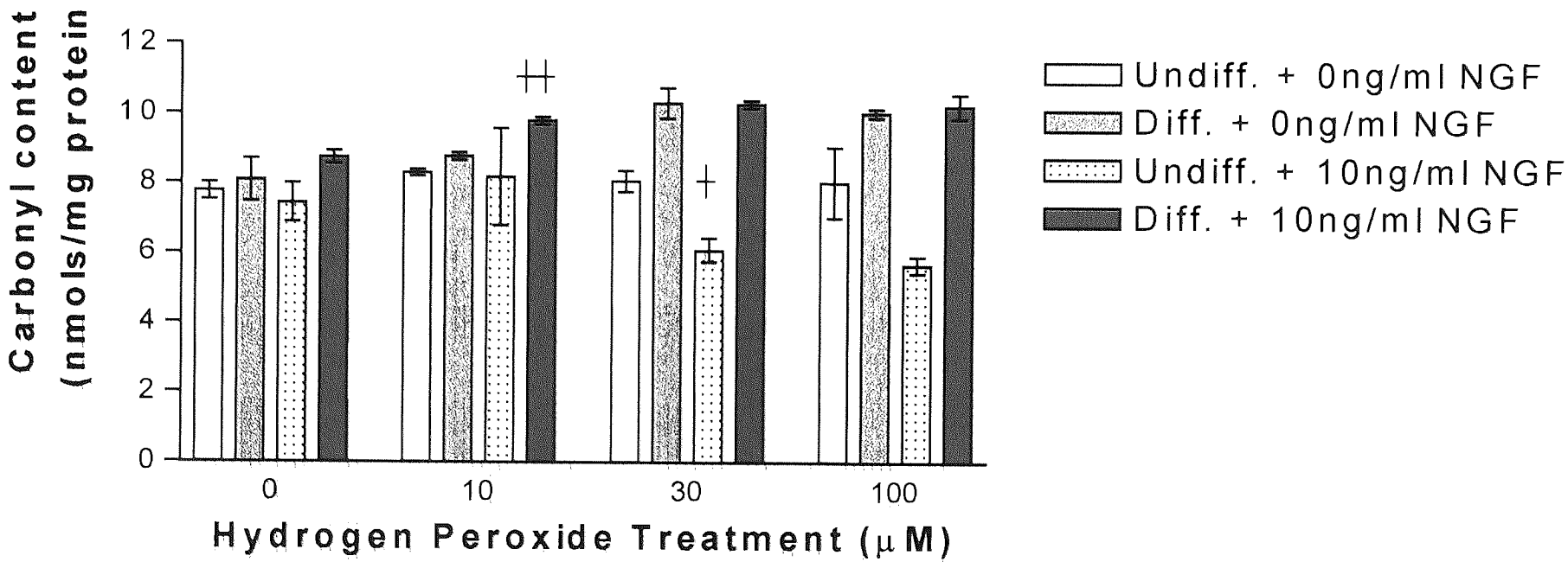

Figure 4.21 The effects of nerve growth factor (NGF) on hydrogen peroxide toxicity in differentiated and undifferentiated controls on protein carbonyl levels. SY5Y cells ($2x10^5$) were incubated with NGF (10ng/ml) at 37°C, 5%CO_2 for 24 hours. H_2O_2 (10, 30 and 100μM) was then added at 37°C, 5%CO_2 for 24 hours. Cells were then harvested and prepared for a carbonyl ELISA as state in method 2.2.7. Figure shows the mean carbonyl content ± SEM for 6 replicates. ┼ represents $P<0.05$, ┼┼ represents $P<0.01$ (Unpaired t-tests) when compared to the same treatment in the absence of NGF.

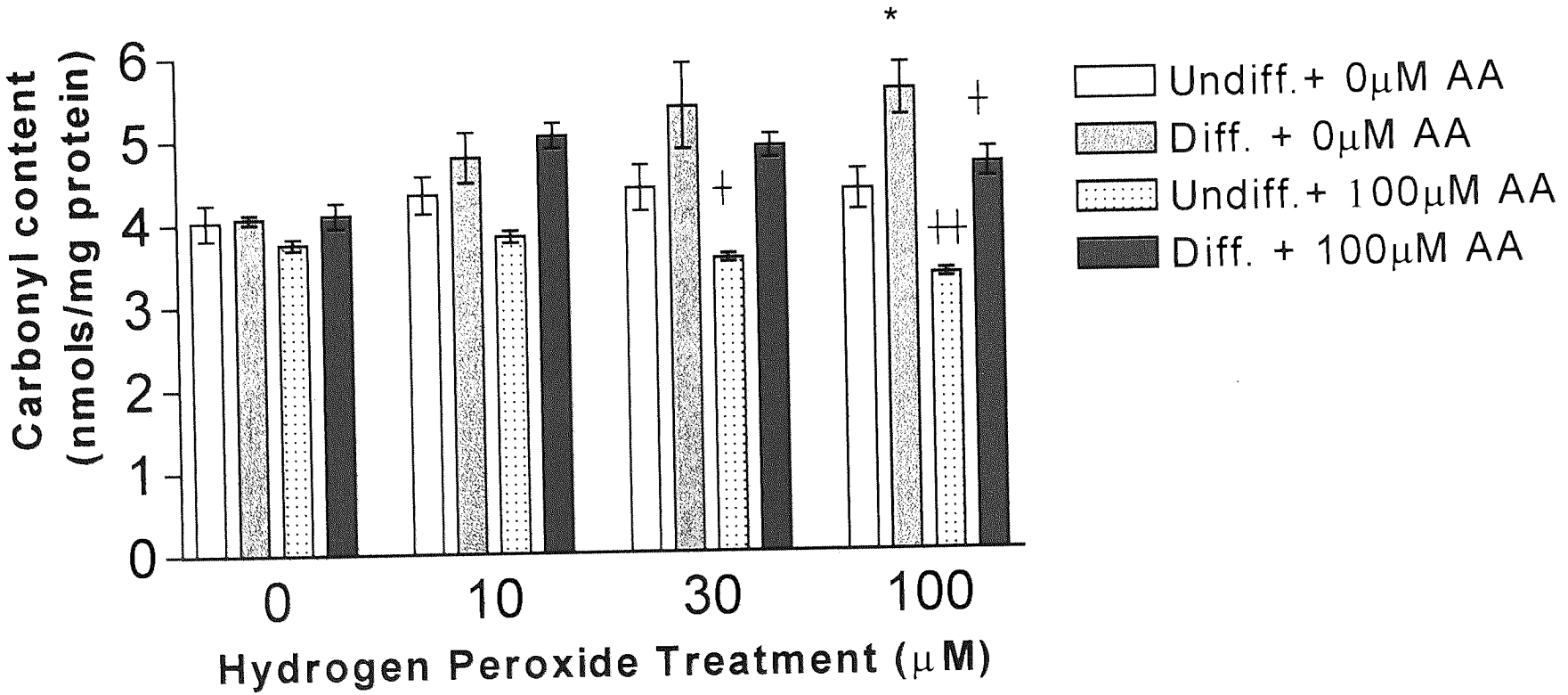

Figure 4.22 The effects of ascorbic acid (AA) on hydrogen peroxide toxicity in differentiated and undifferentiated controls on protein carbonyl levels. SY5Y cells ($2x10^5$) were incubated with AA (100μM) at 37°C, 5%CO_2 for 24 hours. H_2O_2 (10, 30 and 100μM) was then added at 37°C, 5%CO_2 for 24 hours. Cells were then harvested and prepared for a carbonyl ELISA as state in method 2.2.7. Figure shows the mean carbonyl content ± SEM for 6 replicates. * represents $P<0.05$ (Unpaired t-test) when compared to same treatment in undifferentiated cells. + represents $P<0.05$, ++ represents $P<0.01$ when compared to the same treatment in the absence of AA in the same cell type.

those who had undergone AA pre-treatment (P=0.0128 and P=0.0023 respectively, n=6, unpaired t-tests).

In differentiated cells significant reductions were seen at 100μM H_2O_2 in carbonyl levels when comparing untreated cells to those that had undergone AA pre-treatment (P=0.0316, n=6, unpaired t-test).

4.2.4.5 Effect of brain derived neurotrophic factor on hydrogen peroxide toxicity on protein carbonyl levels

The effects of BDNF on H_2O_2 toxicity in both undifferentiated cells and differentiated cells were investigated by measuring protein carbonyls. Figure 4.23 shows that increases in carbonyl levels were observed with increasing H_2O_2 in both cell types. Differences between the two cell types were recorded with differentiated untreated cells having higher carbonyl levels than undifferentiated cells in the absence of BDNF. Differentiated cells showed significantly greater protein carbonyls in the absence of peroxide (P=0.0255, unpaired t-test, n=6), this is in contrast to figure 4.19 where differentiated cells were shown to have lower carbonyl levels, than undifferentiated cells, however, cells had been in culture for 24 hours longer during BDNF pre-treatment.

The effects of BDNF on protein carbonyl induction at each H_2O_2 concentration in each cell type were compared. At 100μM H_2O_2, a significant increase in protein carbonyl levels recorded in the presence of 10ng/ml BDNF ($P<0.05$, Dunnett's test, n=6).

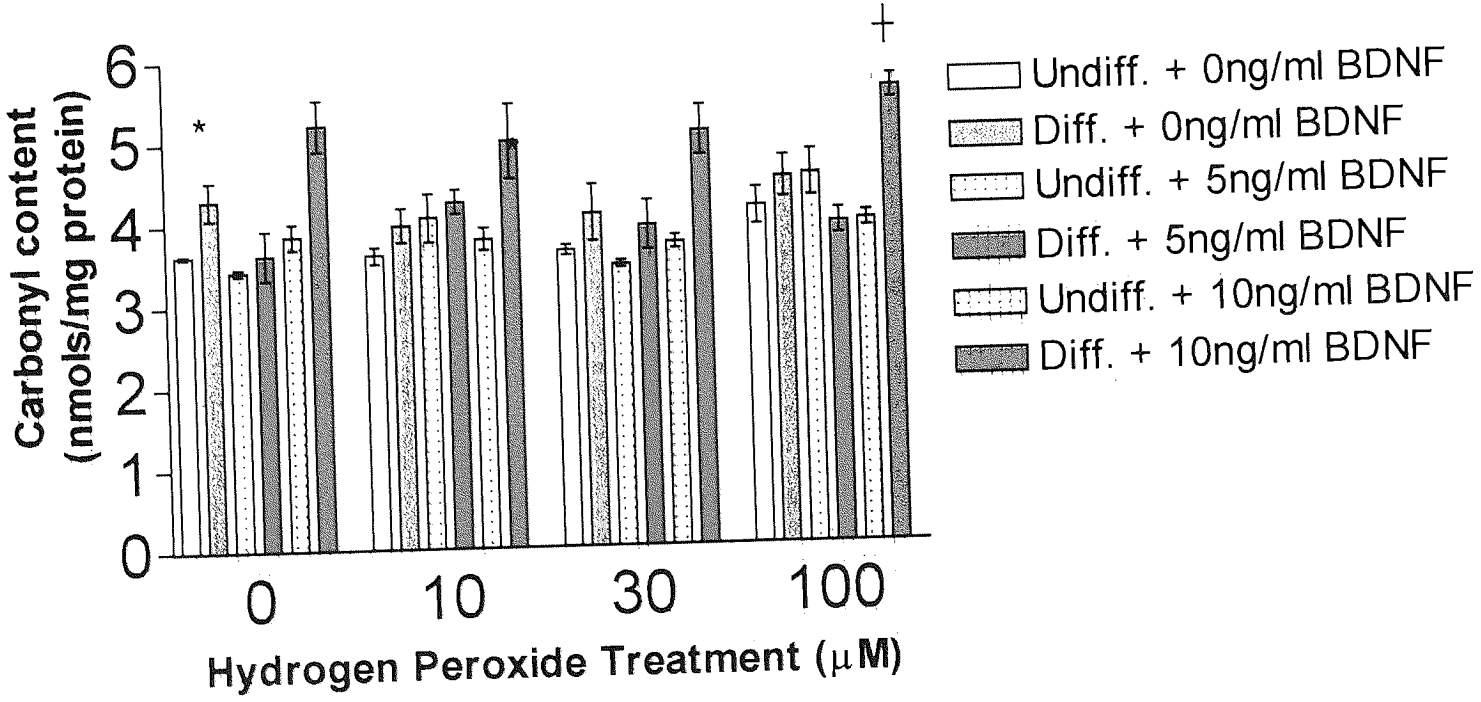

Figure 4.23 The effects of brain derived neurotrophic factor (BDNF) on hydrogen peroxide toxicity in differentiated and undifferentiated controls as assessed by protein carbonyl levels. SY5Y cells ($2x10^5$) were incubated with BDNF (5 and 10ng/ml) at 37°C, 5%CO_2 for 24 hours. H_2O_2 (10, 30 and 100μM) was then added at 37°C, 5%CO_2 for 24 hours. Cells were then harvested and prepared for a carbonyl ELISA as state in method 2.2.7. The figure shows the mean carbonyl content ± SEM for 6 replicates. * represents $P<0.05$ (Unpaired t-test, two tail) when compared to the same treatment in undifferentiated cells. + represents $P<0.05$ (Dunnett's test) when compared to the same treatment in the absence of BDNF in the identical cell type.

4.3 ASCORBIC ACID UPTAKE STUDIES

4.3.1 Uptake of ^{14}C labelled ascorbic acid in PC12 and SY5Y cells

To investigate the actions of AA, uptake studies were conducted, to help to interpret the changes recorded in protein carbonyl levels. Experiments were set up as stated in section 2.2.10.2 incubating radio labelled AA with PC12 and SY5Y cells and harvesting after 4 and 24 hours of treatment. The counts per minute recorded for each sample were equated to the concentration of ^{14}C-ascorbic acid taken up using a standard curve constructed of standards containing known concentrations of radio labelled AA, as shown in figure 4.24.

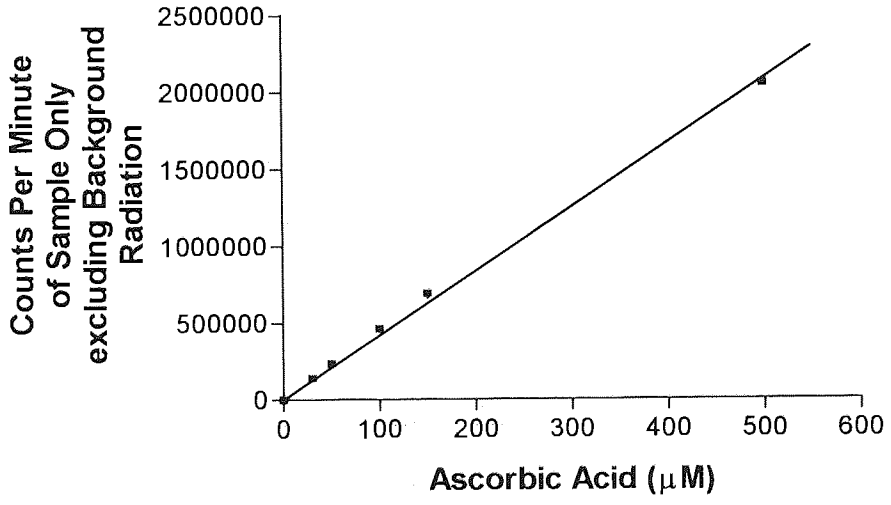

Figure 4.24 Standard curve of radio labelled ascorbic acid standards used to equate the unknown samples to a concentration of AA taken up. Figure shows mean corrected count per minute ± SEM for 3 replicates.

The equivalent concentration of ^{14}C radio labelled AA was found for each cell type as shown in figure 4.25.

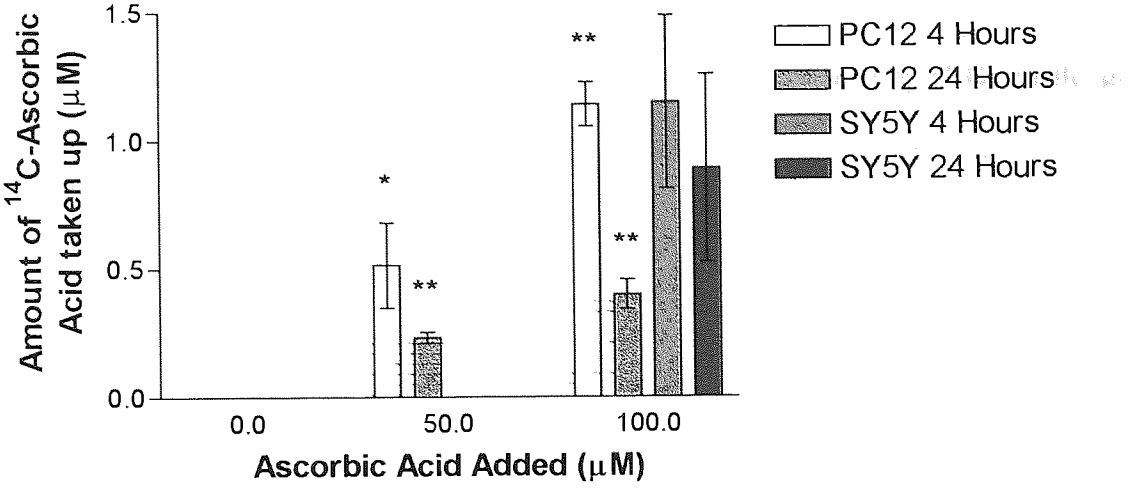

Figure 4.25 The uptake of radio labelled ascorbic acid in PC12 and SY5Y cells over 24 hours. PC12 and SY5Y cells ($2x10^5$) were incubated with ascorbic acid (50 and 100μM) at 37°C, 5%CO_2 for 4 and 24 hours. Cells were then harvested and prepared for scintillation counting as stated in method 2.2.10.2. Figure shows the mean concentration of ^{14}C-ascorbic acid taken up ± SEM for 3 replicates. * represents P<0.05, ** represents P<0.01.

Figure 4.25 shows for PC12 cells, dose dependent uptake of AA at both 4 and 24 hours. Less AA was evident in cells 24 hours after dosing than 4 hours. Results show significant differences between AA treatments at both 4 hours (P=0.0009, n=3, single factor ANOVA), and 24 hours (P=0.0006, n=3, single factor ANOVA).

For SY5Y cells, lower uptake of AA was observed after 24 hours compared to 4 hours, however results were not significant at both time points according to unpaired t-tests, two tailed.

4.4 DISCUSSION

The data presented here has shown that in situations of OS induced by H_2O_2 challenge, protein carbonyl levels increase in both PC12 and undifferentiated and differentiated SY5Y cells. Initial data also showed a general trend that $A\beta_{25-35}$ also increases protein carbonyl levels as tested in PC12 cells. This data goes towards agreeing with the results of Yatin *et al.*, (1999a), who have shown $A\beta_{25-35}$ to cause increases in carbonyls three times that of controls in neuronal proteins isolated from human AD brains. Aksenov *et al.*, (2001) have also shown significant increases in human AD brains in protein carbonyl levels of β-actin (442±23% of control, $P<0.01$) and in creatine kinase BB (CKBB) (336±24% of control, $P<0.01$). However they showed that these individual brain proteins, which were identified as targets of protein carbonyl formation in AD, were not neuronal specific. In addition, they could not demonstrate that excessively carbonylated β-actin was present only in oxidative stressed neurons. They suggested that the OS-induced injury might involve selective modification of different intracellular proteins, including key enzymes and structural proteins, which precedes and may lead to the neurofibrillary degeneration of neurons in the AD brain. This requires further investigation, and may yield improved sensitivity over measurements of global protein damage.

Neurotrophins were employed to investigate their effect on carbonyl formation after peroxide challenge. It could be proposed that NGF may increase cell number in its 24 hours incubation with unchallenged cells. Therefore, experiments were set up to assay cell number after pre-incubation and NGF was shown to decrease cell numbers, and thereby cells may actually have been exposed to more toxic agent per cell rather than less. With NGF no significant effects were recorded against peroxide challenge in both

PC12 and undifferentiated SY5Y cells. BDNF was also employed against differentiated SY5Y cells, these experiments showed that BDNF caused a significant increase in carbonyl levels against peroxide challenge.

Ascorbate was only found to protect against protein carbonyl formation in undifferentiated and differentiated SY5Y cells after 24 hours of AA pre-treatment at 50 and 100μM. Vitamin pre-treatment has previously been shown to reduce carbonyl formation, however it was using the lipid soluble antioxidant vitamin E and not AA. It was shown to protect against carbonyl formation following Aβ challenge in rat embryonic neuronal proteins, decreasing the effect of Aβ from an increase of 3 times to an increase of 1.4 times (Yatin *et al.*, 1999b).

^{14}C labelled ascorbic acid studies showed greater uptake after 4 hours at both 50 and 100μM AA in PC12 cells than at 24 hours. This suggests that the AA in the PC12 cultures has been converted to DHA/ metabolised. Whereas in SY5Y cultures there were no significant differences in AA uptake at 4 and 24 hours suggesting that SY5Y cells do not metabolise AA as efficiently as PC12 cells. This data along with the protein carbonyl values recorded suggest than in SY5Y cells, AA acts mainly extracellularly, directly detoxifying the ROS present in the culture. As the AA is working directly on the ROS it therefore reduces their effects quickly causing little effect of ROS. For PC12 cells the data suggests that AA may act intracellularly, that there is a more efficient metabolism, which does not cause the reductions in carbonyls that are seen in SY5Y cells.

CHAPTER FIVE

ALTERATIONS IN GLUTATHIONE LEVELS

5. GLUTATHIONE

Glutathione is qualitatively the most important AOX and free radical scavenger present in cells (Valencia *et al.*, 2001). Glutathione-associated metabolism is a major mechanism for cellular protection against agents which generate OS, it has become increasingly apparent that within the glutathione detoxification system, as shown in figure 1.19b, there is a substantial inter-dependence between separate component members. Glutathione participates in detoxification at several different levels, and may scavenge ROS, reduce peroxides, or be conjugated with electrophilic compounds. Thus, glutathione provides the cell with multiple defences not only against ROS but also against their toxic products. It is involved in the ultimate removal of detoxified oxidation products from the cell. Most importantly, many of the glutathione-dependent proteins are inducible and therefore represent a means whereby cells can adapt to OS (Hayes & McLellan, 1999). Glutathione is further reviewed in section 1.11.

In situations of increasing OS generated either by H_2O_2 or Aβ, it is expected that there would be a greater GSH to GSSG conversion by GPX. The increased H_2O_2 exposure would then subsequently cause the cell to require more GSH to detoxify the ROS, thus causing an up regulation of GSH production. It has been shown previously that following addition of cytotoxic agents, and at the time of onset of apoptosis caused by other agents, GSH levels decrease (van den Dobbelsteen *et al.*, 1996; Froissard & Duval, 1994). However GSH levels have also been shown to decrease in culture, therefore the effects of agents on cellular GSH levels were investigated 4 hours after seeding (Reiners Jr *et al.*, 2000).

Glutathione (reduced and oxidised) levels were determined using a modified microtitre plate method (Punchard *et al.*, 1994). Actual glutathione levels were calculated by equating the changes in absorbance over time alongside standards of known GSH concentrations included on each plate. Figure 5.1 shows a representative standard curve of glutathione standards used to equate the changes in absorbance to actual glutathione values.

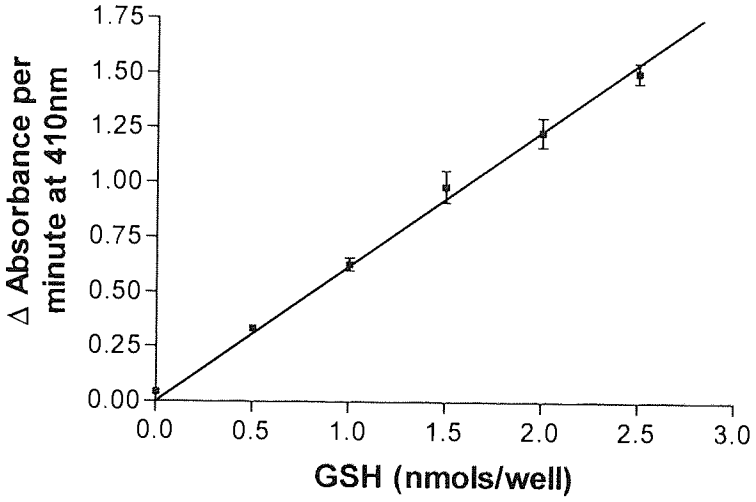

Figure 5.1 Representative glutathione standard curve

To allow comparisons of data from individual experiments, protein concentrations were also measured from another aliquot of the same cell pellet, hence all values are expressed as nmols/mg protein.

5.1 PC12 CELLS

5.1.1 Effect of hydrogen peroxide on glutathione levels

The effects of H_2O_2 on glutathione levels in PC12 cells were investigated. Figure 5.2 shows the effect of increasing the time of incubation with H_2O_2. Levels of GSH were generally higher in H_2O_2 challenged cells compared to those treated with PBS. After 24 hours there was a significant 190.6% increase in glutathione levels comparing 132μM H_2O_2 to control, $P<0.01$ (Dunnett's test). Oxidised glutathione levels were also seen to increase with increasing H_2O_2 concentration.

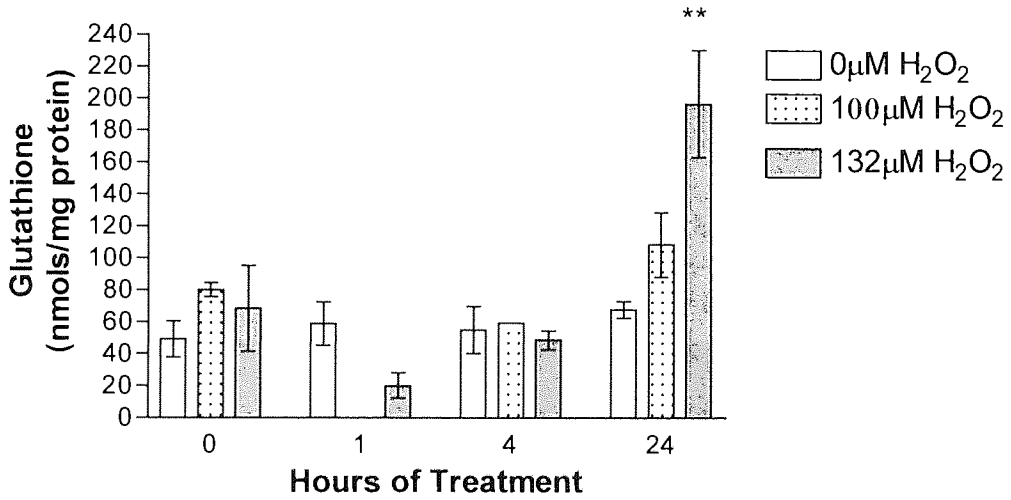

Figure 5.2 Time course of hydrogen peroxide action on glutathione levels in PC12 cells. PC12 cells ($2x10^5$) were incubated with H_2O_2 (100 and 132μM) for 0-24 hours at 37°C, 5%CO_2. Figure shows the mean glutathione value ± SEM of 9 replicates. ** represents $P<0.01$ (Dunnett's test) compared to appropriate control at 0 hours.

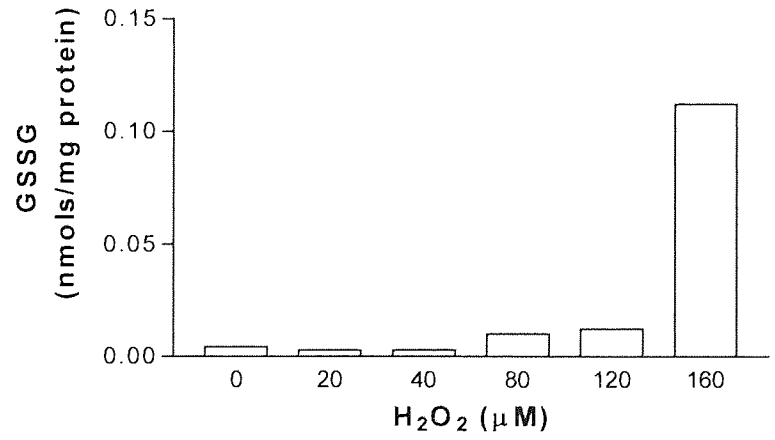

Figure 5.3 Effects of hydrogen peroxide on glutathione (oxidised) levels in PC12 cells. PC12 cells (2x105) were incubated with H_2O_2 (0-160μM) for 24 hours at 37°C, 5% CO_2. Figure shows a representative example.

5.1.2 Effect of amyloid β peptide (fragment 25-35) on glutathione levels

The effects of increasing concentrations of $A\beta_{25-35}$ were investigated using PC12 cells. Figure 5.4 shows no significant effects of Aβ, at any dose or time examined.

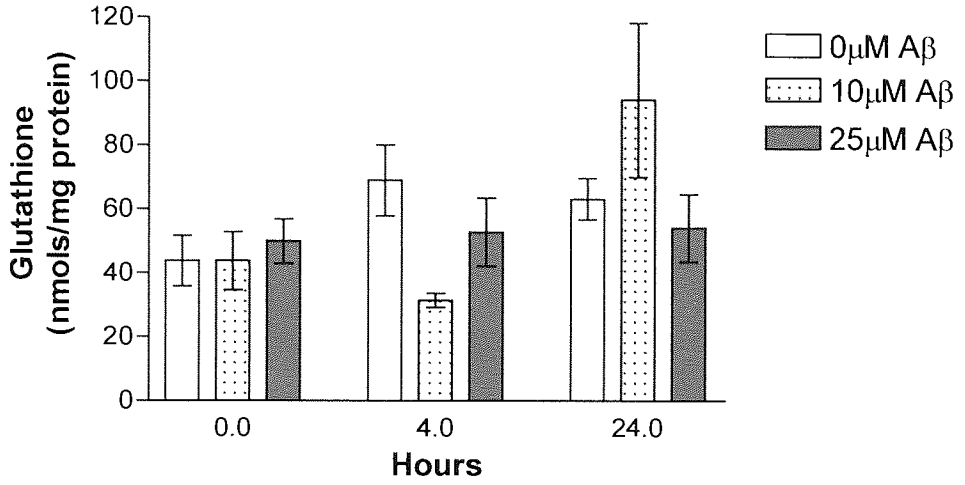

Figure 5.4 The effects of amyloid β peptide on glutathione levels in PC12 cells. PC12 cells ($2x10^5$) were incubated with $A\beta_{25-35}$ (10 and 25μM) for 0-24 hours at 37°C, 5% CO_2. Figure shows the mean glutathione value ± SEM of at least 4 replicates. No significant effects were recorded versus 0μM Aβ at each time point.

5.1.3 Effect of nerve growth factor on glutathione levels

The effects of NGF (5 and 10ng/ml) on levels of glutathione were investigated. Figure 5.5 shows both NGF concentrations caused no-significant decreases in GSH in unchallenged PC12 cells after 24 hours, when analysed with a single factor ANOVA.

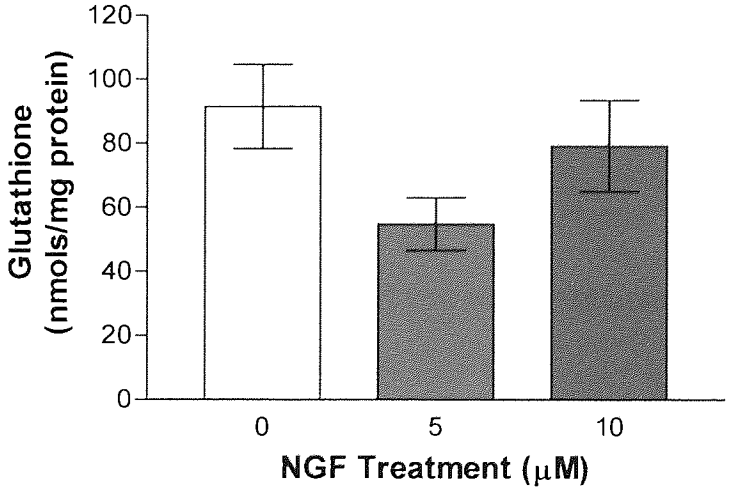

Figure 5.5 The effects of nerve growth factor on glutathione levels in PC12 cells. PC12 cells ($2x10^5$) were incubated with NGF (5 and 10ng/ml) for 24 hours at 37°C, 5% CO_2. Figure shows the mean glutathione value ± SEM of at least 8 replicates.

The effects of NGF (10ng/ml) were further investigated over time, figure 5.6 shows that in the early stages of NGF incubation up to 4 hours NGF caused no significant changes.

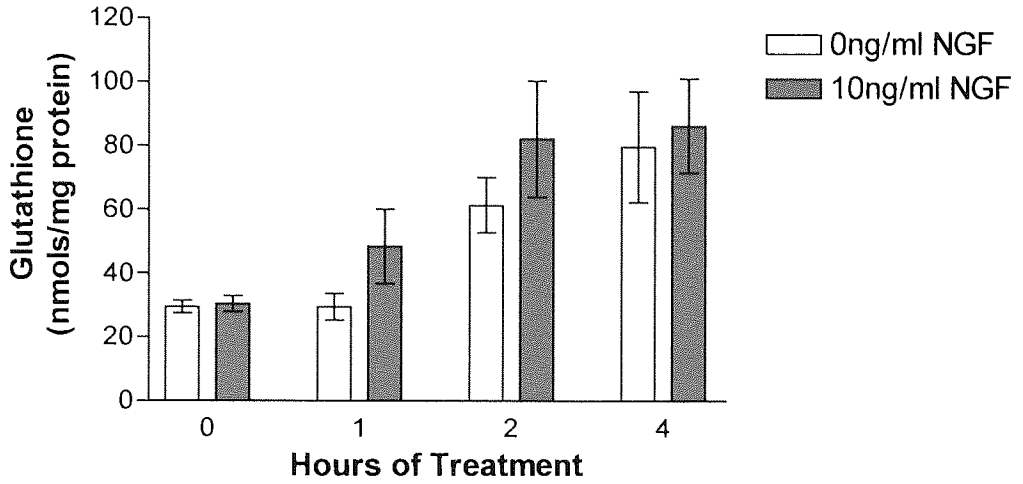

Figure 5.6 The effects of nerve growth factor on glutathione levels in PC12 cells. PC12 cells ($2x10^5$) were incubated with NGF (10ng/ml) for 0-24 hours at 37°C, 5% CO_2. Figure shows the mean glutathione value ± SEM of 6 replicates, there are no significant differences as assessed by a single factor ANOVA.

5.1.3.1 Effect of nerve growth factor on the actions of hydrogen peroxide on glutathione levels

The effects of 24 hours of pre-treatment with NGF (5 and 10ng/ml) on changes in glutathione levels produced by increasing concentrations of H_2O_2 were assessed. Figure 5.7 shows that treatment with 5ng/ml NGF caused a general increasing trend in glutathione levels at all H_2O_2 concentrations compared to control cells except at 50μM (not significant). However, treatment with 10ng/ml NGF caused a non-significant decreasing trend in glutathione levels at all H_2O_2 concentrations compared to control cells .

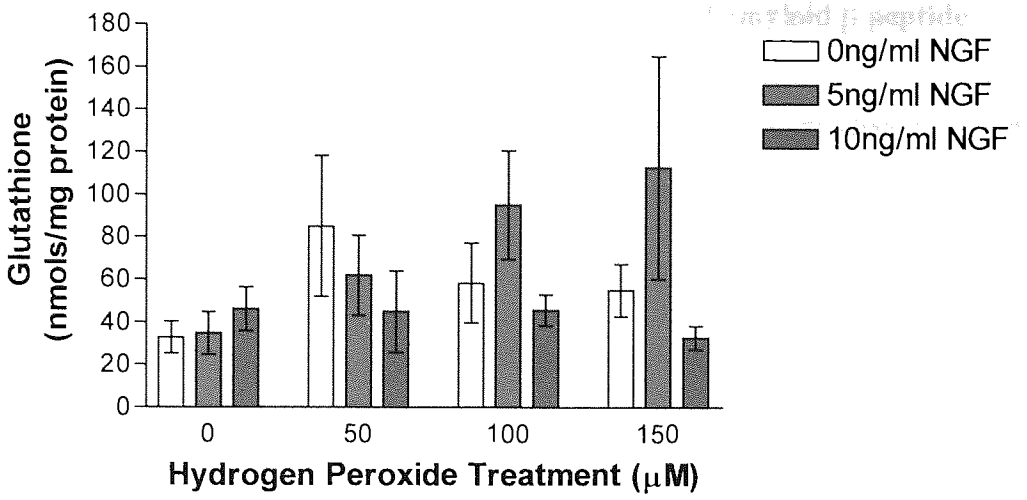

Figure 5.7 The effects of nerve growth factor on the action of hydrogen peroxide on glutathione levels in PC12 cells. PC12 cells ($2x10^5$) were incubated with NGF (5 and 10ng/ml) for 24 hours at 37°C, 5%CO_2 before addition of H_2O_2 (50, 100, 150μM) at 37°C, 5% CO for 24 hours. Figure shows the mean glutathione value ± SEM of 3 investigations.

GSSG levels were also measured. Figure 5.8 shows that with increasing H_2O_2 concentrations GSSG levels increased. However, none of the differences were significant (single factor ANOVA) compared to non-NGF treated cells.

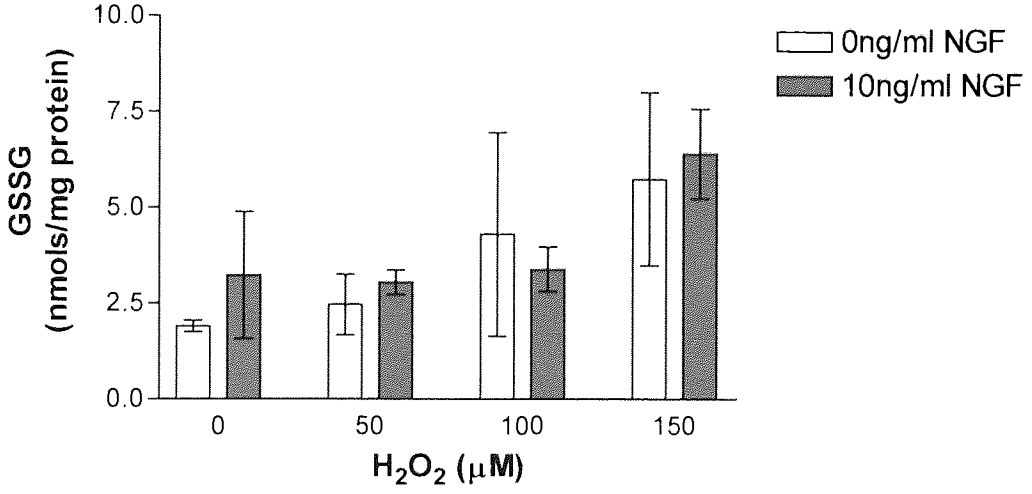

Figure 5.8 The effects of nerve growth factor pre-treatment on the action of hydrogen peroxide on glutathione levels (oxidised) in PC12 cells. PC12 cells ($2x10^5$) were incubated with NGF (10ng/ml) for 24 hours at 37°C, 5% CO_2 before the addition of H_2O_2 (50, 100 and 150μM) at 37°C, 5% CO2. Figures shows the mean GSSG value ± SEM of 3 investigations.

5.1.3.2 Effect of nerve growth factor on the action of amyloid β peptide (fragment 25-35) on glutathione levels

The effects of NGF on changes in glutathione levels produced by increasing concentrations of Aβ peptide were assessed using cells pre-treated with NGF (10ng/ml) for 24 hours before the addition of Aβ. In general, results show that the effects of Aβ on glutathione levels to not be dose related, and a unconvincing effect of NGF. Figure 5.9 shows NGF pre-treatment caused reductions in all glutathione levels compared to untreated cells. Levels were compared statistically at each Aβ treatment and time point, with unpaired t-tests comparing levels recorded in the presence and absence of NGF. At 0 hours there were no significant reductions. After 24 hours of Aβ challenge NGF pre-treatment significantly reduced glutathione levels in 10μM Aβ challenged cells (P=0.0493, unpaired t-test).

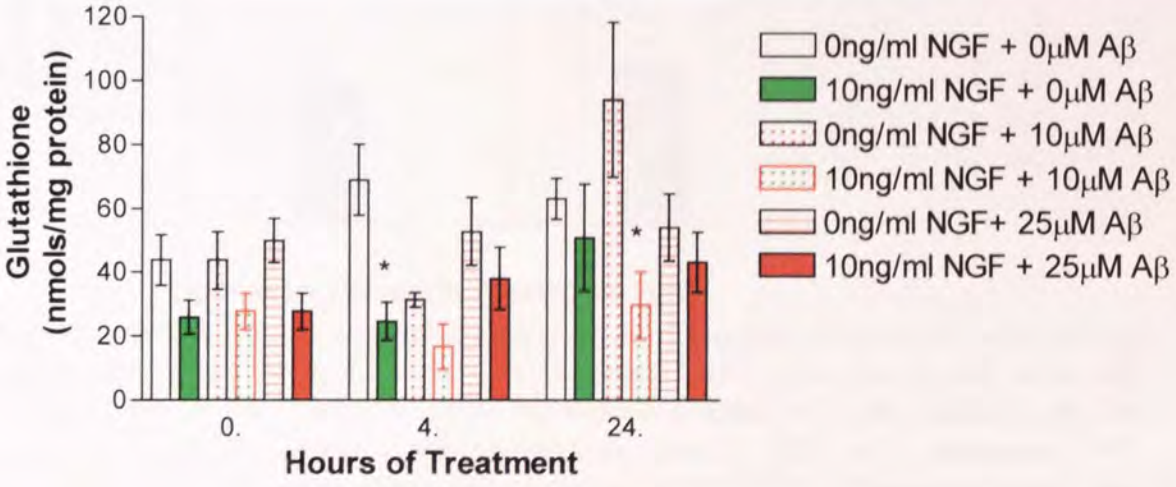

Figure 5.9 The effects of nerve growth factor on amyloid β peptide action on glutathione levels in PC12 cells. PC12 cells ($2x10^5$) were incubated with NGF (5ng/ml) for 24 hours at 37°C, 5% CO_2 before incubation with $A\beta_{25-35}$ (10 and 25μM) for 0-24 hours at 37°C, 5% CO_2. Figure shows the mean glutathione value ± SEM of at least 3 investigations. * represents P<0.05 (Unpaired t-test)

5.1.4 Effect of ascorbic acid on the action of hydrogen peroxide on glutathione levels

The effects of AA on the changes in glutathione levels produced by increasing concentrations of H_2O_2 were assessed using cells pre-treated with AA (100μM) versus control for 24 hours before the addition of H_2O_2. Figure 5.10 shows significant increases in glutathione levels with increasing H_2O_2 dose in non AA pre-treated cells (P=0.0005, Unpaired t-test). No significant changes were recorded in AA pre-treated cells. Only H_2O_2 challenge in non-AA pre-treated cells caused glutathione levels to increase. AA pre-treatment of cells caused a significant decrease in GSH compared to no pre-treatment at 150μM H_2O_2 (P=0.0045, unpaired t-test).

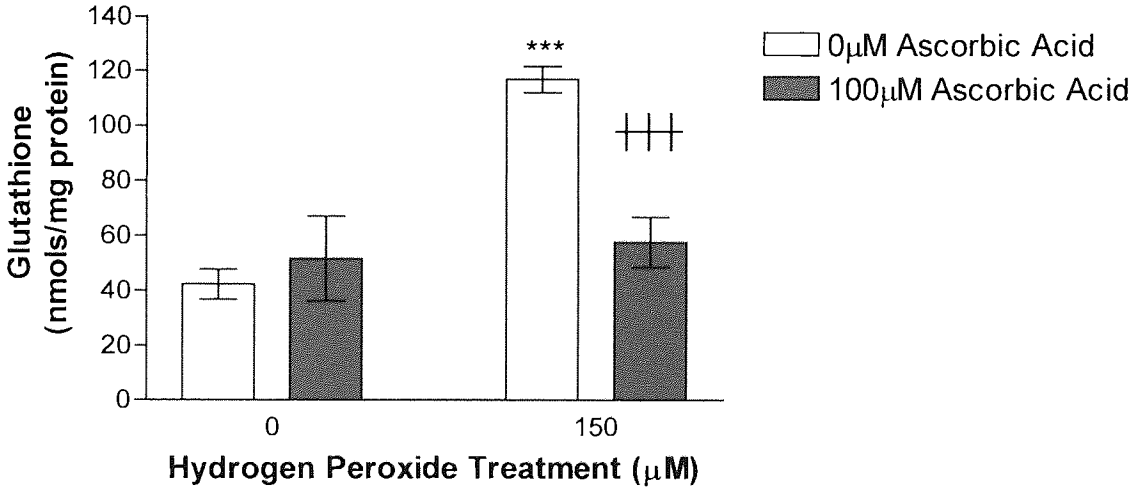

Figure 5.10 The effects of ascorbic acid (AA) on the action of hydrogen peroxide on glutathione levels in PC12 cells. PC12 cells ($2x10^5$) were incubated with AA (100μM) for 24 hours at 37°C, 5%CO_2 before addition of H_2O_2 (150μM) for 24 hours. Figure shows the mean glutathione value ± SEM of 3 replicates. * represents P<0.005 when compared to levels at 0μM H_2O_2 (Unpaired t-test, two tailed, n=3). +++ represents P<0.005 when glutathione levels were compared at 150μM H_2O_2 to each AA pre-treatment (Unpaired t-test, two tailed, n=6 replicates)**

5.1.4.1 Effect of ascorbic acid (washed out) on the action of hydrogen peroxide on glutathione levels

The effects of AA on changes in glutathione levels produced by increasing concentrations of H_2O_2 were assessed using cells pre-treated with 100μM AA versus

control for 24 hours which was subsequently washed out before the addition of H_2O_2. Figure 5.11 shows significant increases in glutathione levels with increasing H_2O_2 dose in untreated cells (P=0.0271, Unpaired t-test) as shown previously in figure 5.10. However no significant effects on oxidant induced changes in GSH levels by AA were observed.

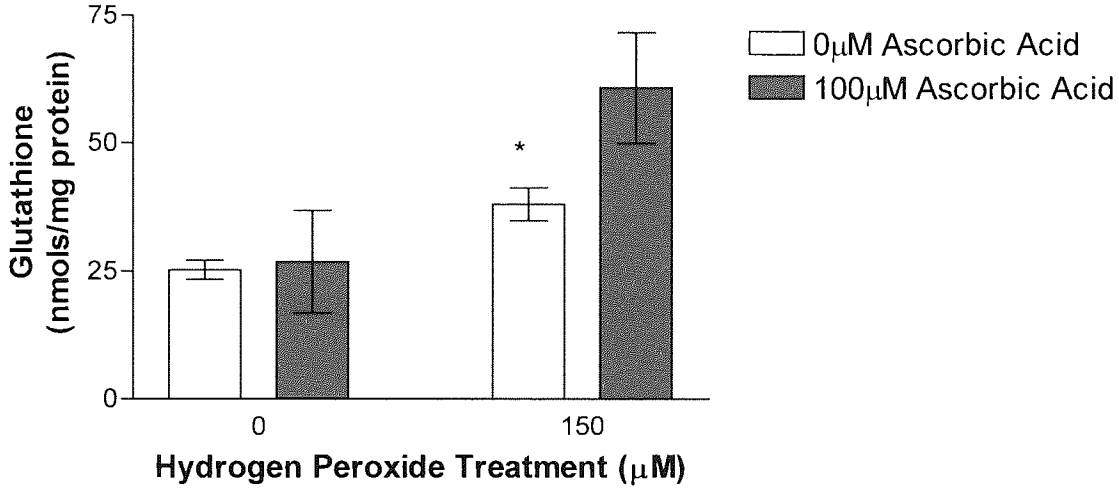

Figure 5.11 The effects of ascorbic acid (AA) on the action of hydrogen peroxide on glutathione levels in PC12 cells. PC12 cells ($2x10^5$) were incubated with AA (100μM) for 24 hours at 37°C, 5% CO_2 before medium was replaced and H_2O_2 (150μM) added for 24 hours. Figure shows the mean glutathione value ± SEM of 3 replicates. * represents P<0.05 versus levels recorded at 0μM H_2O_2, 0μM AA (Unpaired t-test).

5.2 SY5Y CELLS

5.2.1 Effect of hydrogen peroxide on glutathione levels

The effects of H_2O_2 on glutathione levels in SY5Y cells were investigated. Figure 5.12 shows that after 4 hours GSH levels decrease, which are then restored after 24 hours of treatment. However none of the changes recorded were significantly different to those recorded in control treated cells.

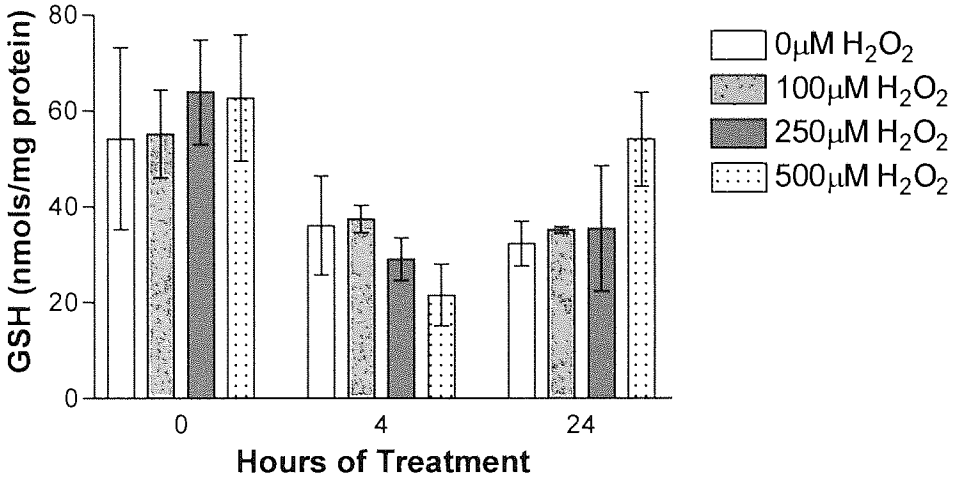

Figure 5.12 Time course of hydrogen peroxide action on glutathione levels in SY5Y cells. SY5Y cells ($2x10^5$) were incubated with H_2O_2 (100, 250 and 500μM) for 0-24 hours at 37°C, 5%CO_2. Figure shows the mean glutathione value ± SEM of 3 replicates.

5.2.2 Effect of ascorbic acid on hydrogen peroxide action on glutathione levels

The effects of AA (50 and 100μM) on changes in glutathione levels produced by increasing concentrations of H_2O_2 were assessed.

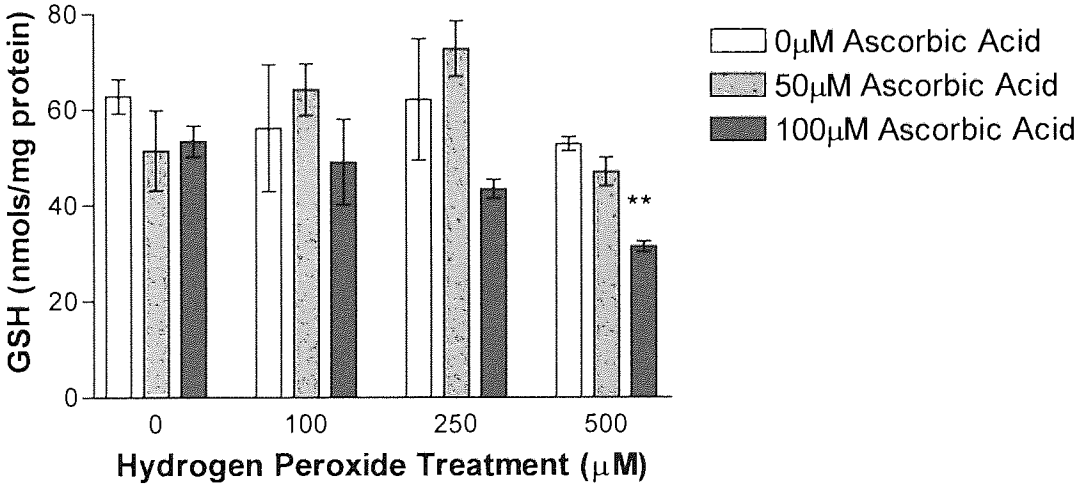

Figure 5.13 The effects of ascorbic acid (AA) on the action of hydrogen peroxide on glutathione levels in SY5Y cells. SY5Y cells ($2x10^5$) were incubated with AA (50 and 100μM) for 24 hours at 37°C, 5%CO_2 before addition of H_2O_2 (10, 250, 500μM) at 37°C, 5%CO_2. Figure shows the mean glutathione value ± SEM of 3 replicates. ** represents P<0.01 (Dunnett's test) when compared to values recorded at same H_2O_2 concentration and 0μM AA.

Figure 5.13 showed 100μM AA caused dose dependent decreases in glutathione levels when compared to control, where the decrease recorded at 500μM H_2O_2 was significant compared to 0μM AA treated cells (0.0023, n=3, Dunnett's test). However, a point to note is that in this experiment no effect of peroxide on GSH levels were observed.

5.3 DIFFERENTIATED SY5Y CELLS

5.3.1 Effect of nerve growth factor on the actions of hydrogen peroxide

The effects of NGF (10ng/ml) on changes in GSH levels produced by increasing concentrations of H_2O_2 were assessed, using cells pre-treated with NGF versus controls for 24 hours before the addition of H_2O_2. Figure 5.14 shows undifferentiated cells treated with NGF showed a general trend of increasing levels, which were significantly higher at 0 and 10μM H_2O_2 (P=0.0022 and P=0.0061, unpaired t-test) compared to non-NGF treated controls. The reverse was recorded in differentiated cells, results showed differentiated cells treated with NGF had generally lower GSH values, which were significantly lower at 100μM H_2O_2 (P=0.0051, unpaired t-test) compared to non-NGF treated controls.

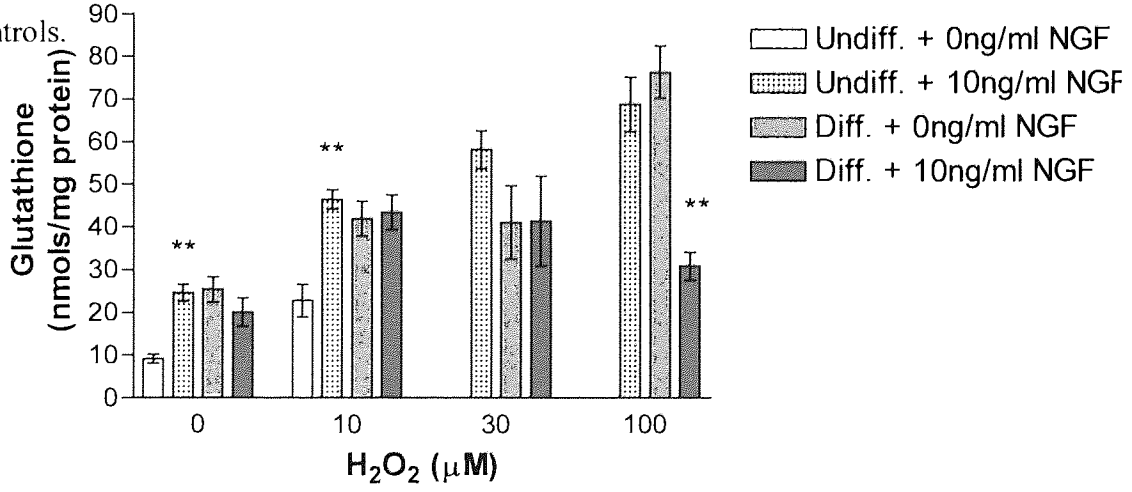

Figure 5.14 The effects of nerve growth factor on the action of hydrogen peroxide on glutathione levels in SY5Y cells. SY5Y cells ($2x10^5$) were incubated with NGF (10ng/ml) for 24 hours at 37°C, 5%CO_2 before addition of H_2O_2 (10, 30, 100μM) at 37°C, 5%CO_2. Figure shows the mean glutathione value ± SEM of 3 replicates. ** represents P<0.01 (Unpaired t-test) when compared to respective control at same H_2O_2 concentration and no NGF pre-treatment in same cell type.

5.3.2 Effect of brain derived neurotrophic factor on the actions of hydrogen peroxide

The effects of BDNF (5ng/ml) on levels of glutathione (reduced and oxidised) were investigated. Figure 5.15 shows the effect of BDNF on reduced glutathione levels and figure 5.16 shows the effect of BDNF on oxidised glutathione levels, where increases in glutathione occurred in both cell types. Lower basal levels were recorded in differentiated cells, and in differentiated cells treated with BDNF there were an increasing trend in glutathione levels. However, changes were apparent in undifferentiated BDNF treated cells and untreated differentiated cells. Oxidised glutathione levels showed relatively little changes with there being no significant differences between BDNF treated and untreated cells of the same type.

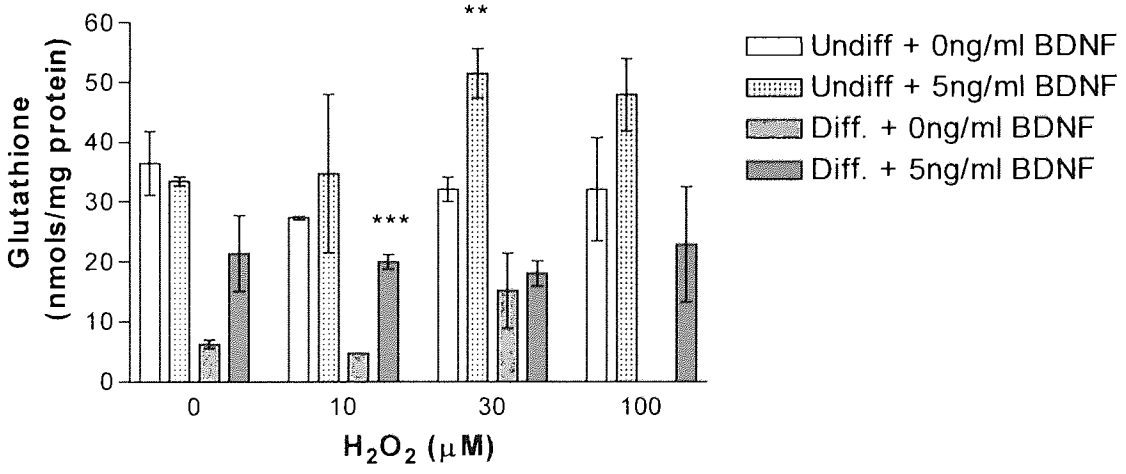

Figure 5.15 Effects of brain derived neurotrophic growth factor on the action of hydrogen peroxide on glutathione levels in SY5Y cells. SY5Y cells ($2x10^5$) were incubated with BDNF (10ng/ml) for 24 hours at 37°C, 5%CO_2 before addition of H_2O_2 (10, 30, 100μM) at 37°C, 5%CO_2. Figure shows the mean glutathione value ± SEM of 3 replicates. **represents P<0.01, ***represents P<0.001 when compared to same cell type at each H_2O_2 concentration, (Unpaired t-test).

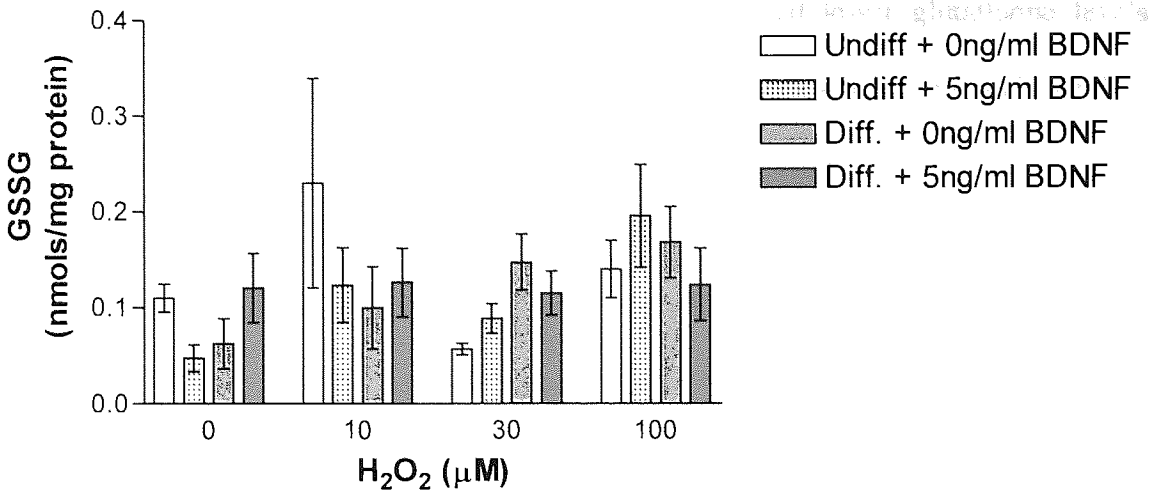

Figure 5.16 Effects of brain derived neurotrophic growth factor on the action of hydrogen peroxide on glutathione levels in SY5Y cells. SY5Y cells ($2x10^5$) were incubated with BDNF (10ng/ml) for 24 hours at 37°C, 5%CO_2 before addition of H_2O_2 (10, 30, 100μM) at 37°C, 5%CO_2. Figure shows the mean GSSG value ± SEM of 3 replicates.

5.4 Discussion

Froissard *et al.*, (1997) have stated that there is strong evidence to support the existence of a close relationship between the level of intracellular glutathione and cell survival in PC12 cells. Seyfried *et al.*, (1999) have also shown that mitochondrial GSH is critical for the maintenance of mitochondrial function and cellular viability.

Glutathione levels were shown to increase with increasing H_2O_2 concentrations in both PC12 and differentiated SY5Y cells after 24 hours. Aβ showed no little evidence for this response with levels only increasing slightly but not significantly. NGF was also shown not to cause any significant changes in GSH levels of unchallenged cells; this is in agreement with Kamata *et al.*, (1996) who showed NGF to protect cells from OS independently of GSH. However under H_2O_2 challenge, NGF in PC12 cells (5ng/ml) was shown to increase levels of GSH versus control, with NGF (10ng/ml) causing lower levels of glutathione versus control. This was consistent with differentiated cells, where 10ng/ml NGF pre-treatment caused lower levels of glutathione versus control. NGF

pre-treatment against Aβ challenge (10ng/ml) also caused lower glutathione levels compared to controls. The data recorded with 5ng/ml NGF is consistent with the data previously published by Pan & Perez-Polo (1993) and Sampath *et al.*, (1994) who have both shown NGF to cause increases in GSH levels. Pan & Perez-Polo (1993) have reported basal GSH levels of approximately 14 nmols GSH/mg protein for PC12 cells and approximately 27 nmols GSH/mg protein for SY5Y cells. Using the employed assay, GSH levels of approximately 12 nmols GSH/ mg protein for PC12 cells and approximately 35 nmols/mg protein for SY5Y cells were achieved. This shows the work conducted is comparable to the work of others, however it has been noted by many workers that the assay is susceptible to changes, therefore each assay was conducted under strict conditions. Glutathione values did vary slightly from assay to assay, as shown by the slightly higher basal values on the included graphs, however an assessment was always made of the glutathione standard to reduce the risk of anomalous values and to ensure data from different data sets of the same investigation was comparable.

Interestingly, 10-15% of the total level of intracellular GSH is localised to mitochondria, and depletion of mitochondrial GSH have been shown to cause an increase in sensitivity to killing by specific agents, which stimulates mitochondrial ROS production by inhibiting the ETC (Garcia-Ruiz *et al.*, 1995). Furthermore, whether a drop in GSH levels precede intracellular ROS production during apoptosis or vice versa is not certain. Hence any role of GSH depletion alone in triggering apoptosis is not clear (Hall, 1999).

AA is intrinsically linked to the metabolism of GSH. Pre-treatment of cells prior to H_2O_2 challenge caused decreases in glutathione levels compared to non AA pre-treated cells. Intracellular AA will modulate the intracellular redox status, and may therefore alter the rates of GSH metabolism through effects on gene expression, or directly utilise GSH for regeneration from the oxidised form of AA. However when the AA pre-treatment was washed out prior to H_2O_2 challenge, glutathione levels increased compared to non-AA pre-treated cells. This demonstrates an extra-cellular role for ascorbate, possibly through provision of reducing equivalents for maintenance of cysteine.

BDNF was also shown to increase glutathione levels in undifferentiated and differentiated cells. This is in agreement with data by Gabaizadeh *et al,* (1997) who have also shown BDNF to cause increases in glutathione levels.

GSSG levels were also assessed in some of the paradigms. Results showed H_2O_2 to cause increases in levels with increasing concentration. With NGF treatment and H_2O_2 challenge GSSG levels were also shown to increase but NGF caused no significant differences. Nevertheless, it is evident from this data that much of the GSH is lost, either through mixed disulphide formation with proteins or through efflux.. The drop in GSH may therefore reflect an inhibition of synthesis, a deficit in the GSH salvage pathway, or an increased rate of efflux (Chandra *et al.,* 2000).

Yonezawa *et al.,* (1996) have shown that deprivation of one of the precursors of glutathione (cysteine) induces glutathione depletion and death in cultures of cells, but that rescue by free radical scavenger and a diffusible glial factor was not associated with

a restoration of normal glutathione content. These authors thus suggest that the protecting agents act distal to glutathione. This is in agreement with Kamata *et al.*, (1996) who showed when cellular GSH was depleted by treatment with BSO, NGF still protected cells. Therefore this study also agrees that NGF exerts its protection independently of GSH. The data presented in this chapter also agrees with this, in that the 'best performing NGF concentration (10ng/ml) in other chapters was shown not to cause any significant increases in glutathione levels indicative of NGF exerting its protection via glutathione up regulation.

CHAPTER SIX

EFFECT OF NERVE GROWTH FACTOR ON GENE EXPRESSION

6. GENE REGULATION & EXPRESSION

Differences or alterations in the levels of protein can occur by a number of different mechanisms including alterations in the level of gene transcription and alterations in the stability or translatability of the resulting RNA (Lillycrop *et al.*, 1992). Figure 6.1a shows a scheme of the action of ROS on modifying molecules and the downstream effects caused.

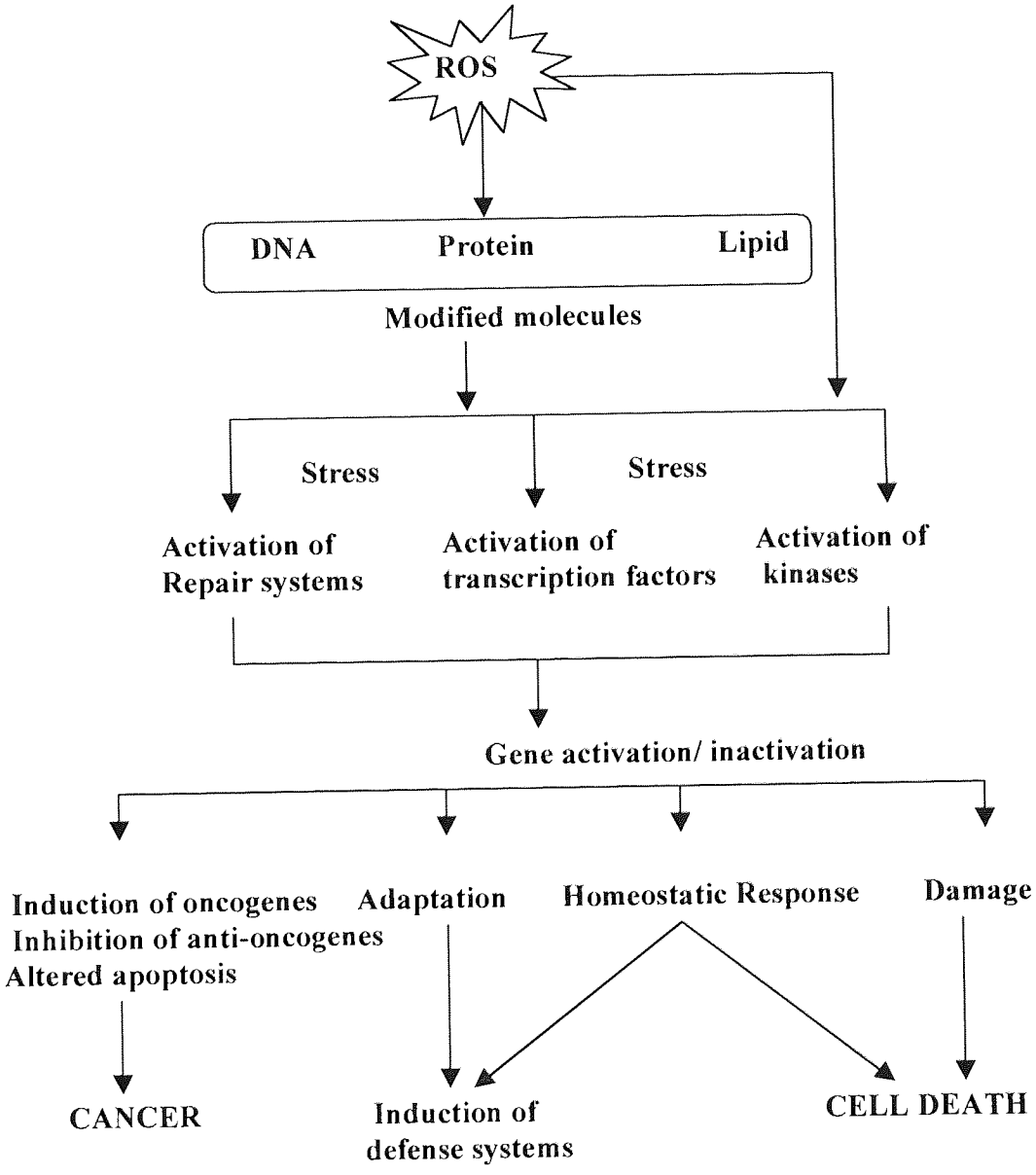

Figure 6.1a The role of ROS in cell signalling processes, adapted from Kehrer (2000).

The Reverse Transcriptase PCR (RT-PCR) has been adopted as a powerful tool to study gene expression. PCR itself was conceived by Kary Mullis in 1983 has been defined as 'a process that could make unlimited copies of genes'. The PCR reaction involves denaturing DNA by heating ay approximately 95°C, thereby completely separating the double stranded DNA molecules forming single strands. These become the templates for gene-specific primers and thermostable DNA polymerase. Primers are then allowed to anneal to the complementary sequences in the DNA at approximately 55°C, before heating to 72°C, which allows for extension of the primers by DNA polymerase in the presence of dNTPs, and for DNA synthesis to proceed. The whole cycle is usually repeated approximately 30 times, and in theory every cycle doubles the amount of DNA present, therefore starting off with 1 molecule of DNA after 30 cycles approximately 1.07×10^9 molecules would have been produced. However in practise amplification efficiency is usually only approximately 70%, and 1 million copies would be a more realistic figure. PCR is a method of amplifying DNA, that was first described in 1988 (Saiki *et al.*, 1988).

Amplification of RNA by PCR can be performed by annealing a primer to the RNA template and then synthesising a cDNA copy using reverse transcriptase (RT) followed by PCR (Newton & Graham, 2000). Because PCR will only amplify DNA and not RNA it is necessary to first prepare a cDNA copy of all the mRNAs in the cell, using reverse transcriptase, and specific primers derived from the sequence of the mRNA of interest can then be used to specifically amplify the cDNA/mRNA hybrid produced in this manner (Lillycrop *et al.*, 1992).

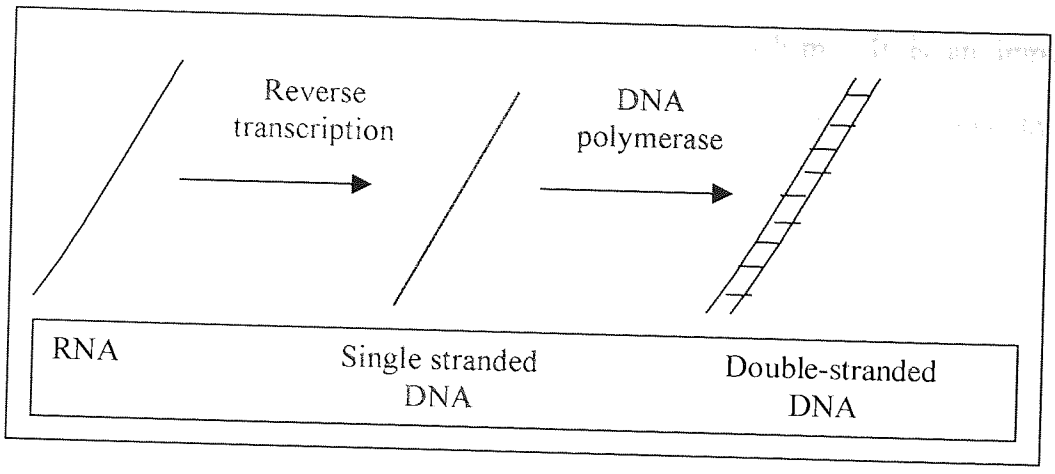

Figure 6.1b Reverse transcription of an RNA template into DNA, adapted from Brown, (1995).

6.1 CONTROL OF GENE EXPRESSION

Housekeeping or control genes are used as the primary control for all gene expression experiments as a parallel measurement to assess differences in sample loading or reaction efficiencies, in order to provide a means to evaluate and subsequently adjust for intrinsic experimental variations. True housekeeping genes do not exist, only pivotal control genes, which have to exhibit two major properties. Firstly they should be essential for the maintenance of cellular function and viability and therefore should be ubiquitously expressed in all tissues, and secondly their transcription should not be affected within the experimental context being investigated. Therefore the expression of invariant control genes should remain at a steady-state level, whilst the transcription of target genes may be up- or down- regulated (Suzuki *et al.*, 2000). Consequently the use of internal controls facilitates the direct and sound measurement of comparative gene expression (Stürzenbaum & Kille, 2001).

Two housekeeping genes have been employed in experiments, glyceraldehyde-3-phosphate (GAPDH / G3PDH) and β-Actin. The glycolytic tetramer GAPDH/G3PDH

is a multifunctional enzyme involved in cellular metabolism. It is an important glycolytic enzyme that catalyses the oxidative phosphorylation of glyceraldehyde-3-phosphate to 1,3-diphosphoglycerate, and it is the most widely used internal control gene (Suzuki *et al.*, 2000). Measurement of GAPDH transcript abundance was originally selected as a normalizer for other expressions because it encodes for a protein with a housekeeping function. As it is a glycolytic intermediate it is therefore expected to be present in all cells and exhibit minimal modulation. However GAPDH gene expression has been reported to increase during other non-glycolytic activities such as programmed neuronal cell death (Ishitani *et al.*, 1996).

β-Actin is one of the major components of cytoplasmic microfilaments in eukaryotic cells. Although actin is the second most widely used control genes, there is increasing evidence suggesting that the relative amounts of each isoform expressed and the total actin content can vary with differing conditions, questioning the usefulness of this molecule as a control (Stürzenbaum & Kille, 2001).

The GSH redox status is critical for various biological events that include transcriptional activation of specific genes, modulation of redox-regulated signal transduction, regulation of cell proliferation, apoptosis, and inflammation (Rahman & MacNee, 2000). A simplified diagram of the response to the imbalance of GSH redox status is shown in figure 6.1c.

The intracellular concentration of GSH is mainly regulated by γ-GCS (Richman & Meister, 1975). The mechanism by which GSH modulates γ-GCS expression is unknown, however evidence has suggested that the thiol redox status of cysteines in

pivotal transcription factors, such as NF-κB and fos/jun alters DNA/protein interactions and functionally changes rates of gene transcription. Thus, the increased uptake of GSH may modify the thiol redox of a transcription factor (Kim *et al.* 1996). The expression of γ-GCS is sensitive to OS, where the existence of OS-response elements such as AP-1 on the γ-GCSh (γ-GCS heavy subunit) promoter have been clarified (Mulcahy *et al.*, 1997).

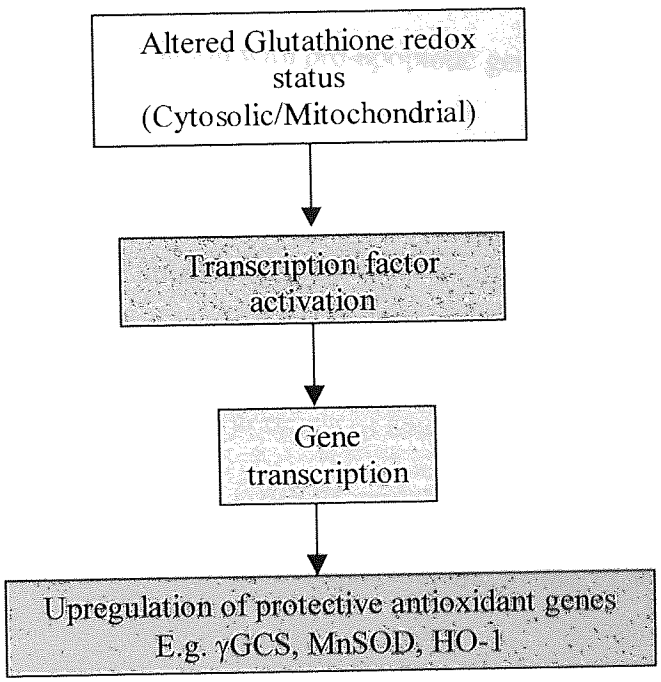

Figure 6.1c Response to the imbalance of GSH redox status, adapted from Rahman & MacNee, 2000

Redox sensitive transcription factors such as nuclear factor-κB (NF-κB) and activator protein 1 (c-Fos/cJun, AP-1) are also known to upregulate protective antioxidant genes. Maintenance of a high intracellular (GSH)/(GSSG) ratio (>90%) minimises the accumulation of disulfides and provides a reducing environment within the cell. This ratio is influenced by the activity of glutathione peroxidase (GPX), where expression of this enzyme has also been suggested to be modulated by redox status. If there is a shift in the GSH/GSSG redox buffer, a variety of cellular signalling processes are influenced, such as activation and phosphorylation of stress kinases (JNK, p38, PI-3K) via sensitive

cysteine-rich domains; activation of sphingomyelinase-ceramide pathway, and activation of the transcription factors AP-1 and NF-κB, eventually leading to increased gene transcription (Rahman & MacNee, 2000).

In order to evaluate the role of the expression of glutathione metabolising enzymes in response to neurotoxic insult in these models, the levels of transcripts for GCS and GPX have been evaluated in association with pro-apoptotic gene BAX.

6.2 RESULTS

To check for successful uncontaminated mRNA extraction after RT reaction, all samples were subjected to a GAPDH PCR, and gels of the PCR products were then run on agarose gels to demonstrate the presence of an approximately sized single band only. The standard gels consisted of all GAPDH samples both positive and negative with a PCR control and a DNA size ladder to check the size of the PCR product on a 1.5% agarose gel.

A GAPDH gel showing only products in the positive lanes and no product in the negative lanes and PCR control, indicated a successful uncontaminated mRNA extraction as shown in figure 4.2.

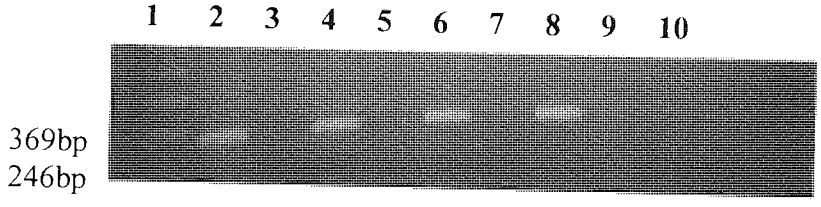

Figure 6.2. A standard GAPDH Control Agarose Gel. Lane 1 – 123bp ladder, Lane 2 – Sample 1 (Positive), Lane 3 – Sample 1 (Negative), Lane 4 – Sample 2 (Positive), Lane 5 – Sample 2 (Negative), Lane 6 – Sample 3 (Positive), Lane 7 – Sample 3 (Negative), Lane 8 – Sample 4 (Positive), Lane 9 – Sample 4 (Negative) and Lane 10 – PCR Control.

6.3 Optimisation of Primers

6.3.1 GAPDH

Product size: 318bp
Cycle Parameters:

98°C	3 minutes	
+ Taq		
60°C	2 minutes	1 cycle
72°C	2 minutes	
94°C	30 seconds	
60°C	30 seconds	26 cycles
72°C	30 seconds	
94°C	30 seconds	
60°C	30 seconds	1 cycle
72°C	4 minutes	

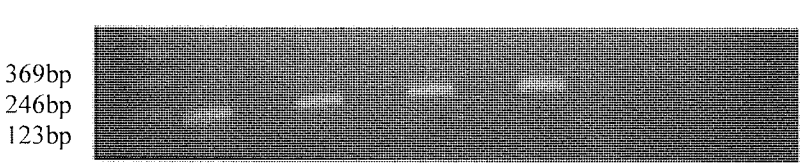

Figure 6.3 1.5% Agarose Gel of GAPDH PCR Products synthesized with a 60°C annealing temperature. Lane 1 – 123bp ladder, Lane 2 – Sample 1 (Positive), Lane 3 – Sample 1 (Negative), Lane 4 – Sample 2 (Positive), Lane 5 – Sample 2 (Negative), Lane 6 – Sample 3 (Positive), Lane 7 – Sample 3 (Negative), Lane 8 – Sample 4 (Positive), Lane 9 – Sample 4 (Negative) and Lane 10 – PCR Control

This gene had previously been optimised in the laboratory.

6.3.2 β-Actin

Product size: 538bp
Cycle Parameters:

94°C	1 minute	1 cycle
94°C	45 seconds	
+ Taq		
67°C	1 minute	
72°C	1 minute	
94°C	45 seconds	
67°C	1 minute	35 cycles
72°C	1 minute	
72°C	10 minutes	1 cycle

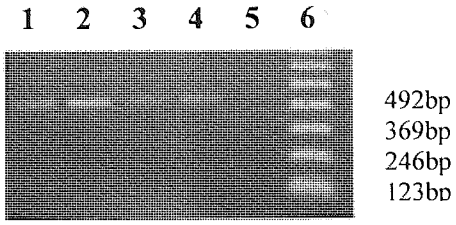

Figure 6.4 1.5% Agarose Gel of β-Actin PCR Products synthesized with a 65°C annealing temperature. Lane 1 – Sample 1 (Positive), Lane 2 – Sample 2 (Positive), Lane 3 – Sample 3 (Positive), Lane 4 – Sample 4 (Positive), Lane 5 – PCR Control and Lane 6 – 123bp DNA ladder

This temperature was ruled out as two bands, the one required and a higher band were produced. The PCR was re-ran at 1°C higher.

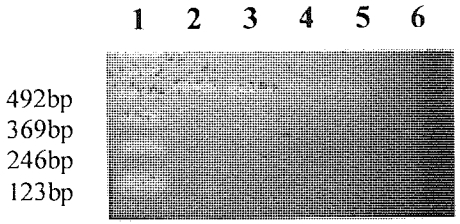

Figure 6.5 1.5% Agarose Gel of β-Actin PCR Products synthesized with a 67°C annealing temperature for 36 cycles. Lane 1 – 123bp DNA ladder, Lane 2 - Sample 1 (Positive), Lane 3 – Sample 2 (Positive), Lane 4 – Sample 3 (Positive), Lane 5 – Sample 4 (Positive) and Lane 6 – PCR Control

Results showed a clear band of the correct product size, this was then used for cycle sampling to determine the optimum number of cycles. Gels were run of products from PCRs of 20, 25, 30 and 35 cycles of which all were blank. A product was only obtained with 36 cycles.

Therefore for β-actin PCRs were conducted at 67°C with 36 cycles.

6.3.3 Gamma glutamyl cysteinyl synthetase (GCS)

Product size: 346bp
Cycle parameters:

94°C	1 minute	1 cycle
94°C	45 seconds	
+ Taq		
56°C	1 minute	
72°C	1 minute	
94°C	45 seconds	
56°C	1 minute	31 cycles
72°C	1 minute	
72°C	10 minutes	1 cycle

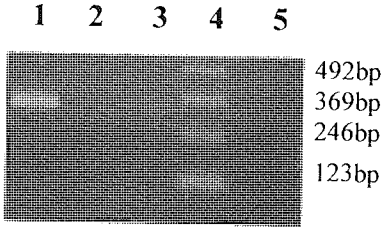

Figure 6.6 1.5% Agarose Gel of GCS PCR Products synthesized with a 56°C annealing temperature. Lane 1 – Sample 1 (Positive), Lane 2 – Sample 2 (Positive), Lane 3 – Sample 3 (Positive), Lane 4 – 123bp Ladder and Lane 5 – PCR Control

Optimisation was conducted on this primer, 56°C showed only one band of the correct size. 32 cycles was found to be the optimum cycle number, where 30 cycle PCRs produced no detectable product.

6.3.4 Glutathione Peroxidase (GPX)

Product size: 197bp
Cycle parameters:

94°C	1 minute	1 cycle
94°C	45 seconds	
+ Taq		
56°C	1 minute	
72°C	1 minutes	
94°C	45 seconds	
56°C	1 minute	27 cycles
72°C	1 minute	
72°C	10 minutes	1 cycle

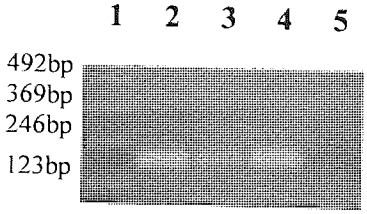

Figure 6.7 1.5% Agarose Gel of GPX PCR Products synthesized with a 56°C annealing temperature. Lane 1 – 123bp Ladder, Lane 2 - Sample 1 (Positive), Lane 3 – Sample 2 (Positive), Lane 4 – Sample 3 (Positive) and Lane 5 – PCR Control

Results showed 56°C to also be the optimum annealing temperature for the GPX primer. At lower temperatures no-specific binding was recorded and at higher temperatures no products were recorded. Cycle sampling was also conducted, which showed large product bands at 30 and 35 cycles, however at these cycle numbers products were too large to differentiate the intensity of the products. Cycle sampling showed 28 cycles to generate products within the exponential phase of PCR cycling.

6.3.5 BAX

Product size: 352bp
Cycle Parameters:

94°C	4 minutes	
94°C	1 minute	
+ Taq		1 cycle
65°C	1 minute	
72°C	1 minute	
---	---	---
94°C	1 minute	
65°C	1 minute	29 cycles
72°C	1 minute	
---	---	---
72°C	10 minutes	1 cycle

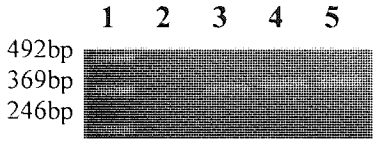

Figure 6.8 1.5% Agarose Gel of BAX PCR Products synthesised with a 65°C annealing temperature. Lane 1 – 123bp ladder, Lane 2 – PCR Control, Lane 3 – Sample 1 (Positive), Lane 4 – Sample 2 (Positive), Lane 5 – Sample 3 (Positive)

Optimisation of the BAX primer showed 65°C and 30 cycles to be the optimal conditions, for a single band in the exponential phase of amplification. (Other ranges tested 60°, 62°C, 64°C and 67°C).

6.4 Investigations into selective apoptotic and GSH metabolism gene expression in PC12 cells under NGF treatment and hydrogen peroxide challenge

Experiments were conducted to investigate any changes in gene expression for selected apoptotic and GSH metabolising enzymes, caused by NGF treatment in PC12 cells before and during H_2O_2 challenge. PC12 cells ($2x10^5$) were incubated with NGF (10ng/ml) for 0 – 24 hours at 37°C, 5%CO_2 before H_2O_2 (150μM) was also added for either 4 or 24 hours. Cells were harvested at various time points indicated in the legends in figure 6.9 and the mRNA extracted (section 2.2.8.1). After extraction the mRNA underwent a RT reaction and then PCRs for GAPDH, GPX, GCS, BAX and β-Actin were conducted.

GAPDH expression remained constant. Levels of GPX expression remained constant until after peroxide challenge, where levels increased after both 4 and 24 hours of challenge in NGF pretreated cells and non NGF pretreated cells. This effect was more marked in NGF pretreated cells. BAX expression also remained constant for the first 24 hours, however, after peroxide challenge expression levels increased in NGF pretreated cells after 4 and 24 hours, increases were only seen after 24 hours in non NGF pre-

treated cells. GCS expression was more variable in NGF treated cells compared to non-NGF treated cells. The only marked differences in non NGF treated cells were after 4 hours of peroxide challenge where expression was virtually nothing and after 24 hours of peroxide challenge where there was the greatest expression. In NGF treated cells GCS levels initially increased up to 2 hours after the NGF treatment then decreased. After 4 hours of peroxide challenge GCS levels were also greatly reduced showing the least expression, expression then increased after 24 hours of peroxide challenge.

These changes were subsequently analysed to semi-quantitate any changes in gene expression. The gene expression analysis tool Phoretix was used to quantify the intensity of each band (product) on every gel. The intensities recorded were then corrected for by adjusting all the results found to the GAPDH. Figure 6.10 shows the percentage of control of each of the 3 test genes (GCS, GPX and BAX) over time.

6.4.1 Gene expression in PC12 cells under NGF treatment and in the presence and absence of hydrogen peroxide challenge

Experiments were conducted using PC12 cells ($2x10^5$) incubated with NGF (10ng/ml) for 0 – 24 hours at 37°C, 5%CO_2. Either H_2O_2 (150μM) or PBS was then subsequently added for either 4 or 24 hours. Cells were harvested at various time points as stated in the gel legends in figure 6.11 and the mRNA extracted as stated in section 2.2.8.1. After extraction the mRNA underwent a RT reaction and then PCR's for GAPDH, GPX, GCS, BAX and β-Actin were also conducted.

Figure 6.9 1.5% Agarose gels of PCR products. PC12 cells ($2x10^5$) were incubated with NGF (10ng/ml) versus control) for 0-24 hours at 37°C, 5%CO_2. H_2O_2 (150μM) was then added for 4 and 24 hours at 37°C, 5%CO_2 and cells were harvested and mRNA extracted as stated in section 2.2.8 and after RT, PCRs were conducted.

- **GAPDH (60°C, 28 cycles) + NGF TREATMENT**

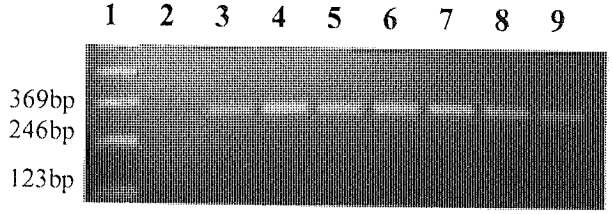

(Hours stated are of NGF treatment).
Lane 1 – 123bp ladder, Lane 2 – Blank, Lane 3- 0 hour, Lane 4 – 1 hour
Lane 5 – 2 hours, Lane 6- 4 hours, Lane 7 – 24 hours
Lane 8 – 24 hours + 4 hours H_2O_2, Lane 9 – 24 hours + 24 hours H_2O_2

- **GPX (56°C, 28 cycles) + NGF**

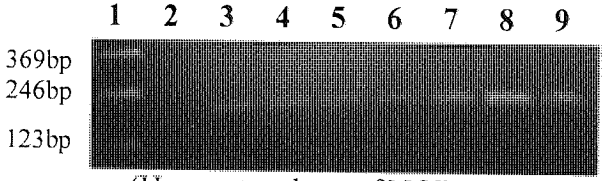

(Hours stated are of NGF treatment).
Lane 1 – 123bp ladder, Lane 2 – Blank, Lane 3- 0 hour, Lane 4 – 1 hour
Lane 5 – 2 hours, Lane 6- 4 hours, Lane 7 – 24 hours
Lane 8 – 24 hours + 4 hours H_2O_2, Lane 9 – 24 hours + 24 hours H_2O_2

GAPDH (60°C, 28 cycles) NO NGF TREATMENT

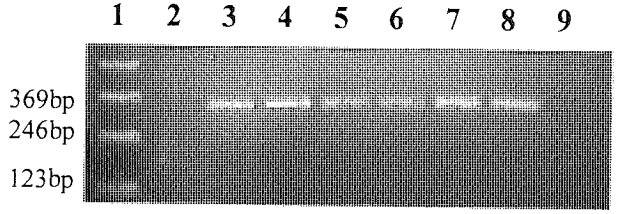

(Hours stated are of control (PBS) treatment).
Lane 1 – 123bp ladder, Lane 2 – Blank, Lane 3 – 1 hour,
Lane 4 – 2 hours, Lane 5 – 4 hours, Lane 6 – 24 hours,
Lane 7 – 24 hours + 4 hours H_2O_2,
Lane 8 – 24 hours + 24 hours H_2O_2, Lane 9 – PCR Control

GPX (56°C, 28 cycles) - NGF

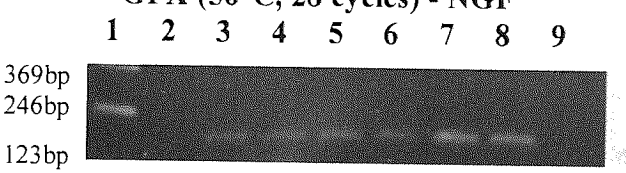

(Hours stated are of control (PBS) treatment).
Lane 1 – 123bp ladder, Lane 2 – Blank, Lane 3 – 1 hour,
Lane 4 – 2 hours, Lane 5 – 4 hours, Lane 6 – 24 hours,
Lane 7 – 24 hours + 4 hours H_2O_2,
Lane 8 – 24 hours + 24 hours H_2O_2, Lane 9 – PCR Control

- **BAX (65°C, 30 cycles)**
  + NGF TREATMENT

1 2 3 4 5 6 7 8 9

492bp
369bp
246bp

(Hours stated are of NGF treatment).
Lane 1 – 123bp ladder, Lane 2 – Blank, Lane 3- 0 hour, Lane 4 – 1 hour
Lane 5 – 2 hours, Lane 6- 4 hours, Lane 7 – 24 hours
Lane 8 – Lane 24 hours + 4 hours H_2O_2, Lane 9 – 24 hours + 24 hours H_2O_2

- **β-Actin (67°C, 36 cycles)**
  +NGF TREATMENT

1 2 3 4 5 6 7 8 9

369bp
246bp
123bp

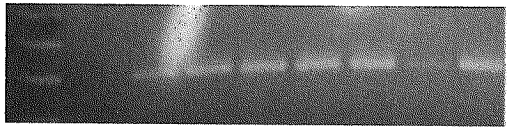

(Hours stated are of NGF treatment).
Lane 1 – 123bp ladder, Lane 2 – Blank, Lane 3- 0 hour, Lane 4 – 1 hour
Lane 5 – 2 hours, Lane 6- 4 hours, Lane 7 – 24 hours
Lane 8 – Lane 24 hours + 4 hours H_2O_2, Lane 9 – 24 hours + 24 hours H_2O_2

BAX (65°C, 30 cycles)
NO NGF TREATMENT

1 2 3 4 5 6 7 8 9

369bp
246bp
123bp

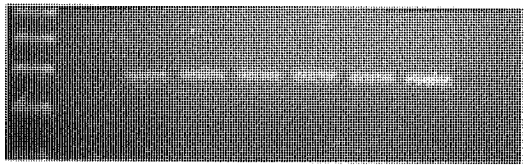

(Hours stated are of Control (PBS) treatment).
Lane 1 – 123bp ladder, Lane 2 – Blank, Lane 3 – 1 hour,
Lane 4 – 2 hours, Lane 5 – 4 hours, Lane 6 – 24 hours,
Lane 7 – 24 hours + 4 hours H_2O_2,
Lane 8 – 24 hours + 24 hours H_2O_2, Lane 9 – PCR Control

β-Actin (67°C, 36 cycles)
- NGF TREATMENT

1 2 3 4 5 6 7 8 9

369bp
246bp
123bp

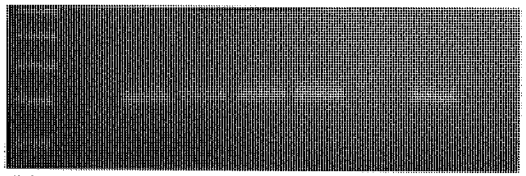

(Hours stated are of NGF treatment).
Lane 1 – 123bp ladder, Lane 2 – Blank, Lane 3 – 1 hour,
Lane 4 – 2 hours, Lane 5 – 4 hours, Lane 6 – 24 hours,
Lane 7 – 24 hours + 4 hours H_2O_2,
Lane 8 – 24 hours + 24 hours H_2O_2, Lane 9 – PCR Control

- **GCS (56°C, 32 cycles) + NGF + NGF TREATMENT**

1 2 3 4 5 6 7 8 9

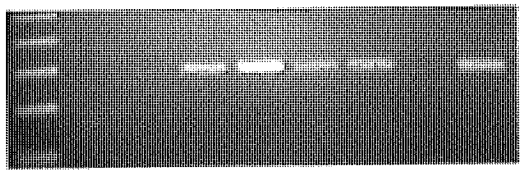

(Hours stated are of NGF treatment).
Lane 1 – 123bp ladder, Lane 2 – Blank, Lane 3- 0 hour, Lane 4 – 1 hour
Lane 5 – 2 hours, Lane 6- 4 hours, Lane 7 – 24 hours
Lane 8 – 24 hours + 4 hours H_2O_2, Lane 9 – 24 hours + 24 hours H_2O_2

GCS (56°C, 32 cycles) -NGF NO NGF TREATMENT

1 2 3 4 5 6 7 8 9

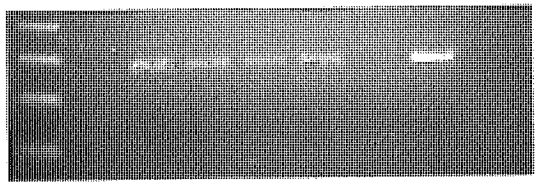

(Hours stated are of control (PBS) treatment).
Lane 1 – 123bp ladder, Lane 2 – Blank, Lane 3 – 1 hour,
Lane 4 – 2 hours, Lane 5 – 4 hours, Lane 6 – 24 hours,
Lane 7 – 24 hours + 4 hours H_2O_2,
Lane 8 – 24 hours + 24 hours H_2O_2, Lane 9 – PCR Control

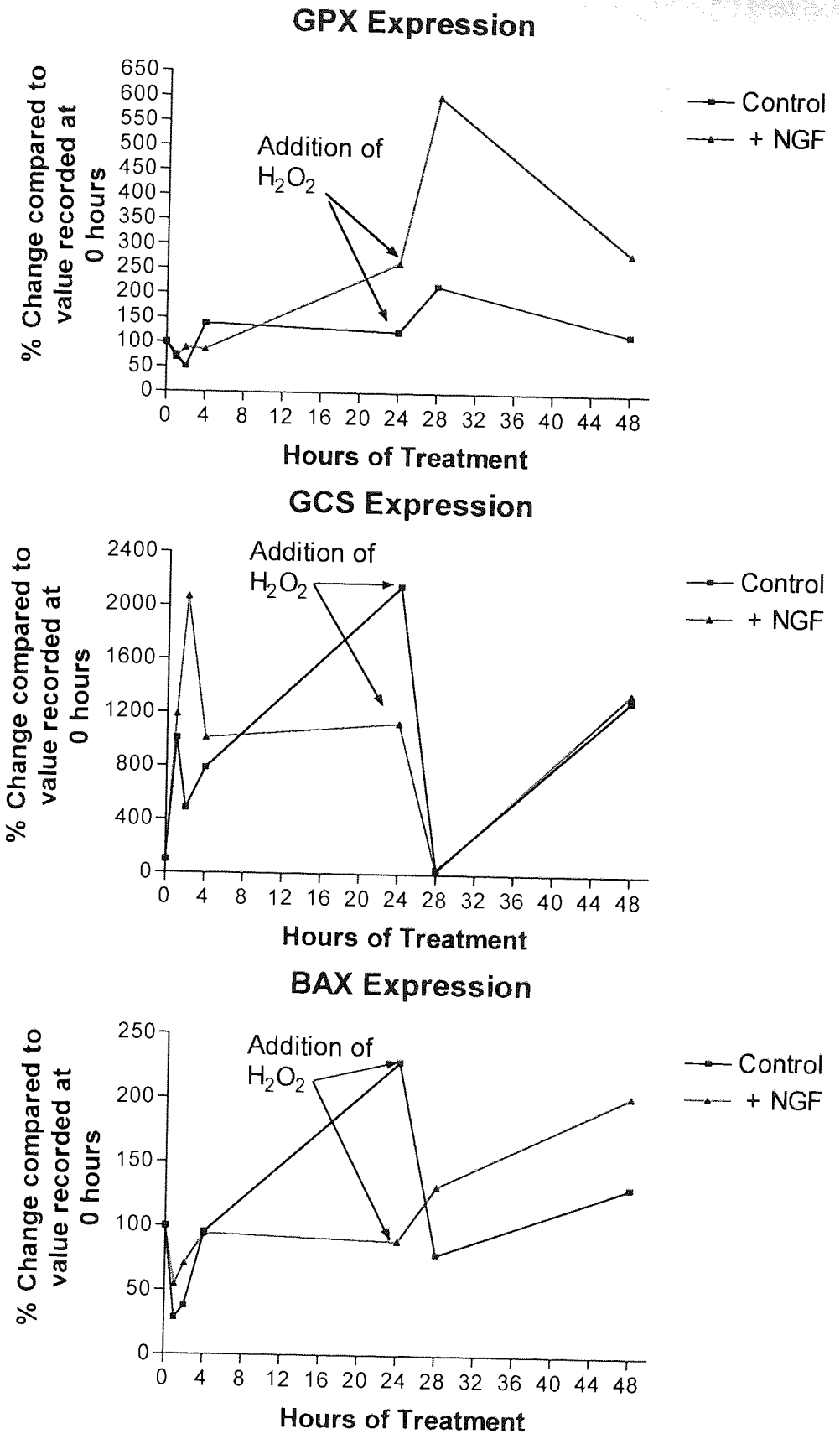

Figure 6.10 GPX, GCS and BAX expression as quantitated using the gene expression tool Phoretix. Figures show the percentage changes in gene expression levels over time.

Figure 6.11 1.5% Agarose gels of PCR products. PC12 cells ($2x10^5$) were incubated with NGF (10ng/ml) for 0-24 hours at 37°C, 5%CO_2. H_2O_2 (150μM) was then added for 4 and 24 hours at 37°C, 5%CO_2 and cells were harvested and mRNA extracted as stated in section 2.2.8 and after RT, PCR reactions were conducted.

- **GAPDH (60°C, 28 cycles)**

1 2 3 4 5 6 7 8 9

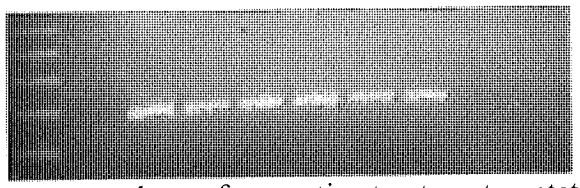

(Hours stated are of respective treatment as stated)
(N= NGF treatment, P=PBS treatment).
Lane 1 – 123bp ladder, Lane 2 – Blank, Lane 3- 1 hour N, Lane 4 – 2 hours N
Lane 5 – 4 hours N, Lane 6- 1 hour P, Lane 7 – 2 hours P
Lane 8 – 4 hours P, Lane 9 – PCR Control

1 2 3 4 5 6 7 8

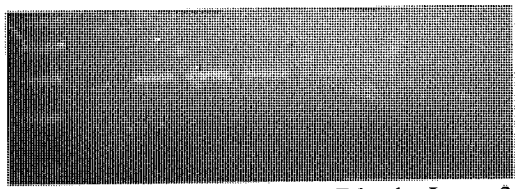

Lane 1 – 123bp ladder, Lane 2 – Blank, Lane 3 – 0 hours
Lane 4 – 24 hours N + 4 hours H_2O_2, Lane 5 – 24 hours N + 4 hours PBS
Lane 6 – 24 hours P + 24 hours H_2O_2, Lane 7 – 24 hours P + 24 hours PBS
Lane 8 – PCR Control

GAPDH (60°C, 28 cycles)

1 2 3 4 5 6 7 8 9 10

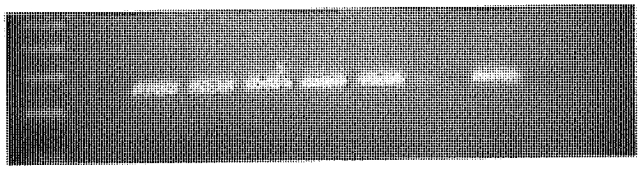

(Hours stated are of respective treatment as stated)
(N= NGF treatment, P=PBS treatment).
Lane 1 – 123bp ladder, Lane 2 – Blank, Lane 3 – 24 hours N,
Lane 4 – 24 hours P, Lane 5 – 24 hours N + 4 hours H_2O_2,
Lane 6 – 24 hours N + 4 hours PBS,
Lane 7 – 24 hours P + 4 hours H_2O_2, Lane 8 – Blank
Lane 9 – 24 hours P + 4 hours PBS, Lane 10 – PCR Control

GPX (56°C, 26 cycles)

1 2 3 4 5 6 7 8 9 10

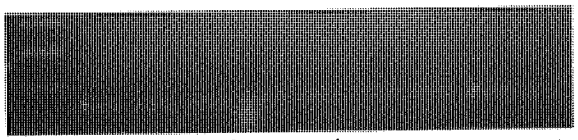

(Hours stated are of respective treatment as stated)
(N= NGF treatment, P=PBS treatment).
Lane 1 –123bp ladder, Lane 2 –0 hours, Lane 3 – 1 hour P,
Lane 4 – 2 hours P, Lane 5 – 4 hours P, Lane 6 – 24 hours P,
Lane 7 – 24 hours P + 4 hours H_2O_2, Lane 8 – 24 hours P + 4 hours PBS
Lane 9 – 24 hours P + 24 hours H_2O_2, Lane 10 – 24 hours P + 24 hours PBS,

- **BAX (65°C, 30 cycles)**

1 2 3 4 5 6 7 8 9 10

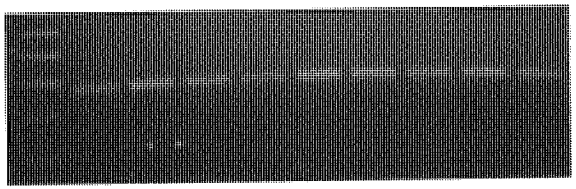

(Hours stated are of respective treatment as stated)
(N= NGF treatment, P=PBS treatment).
Lane 1 – 123bp ladder, Lane 2 – 0 hours, Lane 3 – 1 hour P,
Lane 4 – 2 hours P, Lane 5 – 4 hours P, Lane 6 – 24 hours P,
Lane 7 – 24 hours P + 4 hours PBS, Lane 8 – 24 hours P + 4 hours H_2O_2
Lane 9 – 24 hours P + 24 hours PBS, Lane 10 – 24 hours P + 24 hours H_2O_2

GPX (56°C, 26 cycles)

1 2 3 4 5 6 7 8 9 10

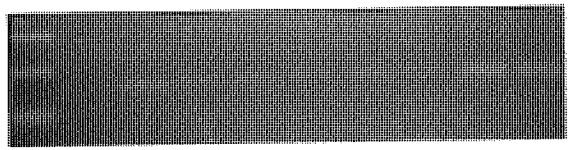

(Hours stated are of respective treatment as stated)
(N= NGF treatment, P=PBS treatment).
Lane 1 – 123bp ladder, Lane 2 – PCR Control, Lane 3 –
1 hour N, Lane 4 – 2 hours N, Lane 5 – 4 hours N, Lane 6 –
24 hours N, Lane 7 – 24 hours N + 4 hours H_2O_2, Lane 8 – 24
hours + 4 hours PBS, Lane 9 – 24 hours N + 24 hours H_2O_2,
Lane 10 – 24 hours N + 24 hours PBS

1 2 3 4 5 6 7 8 9 10

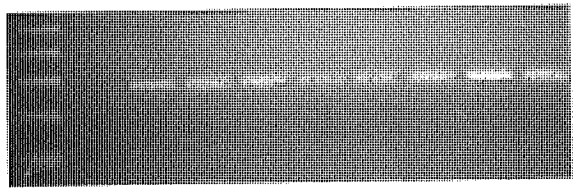

(Hours stated are of respective treatment as stated)
(N= NGF treatment, P=PBS treatment).
Lane 1 – 123bp ladder, Lane 2 – PCR Control,
Lane 3 – 1 hour N, Lane 4 – 2 hours N, Lane 5 – 4 hours N,
Lane 6 – 24 hours N, Lane 7 – 24 hours N + 4 hours PBS,
Lane 8 – 24 hours N + 4 hours H_2O_2, Lane 9 – 24 hours N +
24 hours PBS, Lane 10 – 24 hours N + 24 hours H_2O_2

- **GCS (56°C, 32 cycles)**

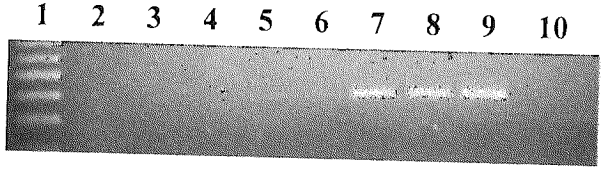

(Hours stated are of respective treatment as stated)
(N= NGF treatment, P=PBS treatment).
Lane 1 –123bp ladder, Lane 2 –0 hours, Lane 3 – 1 hour P,
Lane 4 – 2 hours P, Lane 5 – 4 hours P, Lane 6 – 24 hours P,
Lane 7 – 24 hours P + 4 hours PBS, Lane 8 – 24 hours P + 4 hours H_2O_2
Lane 9 – 24 hours P + 24 hours PBS, Lane 10 – 24 hours P + 24 hours H_2O_2,

GCS (56°C, 32 cycles)

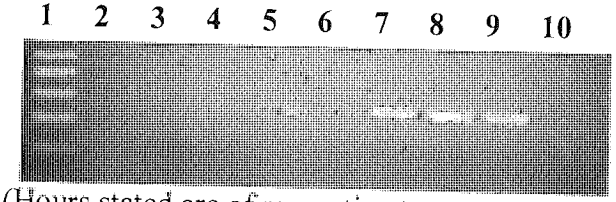

(Hours stated are of respective treatment as stated)
(N= NGF treatment, P=PBS treatment).
Lane 1 – 123bp ladder, Lane 2 – Blank, Lane 3 – PCR Control, Lane 4 - 1 hour N, Lane 5 – 2 hours N, Lane 6 – 4 hours N, Lane 7 – 24 hours N, Lane 8 – 24 hours N + 4 hours PBS, Lane 9 – 24 hours N + 4 hours H_2O_2,
Lane 10 – 24 hours N + 24 hours H_2O_2

6.5 DISCUSSION

The results in this chapter show that in culture conditions, gene expression levels of GCS, GPX and BAX alter. After 24 hours NGF caused increased GPX expression to 264% compared to 123% in controls. Following oxidative insult levels of GPX expression increased to 602% in NGF treated cells and 217% in controls; percentage increases of 228% (NGF treated) and 176% (controls).

GPX utilises GSH in catalysing the breakdown of H_2O_2 to H_2O and O_2 as shown in figure 1.19 (Anderson, 1997). An increased expression would be expected after oxidative insult due to the increased detoxification of H_2O_2. Levels of GPX expression are markedly higher in NGF treated cells suggesting a greater ability of the cells to withstand oxidative insults and therefore show signs of oxidative damage as seen in other markers that have been studied. This increased expression is clearly due to NGF treatment as figure 6.9 shows GPX levels gradually increase over the 24 hours of treatment with NGF. Gene levels after 24 hours of oxidative insult are lower than after 4 hours suggesting the removal of the trigger for upregulation in expression, or loss of stability of mRNA.

The enzyme γ–GCS catalyses the first step in the synthesis of glutathione (GSH) from its precursors glutamic acid and cysteine as shown in figure 1.19a. Although glutathione synthetase (GS) is also involved in the synthesis, γ-GCS is generally regarded as the rate-limiting enzyme. Levels of this precursor (heavy subunit) initially peak at 2-4 hours in control and NGF treated cells inducing an increase in GSH levels in the cell perhaps to counteract OS building up in the culture conditions. Levels continue to rise over the period of non oxidative insult in control cells whereas levels reduce in

NGF treated cells. GSH is also dependent on selenium and cysteine in the medium and therefore fresh medium alone may promote expression, and may be causing the increases recorded. Nonetheless, these levels are grossly elevated after 24 hours GCS levels are 2152% (NGF treated) and 1130% (controls). After 4 hours of oxidative insult, GCS levels greatly diminish in both cell groups to 35% and 25%. GCS levels after 24 hours of oxidative insult are comparable to 0 hours with no noticeable difference between control and NGF treated cells. There was much greater experimental variation in this data and a consistent trend was not established.

Gene expression is modulated by both physiological signals (hormones, cytokines, etc.) and environmental stimuli (physical parameters,xenobiotics, etc.). OS appears to be a key pleiotropic modulator which may be involved in either pathway. The role of ROS in cell signalling processes may be mediated directly by various OS acting through the generation of bioactive mediators (Morel & Barouki, 1999). The number of transcription factors whose activities are modulated by ROS is substantial, and include AP-1, p53, NF-κB, HSF, Sp-1 and GABP (Kehrer, 2000). NF-κB has been shown to regulate a host of genes involved in specific immune, stress and inflammatory responses (Dudek *et al.*, 2001). A growing number of transcription factors have been shown to be modulated by variations in the cellular redox status. Because of the wide specificity of transcription factors, some of them are specifically down-regulated by an OS that is not cytotoxic. In ths respect, ROS appear to be actual modulators of gene transcription, independently of the degradation of biological macromolecules (Morel & Barouki, 1999). The adaptive response to OS and the further place of transcription factors and gene expression is shown in figure 6.12.

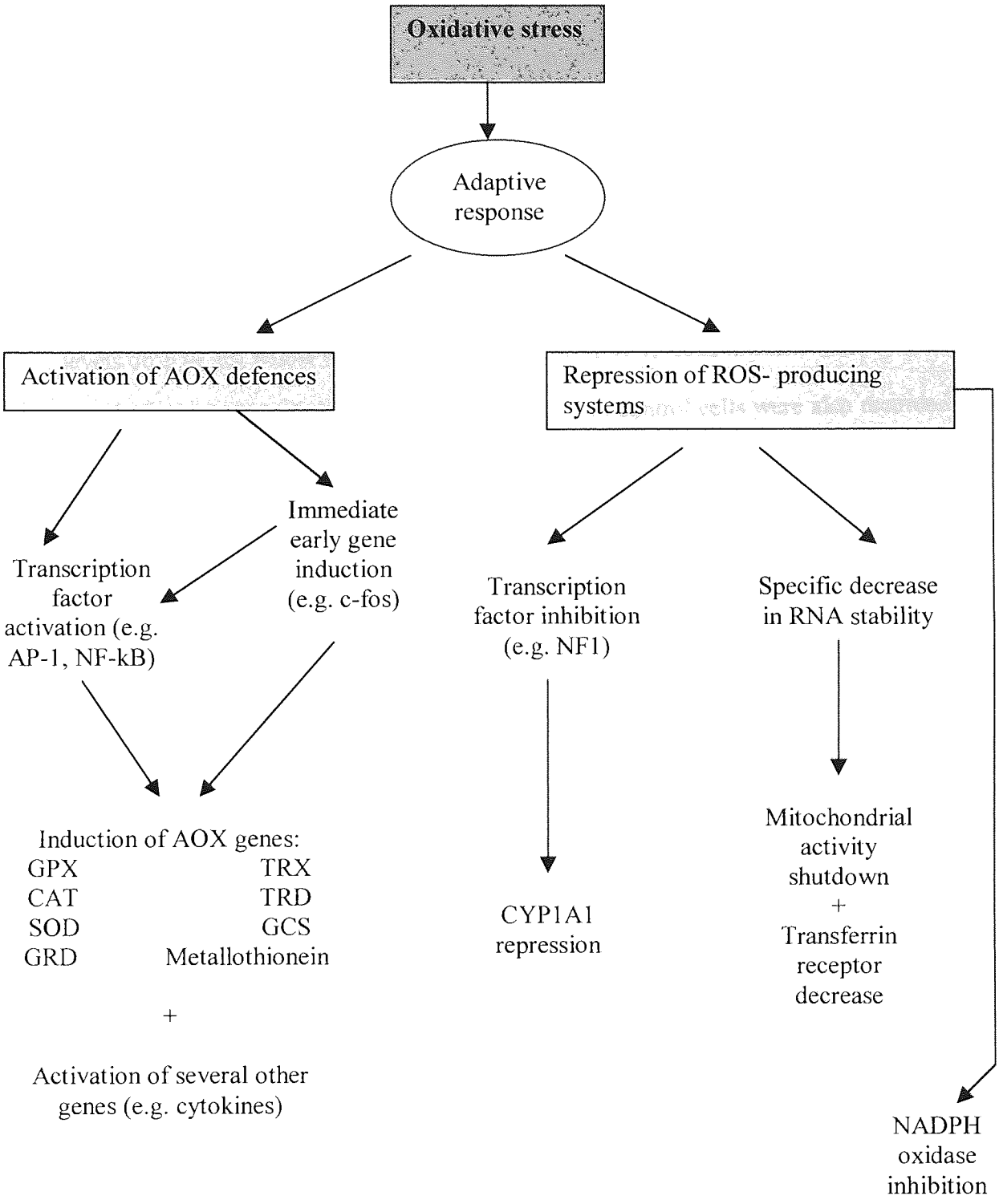

Figure 6.12 The adaptive response to oxidative stress, adapted from Morel & Barouki, (1999).

Bax is a pro-apoptotic gene that has been shown to play an important role in apoptosis. It has been shown that the Bax/Bcl-2 gene ratio can determine whether or not a cell undergoes apoptosis. Bcl-2 is an antiapoptotic gene that has been shown to inhibit apoptosis. Bax expression recorded showed an initial drop in levels at 1 hour which recovered back to basal levels after 4 hours levels then increased in control cells and remained constant in NGF treated cells. This would concur with the increase in OS in culture conditions being encountered causing increases in apoptosis in control cells. After oxidative insult two distinct effects were recorded. In control cells, bax mRNA levels drop to just below basal levels where levels in NGF cells increase and continue to do so for the 24 hours of oxidative insult. Levels in control cells were also recorded to rise in the last 20 hours of oxidative insult.

These results are very hard to interpret alone. Many researchers have studied the Bax:Bcl-2 ratio. Recent studies have shown that neuronal apoptosis induced by Aβ is related to alteration of the Bax/Bcl-2 ratio (Tan *et al., 1999).* However despite trying a couple of sets of mRNA primers no Bcl-2 expression was recorded. This is similar to that recorded by Rong *et al.,* (1999). However, Ray *et al.,* (2000), have published using primers against PC12 cells, which harvested Bcl-2 gene expression products. Despite trying the same primers no expression was recorded, however in the experiments of Ray *et al.,* they used PC12 cells grown on collagen-coated monolayers in Dulbecco's modified Eagles's medium (DMEM). In the experiments presented here, PC12 cells were grown in non-collagen coated plates in RPMI.

Rong *et al.,* (1999), have shown NGF treatment (50ng/ml for 48 hours) to have little or no change on Bax expression levels in the absence of oxidative challenge. This is

similar to the findings here, where over 24 hours Bax expression did not differ greatly. Ray *et al.*, (2000), have shown that H_2O_2 (100μM for 18 hours) did not alter Bax levels and that it was the decrease recorded in Bcl-2 levels that caused the Bax:Bcl-2 ratio to increase by 60.8% compared to controls and to direct the cells to die by apoptosis. The results prevented here show changes in Bax expression, this is in disagreement with the results of a study by Ray *et al.*,(2000), however, it is the ratio of pro-apoptotic to anti-apoptotic genes which is critical in determining commitment to apoptosis.

Sometimes there is a lack of correlation between mRNA and protein levels, as the presence of RNA in a cell is not necessarily indicative of peptide synthesis. Structurally authentic mRNAs may be poorly handled by the translational machinery in a cell. Even the efficient translation of a functional message may not result in biologically active peptide if post translational processes are absent, or if the peptide is rapidly degraded. The analysis of gene expression must therefore extend to the description of the protein end-points of the expression pathway, included in this must be a consideration of protein function (Carter & Murphy, 1999).

CHAPTER SEVEN

EFFECT OF NITROXYBUTYL ESTER OF FLURBIPROFEN (NO-FB) and NOVEL COMPOUNDS ON PC12 CELLS

7.1 INTRODUCTION

It has been noted that inflammation is a secondary response to a primary pathological process. Inflammation occurs in AD brains, where it is most highly evident near plaques, as the presence of activated astrocytes and microglia, and also diverse associated factors including proinflammatory cytokines. Plaques are decorated with complement components and deposits and epidemiological studies suggest that anti-inflammatory drugs may delay the onset or slow the progression of AD (Thal, 2000; O'Banlon & Finch, 1996). Halliday *et al.*, (2000) have shown that long term anti-inflammatory medications in patients with AD enhanced cognitive performance but did not alleviate the progression of the pathological changes. Netland *et al.*, (1998), showed that the NSAID (non-steroidal anti-inflammatory drug) indomethacin reduces the microglia/macrophage response to Aβ infusion, thus providing insight into the role of NSAID in the treatment of AD.

NSAIDs because of their wide availability and relative safety, have been proposed as agents that target the brain, to provide a simple and effective means for the prevention or treatment of AD. Other new agents that target other processes in inflammation, such as complement activation or the interaction between inflammatory mediators and Aβ may also provide additional approaches to treat AD (O'Banlon & Finch, 1996).

A study was conducted using the NSAID, flurbiprofen (FB) and its analogues to investigate whether these agents could alter Aβ and H_2O_2 mediated apoptosis. The study was developed following observations that Aβ toxicity is mediated, at least in part, by ROS. As some of the test agents have been shown to be moieties that inhibit caspase related pathways and protect other cell types including endothelial cells, their

effects on PC12 cells were investigated (Fiorucci *et al.*, 1999). There is also evidence that has suggested that NO generation and metabolism is affected in AD (Hu *et al., 1997).* Therefore NO donating NSAIDs and novel NSAIDs were tested against OS inducing agents in PC12 cells to investigate whether any protection was offered by nitroflurbiprofen (NO-FB), NCX 2216 (NICOX test compound) and FB.

7.2 Effects of hydrogen peroxide

An experimental method was developed where PC12 cells cultures on collagen coated plates showed good sensitivity to H_2O_2. Cells were seeded into 24 well collagen-coated plates at $1x10^5$ cells/ml (ml/well) and cultured in complete (15%) RPMI for 20 hours. Cells were then washed gently with RPMI (1%) and then RPMI (1ml of 1%) was added to each well before the addition of varying concentrations of H_2O_2 and Aβ for 18 hours, in the presence or absence of 100μM FB, NO-FB and NCX 2216. Cells remaining attached to plates were determined by the crystal violet assay.

Figure 7.1 shows NCX 2216 (100μM) to have significant protective effects at both 10 and 30μM H_2O_2 ($P<0.05$, Dunnett's test, n=6). No protection was seen against 100μM H_2O_2, however all viability was virtually eradicated at this dose. In control wells, FB and NO-FB caused significant decreases in viability ($P<0.01$, Dunnett's test, n=6), this trend continued at 10 and 30μM H_2O_2 although the effects were not significantly different to controls.

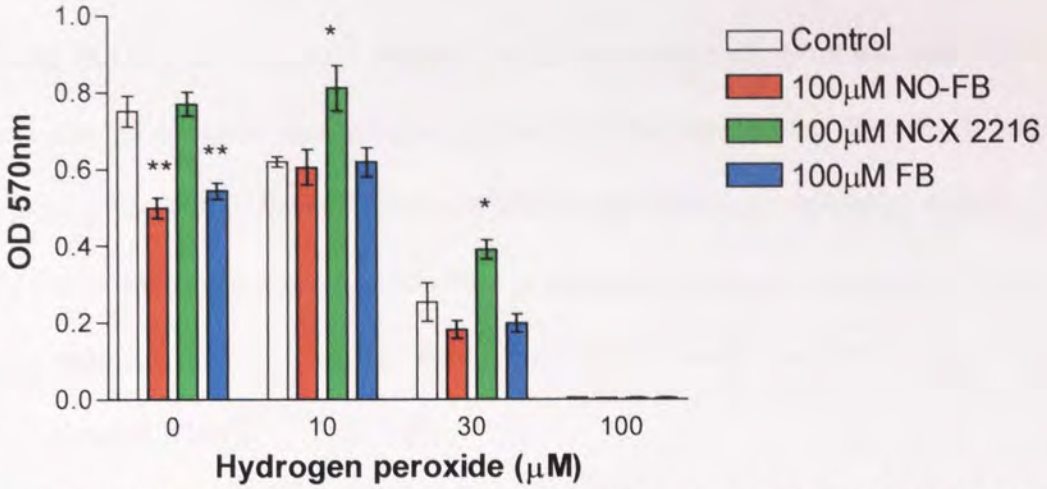

Figure 7.1 Effects of NO-FB, FB and NCX 2216 on the ability of H_2O_2 to cause loss of PC12 cells from the culture plate as measured by crystal violet. Figure shows mean ± SEM. * P<0.05, **P<0.01 (Dunnett's test)

Cells were also analysed for protein carbonyl formation. Figure 7.2 shows at low H_2O_2 concentration (10μM) each of the agents tested, caused reductions in carbonyl levels. At higher H_2O_2 levels (30 and 100μM) increases in carbonyls were recorded in all treatments, however none of the agents tested showing any significant differences to those of control.

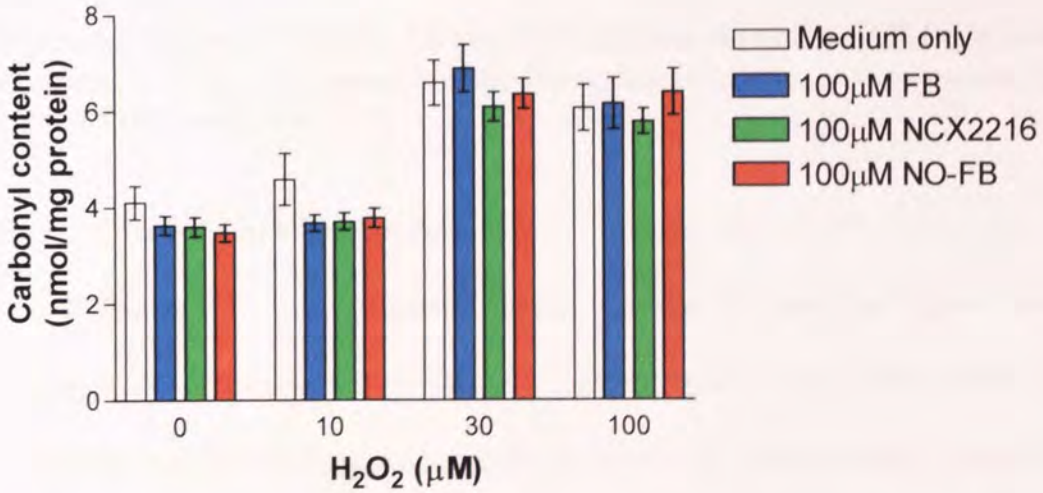

Figure 7.2 Effects of NO-FB, FB and NCX 2216 on the ability of H_2O_2 to cause protein carbonyl formation in PC12 cells. Figure shows mean ± SEM.

Levels of apoptosis were also examined using flow cytometry. Figure 7.3 shows that increasing H_2O_2 levels caused increases in the percentage of apoptotic nucleoids in control cells. There were also changes recorded with the test agents. Between 0-30μM H_2O_2 there were no significant differences between treatments compared to control. At 100μM H_2O_2, each agent caused a reduction in apoptotic nucleoids compared to control, however only the decreases caused by FB and NO-FB were found to be significant ($P<0.05$, Dunnett's test).

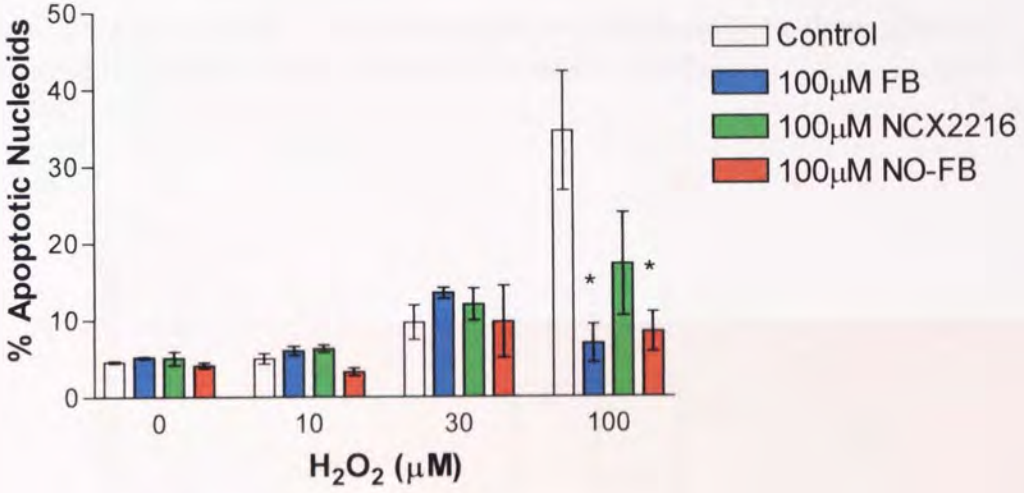

Figure 7.3 Effects of NO-FB, FB and NCX 2216 on the ability of H_2O_2 to cause apoptosis in PC12 cells determined by flow cytometry. Figure shows mean ± SEM. * P<0.05 (Dunnett's test,n=4)

7.3 Effect of amyloid β peptides

The inhibition of $A\beta_{25-35}$ peptide toxicity by the NO-donating agents was also investigated. However, the cytotoxicity (crystal violet assay) assay used was not sensitive to the effects of $A\beta_{25-35}$ as shown in figure 7.4, and in the flow cytometry data as shown in figure 7.5. A relatively high $A\beta_{25-35}$ dose showed no significant toxicity – this is in contrast to data reported in previous chapters.

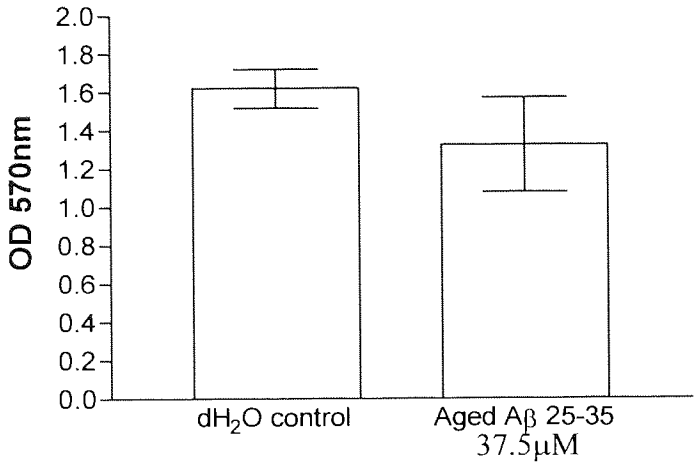

Figure 7.4 Effects of Aβ to cause loss of PC12 cells from the culture plate as measured by crystal violet. Figure shows mean ± SEM.

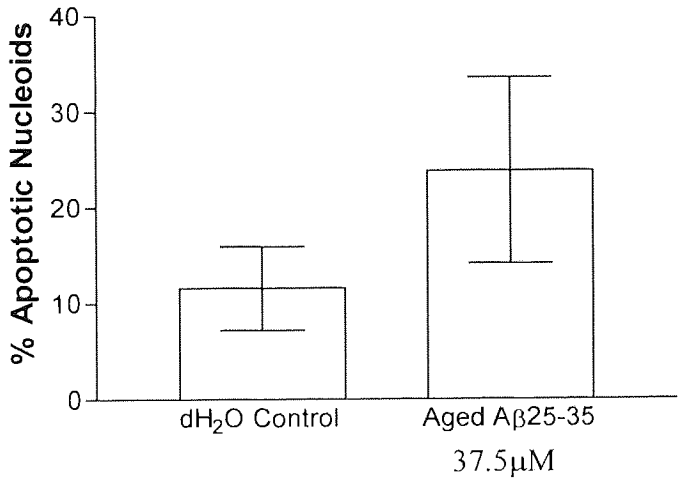

Figure 7.5 Effects of Aβ to cause apoptosis in PC12 cells as measured by flow cytometry. Figure shows mean ± SEM.

The only significant toxicity recorded, was following treatment of PC12 cells with the CT_{105} peptide from the carboxy terminal of the β-amyloid precursor protein, as shown in figure 7.6.

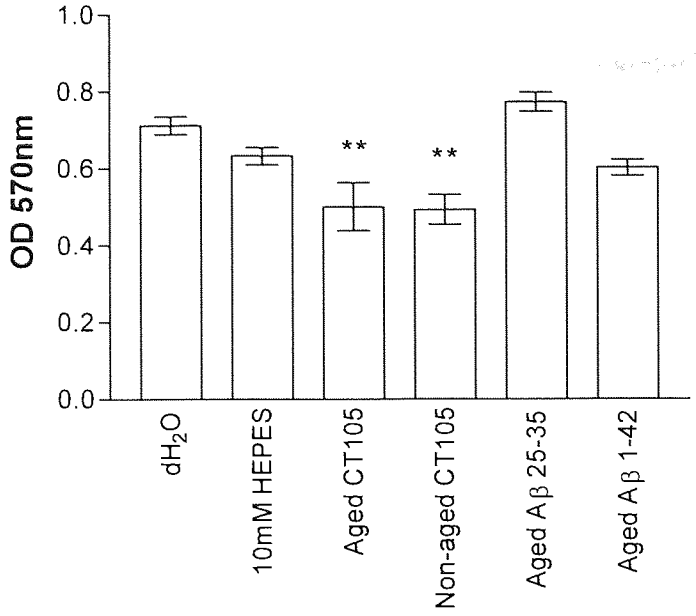

Figure 7.6 Effects of different Aβ peptides to cause loss of PC12 cells from the culture plate as measured by crystal violet. Concentration of agents added: HEPES (10μM) (CT_{105} vehicle), CT_{105} (1μM aged and non-aged), $Aβ_{25-35}$ (10μM) and $Aβ_{1-42}$ (10μM). Figure shows mean ± SEM, ** P<0.01 (Dunnett's test).

7.4 Caspase activity

In order to evaluate whether substrate dependence has an affect on susceptibility to apoptosis, a comparison was made between attached and detached cells, on the levels of caspase 3-like activity after $Aβ_{25-35}$ and H_2O_2 challenge. Figure 7.7 shows the levels of activity in both attached and detached cells. These data show a two fold higher caspase 3 activity in attached cells, and less sensitivity to toxic effects of H_2O_2 and Aβ.

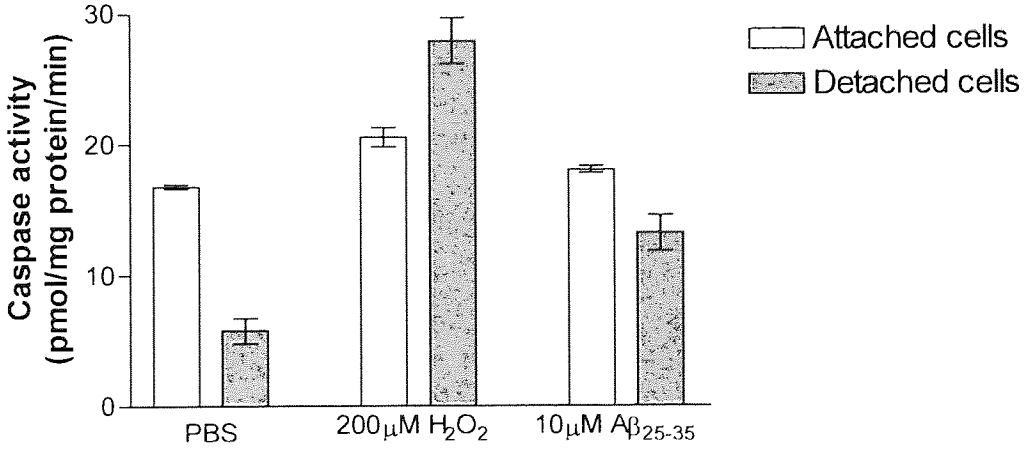

Figure 7.7 Caspase 3-like activity in PC12 cells treated with H_2O_2 (200μM) and $Aβ_{25-35}$ (10μM). Figure shows mean ± SEM, n=4

Data supports the theory that H_2O_2 (and Aβ) mediated apoptosis are caspase-mediated processes due to the increases recorded in caspase 3-like activity.

7.5 Discussion

Again peroxide caused increases in the levels of apoptosis and protein carbonyls, as shown in previous chapters.

The test compounds showed various effects. FB caused a general trend of decreasing crystal violet activity compared to controls, which agreed with flow cytometry data showing increases in apoptosis at each H_2O_2 concentration. However at 100μM H_2O_2, FB caused a significant decrease in apoptosis compared to controls. This is in contrast to data reported by Johal & Hanson (2000) who demonstrated that FB promoted apoptosis, however their data was generated in guinea pig gastric epithelial cells. Clonal cell lines were employed in this present work, Sanfeliu *et al.*, (1999) have stated that the clonal cell lines employed show a cytotoxic response similar to that of human primary neuronal cultures.

NO-FB showed significant effects on crystal violet staining, lowering basal levels compared to controls. Flow cytometry data showed that NO-FB caused significant decreases in the levels of apoptotic nucleoids compared to controls – this is again in agreement with the work by Johal & Hanson, (2000).

In the crystal violet assay, NCX 2216 consistently showed significant protection against oxidant induced toxicity. NCX 2216 also showed a general trend of lower carbonyl values compared to controls. NCX 2216 also showed apoptosis levels the same as

controls or lower, however none were significant. This agent is proposed for further investigation.

CT_{105} is a recombinant carboxy-terminal 105 amino acid fragment. It has been previously demonstrated to inhibit the Na^{+}-Ca^{2+} exchanger, which is considered to play a key role in the Ca^{2+} homeostasis of excitable cells. It has been suggested that CT_{105} may contribute to disruption of intracellular calcium concentration, being possibly involved in inducing the neural toxicity characteristic of AD (Kim *et al.*, 1999a). It has been suggested that CT_{105} can directly attack the cell membrane probably by making pores or non-selective ion channels, whereas it is suggested that Aβ impairs the intracellular metabolic pathway first (Kim & Suh, 1996).

The data generated with CT_{105} peptide is in agreement with that of Hartell & Suh (2000), who also showed CT_{105} to be more potent than Aβ in PC12 cells. The importance of this peptide as a toxic agent, and the relationship with OS should be further investigated.

CHAPTER EIGHT

DISCUSSION, CONCLUSIONS and FURTHER WORK

8.1 Discussion

The hypothesis put forward in chapter one of the proposed mechanism of neurotrophic factor protection on neuronal cells, was reviewed in light of the data generated in chapters three to six. The mechanism was modified to refer to NGF alone and not NGF in general, as BDNF did not show any of the same clear effects recorded with NGF.

It is not known at present whether BDNF reacts with ROS (i.e. trapping the oxygen species) or influences cultured neuronal and glial cells (i.e. activation of enzymes) however, it is certain that BDNF itself changes DNA-binding activity of transcription factors and regulates the expression of functional products that play an important role against OS (Iwata *et al.*, 1997). However, the results generated with BDNF were very disappointing. It has been proposed that the decreased levels of BDNF and the TrkB receptor that have been reported in AD brains, may constitute a lack of trophic support, and thus may contribute to the degeneration of specific neuronal populations in the AD-affected brain (Hock *et al.*, 2000). Therefore it has been proposed that BDNF may be a wonder molecule for AD, if levels of BDNF and TrkB expression can be increased it may have therapeutic potential. However in the paradigms tested no clear effects were observed. Further examination of BDNF is warranted, as the site of BDNF action is still unknown. It needs to be investigated whether the BDNF used was actually binding to the receptors triggering kinase activity, before BDNF action/in-action can actually be evaluated.

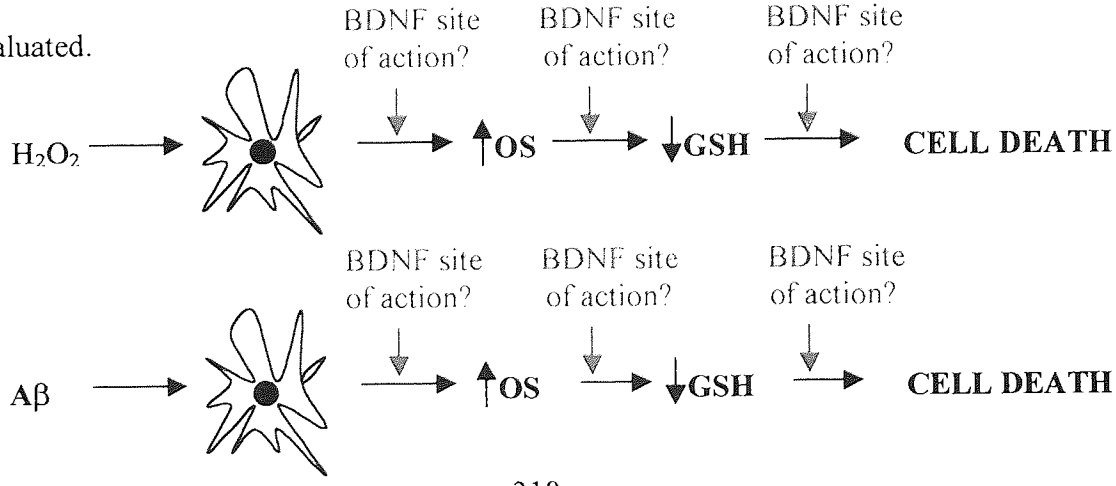

However, in the investigation of NGF there were significant effects recorded. Aβ was shown to cause intraneuronal production of ROS as measured by DCFDA staining (chapter four), where Aβ increased DCF fluorescence indicative of peroxide production in the neuronal model systems used. This further reinforces the proposal of Aβ directly producing OS. The inclusion of the iron chelator DFX further supported this, and also alluded to the fact that Aβ cannot exert its toxicity without the bioavailablity of iron, suggesting the important of metal catalysed production of •OH in toxicity.

Investigations into the effects of NGF, showed with reference to DCF fluorescence that NGF actually caused increases in intracellular peroxide. It is now widely recognised that exposure to low levels of a stressor facilitates the expression of systems, which allow enhanced protection against further exposure to the same stressor. It is interesting to speculate that NGF mediated intracellular oxidant generation may initiate an adaptive response in neuronal cells which further protects against OS. NGF (5ng/ml) showed clear decreases in DCF fluorescence against subsequent Aβ treatment compared to non-NGF pre-treated cells, however against H_2O_2 treatment NGF showed no reductions, it actually showed increases. This lends further support to the hypothesis that the differences in DCF response following NGF treatment between Aβ and H_2O_2 may represent the fact that peroxide is given as a single bolus dose in the latter, whereas the former may produce ROS over a longer period. Alternatively, cell death may also be induced by different pathways.

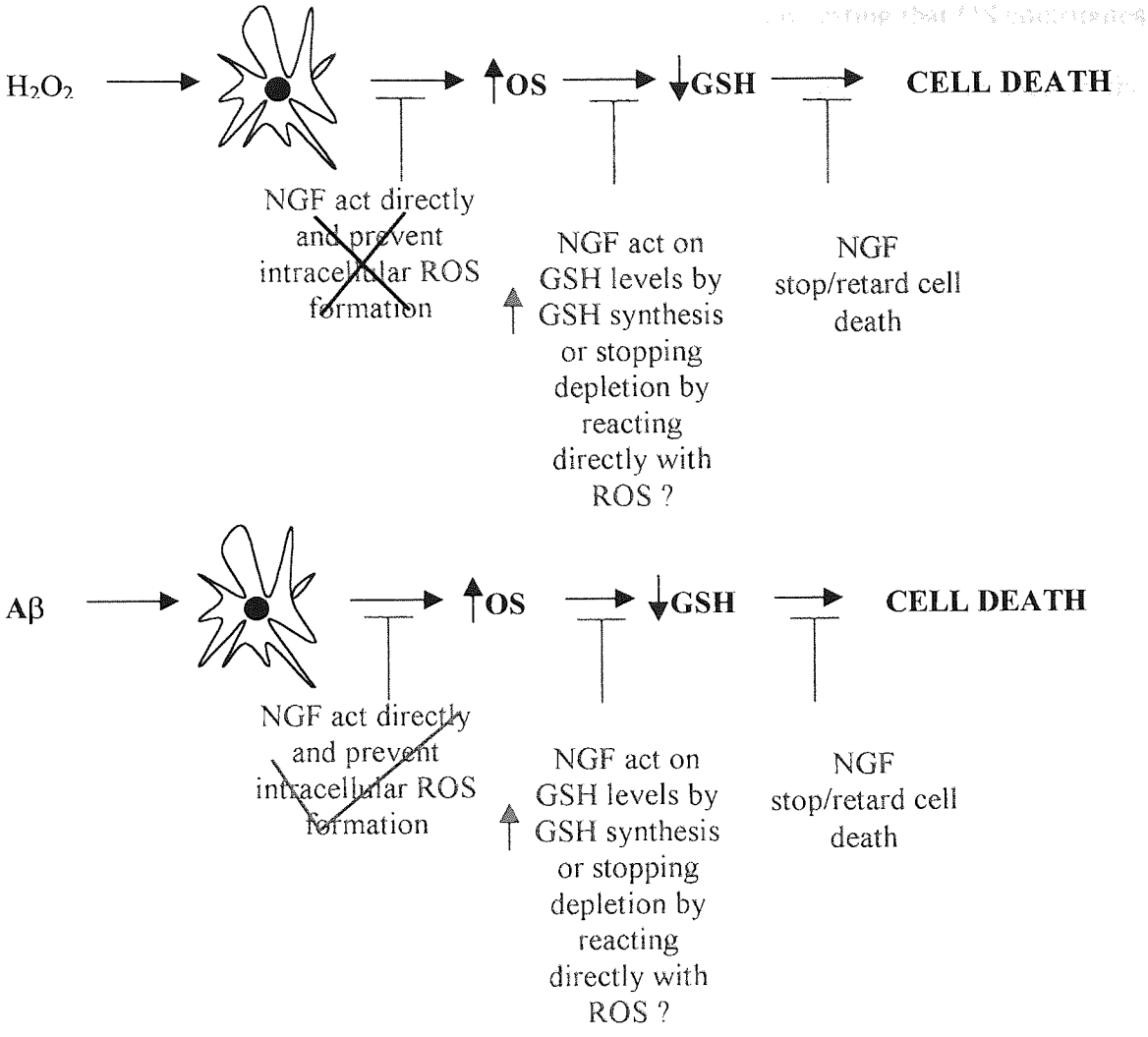

These data suggest that NGF acts early on in the cytotoxic (Aβ) pathway. This is important for two reasons: one is that as it acts so early on in the cell death cascade it has a greater chance of stopping excessive damage, however as the effect is so high up in the cascade, it suggests that NGF treatment may only be useful as a prophylactic treatment and not as an active treatment once ROS are already present.

It has been shown that an increase in ROS causes a disturbance in the balance of ROS and AOX systems in favour of ROS. If there is an imbalance in this system OS will ensue (Sies, 1985). The increase in OS as a consequence of aging and further in AD has shown a tip in the balance of ROS and AOX systems to cause cell death (Li et al., 1998;

Pan & Perez-Polo, 1993). Evidence has also been shown suggesting that OS contributes to the formation of amyloid plaques and NFTs and may therefore by involved in the pathogenesis of AD (Draczynsja-Lusiak *et al.*, 1998). This damage appears to be a major contributor to aging and to degenerative diseases of aging such as cancer, cardiovascular disease, cataracts, immune system decline and brain dysfunctions (Mecocci *et al.*, 1997). In this thesis, OS has been shown to damage cell macromolecules investigated (DNA indirectly and protein directly) and the effects of OS were recorded as protein carbonyls (chapter four), and DNA fragmentation (chapter three). Protein carbonyl data showed that H_2O_2 and Aβ caused increases in levels, indicative of oxidative damage, and Aβ and H_2O_2 also showed increases in DNA fragmentation as assessed by flow cytometry.

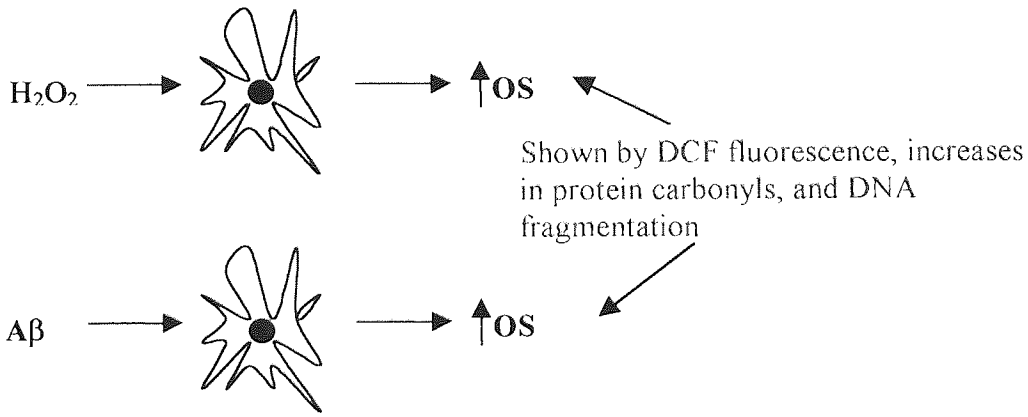

NGF was shown to cause a general trend of decreases in carbonyl values at 10ng/ml and also decreases in the percentage of apoptotic nucleoids in PC12 cells. NGF protection was also recorded in SY5Y cells, with results showing generally lower carbonyl levels with NGF treatment versus controls, and also lower percentages of apoptotic nucleoids. However in differentiated SY5Y cells, NGF showed a general trend of increasing carbonyl levels and the percentage of apoptotic nucleoids.

The effects of OS on GSH levels were also investigated (chapter five). Results showed GSH levels to initially decrease as shown in the hypothetical chain of events, however over increasing time of insult, increases in GSH levels were recorded with increasing peroxide challenge in all cell types investigated. NGF showed no effects on basal levels, however under H_2O_2 challenge NGF did show some effects. In chapter six there were also changes in the glutathione enzyme, GPX mRNA expression recorded, suggesting that NGF may actually be exerting an effect on GSH metabolism, which is not necessary clearly represented at the measured glutathione levels. Kamata *et al.*, (1996) have previously shown NGF to protect PC12 cells from OS independently of GSH, however they only investigated glutathione levels and no mRNA expression.

NGF also caused decreases in GSH levels under Aβ challenge, which were not evident in non-NGF cells. This also suggests that NGF might exert its protective effect against Aβ toxicity by increasing GSH metabolism. Increases in reduced GSH and its oxidative counterpart GSSG have been reported to occur following exposure to oxidants (H_2O_2 and Aβ), suggesting an increase in GSH synthesis (Barker *et al.*, 1996). These workers have concluded that under conditions of OS, such as PD, inactivation of brain glutathione reductase maybe a contributory factor to the loss of GSH. The loss of GSH may further increase the susceptibility of intracellular systems to oxidising systems such as ONOO- giving rise to a destructive cycle of metabolic events leading ultimately to disease.

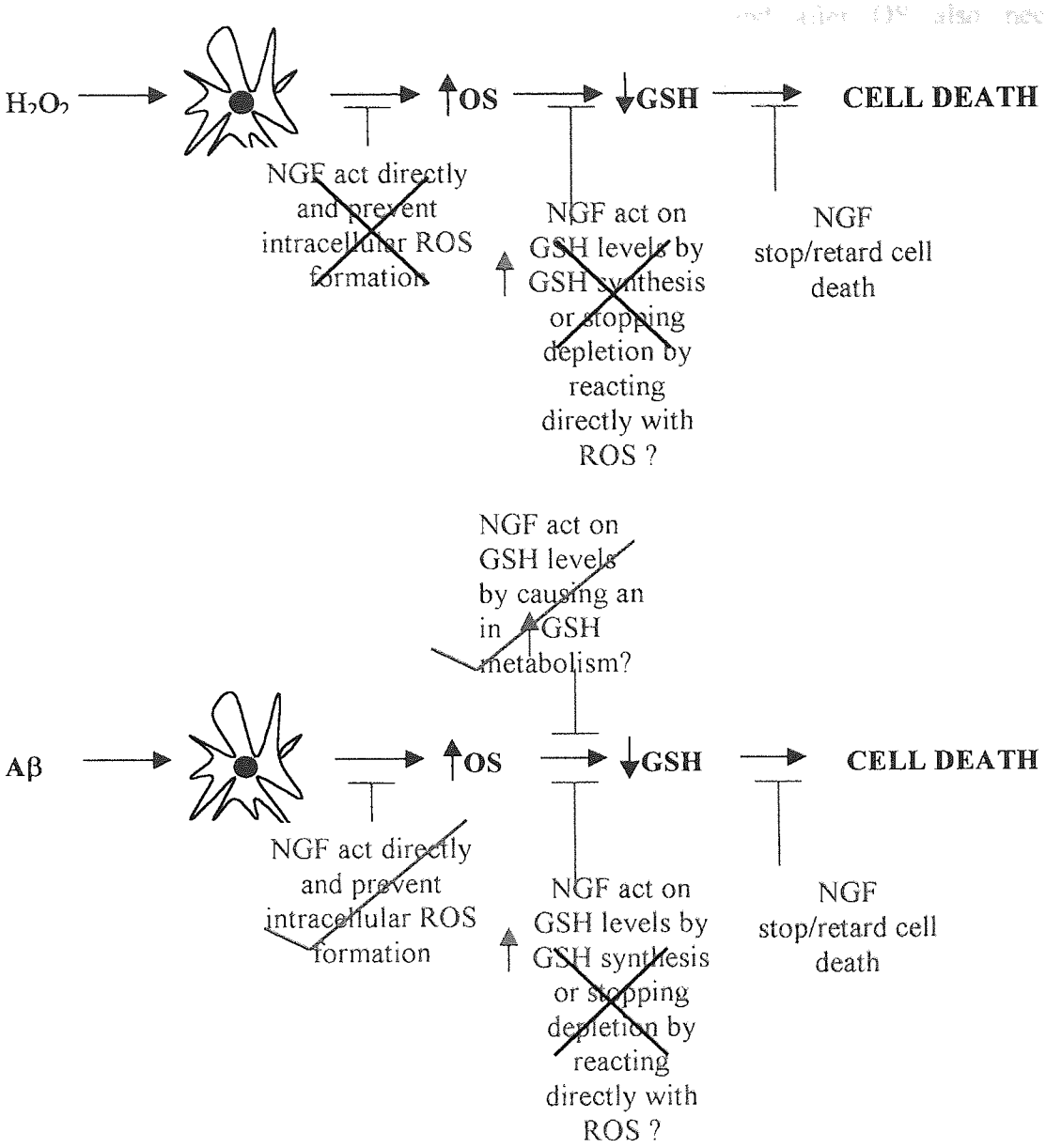

Protection by NGF was also recorded in fluorescence microscopy, which showed protection against cell death caused by H_2O_2 after NGF pre-treatment. This was interesting as Connor *et al.,* (1996) had suggested that apoptosis in AD brain may be due to a reduction in neurotrophic growth factors. The observation that a neurotrophin, in this case NGF reduced the apoptosis infers that neurotrophins may well have a place in AD treatment. However, the effects of NGF reported in this thesis were investigated after pre-treatment and before OS and not after OS insult. Therefore fluorescence

microscopy studies of NGF co-incubation with OS and after OS also needs investigating, along with the effects of Aβ, and NGF and Aβ.

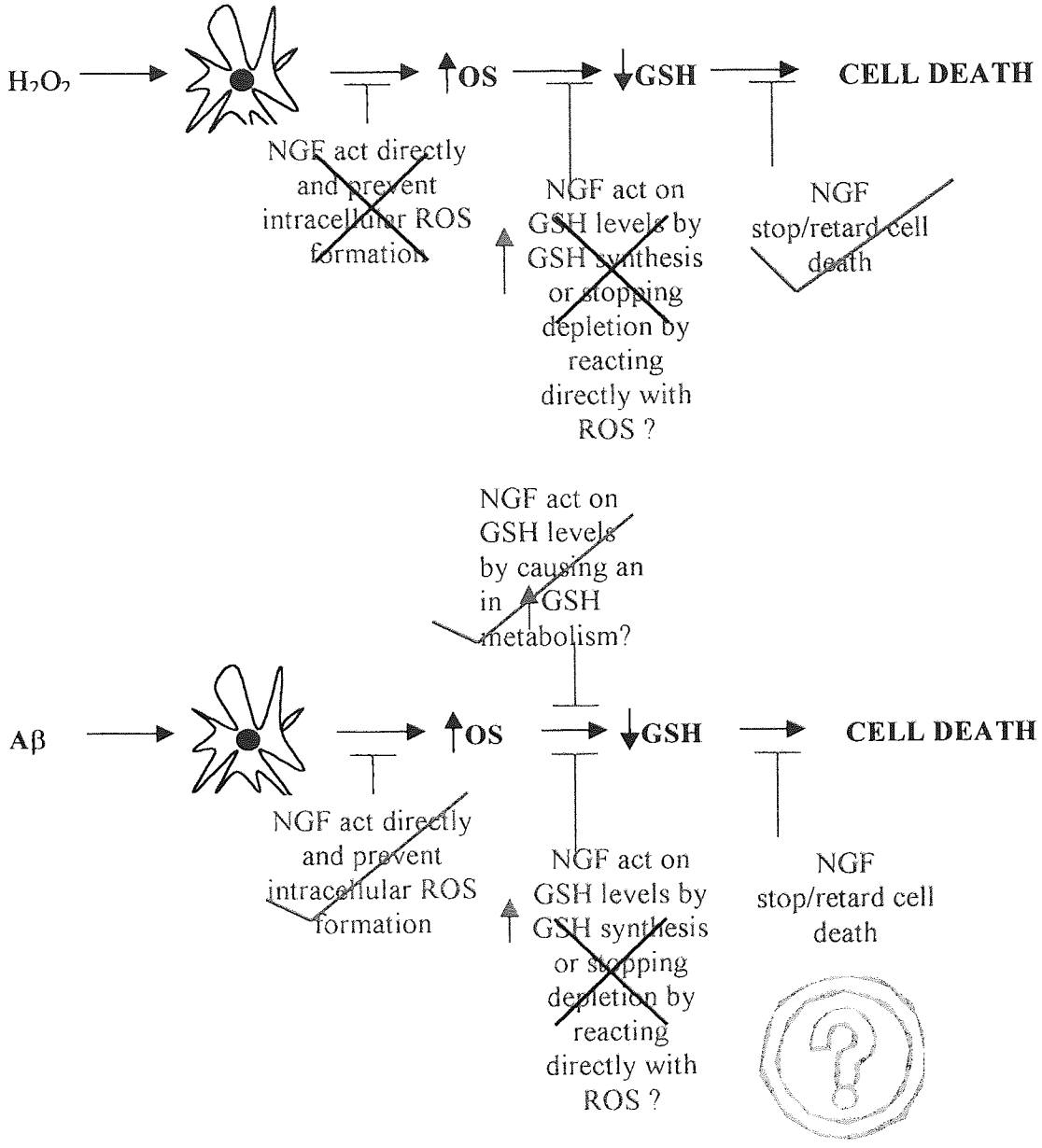

Although there are reductions recorded in some of the neurotrophic factors in AD brains, there are also increases recorded (Narisawa-Saito *et al.*, 1996). It has been shown that there are slightly elevated NGF protein levels in AD patients, whereas NGF mRNA levels remain normal. These data support the hypothesis that a defect in retrograde transport in AD prevents basal forebrain cholinergic neurons from obtaining adequate NGF to maintain normal function, despite sufficient levels of NGF synthesis

in target tissues (Fahnestock *et al.,* 1996). Hock *et al.,*(1998) have reported a reduced expression of the trkA receptor in the parietal cortex, which they have suggested may contribute to impaired NGF-trkA signalling and a reduced transport of NGF in cholinergic neurons. Further support of this theory was the finding that trkA expression was markedly decreased in the parietal cortex of AD patients, whilst the expression of other neurotrophin receptors and neurotrophins was unchanged. Their results reveal a central specific role of the high affinity NGF receptor during neurodegeneration in AD. Also, in contrast to the parietal cortex, the cerebellum is normally not affected by neuronal and synaptic loss in AD, and there was no evidence for reduced trkA expression. Mufson *et al.,* (1997) have also shown a reduction in both mRNA and one of the trkA receptor proteins within the nucleus basalis and frontal cortex in AD, further supporting the theory that it is not changes in NGF levels but receptor expression that are important. Herein, data has demonstrated a mechanism of NGF protection. It is now important to determine whether increasing receptor expression is a better therapy.

The mode of cell death was also investigated. Results showed H_2O_2 to exert its toxicity via an apoptotic means at low concentrations of OS, which changed to a necrotic means at higher OS concentrations. The data produced with Aβ was inconclusive, data showed Aβ to cause cell death via an apoptotic means at the concentrations tested, but testing was not as comprehensive as the analysis of H_2O_2 toxicity.

It is therefore now important to examine the subcellular distribution of this damage, which leads to cell death. For example an important target is the mitochondrion: Reports have shown a decrease in complex I and to a lesser extent in complex IV activities in old age, while complex II and III activities are mostly unaffected (Desai *et*

al., 1996). This is very critical because many subunits of complex I and IV are encoded by mitochondrial DNA whereas complex II is exclusively encoded by nuclear DNA (Richter, 1995). Mandavilli *et al.*, (2000) have shown in PD models that MPTP administration leads to extensive damage to the dopaminergic system and preferential DNA damage in mitochondria. They have also shown age-related increases in DNA damage in mitochondria, which clearly showed that ROS play a major role in aging and age-related neuronal degeneration. They proposed that the neurodegenerative process in 1-Methyl-4-phenyl-1,2,3,6-tetrahydropyridine (MPTP) toxicity may involve OS leading to mitochondrial damage which leads to more ROS, thus contributing to the vicious cycle and ultimately to cell death in the dopaminergic system. Shen *et al.*, (2001) have also clearly shown that mitochondria serve as the main target of $O_2^{\bullet-}$, which is capable of initiating an apoptotic process involving mitochondrial depolarization, cytochrome c release, caspase activation, and eventually irreversible apoptotic cell death.

Rational therapeutic approaches to treating AD are currently being developed that target Aβ production. Such approaches will certainly rely on measurement of Aβ, either in plasma or CSF to document efficacy. Other therapeutic approaches could include target the redox sensitive transcription factor binding sites in the promoter region of the APP gene. As there is a redox component, AOX may alter APP expression. Also the effect of AOX modulation on presenilins and their processing also merits study.

However, one of the dilemmas currently facing the pharmaceutical industry is who to treat with such drugs. If patients with early AD are treated, might anti-Aβ therapy be too little too late? The data presented in this thesis has only investigated 'pre-AD',

treating cell models before any stressors were applied, therefore further investigations are needed to investigate the effects of AA, NGF and BDNF, once a stressor is already present . Would the agents retard, eradicate or even potentiate any of the toxic effects? Clearly if the process is reversible, then such treatment may require the identification of individuals at risk prior to the development of disease. If the disease is already apparent, then a therapy greater than a simple preventative drug treatment may be required. Therefore it has been suggested that a major investment needs to be made in developing predicative tests for who will get the disease so that early pharmacological intervention can be initiated (Golde *et al.*, 2000).

8.2 Conclusion

In summary, the present research has established that the apoptotic effects of oxidative stress generated by either H_2O_2 or Aβ on neuronal cell models is protected against by NGF to varying degrees in the different cell models. The neuroprotection recorded was shown by reductions in morphological changes, increases in cell viability, decreases in protein carbonyls, changes in neuroprotective gene expression and modulations of GSH levels. AA showed a 'janus face' showing either antioxidant or prooxidant action depending on the situation. BDNF was also investigated, however only a few preliminary experiments were conducted which showed any effects to be inconclusive and therefore it warrants further investigations.

8.3 Further Work

Perhaps the first area I would highlight for study is the further investigations into glutathione. The current assays available for glutathione oxidised and reduced are very limiting, as they have no constant internal standards leading to variable results each time the assays were conducted. Levels of enzymes in the glutathione cycle would further clarify changes that are occurring in each paradigm tested. GPX is the enzyme that catalyses the conversion of GSH to GSSG alongside the decomposition of H_2O_2 to H_2O and $O_{2,}$, and it is particularly sensitive to inactivation under OS, however, it is also induced by the adaptive response at the transcriptional level.

The role of GPX in brain could be investigated *in vitro* using cell culture models. It would be interesting to determine the effects that varying concentrations of neurotrophins (such as NGF and BDNF) have on GPX activity and expression. Furthermore, the transfection of GPX cDNA neuronal cells, could be used to assess the role of this enzyme in greater detail. The interactions of the various neurotrophins through specific receptors could be investigated in this way.

Another area for further study is the investigation of the presence of GPX in adult human brain and adult human AD brain. It is necessary to repeat the experiments undertaken in this thesis in human samples. Although there may be differences present due to sample age and condition, some conclusions may be drawn from analysis in this area. Therefore what is the best model? The differentiated SY5Y cells seem to represent a good model, as they were human in origin, sensitive to neurotrophins and very susceptible to oxidative damage.

Further investigation is needed into the effects of neurotrophic factors on gene expression, initial results showed interesting changes in the genes studied. However only the effects of NGF on H_2O_2 insult were studied, and not that of Aβ. More work is needed investigating the effect of NGF on Aβ insult on gene changes.

Further investigation is also needed into intracellular peroxide production in all cell models. Initial data shows that NGF may be exerting its protective effect by reducing levels of intracellular peroxides. Results also showed further evidence indicative of Aβ cannot exert its toxicity without the bioavailability of iron. However further replicates and paradigms should be investigated. Also NGF co-incubation could be investigated, does NGF still exert a protective effect when co-incubated with insults?

Initial studies have also been completed using new proteomic technology with tertiary blotting for protein carbonyls that has become available within the laboratory. Initial results have shown in test samples that when comparing SY5Y cells treated with H_2O_2 and pre-treated with either PBS, AA or NGF results showed fewer protein carbonyls in AA pre-treated cells compared to controls and even fewer in NGF pre-treated cells. Gels showed fewer proteins (spots) with the AA and NGF treatments compared to controls. There were also dramatic differences in isoelectric focussing point (IEP) of the oxidised proteins resolved. In the control treated cells with peroxide challenge only, there was a spread of proteins across the gel (IPG pH 3-10 strips used), however in both the AA and NGF pre-treated peroxide challenged gels, the diversity of the spread was reduced, especially with NGF pre-treatment which caused a near wipe-out of proteins with an IEP in the middle of the gels (neutral proteins). Differentiated cells and their respective undifferentiated controls where also run through this system. Preliminary results

showed that undifferentiated cells expressed approximately 30% more proteins, however the differentiated cells showed greater expression of some of the common proteins, and also a higher number of positively charged proteins. However there were some similarities; both cell types expressed mainly negatively charged oxidised proteins as determined by the IEP in the same positions of the gels.

Further investigations into the effectiveness of peptides are also required, the majority of experiments were conducted using the N terminal Aβ peptides, specifically Aβ25-35. However Aβ25-35 has never actually been isolated from the brains of AD patients. The aggregation state of the peptides also warrants further work, it has been stated that Aβ 1-42 and Aβ1-43 are toxic more than 1-40, due to the aggregational conformations they can achieve which causes Aβ to be laid down as seeds during amyloid plaque formation (Wilfang *et al.*, 1997). Also the majority of work has been completed on the N-terminal peptides not the C-terminal peptides. However, as shown in chapter seven, C terminal fragments are far more toxic than N-terminal peptides. It has been suggested that CT_{105} can directly attack the cell membrane probably by making pores or non-selective ion channels, whereas it is suggested that Aβ impairs the intracellular metabolic pathway first (Kim & Suh, 1996).

CHAPTER NINE

REFERENCES

9. REFERENCES

Ackworth, I. N., and Bailey, B. (1995). The Handbook of Oxidative Metabolism. ESA Publication, USA.

Adamec, E., Vonsattel, J.-P., and Nixon, R. A. (1999). DNA strand breaks in Alzheimer's disease. *Brain Research* **849**, 67-77.

Aksenov, M. Y., Aksenova, M. V., Butterfield, D. A., Geddes, J. W., and Markesberry, W. R., (2001). Protein oxidation in the brain in Alzheimer's disease. *Neuroscience Letters* **103**, 373-383.

Allen, S. J., Wilcock, G. K., and Dawbarn, D. (1999). Profound and selective loss of catalytic TrkB immunoreactivity in Alzheimer's disease. *Biochemical and Biophysical Research Communications* **264**, 648-651.

Allsop, D., and Williams, C. H. (1994). Amyloidosis in Alzheimer's disease. *Biochemical Society Transactions* **22**, 171-175.

Ames, B. N. (1998). Micronutrients prevent cancer and delay aging. *Toxicology Letters* **102-103**, 5-18.

Anderson, M.E. (1997) Free radicals: a practical approach. Editors Punchard, N.A., and Kelly, F. J. IRL Press, Oxford.

Asensi, M., Sastre, J., Pallardo, F. V., Lloret, A., Lehner, M., Asuncion, J. G., and Vina, J. (1999). Ratio of Reduced to Oxidized Glutathione as Indicator of Oxidative Stress Status and DNA Damage. *Methods in Enzymology* **299**, 267-277.

Bains, J. S., and Shaw, C. A. (1997). Neurodegenerative disorders in humans: the role of glutathione in oxidative stress-mediated neuronal death. *Brain Research Reviews* **25**, 335-358.

Beal, M. F., Hyman, B. T., and Koroshetz, W. (1993). Do defects in mitochondrial energy metabolism underlie the pathology of neurodegenerative diseases? *Trends in the Neurosciences* **16 (4)**, 125-131.

Beasley, R., Thomson, C., and Pearce, N. (1991). Selenium, glutathione peroxidase and asthma. *Clinical and Experimental Allergy: Journal of the British Society for Allergy and Clinical Immunology* **21 (2)**, 157-149.

Behl, C., Davis, J., Cole, G. M., and Schubert, D. (1992). Vitamin E Protects Nerve Cells from Amyloid Beta Protein Toxicity. *Biochemica and Biophysic Acta* **186**, 944-950.

Behl, C., Davis, J. B., Klier, F. G., and Schubert, D. (1994a). Amyloid beta peptide induces necrosis rather than apoptosis. *Brain Research* **645**, 253-264.

Behl, C., Davis, J. B., Lesley, R., and Schubert, D. (1994b). Hydrogen Peroxide Mediates Amyloid Beta Protein Toxicity. *Cell Adhesion* 77, 817-827.

Benzi, G., and Moretti, A. (1995). Are Reactive Oxygen Species Involved in Alzheimer's Disease? *Neurobiology* **16**, 661-674.

Benzi, G., and Moretti, A. (1997). Glutathione in brain aging and neurodegenerative disorders in: C. A. Shaw (Ed), Glutathione in the Nervous System, Taylor & Francis, Washington DC.

Berlett, B. S., and Stadtman, E. R. (1997). Protein Oxidation in Aging, Disease, and Oxidative Stress. *The Journal of Biological Chemistry* **272**, 20313-20316.

Bertram, L., Blacker, D., Mullin, K., Keeney, D., Jones, J., Basu, S., Yhu, S., McInnis, M. G., Go, R. C. P., Vekrellis, K. et al (2000). Evidence for genetic linkage of Alzheimer's disease to chromosome 10q. *Science* **290**, 2302-2303

Blakely, W. F., Fuciarelli, A. F., Wegher, B.J. and Dizdaroglu, M. (1990). Hydrogen-peroxide-induced base damage in deoxyribonucleic acid. *Radiation Research* **121 (3)**, 338-343.

Borek, C. (1997). Antioxidants and cancer. *Science and Medicine* **November/December**, 53-61.

Bothwell, M. (1995).Functional interactions of neurotrophins and neurotrophin receptors. *Annual Review of Neuroscience* **18**, 223-253.

Bourdel-Marchasson, I., Delmas-Beauvieux, M.-C., Peuchan, E., Richard-Harston, S., Decamps, A., Reignier, B., Emeriau, J.-P., and Rainfray, M. (2001). Antioxidant defences and oxidative stress markers in erythrocytes and plasma from normally nourished elderly Alzheimer patients. *British Geriatrics Society* **30**, 235-241.

Bournat, J.C., and Allen, J.M. (2001). Regulation of the Y1 neuropeptide Y receptor gene expression in PC12 cells. *Molecular Brain Research* **90**, 149-164.

Bowen, C., Spiegel, S., and Gelmann, E. P. (1998). Radiation-induced apoptosis mediated by retinoblastoma protein. *Cancer Research* **58 (15)**, 3275-3281.

Bowling, A. C., Schulz, J. B., Brown Jr, R. H., and Beal, M. F. (1993). Superoxide dismutase activity, oxidative damage, and mitochondrial energy metabolism in familial amyotrophic lateral sclerosis. *Journal of Neurochemistry* **61 (6)**, 2322-2325.

Bowling, A. C., and Beal, M. F. (1995). Bioenergetic and Oxidative Stress in Neurodegenerative Diseases. *Life Sciences* **56**, 1151-1171.

Brenner, A. J., and Harris, E. D. (1995). A quantitive test for copper using bicinchonic acid. *Analytical Biochemistry* **226**, 80-84.

Brown, T. A. (1995). Genetics: a molecular approach. Second edition. Chapman & Hall, London.

Brown, R. E., Jarvis, K. L., and Hyland, K. J. (1989). Protein measurement using bicinchonic acid: elimination of interfering substances. *Analytical Biochemistry* **180 (1)**, 136-139.

Bruce, A. J., Bose, S., Fu, W., Butt, C. M., Mirault, M.-E., Tanigucji, N., and Mattson, M. P. (1997). Amyloid β-peptide alters the profile of antioxidant enzymes in hippocampal cultures in a manner similar to that observed in Alzheimer's disease. *Pathogenesis* **1**, 15-30.

Buss, H., Chan, T. P., Sluis, K. B., Domigan, N. M., and Winterbourn, C. C. (1997). Protein Carbonyl Measurement by a Sensitive ELISA Method. *Free Radical Biology & Medicine* **23**, 361-366.

Butterfield, D. A., Drake, J., Pocernich, C., and Castegna, A. (2001). Evidence of oxidative damage in Alzheimer's diease brain: central role for amyloid β-peptide. *Trends in Molecular Medicine* **7 (12)**, 548-554.

Butterfield, D. A., Howard, B., Yatin, S., Koppal, T., Drake, J., Hensley, K., Aksenov, M., Aksenova, M., Subramaniam, R., Varadarajan, S., Harris-White, M. E., Pedigo, N. W. Jr., and Carney, J. M. (1999). Elevated oxidative stress in models of normal brain aging and Alzheimer's disease. *Life Sciences* **65 (18-19)**, 1883-1892.

Buttke, T. M., and Sandstrom, P. A. (1994). Oxidative stress as a mediator of apoptosis. *Immunology Today* **15**, 7-10.

Cacabelos, R., Takeda, M., and Winbald, D. (1999). The glutamatergic system and neurodegeneration in dementia: Preventive strategies in Alzheimer's disease. *International Journal of Geriatric Psychiatry* **14**, 3-47.

Cadenas, E., and Davies, K. J. A. (2000). Mitochondrial free radical generation, oxidative stress, and aging. *Free Radical Biology and Medicine* **29 (3/4)**, 222-230.

Camougrand, N. and Rigoulet, M. (2001). Aging and oxidative stress: studies of some gene involved both in aging and in response to oxidative stress. *Respiration Physiology* **128**, 393-401.

Carter, D., and Murphy, D. (1999). Molecular Neuroscience. Longman Publishing, England.

Cassarino, D. S., and Bennett Jr., J. P. (1999). An evaluation of the role of mitochondria in neurodegenerative diseases: mitochondrial mutations and oxidative pathology, protective nuclear responses, and cell death in neurodegeneration. *Brain Research Reviews* **29**, 1-25.

Chandra, J., Samali, A., and Orrenius, S. (2000). Triggering and modulation of apoptosis by oxidative stress. *Free Radical Biology & Medicine* **29**, 323-333.

Chanvitayapongs, S., Draczynska-Lusiak, B., and Sun, A. Y. (1997). Amelioration of oxidative stress by antioxidants and resveratrol in PC12 cells. *NeuroReport* **8**, 1499-1502.

Cirulli, F. (2001). Role of environmental factors on brain development and nerve growth factor expression. *Physiology & Behaviour* **73**, 321-330.

Connor, B., Young, D., Lawlor, P., Gai, W., Waldvogel, H., Faull, R. L. M., and Dragunow, M. (1996). Trk receptor alterations in Alzheimer's disease. *Molecular Brain Research* **42**, 1-17.

Connor, B., Young, D., Yan, Q., Faull, R. L. M., Synek, B., and Dragunow, M. (1997). Brain-derived neurotrophic factor is reduced in Alzheimer's disease. *Molecular Brain Research* **49**, 71-81.

Creagh, E. M., and Martin, S. J. (2001). Caspases:cellular demolition experts. *Biochemical Society Transactions* **29**, 696-702.

Darzynkiewicz, Z., Bedner, E., Tragnos, F., and Murakami, T. (1998). Critical aspects in the analysis of apoptosis and necrosis. *Human Cell* **11 (1)**, 3-12.

Darzynkiewicz, Z., and Li, X. (1997). Measurements of cell death by flow cytometry. From Techniques in apoptosis: a user's guide edited Cotter, T. G., and Martin, S. J. Portland Press, London.

Davis, W., Ronai, J., and Tew, K. D. (2001). Cellular thiols and reactive oxygen species in drug-induced apoptosis.*Journal of Pharmacology and Experimental Therapeutics* **296**, 1-5.

Dean, T. R., Fu, S., Stocker, R., and Davies, M. (1997). Biochemistry and pathology of radical-mediated protein oxidation. *Biochemical Journal* **324**, 1-18.

Denisova, N. A., Cantuti-Castelvetri, I., Hassan, W. N., Paulson, K. E., and Joseph, J. A. (2001). Role of membrane lipids in regulation of vulnerability to oxidative stress in PC12 cells: Implication for aging. *Free Radical Biology & Medicine* **30**, 671-678.

Desai, V. G., Feuers, R. J., Hart, R. W., and Ali, S. F. (1996) MPP+ induced neurotoxicity in mouse is age dependent. Evidence by selective inhibition of complexes of electron transporter. *Brain Research* **715**, 1-8.

de Strooper, B. D., and König, G. (2001). An inflammatory drug prospect. *Nature* **414**, 159-160.

Draczynska-Lusiak, B., Chen, Y. M., and Sun, A. Y. (1998). Oxidized lipoproteins activate NF-KB binding activity and apoptosis in PC12 cells. *NeuroReport* **9**, 527-532.

Dringen, R. (2000). Metabolism and functions of glutathione in brain. *Progress in Neurobiology* **62**, 649-671.

Dudek, E. J., Shang, F., and Taylor, A. (2001). H_2O_2-mediated oxidative stress activated NF-kB in lens epithelial cells. *Free Radical Biology & Medicine* **31 (5)**, 651-658.

Duguid, J. R., Bohmont, C. W., Liu, N., and Tourrellotte, W. W. (1989). Changes in brain gene expression shared by scrapie and Alzheimer disease. *Proceedings National Academy of Sciences* **86**, 7260-7264.

Duke, R. C., Ojcius, D. M., and Young, J.-E. (1996). Cell suicide in health and disease. *Scientific American* **December**, 48-55.

Du Yan, S., Chen, X., Fu, J., Chen, M., Zhu, H., Roher, A., Slattery, T., Zhao, L., Nagashima, M., Morser, J., Migheli, A., Naworth, P., Stern, D., and Schmidt, A. M. (1996). RAGE and amyloid-beta peptide neurotoxicity in Alzheimer's disease. *Nature* **382**, 685-691.

Ekinci, F. J., Linsley, M. D., and Shea, T. B. (2000). Beta-Amyloid-induced calcium influx induces apoptosis in culture by oxidative stress rather than tau phosphorylation. *Molecular Brain Research* **76**, 389-395.

El Mouatassim, S., Guerin, P., and Menezo, Y. (2000). Mammalian oviduct and protection against free oxygen radicals: expression of genes encoding antioxidant enzymes in human and mouse. *European Journal of Obstetrics and Gynecology and Reproductive Biology* **89**, 1-6.

Encinas, M., Iglesias, M., Llecha, N., and Comella, J. X. (1999). Extracellular-Regulated Kinases and Phosphatidylinositol 3-Kinase Are Involved in Brain-Derived Neurotrophic Factor-Mediated Survival and Neuritogenesis of the Neuroblastoma Cell Line SH-SY5Y. *Journal of Neurochemistry* **73**, 1409-1421.

Enkinci, F. J., Linsley, M-D., and Shea, T. B. (2000). β-Amyloid-induced calcium influx induces apoptosis in culture by oxidative stress rather than tau phosphorylation. *Molecular Brain Research*, **76**, 389-395.

Ertekin-Taker, N., Graff-Radford, N., Younkin, L. H., Eckman, C., Baker, M., Adamson, J., Roland, J., Blangero, J., Hutton, M., and Younkin, S. G. (2000). Linkage of plasma Aβ42 to a quantitative locus on chromosome 10 in late-onset Alzheimer's disease pedigrees. *Science* **290**, 2303-2304.

Esteve, J. M., Mompo, J., Garcia De La Asuncion, J., Sastre, J., Asensi, M., Boix, J., Vina, J. R., Vina, J., and Pallardo, F. V. (1999). Oxidative damage to mitochondrial DNA and glutathione oxidation in apoptosis: studies in vivo and in vitro. *FASEB Journal* **13**, 1055-1064.

Evans, P., Lyras, L., and Halliwell, B. (1999). Measurement of Protein Carbonyls in Human Brain Tissue. *Methods: A Companion to Methods in Enzymology* **309**, 145-156.

Fagarasan, M. O., and Efthimiopoulos, S. (1996). Mechanism of amyloid β-peptide (1-42) toxicity in PC12 cells. *Molecular Psychiatry* **1**, 398-403.

Fahnestock, M., Scott, S. A., Jette, N., Weingartner, J.A., Crutcher, K.A. (1996). Nerve growth factor mRNA and protein levels measured in the same tissue from normal and Alzheimer's disese parietal cortex. *Molecular Brain Research* **42**, 175-178.

Fine, R. E. (1999). The Biochemistry of Alzheimer Disease. *Alzheimer's Disease and Associated Disorders* **13**(Supplement 1), S82-S87.

Fiorucci, S., Santucci, L., Federici, B., Antonelli, E., Distrutti, E., Morelli, O., Di Renzo, G., Coata, G., Cirino, G., Del Soldato, P. and Morelli, A. (1999). Nitric oxide-releasing NSAIDs inhibit interleukin-1β converting enzyme-like cysteine proteases and protect endothelial cells from apoptosis induced by TNFα. *Aliment Pharmacology Therapy* **13**, 421-435.

Forloni, G., Chiesa, R., Smiroldo, S., Verga, L., Salmona, M., Tagliavini, F., and Angeretti, N. (1993). Apoptosis mediated neurotoxicity induced by chronic application of beta amyloid fragment 25-35. *NeuroReport* **4**, 523-526.

Fratiglioni, L. (1996). Epidemiology of Alzheimer's disease and current possibilities for prevention. *Acta Neurologic Scandinavia*(**Supplement. 165**), 33-40.

Frei, B. (1994). Reactive Oxygen Species and Antioxidant Vitamins: Mechanisms of Action. *The American Journal Of Medicine* **97** (Supplement. 3A), 5S-13S.

Fridovich, I. (1998). Oxygen toxicity:A radical explanation. *The Journal of Experimental Biology* **201**, 1203-1209.

Froissard, P. and Duval, D. (1994). Cytotoxic effects of glutamic acid on PC12 cells. *Neurochemistry International* **24(5)**, 485-493.

Froissard, P., Monrocq, H., and Duval, D. (1997). Role of glutathione metabolism in the gluatamate-induced programmed cell death of neuronal-like PC12 cells. *European Journal of Pharmacology* **326**, 93-99.

Gabaizadeh, R., Staecker, H., Liu, W., and Van De Water, T. R. (1997). BDNF protection of auditory neurons from cisplatin involves changes in intracellular levels of both reactive oxygen species and glutathione. *Molecular Brain Research* **50**, 71-78.

Garcia-Ruiz, C., Colell, A., Morales, A., Kaplowitz, N., Fernandez-Checa, J. C. (1995). Role of oxidative stress generated from the mitochondrial electron transport chain and mitochondrial glutathione status in loss of mitochondrial function and activation of transcription factor-kappa B: studies with isolated mitochondria and rat hepatocytes. *Molecular Pharmacology* **48**, 825-834.

Gershon, D. (1999). The mitochondrial theory of aging: Is the culprit a faulty disposal system rather than indigenous mitochondrial alterations? *Experimental Gerontology* **34**, 613-619.

Ghibelli, L., Coppola, S., Rotilio, G., Lafavia, E., Maresca, V., and Ciriolo, M. R. (1995). Non-Oxidative Loss of Glutathione in Apoptosis via GSH Extrusion. *Biochemica et Biophysica acta* **216**, 313-320.

Glenner, G. G., and Wong, C. W. (1984). Alzheimer's disease: initial report of the purification and characterization of a novel cerebrovascular amyloid protein. *Biochemical and Biophysical Research Communications* **120**, 885-890

Golde, T. E., Eckman, C. B. and Younkin, S. G. (2000). Biochemical detection of Aβ isoforms: implications for pathogenesis, diagnosis, and treatment of Alzheimer's disease. *Biochimica et Biophysica acta* **1502,** 172-187.

Good, P. F., Werner, P., Hsu, A., Olanow, C. W., and Perl, D. P. (1996). Evidence of neuronal oxidative damage in Alzheimer's Disease. *American Journal of Pathology* **149 (1)**, 21-28.

Gozes, I. (2001). Neuroprotective peptide drug delivery and development:potential new therapeutics. *Trends in the Neurosciences* **24**, 700-705.

Greene, L. A., and Tischler, A. S. (1976). Establishment of a noradrenergic clonal line of rat adrenal pheochromocytoma cells which respond to nerve growth factor. *Proceedings National Academy of Sciences* **73**, 2424-2428.

Griffiths, H. R. (2000). Antioxidants and Protein Oxidation. *Free Radical Research* **33**, S47-S58

Griffiths, H. R., and Lunec, J. (2001). Ascorbic acid in the 21st century- more than a simple antioxidant. *Environmental Toxiciology and Pharmacolgy* **10**, 173-182

Gschwind, M., and Huber, G. (1995). Apoptotic cell death induced by β-Amyloid 1-42 peptide is cell type dependent. *Journal of Neurochemistry* **65**, 292-300.

Hagg, T., Fass-Holmes, B., Vahlsing, H. L., Manthorpe, M., Conner, J. M., and Varon, S. (1989). Nerve growth factor (NGF) reverses axotomy-induced decreases in choline acetyltransferase, NGF receptor and size of medial septum cholinergic neurons. *Brain Research* **505**, 209-238.

Hagg, T., Manthorpe, M., Vahlsing, H. L., and Varon, S. (1988). Delayed treatment with nerve growth factor reverses the apparent loss of cholinergic nbeurons after acute brain damage. *Experimental Neurology* **101**, 303-312

Hall, L. L., Bicknell, G. R., Primrose, L., Pringle, J. H., Shaw, J. A., and Furness, P. N. (1998). Reproducibility in the quantification of mRNA levels by RT-PCR ELISA and RT competitive-PCR ELISA. *Biotechniques* **24 (4)**, 652-658.

Hall, A. G. (1999). The role of glutathione in the regulation of apoptosis. *European Journal of Clinical Investigations* **29**, 238-245.

Halliday, G. M., Shepherd, C. E., McCann, H., Redid, W. G. J., Grayson, D. A., Broe, A., and Kril, J. J. (2000). Effect of anti-inflammatory medications on neuropathlogical findings in Alzheimer disease. *Acta Neurologica* **57**, 831-836

Halliwell, B. (1999). Vitamin C: poison,prophylactic or panacea? *Trends in the Biological Sciences* **24**, 255-259.

Halliwell, B., Clement, M. V., and Long, L. H. (2000). Hydrogen peroxide in the human body. *FEBS Letters* **486**, 10-13.

Halliwell, B., Clement, M. V., and Ramalingma, J., and Long, L. H. (2000). Hydrogen Peroxide. Ubiquitous in cell culture and *in vivo*? *IUBMB Life*, **50**, 251-257.

Hansen, M. B., Nielsen, S. E., and Berg, K. (1989). Re-examination and further development of a precise and rapid dye method for measuring cell growth/ cell kill. *Journal of Immunological Methods* **119**, 203-210.

Harmon, B. V., Winterford, C. M., O'Brien, B. A., and Allan, D. J. (1998). Morphological Criteria for Identifying Apoptosis. *Cell Biology: A Laboratory handbook* **2nd edition**, 327-340.

Hartell, N. A., and Suh Y.-H. (2000). Peptide fragments of β-amyloid precursor protein: effects on parallel fiber- Purkinje Cell synaptic transmission in rat cerebellum. *Journal of Neurochemistry* **74**, 1112-1121.

Hayes, J. D., and McLellan, L. I. (1999). Glutathione and glutathione-dependent enzymes represent a co-ordinately regulated defence against oxidative stress. *Free Radical Research* **31**, 273-300.

Helbock, H. J., Beckman, K. B., and Ames, B. N. (1999). 8-Hydroxydeoxyguanosine and 8-hydroxyguanine as biomarkers of oxidative DNA damage. *Methods in Enzymology* **300**, 156-166.

Hengartner, M. (1998). Death by Crowd Control. *Science* **281**, 1298-1299.

Hock, C., Hesse, K., Hulette, C., Rosenberg, C., and Otten, U. (2000). Region-specific neurotrophin imbalances in Alzheimer's disease. *Archives of Neurology* **57**, 846-851.

Hock, C., Heese, K. Muller-Spahn, F., Hulette, C., Rosenberg, C., and Otten, U. (1998). Decreased trkA neurotrophin receptor expression in the parietal cortex of patients with Alzheimer's disease. *Neuroscience Letters* **241**, 151-154.

Hockenberry, D. M., Oltvai, Z. N., Yin, X. M., Milliman, C. L., and Korsmeyer, S. J. (1993). Bcl-2 functions in an antioxidant pathway to prevent apoptosis. *Cell* **75**, 241-251.

Holscher, C. (1998). Possible causes of Alzheimer's disease: amyloid fragments, free radicals, and calcium homeostasis. *Neurobiology of Disease* **5**, 129-141.

Holsinger, R. M. D., Schnarr, J., Henry, P., Castelo, V. T., and Fahnestock, M. (2000). Quantitation of BDNF mRNA in human parietal cortex by competitive reverse transcription-polymerase chain reaction: decreased levels in Alzheimer's disease. *Molecular Brain Research* **76**, 347-354.

Hoy, A., Leininger-Muller, B., Jolivalt, C., and Siest, G. (2000). Effect of apolipoprotein E on cell viability in a human neuroblastoma cell line: influence of oxidation and lipid-association. *Neuroscience Letters* **285**, 173-176.

Hoyer, S. (1996). Oxidative metabolism deficiencies in brains of patients with Alzheimer's disease. *Acta Neurologica Scandinavia* **(Suppl. 165)**, 18-24.

Hu, J., Ferreira, A., and Van Eldik, L. J. (1997). S100beta induces neuronal cell death through nitric oxide release from astrocytes. *Journal of Neurochemistry* **69 (6)**, 2294-2301.

Hu, H.-L., Forsey, R. J., Blades, T. J., Barratt, M. E. J., Parmar, P., and Powell, J. R. (2000). Antioxidants may contribute in the fight against ageing: an in vitro model. *Mechanisms of Ageing and Development* **121**, 217-230.

Huang, X., Atwood, C. S., Hartshorn, M. A., Multhaup, G., Goldstein, L. E., Scarpa, R. C., Cuajungco, M. P., Gray, D. N., Lim, J., Moir, R. D., Tanzi, R. E., and Bush, A. I. (1999). The Aβ Peptide of Alzheimer's disease directly produces hydrogen peroxide through metal ion reduction. *Biochemistry* **38**, 7609-7616.

Hurley, A. C., and Wells, N. (1999). Past, present, and future directions for Alzheimer research. *Alzheimer's Disease and Associated Disorders* **13**(Supplement 1), S6-S10.
Ishitani, R., Kimura, M., Sunaga, K., Katsube, N., Tanaka, M., and Chuang, D. M. (1996). An antisense oligodeoxynucleotide to glyceraldehyde-3-phosphate dehydrogenase blocks age-induced apoptosis of mature cerebrocortical neurons in culture. *The Journal of Pharmacology and Experimental Therapeutics* **278 (1)**, 447-454.

Ibi, M., Sawada, H., Kime, T., Katsuki, H., Kaneko, S., Shimohama, S., and Akaike, A. (1999). Depletion of intracellular glutathione increases susceptibility to nitric oxide in mesencephalic dopaminergic neurons. *Journal of Neurochemistry* **73**, 1696-1703.

Isobe, I., Michikawa, M., and Yanagisawa, K. (1999). Enhancement of MTT, a tetrazolium salt, exocytosis by amyloid beta-protein and chloroquine in cultured rat astrocytes. *Neuroscience Letters* **266**, 129-132.

Ito, M., Sakai, N., Ito, K., Mizobe, F., Hanada, K., and Mizoue, K. (1999). A novel fungal metabolite NG-061 enhances and mimics neurotrophic effect of nerve growth factor (NGF) on neurite outgrowth in PC12 cells. *Journal of Antibiotics (Tokyo)* **52 (3)**, 224-230.

Iversen, L. L., Mortishire-Smith, R. J., Pollack, S. J., and Shearman, M. S. (1995). The toxicity in vitro of beta-amyloid protein. *Biochemical Journal* **311**, 1-16.

Iwata, E., Asanuma, M., Nishibayashi, S., Kondo, Y., and Ogawa, N. (1997). Different effects of oxidative stress on activation of transcription factors in primary cultured rat neuronal and glial cells. *Molecular Brain Research* **50**, 213-220.

Jakubowski W., and Bartosz, G. (2000). 2,7-dichlorofluorescin oxidation and reactive oxygen species: what does it measure? *Cell Biology International* **24 (10)**, 757-760.

Jang, J.-H., and Surh, Y.-J. (2001). Protective effects of resveratrol on hydrogen peroxide-induced apoptosis in rat pheochromocytoma (PC12) cells. *Mutation Research* **496**, 181-190.

Jiang, D., Jha, N., Boonplueang, R., and Andersen, J. K. (2001). Caspase 3 inhibition attenuates hydrogen peroxide-induced DNA fragmentation but not cell death in neuronal PC12 cells. *Journal of Neurochemistry* **76**, 1745-1755.

Joaquin, A. M., and Gollapudi, S. (2001). Functional Decline in Aging and Disease: A Role for Apoptosis. *Functional Decline in Aging* **49**, 1234-1240.

Johal, K., and Hanson, P. (2000) Opposite effects of flurbiprofen and the nitroxybutyl ester of flurbiprofen on apoptosis in cultured guinea-pig gastric mucous cells. *British Journal of Pharmacology* **130 (4)**, 811-818.

Kamata, H., Tanaka, C., Yagisawa, H., and Hirata, H. (1996). Nerve growth factor and forskolin prevent H_2O_2-induced apoptosis in PC12 cells by glutathione independent mechanism. *Neuroscience Letters* **212**, 179-182.

Kane, D. J., Sarafian, T. A., Anston, R., Hahn, H., Gralla, E. B., Valentine, J. S., Ord, T., and Bredesen, D. E. (1993). Bcl-2 inhibition of neural death: decreased generation of reactive oxygen species. *Science* **262**, 1274-1277.

Kaplan, D. R., Matsumoto, K., Lucarelli, E., and Thiele, C. J. (1993). Induction of TrkB by retinoic acid mediates biologic responsiveness to BDNF and differentiation of human neuroblastoma cells. *Neuron* **11**, 321-331.

Kasapoglu, M., and Ozben, T. (2001). Alterations of antioxidant enzymes and oxidative stress markers in aging. *Experimental Gerontology* **36**, 209-220.

Kehrer, J. P. (2000). The Haber-Weiss reaction and mechanisms of toxicity. *Toxicology* **149**, 43-50.

Khan, A. U., and Kasha, M. (1994). Singlet molecular oxygen in the Haber-Weiss reaction. *Proceedings National Academy of Sciences* **91**, 12365-12367.

Kim, S,-H., Lee, J.-H., and Suh, Y.-H. (1999a). C-terminal fragment of Alzheimer's amyloid precursor protein inhibits sodium/calcium exchanger activity in SK-N-SH cell. *NeuroReport* **10**, 113-116.

Kim, S.–H., and Suh, Y-H. (1996). Neurotoxicity of a carboxyl-terminal fragment of the Alzheimer's amyloid precursor protein. *Journal of Neurochemistry* **67**, 1172-1182.

Kim, Y.-M., Chung, H.-T., Kim, S.-S., Han, J.-A., Yoo, Y.-M., Kim, K.-M., Lee, G.-H., Yun, H.-Y., Green, A., Li, J., Simmons, R. L., and Billiar, T. R. (1999b). Nitric oxide protects PC12 cells from serum deprivation-induced apoptosis by cGMP-dependent inhibition of caspase signaling. *The Journal of Neuroscience* **19**, 6740-6747.

Kim, S., Wilson, J. J., Allen, K. G. D., and Clarke, S. D. (1996). Suppresion of renal γ-glutamylcysteine synthase expression in dietary copper deficiency. *Biochimica et Biophysica Acta* **1313**, 89-94.

Kitani, K., Kanai, S., Ivy, G. O., and carrillo, M. C. (1999). Pharmacological modifications of endogenous antioxidant enzymes with special reference to the effects of

deprenyl: a possible antioxidant strategy. *Mechanisms of Ageing and Development* **111 (2-3)**, 211-221.

Klaunig, J. E., Xu, Y., Isenberg, J. S., Bachowski, S., Kolaja, K. L., Jiang, J., Stevenson, D. E., and Walborg Jr., E. F. (1998). The role of oxidative stress in chemical carcinogenesis. *Environmental Health Prospectives* **106 (Supplement 1)**, 289-295.

Kleinman, W. A., and Richie Jr, J. P. (2000). Status of glutathione and other thiols and disulphides in human plasma. *Biochemical Pharmacology* **60**, 19-29.

Kohring, K., and Zimmermann, H. (1998). Upregulation of ecto-5'-nucleotidase in human neuroblastoma SH-SY5Y cells on differentiation by retinoic acid or phorbolester. *Neuroscience Letters* **258**, 127-130.

Kuner, P., Schubenel, R., and Hertel, C. (1998). βA binds to p75 NTR and activates NF-κB in human neuroblastoma cells. *Journal of Neuroscience Research* **54**, 798-804.

Levi-Montalcini, R. and Hamburger, V. (1951). Selective growth stimulating effects of mouse sarcoma on the sensory and sympathetic nervous system of chick embryo. *Journal of Experimental Zoology* **116**, 321-361.

Levine, R. L., and Stadtman, E. R. (2001). Oxidative modification of proteins during aging. *Experimental Gerontology* **36**, 1495-1502.

Li, Y.-P., Bushnell, A. F., Lee, C.-M., Perlmutter, L. S., and Wong, S. H.-F. (1996). β-amyloid induces apoptosis in human derived neurotypic SH-SY5Y cells. *Brain Research* **739**, 196-204.

Lightowlers, R. N., Jacobs, H. T., and Kajander, O. A. (1999). Mitochondrial DNA – All things bad? *Trends in Genetics* **15 (3)**, 91-93

Lillycrop, K. A., Budrahan, V. S., Lakin, N. D., Terrenghi, G., Wood, J. N., Polak, J. M., and Latchman, D. S. (1992). A novel POU family transcription factor is closely related to Brn-3 but has a distinct expression pattern in neuronal cells. *Nucleic Acids Research* **20(19)**,

Limoli, C. L., Hartmann, A., Shephard, L., Yang, C., Boothman, D. A., Bartholomew, J., and Morgan, W. F. (1998). Apoptosis, reproductive failure and oxidative stress in chinese hamster ovary cells with compromised genomic integrity. *Cancer Research* **58**, 3712-3718.

Lindenboim, L., Haviv, R., and Stein, R. (1995). Inhibition of Drug-Induced Apoptosis by Survival Factors in PC12 Cells. *Journal of Neurochemistry* **64**, 1054-1063.

Linton, S., Davies, M. J., and Dean, R. T. (2001). Protein oxidation and ageing. *Experimental Gerontology* **36**, 1503-1518.

Lledias, F., Rangel, P., and Hansberg, W. (1998). Oxidation of catalase by singlet oxygen. *The Journal of Biological Chemistry* **273 (17)**, 10630-10637.

Loo, D. T., Copani, A., Pike, C. J., Whittemore, E. R., Walencewicz, A. J., and Cotman, C. W. (1993). Apoptosis is induced by beta-amyloid in cultured central nervous system neurons. *Neurobiology* **90**, 7951-7955.

Lovell, M. A., Ehmann, W. D., Butler, S. M., and Markesberry, W. R. (1995). Elevated thiobarbituric acid-reactive substances and antioxidant enzyme activity in the brain in Alzheimer's disease. *Neurology* **45**, 1594-1601.

Lyras, L., Cirns, N. J., Jenner, A., Jenner, P., and Halliwell, B. (1997). An Assessment of Oxidative Damage to Proteins, Lipids, and DNA in Brain from Patients with Alzheimer's Disease. *Journal of Neurochemistry* **68**, 2061-2069.

Majima, H. T., Oberley, T. D., Furukawa, K., Mattson, M. P., Yen, H. C., Szweda, L. I., and St Clair, D.K. (1998). Prevention of mitochondrial injury by manganese superoxide dismutase reveals a primary mechanism for alkaline-induced cell death. *The Journal of Biological Chemistry* **273 (14),** 8217-8224.

Makar, T. K., Cooper, A. J. L., Tofel-Grehl, B., Thaler, H. T., and Blass, J. P. (1995). Carnitine, carnitine acetyltransferase, and glutathione in Alzheimer brain. *Neurochemical Research* **20**, 705-711.

Makar, T. K., Nedergaard, M., Preuss, A., Gelbard, A. S., Perumal, A. S., and Copper, A. J. L. (1994). Vitamin E, ascorbate, glutathione, glutathione disulphide, and enzymes of glutathione metabolism in cultures of chick astrocytes and neurons: Evidence that astrocytes play an important role in antioxidative processes in the brain. *Journal of Neurochemistry* **62**, 45-53.

Mandavilli, B. S., Ali, S. Y., and van Houten, B. (2000). DNA damage in brain mitochondria caused by aging and MPTP treatment. *Brain Research* **885**, 45-52.

Marcus, D. L., Thomas, C., Rodriguez, C., Simberkoff, K., Tsai, J. S., Strafaci, J. A., and Freedman, M. L. (1998). Increased peroxidation and reduced antioxidant enzyme activity in Alzheimer's disease. *Experimental Neurology* **150 (1)**, 40-44.

Markesberry, W. R., and Carney, J. M. (1999). Oxidative alterations in Alzheimer's disease. *Brain Pathology* **9**, 133-146.

Martin, D., Salinas, M., López-Valdaliso, R., Serrano, E., Recuero, M., and Cuadrado, A. (2001). Effect of the Alzheimer amyloid fragment Aβ(25-35) on Akt/PKB kinase and survival of PC12 cells. *Journal of Neurochemistry* **78**, 1000-1008.

Mason, P. (1995). Antioxidant Supplements: Should they be recommended? *The Pharmaceutical Journal* **254**, 264-266.

Mates, J. M. (2000). Effects of antioxidant enzymes in the molecular control of reactive oxygen species toxicology. *Toxicology* **153**, 83-104.

Mates, J. M., and Sanchez-Jimenez, F. M. (2000). Role of reactive oxygen species in apoptosis: implications for cancer therapy. *International Journal of Biochemistry and Cell Biology* **32**, 157-170.

Matsuoka, Y., Picciano, M., La Francois, J. and Duff, K. (2001). Fibrillar beta-amyloid evokes oxidative damage in a transgenic mouse model of Alzheimer's disease. *Neuroscience* **104 (3)**, 609-613.

Mazziotti, M., and Perlmutter, D. H. (1998). Resistance to the apoptotic effect of aggregated amyloid-beta peptide in several different cell types including neuronal- and hepatoma- derived cell lines. *Biochemical Journal* **332**, 517-524.

Mecocci, R., Beal, M. F., Cecchetti, R., Polidori, M. C., Cherubini, A., Chionne, F., Avellni, L., Romano, G., and Senin, U. (1997) Mitochondrial membrane fluidity and oxidative damage to mitochondrial DNA in aged and AD human brain. *Molecular and Chemical Neuropathology* **31 (1)**, 53-64.

Miller, L. J., and Marx, J. (1998). Apoptosis. *Science* **281**, 130.

Miranda, S., Opazo, C., Larrondo, L. F., Muñoz, F. J., Ruiz, F., Leighton, F., and Inestrosa, N. C. (2000). The role of oxidative stress in the toxicity induced by amyloid β-peptide in Alzheimer's disease. *Progress in Neurobiology* **62**, 633-648.

Misonou, H., Morishima-Kawashima, M., and Ihara, Y. (2000). Oxidative stress induces intracellular accumulation of amyloid β protein (Aβ) in human neuroblastoma cells. *Biochemistry* **39**, 6951-6959.

Monji, A., Utsumi, H., Ueda, T., Imoto, T., Yoshida, I., Hashioka, S., tashiro, K., and Tashiro, N. (2001). The relationship between the aggregational state of the amyloid-β peptides and free radical generation by the peptides. *Journal of Neurochemistry***77**, 1425-1432.

Mookherjee, P., and Johnson, G. V. W. (2001). Tau phosphorylation during apoptosis of human SH-SY5Y neuroblastoma cells. *Brain Research* **921**, 31-43.

Morel, Y. and Barouki, R. (1999). Repression of gene expression by oxidative stress. *Biochemical Journal* **342**, 481-496.

Moriya, R., Uehara, T., and Nomura, Y. (2000). Mechanism of nitric oxide-induced apoptosis in human neuroblastoma SH-SY5Y cells. *FEBS Letters* **484**, 253-260.

Morris, M. C., Beckett, L. A., Scherr, P. A., Hebert, L. E., Bennett, D. A., Field, T. S., and Evans, D. A. (1998). Vitamin E and Vitamin C supplement use and risk of incident Alzheimer disease. *Alzheimer's Disease and Associated Disorders* **12**, 121-126.

Mulcahy, R. T., Wartman, M. A., Bailey, H. H., and Gipp, J. J. (1997). Constitutive β-naphthoflavone-induced expression of the human γ-glutamylcysteine synthetase heavy subunit gene is regulated by a distal antioxidant response element/TRE sequence. *Journal of Biological Chemistry* **272**, 7445-7454.

Murer, M. G., Yan, Q., and Raisman-Vozari, R. (2001). Brain-derived neurtotrophic factor in the control human brain, and in Alzheimer's disease and Parkinson's disease. *Progress in Neurobiology* **63**, 71-124.

Muroya, K., Hattori, S., and Nakamura, S. (1992). Nerve growth factor induces rapid accumulation of the GTP-bound form of p21ras in rat pheochromocytoma PC12 cells. *Oncogene* 7, 277-281.

Nagy, Z. (2000). Cell cycle regulatory failure in neurones: causes and consequences. *Neurobiology of Aging* **21**, 761-769.

Narisawa-Saito, M., Wakabayashi, K., Tsuji, S., Takahashi, H., and Nawa, H. (1996). Regional specificity of alterations in NGF, BDNF and NT-3 levels in Alzheimer's disease. *NeuroReport* 7, 2925-2928.

Naoi, M., Maruyama, W., Akao, Y., Zhang, J., and Parvez, H. (2000). Apoptosis induced by an endogenous neurotoxin, N-methyl(R)salsolinol, in dopamine neurons. *Toxicology* **153**, 123-141.

Netland, E. E., Newton, J. L., Majocha, R. E., and Tate, B. A. (1998). Indomethacin reverses the microglial response to amyloid beta-protein. *Neurobiology of Aging* **19 (3)**, 201-204.

Newton, C. R., and Graham, A. (2000) Introduction to biotechniques: PCR. BIOS Scientific Publishers Ltd, Oxford.

Nicholson, D. W., and Thornberry, N. A. (1997). Caspases: killer proteases. *Trends in Biological Sciences* **22**, 299-306.

Nicoletti, I., Migliorati, G., Pagliacci, M. C., Grignani, F., and Riccardi, C. (1991). A rapid and simple method for measuring thymocyte apoptosis by propidium iodide staining and flow cytometry. *Journal of Immunological Methods* **139**, 271-279.

Nordberg, J., and Arner, S. J. (2001). Reactive oxygen species, antioxidants, and the mammalian thioredoxin system. *Free Radical Biology & Medicine* **31**, 1287-1312.

O'Banion, M. K., and Finch, C. E. (1996). Inflammatory mechanisms and anti-inflammatory therapy in Alzheimer's disease. *Neurobiology of Aging* **17 (5)**, 669-671.

Oberdoerster, J., and Rabin, R. A. (1999). NGF-Differentiated and undifferentiated PC12 cells vary in induction of apoptosis by ethanol. *Life Sciences* **64**, 267-272.

Oh-Hashi, K., Maruyama, W., and Isobe, K. (2001). Peroxynitrite induces GADD34, 45, and 153 via p38 MAPK in human neuroblastoma SH-SY5Y cells. *Free Radical Biology & Medicine* **30**, 213-221.

Okuda, S., Nishiyama, N., Saito, H., and Katsuki, H. (1998). 3-Hydroxykynurenine, an endogenous oxidative stress generator, causes neuronal cell death with apoptotic features and region selectivity. *Journal of Neurochemistry* **70**, 299-307.

Oliver, C. N., Ahn, B. W., Moerman, E. J., Goldstein, S., and Stadtman, E. R. (1987). Age-related changes in oxidized proteins. *Journal of Biological Chemistry* **262**, 5488-5491.

Olivieri, G., Baysang, G., Meier, F., Muller-Spahn, F., Stähelin, H. B., Brockhaus, M., and Brack, C. H. (2001). N-Acetyl-L-Cysteine protects SHSY5Y neuroblastoma cells from oxidative stress and cell cytotoxicity: effects on β-amyloid secretion and tau phosphorylation. *Journal of Neurochemistry* **76**, 224-233.

Olson, L. (1993). NGF and the treatment of Alzheimer's disease. *Experimental Neurology* **124**, 5-15.

O'Neill, L. A. J., and Kaltschmidt, C. (1997). NF-kB: a crucial transcription factor for glial and neuronal cell function.. *Trends in the Neurosciences* **20**, 252-258.

Ormerod, M. G. (1998). Flow Cytometry of Apoptotic Cells. *Cell Biology: A Laboratory Handbook* **2nd edition**, 351-356.

Påhlman, S., Hoehner, J. C., Nanberg, E., Hedborg, F., Fagerstrom, S., Gestblom, C., Johansson, I., Larsson, U., Lavenius, E., Ortoft, E., and Soderholm, H. (1995). Differentiation and survival influences of growth factors in human neuroblastoma. *European Journal of Cancer* **31A**, 453-458.

Pan, Z., and Perez-Polo, R. (1993). Role of nerve growth factor in oxidant homeostasis: Glutathione metabolism. *Journal of Neurochemistry* **61**, 1713-1721.

Panet, H., Barzilai, A., Daily, D., Melamed, E., and Offen, D. (2001). Activation of nuclear transcription factor kappa B (NF-kB) is essential for dopamine-induced apoptosis in PC12 cells. *Journal of Neurochemistry* 77, 391-398.

Pascale, A., and Etcheberrigaray, R. (1999). Calcium alterations in Alzheimer's disease: Pathophysiology, models and therapeutic opportunities. *Pharmacological Research* **39**, 81-88.

Pereira, C., Sancha Santos, M., and Oliveira, C. (1999). Involovement of oxidative stress on the impairment of energy metabolism induced by amyloid beta peptides on PC12 cells: Protection by antioxidants. *Neurobiology of Disease* **6**, 209-219.

Peter, M. E., Heufelder, A. E., and Hengartner, M. O. (1997). Advances in apoptosis research. *Proceedings National Academy of Sciences* **94**, 12736-12737.

Petersen, A., Larsen, K. E., Behr, G. G., Romero, N., Przedborski, S., Brundin, P., and Sulzer, D. (2001). Brain-derived neurotrophic factor inhibits apoptosis and dopamine-induced free radical production in striatal neurons but does not prevent cell death. *Brain Research Bulletin* **56**, 331-335.

Pike, C. J., Burdick, D., Walencewicz, A. J., Glabe, C. G., and Cotman, C. W. (1993). Neurodegeneration induced by beta-amyloid peptides in vitro: the role of the peptide assembly state. *The Journal of Neuroscience* **13**, 1676-1687.

Pitchumoni, S. S., and Doraiswamy, P. M. (1998). Current status of antioxidant therapy for Alzheimer's disease. *Journal of the American Geriatric Society* **46**, 1566-1572.

Pollwein, P., Masters, C. L., and Beyreuther, K. (1992). The expression of the amyloid precursor protein (APP) is regulated by two GC-elements in the promoter. *Nucleic Acids Research* **20**, 63-68.

Potters, G., De Gara, L., Asard, H., and Horemans, N. (2002). Ascorbate and glutathione: guardians of the cell cycle, partners in crime? *Plant Physiology and Biochemistr. In press.*

Pratico, D. (2002). Alzheimer's disease and oxygen radicals: new insights. *Biochemical Pharmacology* **7109**, 1-5.

Pratico, D., Uryu, K., Leight, S., Trojanoswki, J. Q., and Lee, V. M (2001). Increased lipid peroxidation precedes amyloid plaque formation in an animal model of Alzheimer amyloidosis. *Journal of Neuroscience (Online)* **21 (12)**, 4183-4187.

Price, D. L., Sisodia, S. S., and Borchelt, D. R. (1998). Genetic neurodegenerative diseases: the human illness and transgenic models. *Science* **282 (5391)**, 1079-1083.

Punchard, N. A., Watson, D. J., and Thompson, R. P. H. (1994). Analysis of glutathione in endothelial cells grown in 96 well microtitre plates. *Biochemical Society Transactions* **22**, 198S.

Puskas, F., Gergely Jr, P., Banki, K., and Perl, A. (2000). Stimulation of the pentose phosphate pathway and glutathione levels by dehydroascorbate, the oxidised form of vitamin C. *FASEB Journal* **14**, 1352-1361.

Rahman, I. And MacNee, W. (2000). Regulation of redox glutathione levels and gene transcritpion in lung inflammation: therapeutic approaches. *Free Radical Biology & Medicine*, **28(9)**, 1405-1420.

Ramassamy, C., Averill, D., Beffert, U., Bastianetto, S., Theroux, L., Lussier-Cacan, S., Cohn, J. S., Christen, Y., Davignon, J., Quirion, R., and Poirier, J. (1999). Oxidative damage and protection by antioxidants in the frontal cortex of Alzheimer's disease is related to the apolipoprotein E genotype. *Free Radical Biology & Medicine* **27**, 544-553.

Ray, S. K., Fidan, M., Nowak, M. W., Wilfor, G. G., Hogan, E. L., and Banik, N. L. (2000). Oxidative stress and Ca^{2+} influx upregulate calpain and induce apoptosis in PC12 cells. *Brain Research* **852**, 326-334.

Reed, J. C. (2000). Mechanisms of Apoptosis. *American Journal of Pathology* **157 (5)**, 1415-1430.

Reiners Jr, J. J., Mathieu, P., Okafor, C., Putt, D. A., and Lash, L. H. (2000). Depletion of cellular glutathione by conditions used for the passaging of adherent cultured cells. *Toxicology* **115**, 153-163.

Reiter, R. J. (1995). Oxidative processes and antioxidative defense mechanisms in the aging brain. *FASEB Journal* **9 (7)**, 526-533.

Riaz, S., Malcangio, M., Miller, M., and Tomlinson, D. R. (1999). A vitamin D_3 derivative (CB1093) induces nerve growth factor and prevents neurotrophic deficits in streptozotocin-diabetic rats. *Diabetologia* **42 (11)**, 1308-1313.

Rice, M. E. (2000). Ascorbate regulation and its neuroprotective role in the brain. *Trends in Neurosciences* **23**, 209-216.

Richman, P. G., and Meister, A. (1975). Regulation of γ-glutamylcysteine synthetase by nonallosteric feedback inhibition by glutathione. *Journal of Biological Chemistry* **250,** 20578-20583.

Richter, C. (1995). Oxidative damage to mitochondrial DNA and its relationship to ageing. *International Journal of Biochemistry and Cell Biology* **27**, 647-653.

Rong, P., Bennie, A. M., Epa, W. R., and Barrett, G. L. (1999). Nerve growth factor determines survival and death of PC12 Cells by regulation of the bcl-x, bax, and caspase-3 genes. *Journal of Neurochemistry* **72**, 2294-2300.

Ryazanov, A. G. and Nefsky, B. S. (2002). Protein turnover plays a key role in aging. *Mechanisms of Ageing and Development* **123**, 207-213.

Saiki, R. K., Gelfand, D. H., Stoffel, S., Scharf, S. J., Higuchi, R., Hoen, G. T., Mullis, K. B., and Erlich, H. A. (1988). Primer-directed enzymatic amplification of DNA with a thermostable DNA polymerase. *Science* **239 (4839),** 487-491.

Saito, T., Kijima, H., Kiuchi, Y., Isobe, Y., and Fukushima, K. (2001). β-amyloid induces caspase-dependent early neurotoxic change in PC12 cells: correlation with H_2O_2 neurotoxicity. *Neuroscience Letters* **305**, 61-64.

Salvi, A., Carrupt, P-A, Tillement, J-P and Testa, B. (2001). Structural damge to proteins caused by free radicals: assessment, protection by antioxidants, and influence of protein binding. *Biochemical Pharmacology* **61**, 1237-1242.

Sampath, D., Jackson, G. R., Werrbach-Perez, K. and Perez-Polo, J. R. (1994). Effects of nerve growth factor on glutathione peroxidase and catalase in PC12 cells. *Journal of Neurochemistry* **62 (6)**, 2476-2479.

Sanfeliu, C., Cristofol, R., Toran, N., Rodrigez-Farre, E., and Kim, S. U. (1999). Use of human central nervous system cell cultures in neurotoxicity testing. *Toxicology in Vitro* **13**, 753-759.

Sastry, P. S., and Rao, K. S. (2000). Apoptosis and the Nervous System. *Journal of Neurochemistry* **74**, 1-20.

Satoh, T., Enokido, Y., Aoshima, H., Uchiyama, Y., and Hatanaka, H. (1997). Changes in mitochondrial membrane potnetial during oxidative stress-induced apoptosis in PC12 cells. *Journal of Neuroscience Research* **50**, 413-420.

Scheuner, D., Eckman, C., Jensen, M., Song, X., Citron, M., Suzuki, N., Bird, T. D., Hardy, J., Hutton, M., Kukull, W., Larson, E., Levy-Lahad, E., Viltanen, M., Peskind, E., Poorkaj, P., Schellenberg, G., Tanzi, R., Wasco, W., Lannfelt, L., Selkoe, D., and Younkin, S. (1996). Secreted amyloid β-protein similar to that in the senile plaques of Alzheimer's disease is increased *in vivo* by the presenilin 1 and 2 and APP mutations linked to familial Alzheimer's disease. *Nature Medicine* **2**, 864-870.

Schubert, D., Behl, C., Lesley, R., Brack, A., Dargusch, R., Sagara, Y., and Kimura, H. (1995). Amyloid peptides are toxic via a common oxidative mechanism. *Proceedings of the National Academy of Sciences* **92**, 1989-1993.

Selkoe, D. J. (1996). Amyloid Beta-Protein and the Genetics of Alzheimer's Disease. *The Journal of Biological Chemistry* **271**, 18295-18298.

Selkoe, D. J. (1998). The cell biology of beta-amyloid precursor protein and presenilin in Alzheimer's disease. *Trends in Cell Biology* **8**, 447-453.

Semkova, I., and Krieglstein, J. (1999). Neuroprotection mediated via neurotrophic factors and induction of neurotrophic factors. *Brain Research Reviews* **30**, 176-188.

Sen, C. K. (1998). Redox signalling and the emerging therapeutic potential of thiol antioxidants. *Biochemical Pharmacology* **55 (11)**, 1747-1758.

Serrano, T., Lorigados, L. C., and Armenteros, S. (1996). Nerve growth factor levels in normal human sera. *NeuroReport* **8**, 179-181.

Seyfried, J., Soldner, F., Schulz, J. B., Klockgether, T., Kovar, K. A., and Wullner, U. (1999). Differential effects of L-buthionine sulfoxamine and ethacrynic acid on glutathione levels and mitochondrial function in PC12 cells. *Neuroscience Letters* **264**, 1-4.

Shackleford, R. E., Kaufmann, W. K., and Paules, R. S. (2000). Oxidative stress and cell cycle checkpoint function. *Free Radical Biology & Medicine* **28**, 1387-1404.

Shaw, P. J., Ince, P. G., Falkous, G., and Mantle, D. (1995). Oxidative damage to protein in sporadic motor neuron disease spinal cord. *Annals of Neurology* **38 (4)**, 691-695.

Shearman, M. S., Hawtin, S. R., and Tailor, V. J. (1995). The intracellular component of cellular 3-(4,5-dimethylthiazol-2-yl)-2,5-diphenyltetrazolium bromide (MTT) reduction is specifically inhibited by beta-amyloid peptides. *Journal of Neurochemistry* **65 (1)**, 218-227.

Shearman, M. S., Ragan, C. I., and Iversen, L. L. (1994). Inhibition of PC12 cell redox activity is a specific, early indicator of the mechanism of beta-amyloid-mediated cell death. *Proceedings National Academy of Sciences* **91**, 1470-1474.

Shen, H-M., Yang, C-F., Ding, W-X., Liu, J., and Ong, C-N. (2001). Superoxide radical-initiated apoptotic signalling pathway in selenite-treated $HEPG_2$ cells:Mitochondria serve as the main target. *Free Radical Biology and Medicine* **30(1)**, 9-21.

Sherer, T. B., Trimmer, P. A., Borland, K., Parks, J. K., Bennett Jr, J. P., and Tuttle, J. B. (2001). Chronic reduction in complex I function alters calcium signalling in SH-SY5Y neuroblastoma cells. *Brain Research* **891**, 94-105.

Sherwood, L. (1993). Human Physiology: From cells to systems. Second edition. West Publishing Company, Minneapolis, USA.

Shooter, E. M. (2001). Early days of the nerve growth factor. *Annual Review of Neuroscience* **24**, 601-629.

Si, F., Ross, G. M., and Shin, S. H. (1998). Glutathione protects PC12 cells from ascorbate-and dopamine-induced apoptosis. *Experimental Brain Research* **123**, 236-268.

Siegel, G. J., and Chauhan, N. B. (2000). Neurotrophic factors in Alzheimer's and Parkinson's disease brain. *Brain Research Reviews* **33**, 199-227.

Sies, H. (1985). Chapter 1: Oxidative Stress: introductory remarks. In: Sies H., ed Oxidative stress, London Academic Press.

Simon, N., Jolliet, P., Morin, C., Zini, R., Urien, S., and Tillement, J-P. (1998). Glucocorticoids decrease cytochrome c oxidase activity of isolated rat kidney mitochondria. *FEBS Letters* **435**, 25-28.

Slater, A. F. G., Stefan, C., Nobel, I., Dobbelsteen, D., and Orrenius, S. (1995). Signalling mechanisms and oxidative stress in apoptosis. *Toxicology Letters* **82/83**, 149-153.

Sloviter, R. S. (2002). Apoptosis: a guide for the perplexed. *Trends in Pharmacological Sciences* **23 (1)**, 19-24.

Smith, C. U. M. (1996). Elements of Neurobiology. Second Edition. John Wiley & Sons, England

Smith, M. A., Nunomura, A., Zhu, X., Takeda, A., and Perry, G. (2000). Metabolic, metallic, and mitotic sources of oxidative stress in Alzheimer's disease. *Antioxidants and Redox Signaling* **2**, 413-420.

Smith, M. A., Sayre, L., and Perry, G. (1996). Is Alzheimer's a disease of oxidative stress? *Alzheimer's Disease Review* **1**, 63-67.

Smith, M. A., Sayre, L. M., Anderson, V. E., Harris, P. L. R., Beal, M. F., Kowall, N., and Perry, G. (1998). Cytochemical Demonstration of Oxidative Damage in Alzheimer Disease by Immunochemical Enhancement of the Carbonyl Reaction with 2,4-Dinitrophenylhydrazine. *The Journal of Histochemistry & Cytochemistry* **46**, 731-735.

Smith, P. K., Krohn, R. I., Hermanson, G. T., Mallia, A. K., Gartner, F. H., Provenzano, M. D., Fujimoto, E. K., Goeke, N. M., Olson, B. J. and Klenk, D. C. (1985). Measurement of protein using Bicinchoninic acid. *Analytical Biochemistry* **150**, 76-85.

Sofroniew, M. V., Howe, C. L., and Mobley, W. C. (2001). Nerve growth factor signalling, neuroprotection, and neural repair. *Annual Review of Neuroscience* **24**, 1217-1281.

Sohal, R. S., Agarwal, S., Sohal, B. H. (1995). Oxidative stress and aging in the Mongolian gerbil (Mreiones unguiculatus). *Mechanisms of Ageing and Development* **81**, 15-25.

Sohal, R. S., Ku, H. H., Agarwal, S., Forster, M. J. and Lah, H. (1994). Oxidative damage, mitochondrial oxidant generation and antioxidant defenses during aging and in response to food restriction in the mouse. *Mechanisms of Ageing and Development* **74**, 121-133.

Sommer, B. (2002). Alzheimer's disease and the amyloid cascade hypothesis: ten years on. *Current Opinion in Pharmacology* **2**, 87-92.

Song, J. H., Shin, S. H., and Ross, G. M. (2001). Oxidative stress induced by ascorbate causes neuronal damage in an in vitro system. *Brain Research* **895**, 66-72.

Spillantini, M. G., and Goedert, M. (1998). Tau protein pathology in neurodegenrative diseases. *Trends in Neurosciences* **21**, 428-433.

Spina, M. B., Squinto, S. P., Miller, J., Lindsay, R. M., and Hyman, C. (1992). Brain-Derived Neurotrophic Factor Protect Dopamine Neurons Against 6-Hydroxydopamine and N-Methyl-4-Phenylpyridinium Ion Toxicity: Involvement of the Glutathione System. *Journal of Neurochemistry* **59**, 99-106.

Squier, T. C. (2001). Oxidative stress and protein aggregation during biological aging. *Experimental Gerontology* **36,** 1539-1550.

Squinto, S. P., Stitt, T. N., Aldrich, T. H., Davis, S., Bianco, S. M., Radziejewski, C., Glass, D. J., Masiakowski, P., Furth, M. E., Valenzuela, D. M., DiStefano, P. S., and Yancopoulos, G. D. (1991). trkB encodes a functional receptor for Brain-Derived Neurotrophic Factor and Neurotrophin-3 but Not Nerve Growth Factor. *Cell* **65**, 885-893.

Steiner, H., Capell, A., and Haass, C. (1999). Proteolytic processing and degradation of Alzheimer's disease relevant proteins. *Biochemical Society Transactions* **27**, 234-241.

Strittmater, W. J., Saunders, A. M., Schmechel, D., Pericak-Vance, M., Enghild, J., Salvesen, G. S., and Roses, A. D. (1993). Apolipoprotein E: High avidity binding to β-amyloid and increased frequency of type 4 allele in late-onset familial Alzheimer disease. *Proceedings National Academy of Sciences* **90**, 1977-1981.

Stürzenbaum, S. R., and Kille, P. (2001). Control genes in quantitative molecular biological techniques:the variability of invariance. *Comparitive Biochemistry and Physiology Part B* **130**, 281-289.

Su, J. H., Anderson, A. J., Cummings, B. J., and Cotman, C. W. (1994). Immunohistochemical evidence for apoptosis in Alzheimer's disease. *NeuroReport* **5**, 2529-2533.

Supino, R. (1995). MTT Assays. *Methods in Molecular Biology* **43**, 137-149.

Suzuki, A. (1997). Amyloid beta-protein induces necrotic cell death mediated by ICE cascade in PC12 cells. *Experimental Cell Research* **234**, 507-511.

Suzuki, T., Higgins, P. J., and Crawford, D. R. (2000). Control selection for RNA quantitation. *Biotechnology and Applied Biochemistry* **29**, 332-337.

Takuma, K., Yoshida, T., Lee, E., Mori, K., Kishi, T., Baba, A., Matsuda, T. (2000). CV-2619 protects cultured astrocytes against reperfusion injury via nerve growth factor production. *European Journal of Pharmacology* **406 (3)**, 333-339.

Tan, J., Town, T., Placzek, A., Kundtz, A., Yu, H., and Mullan, M. (1999). Bcl-xl inhibits apoptosis and necrosis produced by Alzheimer's beta-amyloid 1-40 peptide in PC12 cells. *Neuroscience Letters* **272**, 5-8.

Thal, L. J. (2000). Anti-inflammatory drugs and Alzheimer's disease. *Neurobiology of Aging* **21**, 449-450.

Thannickal, V. J., and Fanburg, B. L. (2000). Reactive oxygen species in cell signaling. *American Journal Physiology of Lung Cell Molecular Physiology* **279**, l1005-l1028.

Thomas, M., Nicklee, T., and Hedley, D. W. (1995). Differential effects of depleting agents on cytoplasmic and nuclear non-protein sulphydryls: a fluorescence image cytometry study. *British Journal Of Cancer* **72**, 45-50.

Thomas, M. J. (2000). The role of free radicals and antioxidants. *Nutrition* **16**, 716-718.

Thornberry, N. A., and Lazebnik, Y. (1998). Caspases: enemies within. *Science* **281 (5381)**, 1312-1316.

Tomita, T., Maruyama, K., Saido, T. C., Kume, H., Shinozaki, K., Tokuhiro, S., Capell, A., Walter, J., Grunberg, J., Haass, C., Iwatsubo, T., and Obata, K. (1997). The presenilin 2 mutation (N141I) linked to familial Alzheimer disease (Volga German families) increases the secretion of amyloid β protein ending at the 42nd (43rd) residue. *Proceedings of the National Academy of Sciences, USA*, **94**, 2025-2030.

Tsuchiya, M., Suematsu, M., and Suzuki, H. (1994). In vivo visualization of oxygen radical-dependent photoemission. *Methods in Enzymology* **233**, 128-140.

Tuszynski, M. H., U, H. S., Amaral, D. G., and Gage, F. H. (1990). Nerve growth factor infusion in the primate brain reduces lesion-induced cholinergic neuronal degeneration. *Journal of Neuroscience* **10**, 3604-3614.

Twaroski, T. P., O'Brien, M. L., and Robertson, L. W. (2001). Effects of selected polychlorinated biphenyl (PCB) congeners on hepatic glutathione, glutathione-related enzymes, and selenium status: implications for oxidative stress. *Biochemical Pharmacology* **62**, 273-281.

Uberti, D., Yavin, E., Gil, S., Ayasola, K. R., Goldfinger, N., and Rotter, V. (1999). Hydrogen peroxide induces nuclear translocation of p53 and apoptosis in cells of oligodendroglia origin. *Brain Research and Molecular Brain Research* **65**, 167-175.

Valencia, E., Hardy, G., and Marin, A. (2001). Glutathione- Nutritional and pharmacologic viewpoints: Part v. *Nutrition* **17**, 978.

van den Dobbelsteen, D. J., Nobel, C. S. I., Schlegel, J., Cotgreave, I. A., Orrenius, S., and Slater, A. F. G. (1996). Rapid and specific efflux of reduced glutathione during apoptosis induced by Anti-Fas/APO-1 antibody. *The Journal of Biological Chemistry* **271**, 15420-15427.

Villa, A., Latasa, M. J., and Pascual, A. (2001). Nerve growth factor modulates the expression and secretion of β-amyloid precursor protein through different mechanisms in PC12 cells. *Journal of Neurochemistry***77**, 1077-1084.

Voigt, A., Hartmann, P., and Zintl, F. (2000). Differentiation, proliferation and adhesion of human neuroblastoma cells after treatment with Retinoic Acid. *Cell Adhesion* 7, 423-440.

Weber, G. F. (1999). Final common pathways in neurodegenerative diseases: regulatory role of the glutathione cycle. *Neuroscience and Biobehavioural Reviews* **23**, 1079-1086.

Weitzman, J. (2001) Pioneering gene therapy for Alzheimer's. *Trends in Molecular Medicine* 7 **(6)**, 245.

Wilcock, G. K., and Harrold, P. L. (1996). Treatment of Alzheimer's disease: future directions. *Acta Neurologica Scandinavia* **(Supplement 165),** 128-136.

Williams, L.R. (1995). Oxidative stress, age-related neurodegeneration and the potential for neurotrophic treatment. *Cerebrovascular and Brain Metabolism Reviews* 7 **(1),** 55-73.

Willingham, M. C., (1999). Cytochemical methods for the detection of apoptosis. *The Journal of Histochemistry and Cytochemistry*, **47(9)**, 1101-1109.

Winkler, J., Thal, L. J., Gage, F. H., and Fisher, L. J. (1998). Cholinergic strategies for Alzheimer's disease. *Journal of Molecular Medicine* **76(8)**, 555-567.

Winterbourn, C. C., and Buss, I. H. (1999). Protein carbonyl measurement by enzyme-linked immunosorbent assay. *Methods: A Companion to Methods in Enzymology*, 106-111.

Wondrak, G., T, Cervantes-Laurean, D., Jacobson, E. L., and Jacobson, M. K. (2000). Histone carbonyation in vivo and in vitro. *Biochemical Journal* **351**, 769-777.

Wong, G. H. (1995). Protective roles of cytokines against radiation: induction of mitochondrial MnSOD. *Biochemica and Biophysica Acta* **127**, 205-209.

Wooten, M. W., Seibenhener, M. L., Heikkila, J. E., and Mischak, H. (1998). δ-Protein kinase C phosphorylation parallels inhibition of nerve growth factor – Induced differentiation independent of changes in Trk A and Map kinase signalling in PC12 cells. *Cell Signalling* **10 (4)**, 265-276.

Xiao, X. Q., Yang, J. W., and Tang, X. C. (1999). Huperzine A protects rat pheochromocytoma cells against hydrogen peroxide-induced injury. *Neuroscience Letters* **275**, 73-76.

Yallampalli, S., Micci, M.-A., and Taglialatela, G. (1998). Ascorbic acid prevents β-amyloid-induced intracellular calcium increase and cell death in PC12 cells. *Neuroscience Letters* **251**, 105-108.

Yamada, K., and Nabeshima, T. (2000). Animal models of Alzheimer's disease and evaluation of anti-dementia drugs. *Pharmacology and Therapeutics* **88**, 93-113.

Yankner, B. A. (1996). Mechanisms of neuronal degeneration in Alzheimer's Disease. *Neuron* **16**, 921-932.

Yao, X.-X., Drieu, K., and Papadopoulos, V. (2001). The Ginkgo biloba extract EGb 761 rescues the PC12 neuronal cells from β-amyloid-induced cell death by inhibiting the formation of β-amyloid-derived diffusible neurotoxic ligands. *Brain Research* **889,** 181-190.

Yao, Z.-X., Drieu, K., Szweda, L. I., and Papadopoulos, V. (1999). Free radicals and lipid peroxidation do not mediate beta-amyloid-induced neuronal cell death. *Brain Research* **847**, 203-210.

Yatin, S. M., Asenov, M., and Butterfield, D. A. (1999a). The Antioxidant vitamin E modulates amyloid β-peptide-induced creatine kinase activity inhibition and increased protein oxidation: Implications for the free radical hypothesis of Alzheimer's disease. *Neurochemical Research* **24**, 427-435.

Yatin, S. M., Yatin, M., Aulick, T., Ain, K. B., and Butterfield, D. A. (1999b). Alzheimer's amyloid beta-peptide associated free radicals increase rat embryonic neuronal polyamine uptake and ornithine decarboxylase activity: protective effect of vitamin E. *Neuroscience Letters* **263**, 17-20.

Yatin, S. M., Varadarajan, S., Link, C. D., and Butterfield, D. A. (1999c). In vitro and in vivo oxidative stress associated with Alzheimer's amyloid beta-peptide (1-42). *Neurobiology of Aging* **20 (3)**, 325-330.

Yonezawa, M., Back, S. A., Gan, X., Rosenberg, P.A., and Volpe, J. J. (1996). Cystine deprivation induces oligodendroglial death: rescue by free radical scavengers and by a diffusible glial factor. *Journal of Neurochemistry* **67**, 566-573.

Zamzani, N., Brenner, C., Marzo, I., Susin, S. A., adnd Kroemer, G. (1998). Subcellular and submitochondrial mode of action of Bcl-2 like oncoproteins. *Oncogene* **16**, 2265-2282.

Zastawny, T. H., Dabrowska, M., Jaskolski, T., Klimarczyk, M., Kulinski, L., Koszela, A., Szczesniewicz, M., Sliwinska, M., Witkowski, P., and Olinski, R. (1998). Comparison of oxidative base damage in mitochondrial and nuclear DNA. *Free Radical Biology & Medicine* **24 (5)**, 722-725.

Zhan, Q., Lord, K. A., Alamo Jr, I., Hollander, M. C., Carrier, F., Ron, D., Kohn, K. W., Hoffman, B., Libermann, D. A., and Fornace Jr, A. J. (1994). The GADD and myc D genes define a novel set of mammalian genes encoding acidic proteins that synergistically suppress cell growth. *Molecular Cell Biology* **14**, 2361-2371.

Zhang, L., Zhao, B., Yew, D. T., Kusiak, J. W., and Roth, G. S. (1997). Processing of Alzheimer's amyloid presursor protein during H_2O_2-induced apoptosis in human neuronal cells. *Biochemica and Biophysica Acta* **235**, 845-848.